LEABHARLANN CHOLÁISTE NA TRÍONÓIDE, BAILE ÁTHA CLIATH | TRINITY COLLEGE LIBRARY DUBLIN
Ollscoil Átha Cliath | The University of Dublin

**Terms and Conditions of Use of Digitised Theses from Trinity College Library Dublin**

**Copyright statement**

All material supplied by Trinity College Library is protected by copyright (under the Copyright and Related Rights Act, 2000 as amended) and other relevant Intellectual Property Rights. By accessing and using a Digitised Thesis from Trinity College Library you acknowledge that all Intellectual Property Rights in any Works supplied are the sole and exclusive property of the copyright and/or other IPR holder. Specific copyright holders may not be explicitly identified. Use of materials from other sources within a thesis should not be construed as a claim over them.

A non-exclusive, non-transferable licence is hereby granted to those using or reproducing, in whole or in part, the material for valid purposes, providing the copyright owners are acknowledged using the normal conventions. Where specific permission to use material is required, this is identified and such permission must be sought from the copyright holder or agency cited.

**Liability statement**

By using a Digitised Thesis, I accept that Trinity College Dublin bears no legal responsibility for the accuracy, legality or comprehensiveness of materials contained within the thesis, and that Trinity College Dublin accepts no liability for indirect, consequential, or incidental, damages or losses arising from use of the thesis for whatever reason. Information located in a thesis may be subject to specific use constraints, details of which may not be explicitly described. It is the responsibility of potential and actual users to be aware of such constraints and to abide by them. By making use of material from a digitised thesis, you accept these copyright and disclaimer provisions. Where it is brought to the attention of Trinity College Library that there may be a breach of copyright or other restraint, it is the policy to withdraw or take down access to a thesis while the issue is being resolved.

**Access Agreement**

By using a Digitised Thesis from Trinity College Library you are bound by the following Terms & Conditions. Please read them carefully.

I have read and I understand the following statement: All material supplied via a Digitised Thesis from Trinity College Library is protected by copyright and other intellectual property rights, and duplication or sale of all or part of any of a thesis is not permitted, except that material may be duplicated by you for your research use or for educational purposes in electronic or print form providing the copyright owners are acknowledged using the normal conventions. You must obtain permission for any other use. Electronic or print copies may not be offered, whether for sale or otherwise to anyone. This copy has been supplied on the understanding that it is copyright material and that no quotation from the thesis may be published without proper acknowledgement.

# THE STRUCTURAL EVOLUTION AND GIANT LANDSLIDES OF LA PALMA, CANARY ISLANDS

Submitted to the University of Dublin for the degree of Doctor of Philosophy

September 2005

*By* Karl Roa

A view of La Palma from El Garajonay, the highest point on the neighbouring island of La Gomera showing the incomplete shield of Taburiente Volcano (right) and the recently active Cumbre Vieja Volcano (left). The saddle between the two forms a part of the Cumbre Nueva lateral collapse escarpment.

Dept of Geology, Trinity College, Dublin 2. Ireland

TRINITY COLLEGE
13 NOV 2006
LIBRARY DUBLIN
THOSIS
8015

# Declaration

This thesis has not been submitted as an exercise for a degree at any other university. Except where stated, the work described therein was carried out by me alone.

I give permission for the Library to lend or copy this thesis upon request.

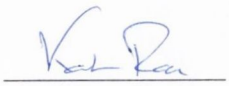

Karl Roa

# CONTENTS


| | | page |
|---|---|---|
| DECLARATION | | ii |
| CONTENTS | | iii |
| LIST OF FIGURES | | iv |
| LIST OF TABLES | | vii |
| ACKNOWLEDGEMENTS | | viii |
| SUMMARY | | ix |
| METHODOLOGY | | xii |
| GLOSSARY | | xiii |
| CHAPTER 1. | STRUCTURAL, STRATIGRAPHIC AND VOLCANOLOGICAL ASPECTS OF LA PALMA | |
| 1.1. | PROJECT LOCATION - LA PALMA | 1 |
| 1.1.1 | The Canary Archipelago – regional tectonics | 4 |
| 1.1.2 | La Palma; contemporary studies | 5 |
| 1.2 | THE CALDERA DE TABURIENTE; STRUCTURE AND ORIGIN OF A COLLAPSE AMPHITHEATRE | 12 |
| 1.2.1 | Introduction | 12 |
| 1.2.2 | The Caldera/Cumbre Nueva embayment – access and physiography | 13 |
| 1.2.3 | Geological map | 18 |
| 1.2.4 | The amphitheatre headwalls | 18 |
| 1.2.5 | The interior of the collapse amphitheatre | 23 |
| 1.2.6 | On the origin of the Caldera de Taburiente | 28 |
| 1.2.7 | Conclusion | 39 |
| 1.3 | THE RIFT ZONE MORPHOLOGY OF LA PALMA | 40 |
| 1.3.1 | Introduction | 40 |
| 1.3.2 | Rift zones, rifting and gravitational spreading; general aspects | 41 |
| 1.3.3 | The morphology of La Palma | 42 |
| 1.3.4 | Origin and evolution of the rift zone architecture | 53 |
| 1.3.5 | Conclusion | 67 |
| CHAPTER 2. | VOLCANO-TECTONIC UNITS AT THE BASE OF THE CALDERA & CUMBRE NUEVA ESCARPMENT | 68 |
| 2.1 | THE TENERRA COLLAPSE BRECCIA | 69 |
| 2.1.1 | Introduction | 69 |
| 2.1.2 | The location and geometry of the TCB from outcrop and subcrop studies | 70 |
| 2.1.3 | The geology of the TCB | 74 |
| 2.1.4 | Discussion | 84 |
| 2.1.5 | Lithificition and substratum expulsion | 91 |
| 2.1.6 | Conclusion | 96 |
| 2.2 | THE CUMBRE NUEVA DETACHMENT FAULT | 97 |
| 2.2.1 | Introduction | 97 |
| 2.2.2 | The basic nomenclature and properties of fault rocks | 98 |
| 2.2.3 | Structure of the Cumbre Nueva detachment fault | 99 |
| 2.2.4. | Synthesis of the structural data | 114 |
| 2.2.5. | Conclusion | 119 |

CHAPTER 2.2 THE CUMBRE NUEVA DETACHMENT


| | | |
|---|---|---|
| 2.2.1 | A weathered section of the Cumbre Nueva detachment | 97 |
| 2.2.2 | Fracture array and geometric relations in fault gouge | 99 |
| 2.2.3 | Fault scaling relationship $W_f/L$ | 99 |
| 2.2.4 | Components of the Cumbre Nueva detachment | 100 |
| 2.2.5 | Distribution of mineral zones in the Seamount Series | 101 |
| 2.2.6 | Locations of stratigraphic profiles, sections etc. | 103 |
| 2.2.7 | Orientated chip sample from the polished fault surface | 104 |
| 2.2.8 | Schmidt projections, rose and contour diagrams | 105 |
| 2.2.9 | Stratigraphic profiles through the detachment | 106 |
| 2.2.10 | Outcrop appearances of the Cumbe Nueva detachment fault | 107 |
| 2.2.11 | Scaled sections of shear fracture geometries and PSD | 108 |
| 2.2.12 | Offset and overthrust features along the detachment | 109 |
| 2.2.13 | Distribution of particle sizes through a section of the fault core | 109 |
| 2.2.14 | Section of the fault core | 110 |
| 2.2.15 | Orientated specimen of chloritic gouge with photomicrographs | 111 |
| 2.2.16 | XRD analysis | 112 |
| 2.2.17 | Orientated chip samples and XRD traces | 113 |
| 2.2.18 | Flank-scale evolution toward gravitational spreading | 114 |
| 2.2.19 | Conceptual evolution of the footwall | 117 |
| 2.2.20 | Fault scaling relationship $D/T$ | 118 |


CHAPTER 3.1 DEBRIS AVALANCHE DEPOSITS AND SOURCE REGIONS


| | | |
|---|---|---|
| 3.1.1. | View of the dismantled summits of Taburiente and Bejenado | 120 |
| 3.1.2. | The dismantled Plio-Pleistocene volcanoes forming northern La Palma | 121 |
| 3.1.3. | End-member classification scheme for mass wasting events | 122 |
| 3.1.4. | Debris avalanche deposits of the Canary Archieplago | 123 |
| 3.1.5. | Outcrop pattern of the discordance surfaces at Playa de la Veta | 125 |
| 3.1.6. | Contemporary interpretations of debris avalanche boundaries | 126 |
| 3.1.7. | Structural elements of the Cumbre Nueva embayment | 127 |
| 3.1.8. | Bejenado embankment | 128 |
| 3.1.9. | Embayment filling volcanism – scaled cross sections | 128 |
| 3.1.10. | Re-evaluations of re-entrant geometry | 129 |
| 3.1.11. | Spatial/dimensional analysis of re-entrant and associated slide blocks | 130 |
| 3.1.12. | HL diagrams for the Cumbre Nueva collapse | 131 |
| 3.1.13. | Slide track and landslide profile for the Cumbre Nueva collapse | 131 |
| 3.1.14. | Re-evaluation of debris avalanche deposit dimensions and sources | 133 |
| 3.1.15. | Shaded relief images of the west flank and associated slide deposits | 134 |
| 3.1.16. | Spatial and temporal evolution of the collapse sectors/embayments | 135 |


CHAPTER 3.2 THE CUMBRE NUEVA LATERAL COLLAPSE


| | | |
|---|---|---|
| 3.2.1 | High oblique SRM of the Cumbre Nueva embayment | 137 |
| 3.2.2 | Mohr diagrams for stress perturbation influenced by fluid pressure | 138 |
| 3.2.3 | The intrusion of magma into a dike-bound aquifer | 140 |
| 3.2.4 | Mohr diagrams for rock mass strength | 141 |
| 3.2.5 | Geotechnical architecture of northern La Palma | 142 |
| 3.2.6 | Outcrop-scale deformation structures on Tenerife and Gran Canaria | 144 |
| 3.2.7 | Components of the Cumbre Nueva embayment. | 145 |
| 3.2.8 | Plan and interpretative north-south cross-section of the embayment | 146 |
| 3.2.9 | Cross-section of the western flank of Cumbre Vieja Volcano | 147 |
| 3.2.10 | A limit equilibrium model for La Palma (subaerial/submarine) | 148 |
| 3.2.11 | Instabilty flow sheet | 149 |
| 3.2.12 | Scaled topographic sections through the Caldera | 151 |
| 3.2.13 | Possible geometry of the critical failure surface | 151 |
| 3.2.14 | Limit equilibrium models for circular failures | 153 |
| 3.2.15 | Method of slices | 153 |
| 3.2.16 | Alternative models for the collapse initiator | 155 |

CHAPTER 4 CONCLUSIONS AND CONTRIBUTIONS

4.1 Revised stratigraphic nomenclature of La Palma 159
4.2 Composite map of La Palma 160
4.3 Event chronology of La Palma 162

LIST OF TABLES

1.2.1 Basic grouping of volcaniclastic units in northern La Palma 25
2.2.1 Range of particle sizes and nomenclature of cataclastic rocks 98
2.2.2 Summary data for large and small displacement thrusts 119
3.1.1 Debris avalanche deposits, source, geometry and age data for La Palma 124
3.1.2 Modifications to table 3.1.1 135
3.2.1 Geotechnical database of volcanic and intrusive rocks 144

# Acknowledgements

Dublin

I wish to extend a great thanks to Chris Stillman who instigated this study and to John Walsh and Valentine Troll for thoroughly reviewing the thesis, for discussions and providing important literature. Very special thanks to John Murray, Zoe Shipton, Brian McSharry, Declan Bourke, Neil Kearney, Joann Laynng, Kate Walsh and most especially my parents Mary and Carl, brother Richard and sister Fiona. Funding provided by Trinity College Dublin, the Spanish Ministry of Foreign affairs, Chris Stillman and especially my own family is gratefully acknowledged. I am very grateful to Kirstin Hetfield and Robbie Goodhue for performing XRD analyses.

Canary Islands

I am very grateful to Pauline Agnew and her children (esp. Ailbhe and Yeyo) in Guamasa, Tenerife for their warmth and help during my studies in the Canary Islands. Juan Carlos Carracedo provided invaluable assistance in the early stages of the research project and continued to help later when differences in scientific opinion began to emerge. Juan Carlos provided topographic maps, GIS data, access to aerial photographs, office space at the CSIC, and temporary financial support. The staff of the *Consejo Superior de Investigaciones Científicas* (CSIC) in La Laguna, Tenerife are also thanked for their cooperation. I would like to thank the staff of the *Parque Nacional de la Caldera de Taburiente*, La Palma (Domingo Peréz, Borca, Pedro, Victor, Angel Palomares Martínez and Ezequiel Alfonso Leon) for their cooperation and friendship during fieldwork.

Hawaiian Islands

A special Mahalo nui loa e a hui ho to my great friends Kathryn and Ken in Volcano Village, Hawai'i for aloha and accommodation during write up in May-June and Oct-Nov-Dec 2003. This thesis has benefited from discussions with Emilio Herrero Berverra, Mike Garcia (SOEST, University of Hawaii) and Jack Lockwood (GeoHazards Consultants) who pointed out important literature and contacts.

Mongolia

Finally, I would like to extend my appreciation to Edward Rochette and Doug Kirwin for granting me extended leave in order to complete the thesis whilst under the employ of Ivanhoe Mines Mongolia Inc., and for finanical/technical support. Critical comments and assistance with the last moment production of this thesis by my subversive Antipodean and Canadian co-workers Adrian Benson (Ch. 1.2), Rohan Wolfe (Ch. 1.3) and Andy Stewart (Ch. 2.1). I would also like to thank Andrew Gourlay (Asia Gold Corp) for reviewing the abstract/introduction and Ch. 1.3.

# SUMMARY

The island of La Palma, in the western Canary Archipelago, is formed by a partially dismantled and eroded Plio-Pleistocene strato-shield volcano (Taburiente/Cumbre Nueva) that is overlapped and elongated to the south by an active rift-centred volcano – Cumbre Vieja. Stratigraphic measurements were used to systematically profile the basal part of the giant Quaternary landslide escarpments that form prominent morphological features on the island. An exhumed detachment fault was discovered in the process. The escarpments, which are 45 km in perimeter and up to 1 km high, are interpreted in the light of this discovery to have developed by synchronous lateral collapses that were preceded by a geologically significant period of gravitational spreading. The detachment occupies the position of what has been classified in contemporary studies as an erosional unconformity, separating an uplifted Pliocene seamount from the subaerial volcanic successions forming the Taburiente/Cumbre Nueva strato-shield. The Cumbre Nueva Detachment, as it is named herein, together with the overlying pyroclast-rich collapse breccias (herein named the Tenerra Collapse Breccia), have not been the subject of any previous academic studies. Both of these units are separated by the detachment plane which geometrically emulates the domal topography of the seamount basement. Together they provide an opportunity to increase our understanding of the geometry and mechanisms of giant landslides on La Palma, past and future. The present study is unique in that it describes field kinematic evidence for the development and exhumation of a low angle fault zone that penetrates the exhumed intrusive core of an isolated volcano. Such data are rare in volcanic environments*, irrespective of the wealth of observations of exhumed detachments in continental/orogenic environments. By investigating the newly discovered detachment and toreva remnants and by evaluating the structural and bathymetric data around La Palma, this doctorate has four main objectives that fundamentally focus upon three major sector collapses.

- To document the geology of the detachment and hangingwall collapse breccias and assess their significance in the structural evolution of La Palma.
- Re-evaluate the dimensions of the Cumbre Nueva embayment and the associated debris avalanche deposits through correlations with the onshore and offshore data, and to assess the implications of the detachment in the Cumbre Nueva lateral collapse.
- Provide new constraints for the spatial and temporal development of La Palma's rift zones through analyses of morphology and structure. This approach compliments the interpretations that follow regarding landslide dimensions and source regions.
- Reveal evidence that the intra-collapse edifice, Bejenado Volcano, underwent failure of its north flank and subsequent remobilization of the associated debris avalanche deposit towards the SW.

Although the Cumbre Nueva detachment presents explicit evidence that the eastern and western flanks were mobile prior to the lateral collapse, the period of mobility and the net displacement distance prior to slope failure are undetermined. The steep and often unstable terrain is a major obstacle to fault-wide correlation. Radiometric facilities were not available to constrain the period of fault activity, while the hydrous metamorphosed and often heavily weathered fault rocks may not even be suitable for such an endeavour.

*An exhumed fault zone exists at Ayacata on Gran Canaria [*Perez-Torrado*, 1992].

***Subject background***

The magnitude and importance of mass wasting as a geomorphic process in the evolution of oceanic volcanoes first emerged from bathymetric studies around the islands and more numerous seamounts that form the Hawaiian-Emperor chain in the north Pacific Ocean [*Moore et al.,* 1989]. Since then, integrated swath bathymetry, coincident acoustic backscatter and seismic reflection surveys, together with onshore structural studies, have been used to systematically identify giant debris avalanche deposits dispersed around the submarine flanks of the island of Reunion in the Indian Ocean, [*Labuzuy* 1996], the Canary Islands [*Watts and Masson* 1995] Tahiti and other Society Islands [*Clouard et al.*, 2001], the Galapagos Islands [*Geist et al.*, 2002], and also in Island arc environments (e.g., Lihir, Papau New Guinea [*Peterson et al.,* 2002] and the Lesser Antilles [*Deplus et al.*, 2001]). It is well established that slope failures, both gigantic and piecemeal, are a process integrated into the very development of volcanoes in oceanic environments. The archetypal stratigraphic architecture of an oceanic/arc volcano should therefore comprise numerous unconformity-bound debris avalanche deposits and volcano-building lavas/volcaniclastics, interlaced with sheeted intrusions [e.g., *Schmincke and Sumita*, 1998; *Clague et al.*, 2002]. Dike swarms form the structural framework of most oceanic island volcanoes, supporting the structural/thermal development of intrusive complexes [e.g., *Walker,* 1992].

The density of sheeted intrusions becomes focused towards the centre of many oceanic volcanoes, extending laterally along high relief or topographically subdued rift zones that display a preferred alignment or clustering of emission centres {e.g., *Carracedo* 1994; *Cronin et al.*, 2001]. In the Hawaiian and Canary archipelagos' there is a demonstrated relationship between the orientations of rift zones and the positions of lateral collapse escarpments/active slumps at the junction of rift axes or at one side of a rift zone [*Delinger and Okubo*, 1995; *Carracedo*, 1996]. A prominent theme in the flank-tectonic behaviour of oceanic volcanoes is the relationship between dike injection and flank instability [*Swanson et al.*, 1976; *Iverson* 1996; *Voight and Ellsworth*, 1997; *Delaney et al.*, 1998]. The question often poised concerns the critical stage of flank instability and if the forceful injection of magma within a rift axis can promote instability over the length of the intrusion or the entire flank.

It is accepted that slope failures on volcanoes result from the conjunction of geological processes that operate throughout their constructional stages. In essence, the processes central to construction and deformation (e.g., eruptions, faulting, seismicity and continuous hydrothermal alteration), ultimately conspire to dismantle large parts of the edifice; a design flaw in a manner of speaking in the scheme of volcano evolution. The construction of oceanic island volcanoes upon kilometre-thick successions of volcanic breccia hyaloclastites, fragmented shoreline-crossing lavas and old debris avalanche deposits leads to the development of poorly supported and/or unstable flanks that can deform due to gravity, spreading laterally or collapsing catastrophically under their own weight [*Lipman et al.*, 2002; *Clague et al.*, 2002]. The cyclic scale of landslides is such that the larger cataclysmic events (between 1 and 1000 $km^3$) occur with less frequency than smaller events (<<1 $km^3$), such as localized rock slides and debris flows. Thc cycle of instability can recur around the same structural weaknesses and/or topographic features where landslides have developed in the past [e.g., *Belousov et al.*, 1999; *Tibaldi*, 2001, *Masson et al.,* 2002]. The morphological profiles of oceanic volcanoes are thus maintained by the coherence of erupted materials and by the load-bearing capacity of their substrates under numerous intrinsic and extrinsic stresses. Intrinsic stresses include the inertial forces due to gravity, volcanic eruptions and associated volcano-seismicity [*Voight and Ellsworth*, 1997 *Hurlimann* 1999]. Extrinsically induced stresses include the dynamic loading imposed due to rainfall, and the associated deviatoric stresses that arise due to excess pore fluid pressure [*Jimenéz and García Fernández*, 2000; *Cervelli et al.,* 2002].

Other seismic events related to regional tectonics may also fit into this category. The size, shape and volume of oceanic volcanoes are necessarily limited by these and other factors that include magma supply rates and pre-existing tectonic and morphological structures (fracture zones and detachments in the oceanic crust, pre-existing seamounts and the extent of lithospheric flexure).

A volcanic edifice will exert immense loading stresses on its foundations; the distributions of these stresses are controlled by structural and compositional anisotropies in the substrates. If deformable substrates are present at the interface between the edifice and its basement, then the volcano may undergo sector spreading in the direction of least resistance (from morphological barriers). Weak layers (particularly tephra and epiclastics), form an integral part of the subaerial stratigraphic architecture of volcanoes, hence the structural integrity can be compromised at numerous levels (e.g., bedding plane instabilities), not just in the underlying substrates. Gravitational or "volcanic spreading" is therefore a simple mass balance response to volcano growth that translates subsidence around volcano summits to outward horizontal displacements around the flanks and peripheries under evolving stress conditions [e.g., *Borgia*, 1994; *Borgia* et al. 2000; *van Wyk de Vries and Matela*, 1998]. The evidence from past landslides (e.g., Mombacho Volcano in Nicaragua and Socompa Volcano in Chile) suggests that in case-specific scenarios there is a cause and effect relationship between giant sector collapses that were preceded by stages of prolonged gravitational spreading focused on one sector [*van Wyk de Vries and Francis*, 1997; *van Wyk de Vries et al.*, 2001].

***La Palma***

The legacy of subaerial volcano instability on La Palma began with the partial destruction of Ancestral Taburiente at around 1.2 Ma [*Ancochea et al.*, 1994]. Although the collapse escarpment is completely buried by later volcanic successions, the proximal part of the associated debris avalanche breccias have been exhumed by the Cumbre Nueva lateral collapse. These well-consolidated volcaniclastics (the Tenerra Collapse Breccia) contain >30% vol juvenile pyroclastic materials, and they reveal important information as to the nature of the ancestral collapse and the syn-depositional rheology of the debris avalanche. It is posible that the collapse was initiated by a powerfull volcanic eruption, or the collapse itself un-roofed and decompressed the high-level magmatic system in a manner reminiscent of the Mt. St Helens eruption in 1980.

For the Caldera/Cumbre Nueva lateral collapse, the mechanism of slope failure is not deemed as being straight-forward, since slivers of the pre-slide western flank (or slump sector) survived the cataclysm. Additionally, the substantial relief below the detachment suggests that the detachment itself was merely exhumed by the lateral collapses, not initiated upon it. Criteria for the precise shape and location of the failure surface are lacking, as is knowledge regarding failure through intact rock versus failure along the detachment. A longitudinal sliver of the former mobile flank fronts a SW-striking dextral wrench fault, inferred to have facilitated rupture of the slump sector from the immobile northern part of the west flank. When failure was initiated, perhaps by an intrusion or by a period of intense rainfall, the shifting loads rapidly overstressed the west flank, producing a cascading or domino effect that culminated in the disintegration and south-westward translation of the flank into the ocean.

The third landslide affected the development of Bejenado volcano, a stratocone that develped within the structural confines of the Cumbre Nueva embayment. Although minor by comparisson with the antecedent landslide events, the Bejenado slope failure event demonstates the underlying principle of how slope failures on La Palma have been controlled by the geometry of previous collapse escarpments and by structures in the basement.

This is perhaps key to understanding the future of potential flank instability on the subaerial sector of Cumbre Vieja Volcano.

## Methodology

### 1. Stratigraphic profiling

A stratigraphic profiling convention, adapted from core logging schemes used in the mineral exploration industry, was used to graphically represent the target stratigraphy. The structure of a typical profile is shown in Fig.1 below.

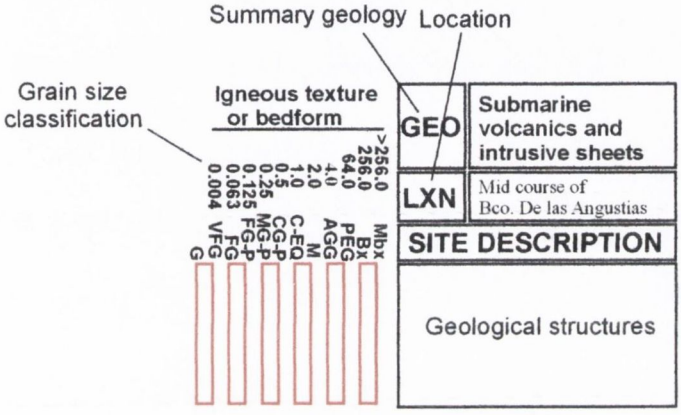


**Fig. 1.** Grain size scheme used in field logging. The abbreviations are as follows. G: glassy, VFG: very fine grain, FG: fine grain, FG-P: finegrain porphyritic, MG-P: medium grain porphyritic, C-EQ: coarse grain equigranular, M: mega-crystic, AGG: aggregate, PEG: Pegmatic, Bx: Breccia, Mbx: mega-breccia.

### 2. GIS data

Highly versatile GIS data, sourced from the *Spanish National Map Project*, were instrumental for the remote analysis of morphology and dimensions. The GIS data comprise the seven 5 m contour CAD drawings (produced by GRAFCAN) that make up La Palma, and three ASCII matrices of La Palma (4 m resolution), El Hierro (10 m resolution) and the Canary Archipelago (40 m resolution). The GIS data were used in volume calculations, scaled sectioning of the island slopes, slope mapping, spatial analyses, for assigning UTM coordinates, assigning heights and slope inclination values to distinctive geographic features, for distance measuring between islands and for contouring of slopes. Shaded relief images were generated using the 3D analyst extension in *Arcview (*version 3.2), most of which were processed on a SUN workstation at the Ivanhoe Mines Exploration office in Ulaanbaatar. Geo-referencing operations utilized *MAP INFO* version 7.

### 3. Remote sensed and aerial images

Aerial ortho-photographs (1:5000 and 1:50,000), aerial photographs (1:25,000) and digital elevation models (1m resolution) sourced from the *Spanish National Map*, were used in the production of geological maps. Earth orbit and Landsat images, shaded relief images and seismic section data of La Palma and other oceanic and continental volcanoes were downloaded from www.visibleearth.nasa.gov and https://zulu.ssc.nasa.gov/mrsid/

# GLOSSARY

| | |
|---|---|
| **Agglomerate** | Masses of volcanic fragments that may or may not be fused together by heat during the bodily motion and disintegration of active lavas, or by the accretion of air-fall pyroclasts. (synonymous with autobreccia) |
| **Asperity** | A protruding surface on a fault plane |
| **Cataclastite†** | Fault rock that is cohesive with a poorly developed or absent schistosity, or which is incohesive, chatacerized by generally angular porphyroclasts and lithic fragments in a finer graned matrix of similar composition. A preferred orientation of grains and fractures is noticable |
| **Epiclastic** | Refers to the remobilisation of mass wasted or eroded volcanic materials. |
| **Plexus** | i.e., intrusive plexus – a structurally complex region of intertwined sheeted intrusions with many individual dike/sill members, often interlacing and cross cutting. |
| **Toreva*** | A landslide block, formerly a stratigraphic segment of a volcano. |
| **Ultracataclastite†** | A cataclastite where the fine grained matrix forms >90% of the rock volume |
| **Volcanic spreading ©** | The gravity-driven cycle of extensional faulting of the summit and outward thrusting and shape change of volcano flanks due to loading, substratum deformation and the growth of intrusive complexes. |
| **Volcaniclastic** | Volcaniclastics encompass all volcanic particles regardless of the mode of fragmentation. Juvenile fragments can be important (accidental) components. |

**Francis et al.*, 1985
†*Brodie et al.*, 2002
© *Borgia*, 1994

# CHAPTER 1

# STRUCTURAL, STRATIGRAPHIC AND VOLCANOLOGICAL ASPECTS OF LA PALMA

# PROJECT LOCATION - LA PALMA

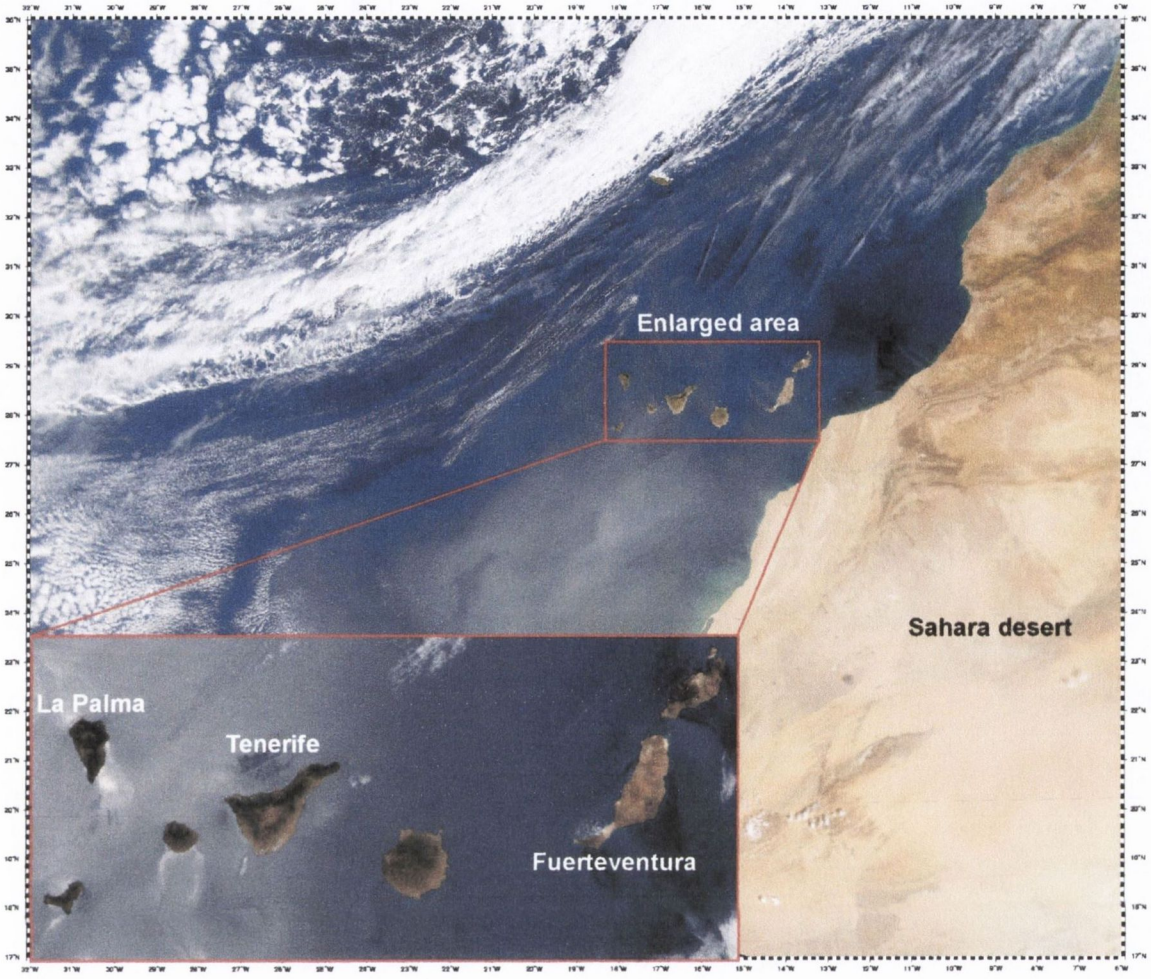


**Fig. 1.** Satellite images showing the proximity of the Canary Islands to continental west Africa. Prominent atmospheric features include a dust storm emanating from the western Sahara and a cloud front approaching Madeira. The enlarged area inset is part of a Landsat image of the archipelago. Images sourced from www.visibleearth.nasa.gov

*Location*

La Palma, one of the western Canary Islands, is located between longitudes 17°43'42" to 18°00'15"W, and latitudes 28° 25' 07" to 28° 51' 15" N, approximately 84 km from the northwest coast of Tenerife and opposite to the Atlas region of northern Morocco. The steep-sided island presents embayed western slopes scalloped by a gigantic collapse amphitheatre, the Caldera de Taburiente, at the former summit region. The highest elevation is on the rim of the Caldera at Roque de Los Muchachos (2426 m) where a cluster of manned astrophysical observatories has been in operation since 1985. The population of >90,000 is focused in the towns of Santa Cruz de La Palma, Los Llanos de Aridane, El Paso and San Andrés and is predominantly of mixed Cuban, Venezuelan, Spanish descent.

*Climate*

Because of the islands' substantial relief and its isolated position relative to the NE trades, there is significant climatic variation between the sub tropical coastal regions, transitional to sub-alpine (above 800 m) and semi-arid (characterized by low scrub vegetation) above 2100 m. The temperature range during summer months is between 11° and 33°C while the range in winter is between –2° to 24°C depending on altitude. Snow is not uncommon above 1700 m during winter (typically between December and early February), while winter cyclones and associated flash floods are occasionally severe.

**Fig. 1.1.1.** *Top left.* High oblique Shuttle image STS-047-085-092 - La Palma. Taken in September 1992. North is to the top right. Source: www.earth.jsc.nasa.gov. *Top right.* Hawaiian-Strombolian activity from the multi-vent Teneguia eruption of 1971 (Cumbre Vieja Volcano). Photo by Kalevi Kuha.

*Middle:* Panoramic image of the cloud-filled Caldera de Taburiente.

*Bottom left.* Front cover of El Dia, (Canarian newspaper) announcing the Teneguia eruption on November 26th 1971. *Bottom right.* Geologists and local officials at the San Juan eruption of 1949. Photo by Manuel Martel.

*Bio-sphere*

Large parts of La Palma are national park or prortected space, conserving cloud forests, the Caldera de Taburiente and its reliant fauna. The interior of the Caldera is heavily wooded with Canarian pine and, to a lesser extent, by beach and willow and by species of Mexican cactus. Bird, lizard and insect life is profuse.

### 1.1.1 The Canary Archipelago – regional tectonics

The Canary Islands are formed by a 450 km long chain of oceanic shield and composite strato-shield volcanoes, located in proximity to northern West Africa. They are among the numerous seamounts and elongate submarine ridges that characterize the abyssal morphology of the NE Atlantic region [*Romero Ruiz et al.*, 2000; *Krastel et al.*, 2001]. Age data for the constructional stages of each island generally increase along the chain with distance from westernmost island, El Hierro, consistent with an origin related to hot-spot activity [e.g., *Morgan*, 1983; *Carracedo et al.*, 1998; *Dañobeitia and Canales*, 2000]. The mantle plume is less productive and spatially more diffuse than the plume inferred to exist beneath Hawaii [*Hoenle and Schmincke*, 1993; *Abratis et al.*, 2002]. Some workers favour a genetic link between the formation of the Canary Archipelago and the Atlas Mountains Orogeny, through a system of seaward propagating fractures [*Araña and Ortiz*, 1991; *Anguita and Hernán*, 2000] (see section 1.3.4.2 for a more detailed discussion).

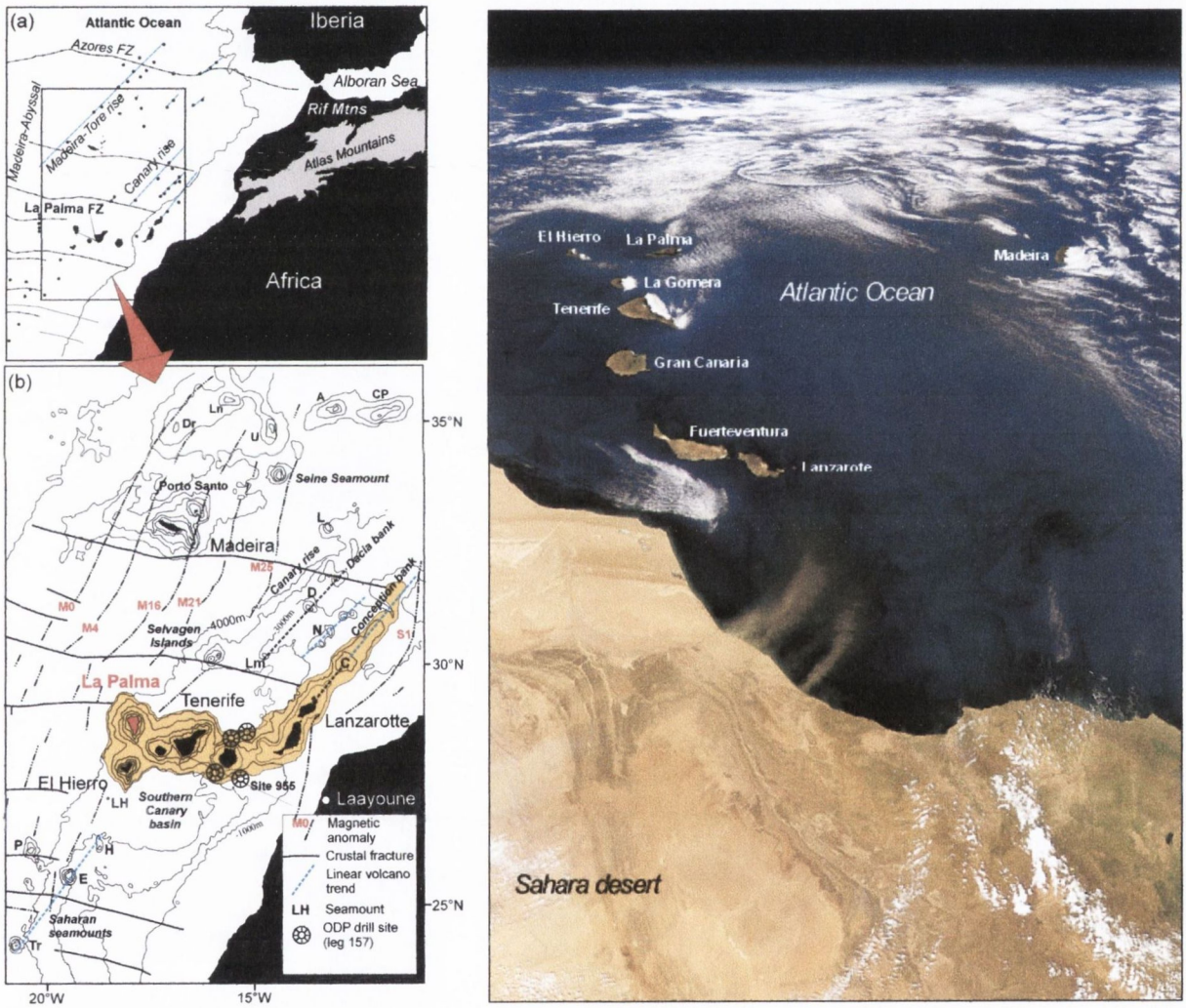


**Fig. 1.1.2.** (a) The regional tectonic framework of the Canary Islands showing the orientations of bathymetric ridges, the locations of individual submarine volcanic centres (dots) and the location of the Atlas Mountain Range (the 2000 m contour interval is plotted for the Atlas Mountains). (b) Close-up of the NE Atlantic with the tectonic trends and alignments of seamounts in the vicinity of the Canary Islands. The yellow shaded area is the apparent bathymetric rise or plume topography generated by the Canarian hot spot.

Seamounts are named as follows: A – Ampere, C- Conception, CP – Coral Patch, D – Dacia, Dr – Dragon, E – Endeavour, H – Hierro, L – Lars, LH – Las Hijas, Lm – Last minute, Ln – Lion, N – Nico, P – Paps group, T – Tropic, U - Unicorn Modified from *Ye et al.* [1998] and *Geldmacher et al.* [2000].

EV487-519990-80125-646. A view west from Earth orbit showing, in the foreground, the active fold belts associated with the Atlas Mountains Orogenic System, and, towards the horizon – the Canary Islands. The dust trails emanating from the Sahara are a source of sediments that exist in westward decreasing abundance in the stratigraphic architecture of the Canary Island volcanoes [e.g., *Schmincke and Sumita*, 1998; *Urgeles et al.*, 1998]. Image source: www.visibleearth.nasa.gov

The individual and coalescing volcanic centers rise between 3.4 and 4.4 km from the sea floor, with submarine slopes between 7° and 18° [*Urgeles et al.*, 1999; *Mitchell et al.*, 2002]. Tenerife, with a vertical extent of nearly 8km, is among the four largest volcano complexes on Earth [*Albay and Marti*, 2000].

The seven islands have evolved as contiguously overlapping or spatially separated edifices of rift zone and non-rift zone affinity [*Navarro and Farrujía*, 1989; *Ancochea et al.*, 2002]. The islands are founded upon an eastward thickening wedge of terrigenous and oceanic sediments that overlie or become transitional with oceanic crust of Jurassic age, between magnetic anomalies M25 (156 Ma) and S1 (170 Ma) [*Urgeles et al.*, 1998; *Dañobeitia and Canales*, 2000]. Thick sequences of clastic and carbonate sediment, exposed in the basal complex of Fuerteventura, record the early Jurassic stage of sea floor spreading [*Robertson and Stillman*, 1979; *Steiner et al.*, 1998]. The regional seafloor is transected by east-west orientated fracture systems, abyssal hills and plateau that extend from the Mid Atlantic Ridge [*Roest et al.*, 1992] (Fig.1.1.2.a).

The collapsed and heavily eroded remnants of the oldest shield volcanoes, dating from the Miocene, are preserved on the islands of Fuerteventura and Lanzarote that straddle the continental rise [e.g., *Stillman*, 1987, 1999]. These islands form the emergent southern part of a 500 km long NE-SW orientated bathymetric ridge, (named Conception bank), that merges onto the northern part of the Western Saharan petroleum-bearing province.

### 1.1.2 La Palma; contemporary studies

La Palma, as a site of geological investigation, has a history dating back to the 19th century to the works of *Von Buch*, [1825] and *Lyell*, [1855]. The level of academic interest on the geology of La Palma is well demonstrated with over 50 publications in the period 1998-2004, focusing on geochemistry, palaeomagnetism, flank instability and overall structural evolution. The shaded relief and Landsat-7 images in Fig. 1.1.3 illustrate the morphological structure and the distinct variations in the intensity of erosion between the extinct strato-shield 'Taburiente' forming the northern part of the island and the active rift-centered edifice 'Cumbre Vieja' in the south. The false colour infra red Landsat-7 scene accentuates the contrast in vegetation cover as a function of elevation.

The island is constructed of alkali basalt lava flows, cinder and tuff cone-forming pyroclasts and associated epiclastics, the petrochemical compositions of which vary from basanites to tephrites with lesser amounts of differentiated lava, for example trachytes and phonolites (the later occurring at higher elevations) [*Nikogossian et al.*, 2001; *Carracedo et al.*, 2001; *Abratis et al.*, 2002]. Taburiente Volcano is the oldest and largest of the three overlapping Pleistocene edifices in the north of La Palma, which are founded upon an uplifted Pliocene seamount (Fig. 1.1.5a) [*Staudigel et al., 1986*; *Navarro and Coello*, 1993]. A prominent discordance separates the subaerial and submarine sequences, with two distinct volcano tectonic sequences in between [*Roa*, 2002; 2003] (Ch. 2 this work). The unroofed seamount/intrusive core complex is exposed within the northern part of the Cumbre Nueva embayment and from within the adjoining Caldera de Taburiente [e.g., *Staudigel and Schmincke*, 1984; *Schiffman and Staudigel*, 1994]. These structures form a continuous escarpment, 45 km in perimeter that is enveloped at its southern end by the recently active Cumbre Vieja Volcano.

The Caldera de Taburiente marks the morphological center of northern La Palma, a 6 km wide, amphitheatre-shaped depression, floored with deep narrow canyons and sharp ridges. The surrounding escarpments add to the topographic relief (maximum - 1.5 km) and offer exceptional views of the stratigraphy of a Canarian volcano. The Caldera is drained to the SW by a deep canyon (or *Barranco or Bco.* in Spanish) - the Bco. De Las Angustias. The walls of the canyon expose the oldest rocks on La Palma (between 4.0 and 2.9 Ma [*Staudigel et al.*, 1986]), comprising tilted, faulted and eroded hydrous metamorphosed pillow lavas (Fig. 1.1.5b,c) and hyaloclastites with interspersed sheeted intrusions.

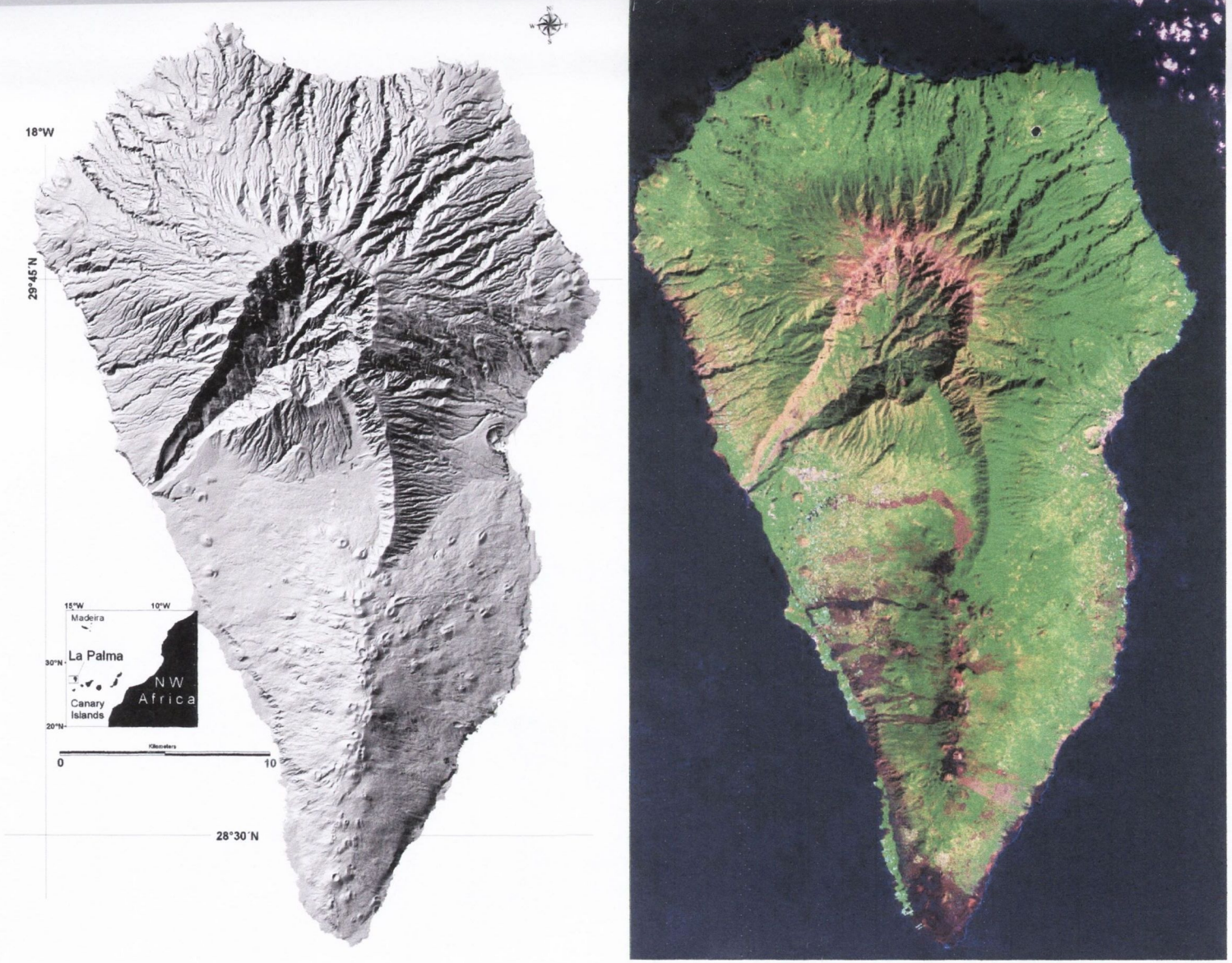


**Fig. 1.1.3**. Left. Shaded relief image of La Palma. Source: *Spanish National Map Project*. Right: Landsat-7 image of La Palma (2000). Source: https://zulu.ssc.nasa.gov/mrsid/

*Fernandez et al.* [2002] present kinematic data for normal faults penetrating the basement and Ancestral Taburiente volcanic successions.

The stratigraphic nomenclature and structural subdivisions of La Palma have evolved significantly since the first radiometric data were published [*Abdel Monem et al.*, 1971] (see appendix 1). The geological map with scaled cross sections (Fig. 1.1.4) illustrates the principal geological units. The Pleistocene subaerial volcanic activity, forming the northern part of the island, is separated into at least three constructional stages, each one climaxing with voluminous flank collapses listed as follows: (1) Ancestral Taburiente or Taburiente-1*, (2) Taburiente/Cumbre Nueva, and (3) Bejenado volcano [*Navarro and Coello*, 1993; *Ancochea et al.*, 1994; *Roa*, 2003]. Construction of the ancestral edifice began at around 1.77 Ma, reaching an elevation above sea level of between 2500 and 3000 m and culminating in giant southward-directed flank collapses at around 1.2 Ma [*Carracedo et al.*, 2001a,b]. The southward direction of failure is confirmed by the shape of the discordance between the ancestral edifice and the overlying Taburiente Volcano [*Coello*, 1987; *Ancochea et al.,* 1994].

Thick sequences of volcaniclastics and intercalated pyroclasts are found at the base of the Caldera/Cumbre Nueva escarpment, overlying most of the observable part of the discordance. From previous sub-crop and outcrop studies these deposits have been generically classified as "agglomerates (*agglomerados* in Spanish)" [*Gastesi et al.*, 1966; *Hernández-Pacheco and De la Nuez*, 1983; *Bravo and Coello*, 1984; *Coello,* 1987; *Navarro and Coello*, 1993]. In their evaluation, *Ancochea et al.* [1994] imply that these agglomerates are in fact the remains of subaerial debris avalanche breccias, sourced by the partial collapse of the ancestral edifice. Vestiges of this edifice are visible as erosional inliers along the deep canyons on the upper slopes of northern La Palma [*Navarro and Coello,* 1993] and from the array of water capture tunnels (galerías) that penetrate the interior stratigraphy of the island [*Bravo and Coello*, 1979; *Coello*, 1987] (Fig. 1.1.4).

Following the partial collapse of Ancestral Taburiente, the emplacement of collapse-filling lavas resumed without hiatus, forming Taburiente Volcano [*Carracedo et al.*, 2001a; *Guillou et al.*, 2001]. The new edifice enlarged and subsequently enveloped Ancestral Taburiente. Most workers are in agreement that at around 0.8 Ma volcanism on La Palma migrated southwards toward the construction of a rift-centred edifice called 'the Cumbre Nueva Volcano [*Ancochea et al.,* 1994], while rift-related volcanism persisted on the slopes of Taburiente, [*Guillou et al.,* 1998; *Carracedo et al.*, 1999].

The latter stages of the development of Taburiente Volcano were characterised by increased levels of phonolitic volcanism from a steepening central cone [*Carracedo et al.*, 2001]. The over-development of Cumbre Nueva (with Cumbre Nueva overlapping the southern part of Taburiente), culminated at around 0.55 Ma with the lateral collapse of the west flank towards the southwest [*Ancochea et al.*, 1994; *Guillou et al.*, 2001]. *Hildenbrand et al.* [2003] suggest that the collapse may have been influenced by persistent uplifting of the seamount and by a N-S orientated fault they infer to exist in the basement. Using analogue gelatine models, *Walter and Troll* [2003] "*conjecture*" that the southward migration of the Cumbre Nueva rift was "*a consequence of the unstable and creeping southwestern volcano sector, with the sequence above the SW-tilted seamount forming the detachment*". Field evidence of detachment was reported at this level by *Roa* [2002], following the discovery of an exhumed decollement in 1998 (*Roa* [2003], Ch's. 2.2 and 2.3 this work).

Post-Cumbre Nueva volcanism was centred on the construction of an intra-collapse stratocone (Bejenado volcano) while residual rift zone volcanism continued on the flanks of Taburiente [*Guillou et al.,* 2001; *Carracedo et al.*, 2001]. After destabilizing upon the debris avalanche breccias of the Cumbre Nueva collapse (forming the edifice substrate), the north flank and summit of Bejenado collapsed northward into the confines of the Caldera de Taburiente and adjoining Cumbre Nueva escarpment. Dismantled segments of the former Bejenado edifice (toreva remnants) remain inside the Caldera [*Roa*, 2003].

*The convention adopted by *Navarro and Coello,* [1993].

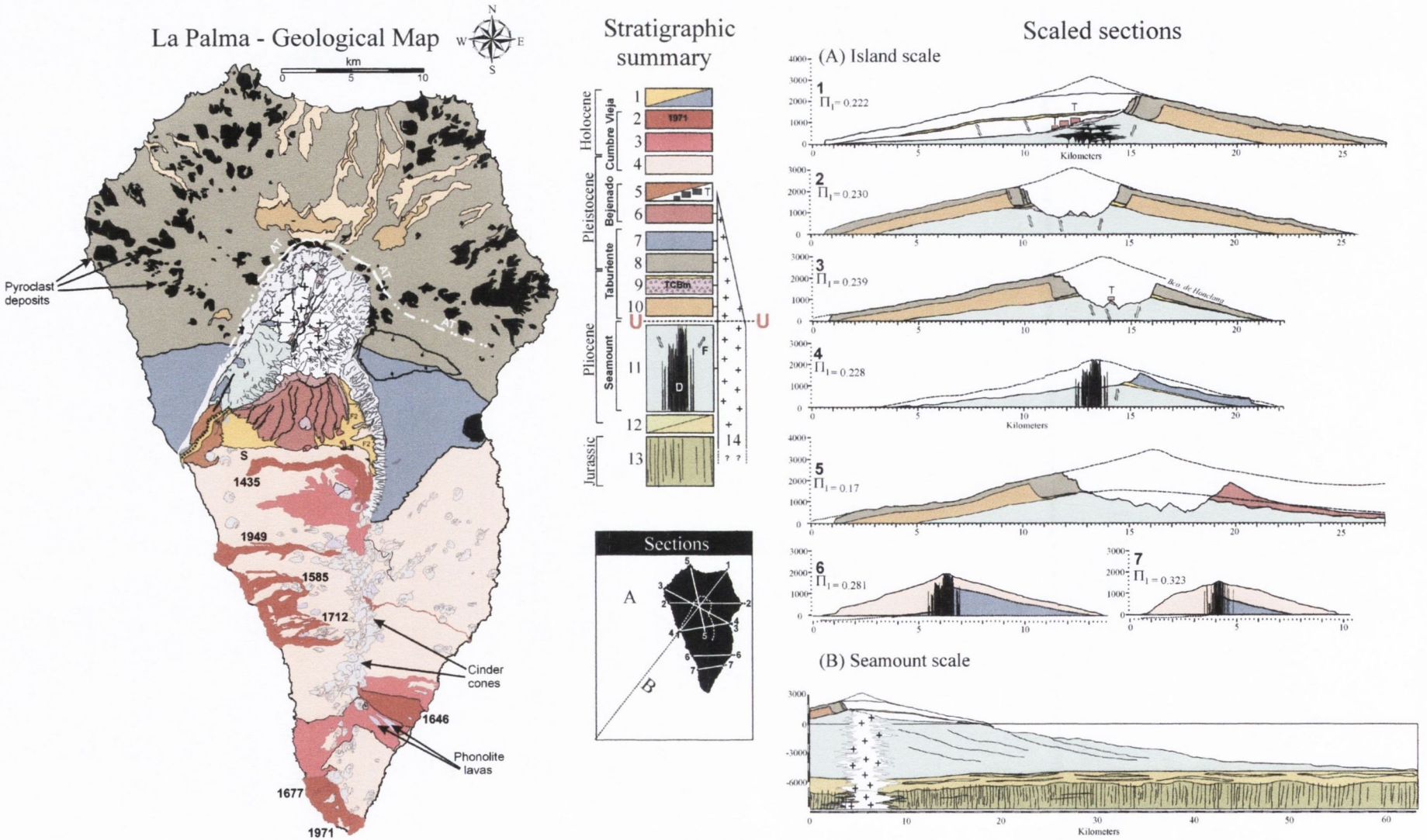


**Figure 1.1.4**. Geologic map and scaled sections of La Palma. Stippled lines mark the reconstructed topography. Abbreviation U: unconformity? (the subject of chapter 2.2). 1. Recent alluvials and rock avalanche deposits, 2. Historic lavas, 3. Sub-historic lavas, 4. Pleistocene/Holocene lavas and pyroclasts, 5. El Time volcaniclastics, 6. Bejenado lavas and pyroclasts, 7. Cumbre Nueva lavas, 8. Taburiente lavas, 9. Tenerra Collapse Breccia, 10. Ancestral Taburiente lavas and pyroclasts, 11. Seamount series lavas/hyaloclastites and debris avalanche breccias, 12. Pelagic/hemipelagic sediments and island-derived volcaniclastics, 13. Oceanic crust, 14. Intrusive complex. Data compiled from *Navarro and Coello* [1993], *Ancochea et al.* [1994], *Urgeles et al.* [1998; 1999], *Schmincke and Sumita,* [1998], *Wynn et al.* [2000], *Carracedo et al.* [2001] and *Roa*, [2002; 2003]. Abbreviations: D. dikes, F. Faults. T- toreva remnant, $\Pi_1$, aspect ratios.

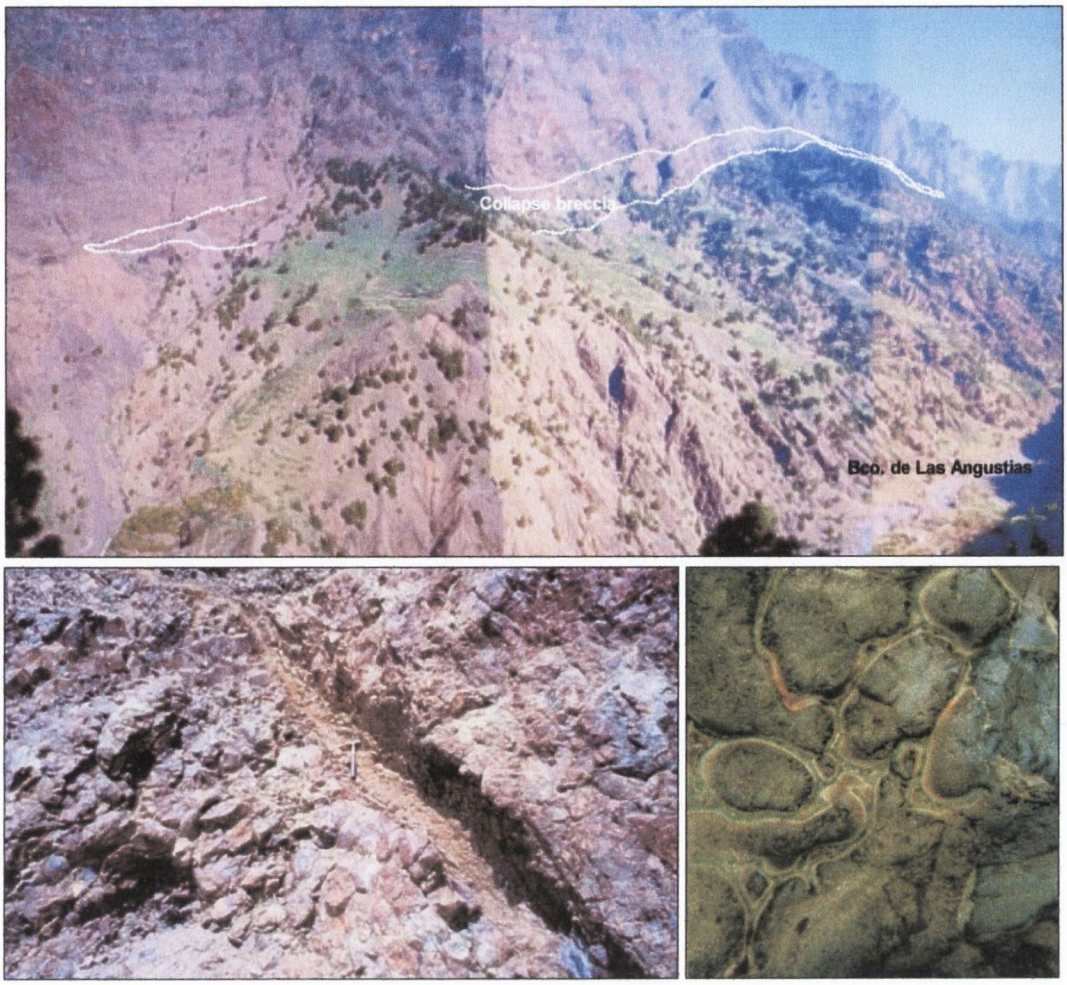


**Fig. 1.1.5.** *Top.* Photomosaic of the Pliocene Seamount Series and shield volcanics. The subaerial collapse breccias (agglomerados) overly what has been interpreted through contemporary studies as an uplift unconformity. *Left.* Steeply dipping fault zone striking 274° penetrating the seamount series. The ferric/chlotitic granular gouge is between 0.05 to 0.34 thick. Location: Hacienda del Cura. Right. Digitizing pillow lavas with enriched intersticial chlorite and epidote. Location: Bco. de Las Angustias.

The most productive (shield stage) volcanic activity on northern La Palma ceased shortly after 0.4 Ma [*Guillou et al.*, 2001]* although evidence of residual volcanism is preserved from youthful, often partially remobilized scoria deposits and occasional clasto-genic lavas flows exposed within the Caldera and Cumbre Nueva embayment.

The oldest rocks on the currently active southern part of the island (Cumbre Vieja Volcano) are dated at around 0.125 Ma [*Guillou et al.,* 1998]. Following the destruction of the Cumbre Nueva rift and the adjacent west flank, Cumbre Vieja Volcano (Fig. 1.1.6) developed along the contours of the headwall escarpment, enveloping the southern segment of the Cumbre Nueva embayment [*Carracedo et al.*, 1997; 1999a,b; *Day et al.*, 1999]. Historically infrequent eruptive activity has been focused along the north-south striking axial rift zone of Cumbre Vieja; the last two eruptions were in 1949 and 1971.

* The youngest rocks dated from northern La Palma are 410±80 ka [*Guillou et al.,* 2001].

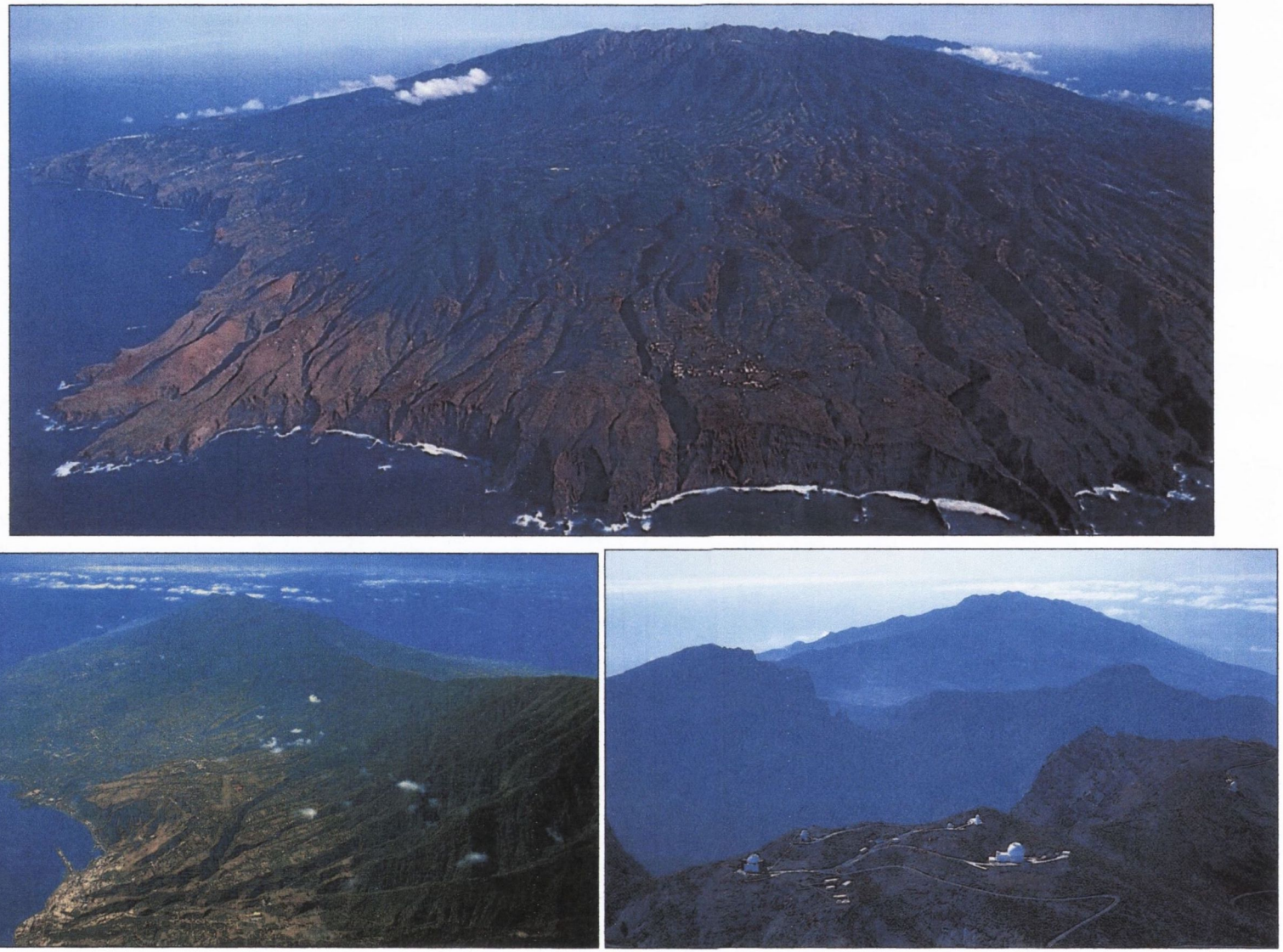

Fig. 1.1.6. *Top.* The north coast of La Palma between Barlovento with a view across the heavily vegetated canyon terrain towards the decapitated summit region of Taburiente Volcano. The locally protruding sea cliffs are up to 200 m high (just below the village of Garafia). *Left.* The southern part pf La Palma, showing the arcuate segment of the Cumbre Nueva escarpment and Cumbre Vieja Volcano. *Right*. View to the south from the highest point (2426 m) on the rim of the Caldera de Taburiente with the astrophysical observatories at Roque de Los Muchachos in the foreground. Photos by Juan Jose Santos.

The first side-scanning sonar surveys were conducted in 1997, with emphasis on the western submarine slopes of La Palma. These and subsequent studies revealed expansive debris avalanche deposits extending west and east of the island [*Urgeles et al.*, 1999]. Studies of multi-beam bathymetry and its derivative back-scatter intensity have been used in correlation with seismic reflection data to define the distributions and amounts of sediment cover, hence the relative age of each debris avalanche deposit [*Urgeles et al.*, 1999; *Masson et al.*, 2002]. These authors delineate an amalgamation of old landslide units on the western submarine slopes, designated collectively as the Playa de la Veta Avalanche Complex (Figure 1.1.7). Overlying this is a large debris avalanche lobe emanating from the Caldera/Cumbre Nueva collapse headwall, referred to as the Cumbre Nueva debris avalanche deposit [*Urgeles et al.*, 1999]. A less distinct debris avalanche lobe, referred to as the Santa Cruz debris avalanche, emanates from the eastern part of La Palma [*Masson et al.*, 2002]. A detailed review of the criteria used in constraining the dimensions of these landslides, the source regions and relative ages is presented in Ch. 3.1.

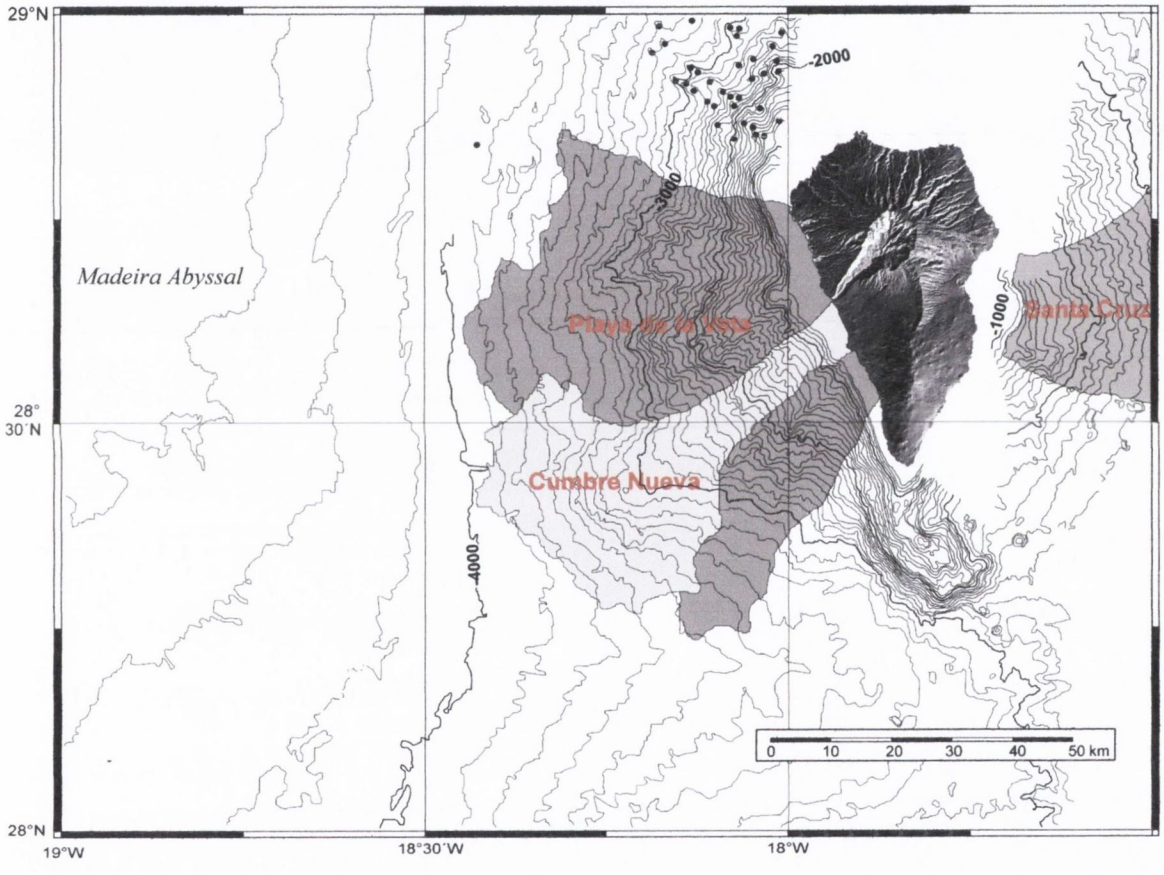


**Fig. 1.1.7.** Debris avalanche deposits and their inferred source regions, as interpreted by *Urgeles et al.* [1999] and *Masson et al.* [2002]. The dots in the to the northeast of La Palma are aligned vents.

# 1.2 The Caldera de Taburiente
# Structure and Origin of a Collapse Amphitheatre

The morphology of the Caldera de Taburiente can be linked to the collapse of the summit region of Taburiente Volcano during or shortly after the Cumbre Nueva lateral collapse. Modifications to its morphology by fluvial erosion, undercutting and piecemeal collapses have, among other structural processes resulted in the deeply dissected relief and unstable intra-Caldera escarpments.

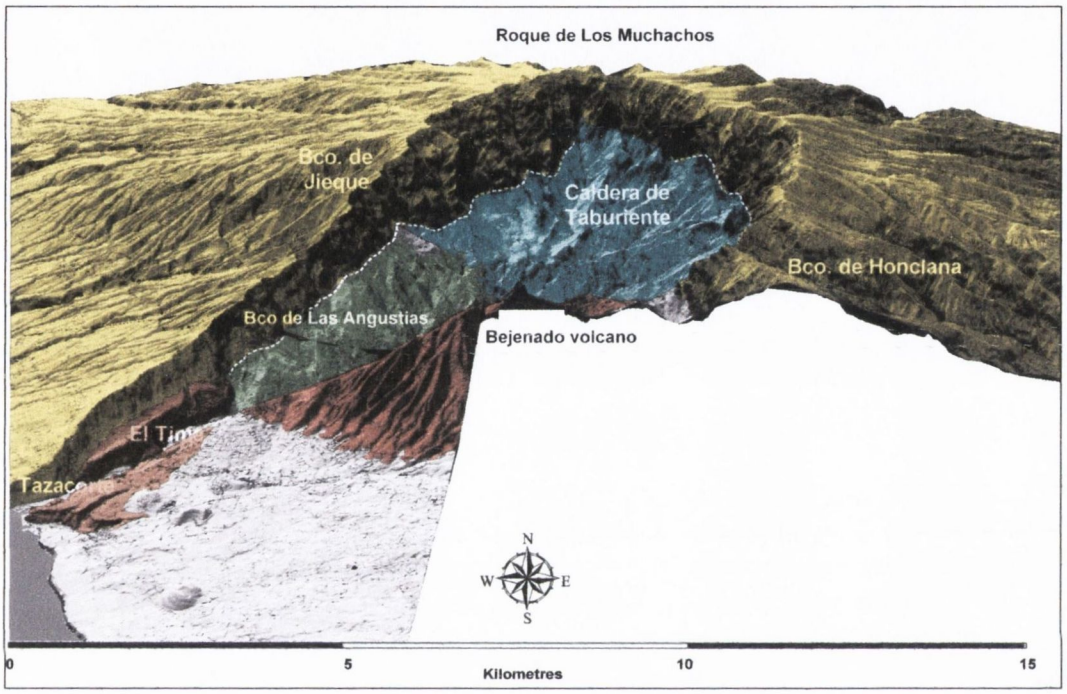


**Fig. 1.2.1.** Cutaway low oblique shaded relief image looking north at the Quaternary collapse escarpments of Taburiente volcano. The stippled lines mark the extent of the detachment fault discussed in Ch. 2.2. Light green shade represents exposed seamount rocks. Blue shading within the Caldera represents the intrusive core.

## 1.2.1 Introduction

Dominating the morphology of La Palma, the Caldera de Taburiente is a giant amphitheatre-shaped depression located in the north central part of the island. This section presents structural, morphological and geological observations from the subvertical walls of the Caldera and the heavily eroded basement rocks. The headwalls exhibit a complex stratigraphic architecture, consisting of myriad pyroclastic deposits, stacks of disjointed sub-horizontal lava flows and occasional laccolith-shaped bodies, all of which are cross-cut by interlacing dikes. The canyons leading to the interior of the Caldera expose a complex of sheeted intrusions consisting of many thousands of dikes and sills that cross-cut gabbro-pyroxenite stocks. A thick mélange of volcaniclastic deposits, with interspersed dikes, is exposed at the upper parts of the canyon walls. These deposits were emplaced by gigantic flank collapses that partially dismantled the Pliocene seamount and the subaerial edifice. This section also introduces the geological context of the tectonic units described in chapter 2 and explores the origin of the Caldera in relation to the Cumbre Nueva escarpment. Interpretations of its origin revolve around a hypothesis of gradual fluvial erosion and undercutting [*Lyell*, 1885; *Middlemost*, 1971; *Carracedo et al.*, 2001; *Hildenbrand et al.*, 2003], although giant collapses have also been proposed [*Ancochea et al.*, 1994]. An advancement of the latter hypothesis is put forth here.

### 1.2.2 The Caldera/Cumbre Nueva embayment – access and physiography.

The Caldera de Taburiente, from which the word 'caldera' is eponymous, forms a large central depression in the northern part of La Palma. The 'Caldera', as it is known locally, is open to the southwest and is over 6 km across and nearly 1.6 km deep. The remote interior of the Caldera is accessed from the town of Los Llanos de Aridane from where a paved road leads on to a dirt track (parts of which are sealed) that traverses the main canyon draining the Caldera to the SW - the Barranco de Las Angustias. The dirt track ends at the overlook at Los Brecitos from where a 3 km long trail descends onto the gravel and boulder beds at Playa de Taburiente, the relative centrepoint of the Caldera. From this point (elevation ~750-m amsl) the enclosing amphitheatre headwalls encompass an area of 28.3 km$^2$. These geomorphologic limits roughly coincide with the geographic limits of the national park above Dos Aguas. The localities of Tenerra and La Cumbrecita mark both sides of the amphitheatre opening where it coalesces with the Cumbre Nueva escarpment. To the south of the Caldera the dismantled north flank of Bejenado Volcano (Fig. 1.2.4) forms a topographic barrier to the basin-shaped drainage system sourced by the Caldera. The orthophoto in Fig 1.2.2 shows these physiographic features and the municipal access routes to the study area. The rim of the Caldera, which is 14.6 km in circumference, reaches its highest point at the degraded scoria cone of Roque de Los Muchachos (2426 m). It is one of many truncated scoria cones found along the amphitheatre rim (e.g., Pico de La Cruz (2351 m), Piedra Llana (2321 m) and Roque Palmero (2310 m)). A second access route by a paved road from the south, near the town of El Paso, leads to La Cumbrecita. From here the trail leading to Playa de Taburiente is longer and is often made impassable by frequent rock-slides, steep slopes and seasonally heavy rain. Steep-sided ridges, up to 3 km in length, some in a state of partial collapse, rise from the amphitheatre floor and extend upwards towards the headwalls at angles typically between 2° and 5°, steepening sharply (to 30°) below the headwalls. The ramp-like profile of these ridges contributes to the cuspate geometry of the Caldera's floor.

The Caldera contains the only permanently active catchment area in the Canary Islands; sourced from the narrow hanging canyons that dissect the amphitheatre escarpments. Precipitous waterfalls (e.g. *Cascada de la Desfondada* and *Verduras Afonso*) cascade from these hanging canyons into the chasms on the amphitheatre floor. Over seventy 4$^{th}$ order gullies and hanging canyons incise the Caldera's rim, feeding into the longer 3$^{rd}$ order canyons such as Bco. de los Cantos (3.06 km), Bco. Verduras Afonso (1.2 km) and Bco. del Diablo (2.5 km). These in turn drain into the two 2$^{nd}$ order canyons - Bco. de Taburiente (3.8 km) and Bco. Almendro Amargo (4.3 km), both of which merge at Dos Aguas. This locality marks the beginning of the Bco. de las Angustias, a SW-striking canyon that drains out over a distance of 9.6 km into the Atlantic at Puerto de Tazacorte. The flow regime of the Angustias catchment area has been heavily depleted since the construction of numerous galerías and channels at the turn of the 19$^{th}$ century (used to irrigate the islands plantations). The galerías are generally excavated in the footwall of the Cumbre Nueva detachment fault (Ch. 2.2) and they extend as a radiating network for up to 2 km in diameter. The aquifers that the galerías exploit are among the most productive in the Canaries, producing between 75 and 172 m$^3$/h [*Bravo and Coello*, 1979]. They are sustained hydrologically by the interface of rain clouds with the high volcano slopes (orographic precipitation), and by severe seasonal flash floods. Annual precipitation rates within the Caldera have been measured between 629 and 850 mm/yr [*Bravo and Coello*, 1979]. Fig. 1.2.5 is a 3D Geographic Information System rendering of the Caldera that illustrates the configuration of the drainage system and the symmetric cuspate shape it preserves.

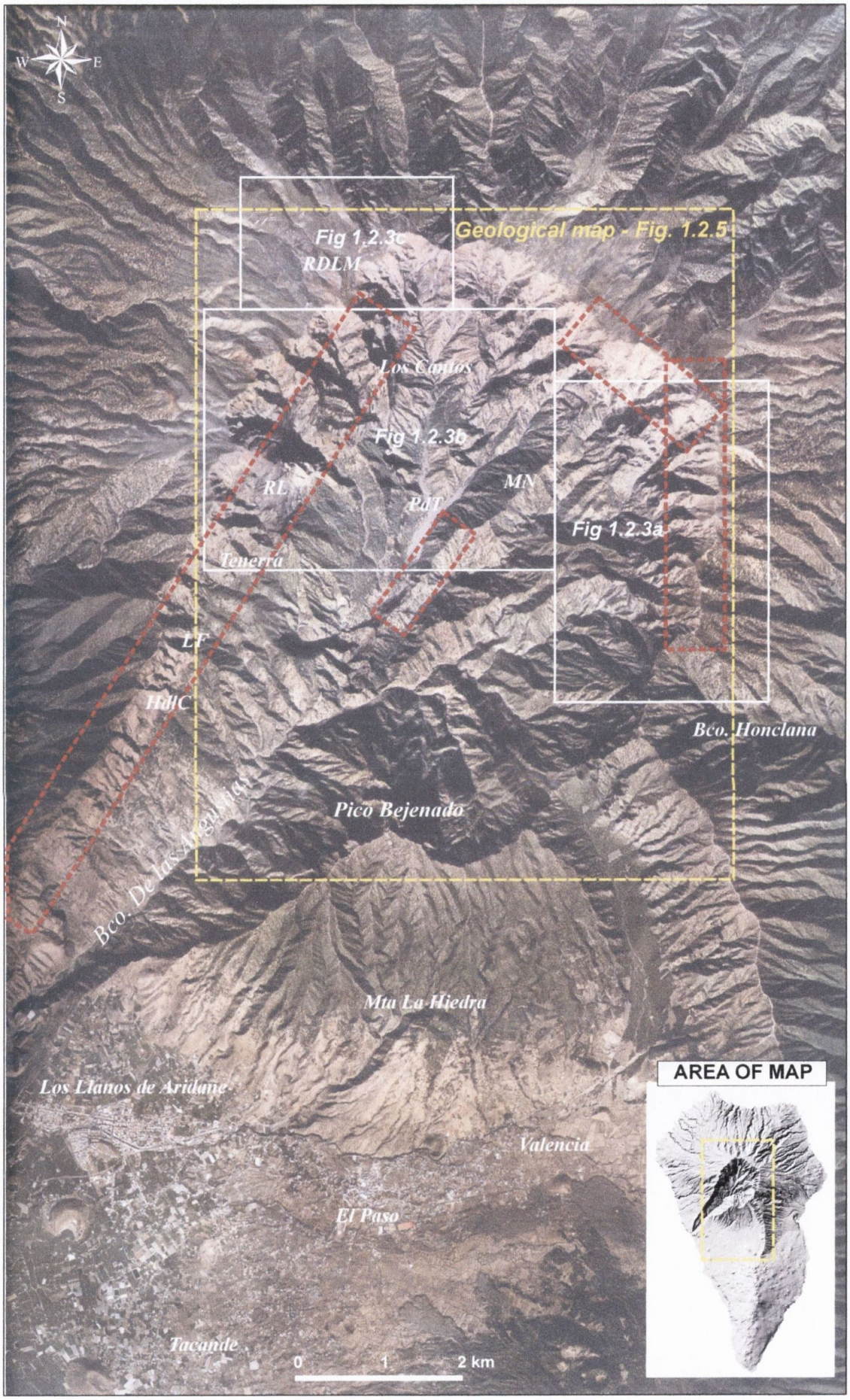


**Fig. 1.2.2**. Orthophotographic image of the study area in northern La Palma taken in November 1998. Stippled red rectangles represent the main areas of interest. Abbreviations: HdlC – Hacienda Del Cura, LF – La Farola, RL – Risco Liso, PdT – Playa de Taburiente, MN – Morro Negro, MN – Morro Negro. Image source - GRAFCAN 2001.

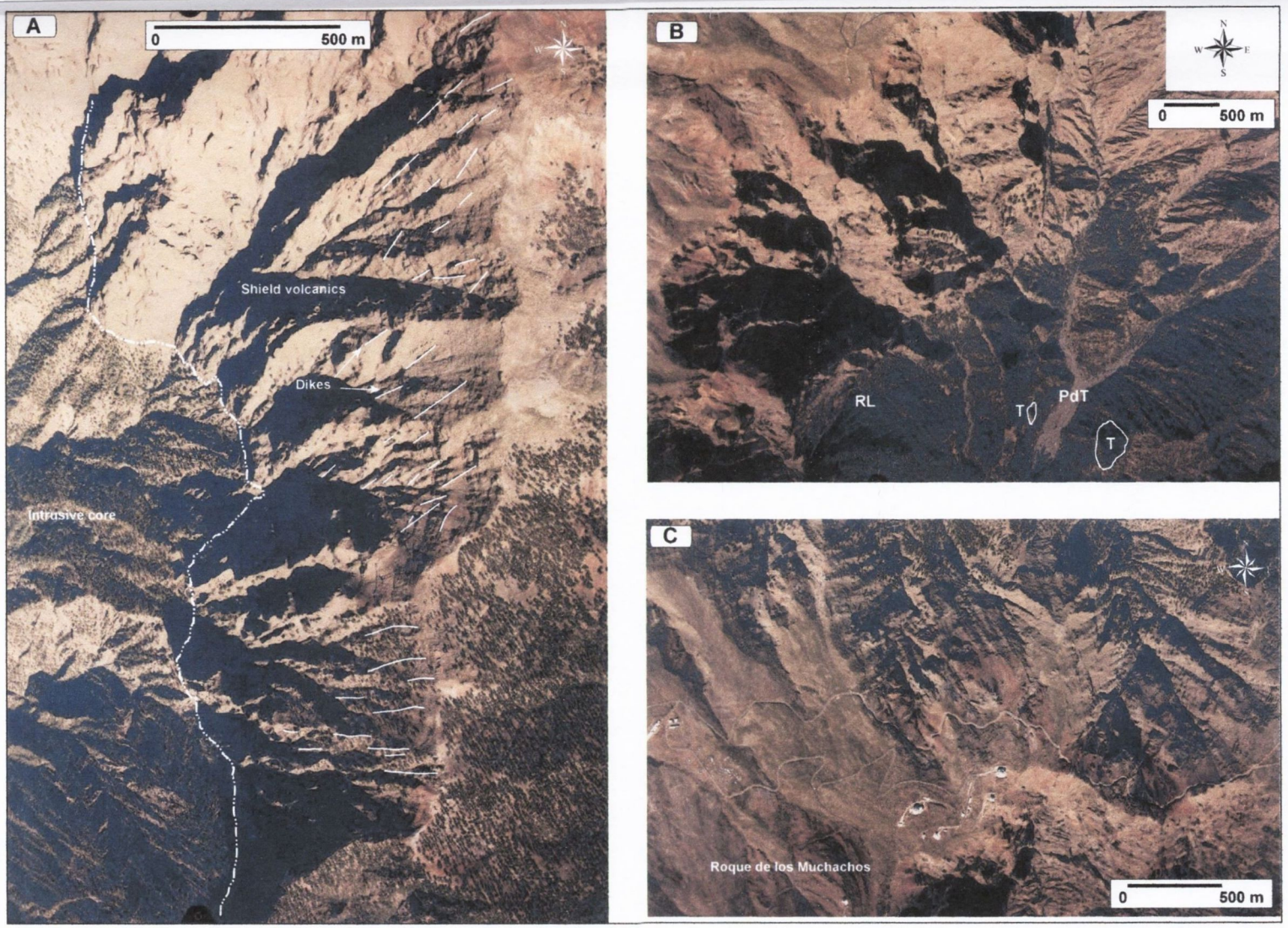


**Fig. 1.2.3.** A Section of the ABZ at La Cumbrecita with the discordance marked in white stipple. Stacked lava flows can be distinguished in the uppermost amphitheater walls while major benches, prominences and scarps extend outwards by to 1.4 km into the amphitheatre. Rust-colored tones on the amphitheatre rim are the remains of degraded scoria cones. B: A section of the ABZ along the NE wall of the Caldera from Risco Liso (RL) toward Bco. de Los Cantos. Toreva remnants abbreviated T. PdT is Playa de Taburiente. The north fork of Playa de Taburiente leads up to Bco. de Los Cantos (see text). C: The Caldera wall at Roque de Los Muchachos. The astrophysical observatory domes give scale to this part of the Caldera rim. Source - Spanish Geological Map Project.

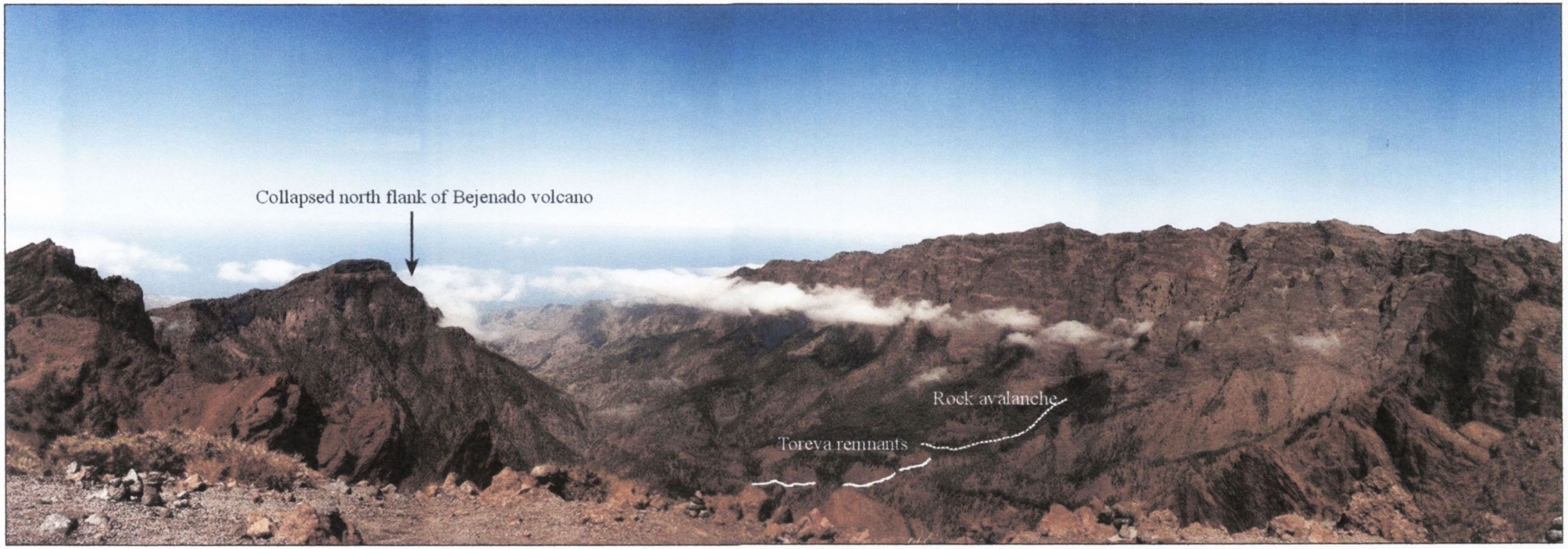


**Fig. 1.2.4.** Panoramic photo-mosaic looking west and north west from Pico de Las Nieves across the Caldera/Cumbre Nueva escarpment. The collapsed north flank of Bejenado volcano and the toreva remnants/rock avalanche deposits are discussed elsewhere [see *Roa*, 2003]. Basal slip surfaces of toreva remnants represented by solid white line.

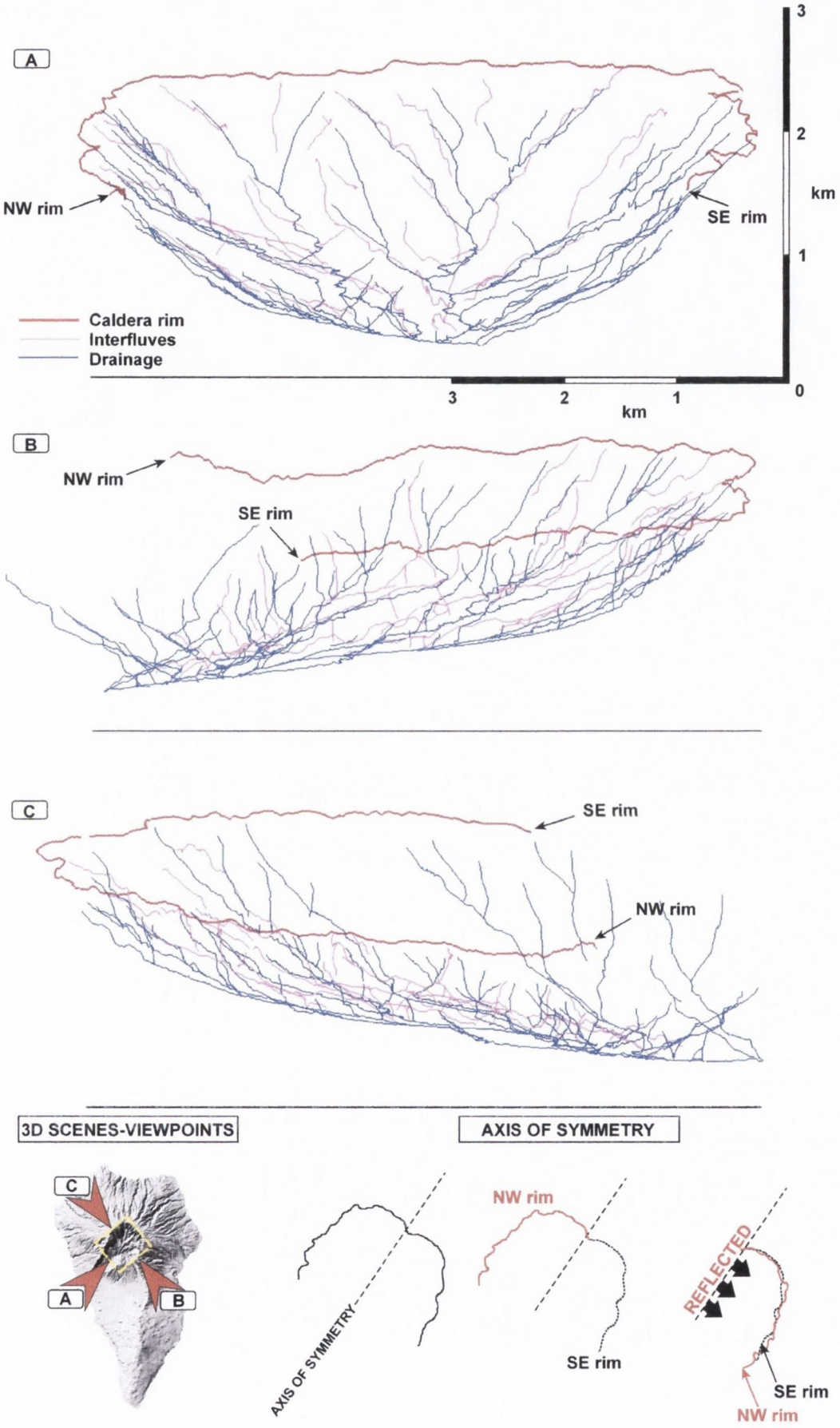


**Fig. 1.2.5**. 3D scenes showing the relief and basin-shaped morphology of the Caldera and its axis of symmetry. The scenes were created using the 3D Analyst extension in Arcview version 3.2

### 1.2.3 Geological map

The geological map in Fig. 1.2.6 was compiled from 1:5000 colour ortho-photographs, 1:25,000 colour aerial photographs (e.g., Fig. 1.2.3) and GIS data. These data were supplemented by scan-line surveys and selective geological mapping at 1:5000 scale inside the Caldera. The amphitheatre walls are, for the most part inaccessible, as is the eastern half of the amphitheatre floor (east of the toreva remnants (see *Roa*, [2003]).

The swarms of sheeted intrusion that transect the amphitheatre walls were traced from ortho-photos and colour aerials. Benches, scarps and topographic prominences were mapped only from GIS data due to the shadow effects from aerial images. Spatially extensive boulder deposits (herein referred to as boulder trains) and slabs (10's of meters across) are ubiquitous throughout the amphitheatre and the embayment (see Ch. 2.1). They are composed of dislodged hangingwall breccia materials (TCB) derived from the base of the Caldera/Cumbre Nueva embayment wall. Although they are far too numerous to log individually, the positions of some of the larger blocks/slabs were fixed with a GPS receiver (see BT in Fig. 1.2.6).

It is important to note that the transition between the seamount series extrusives and the intrusive core occurs over a 1 to 2 km interval, hence the mapping of a distinct transition zone (shaded zone marked T in the geological map).

### 1.2.4 The amphitheatre headwalls

The 700 to 950-m high amphitheatre walls form the highest part of the continuous Cumbre Nueva/Caldera de Taburiente escarpment. The amphitheatre rim (Fig.1.2.8a) is incised by gullies and v-shaped bluffs that penetrate into the flanking canyon terrain, and are widest on the upper flanks. The kilometre high amphitheatre walls expose the archetypal stratigraphic architecture of a Canarian shield volcano (Fig. 1.2.9c), typified by stacked tube-fed sequences of disjointed pahoehoe and a'a lava and truncated pyroclastic deposits between 1 and 200 m thick, all meshed together by interlacing dikes (Figs 1.2.8a,b). Individual lava flows are laterally continuous with a shallow-dip (2°-7°) away from the Caldera's centre. The dikes are emplaced along sinuous and linear trajectories, diffusing out from the centre of the intrusive core, while laccolith-shaped bodies up to 40-m thick occur locally in the Caldera wall stratigraphy. Lava flows (typically sheet flow pahoehoe and stacked a'a) occur with most frequency on the lower slopes while pyroclastic horizons are more predominant in the central part of the volcano along the upper slopes.

The vertical continuity of the precipitous amphitheatre walls is disrupted by discontinuous scarps, benches, terraces and steep talus slopes that feed onto large piedmont deposits. These prominent benches extend the amphitheatre walls outwards by up to 1.6 km, with vertical drops in the order of 100 to 700 m along the scarp faces. Parts of the benches extend into the Caldera along sharp eroded ridges (e.g., *Roque de la Fortaleza*) that separate deep, narrow ravines feeding into the Caldera (Fig. 1.2.9b). The prominences terminate along the marked slope break between the shield volcanics and Pliocene basement. The aerial images in Fig. 1.2.3 illustrate the width of this zone of benches, scarps and prominences herein referred to as the 'amphitheatre bench zone' or ABZ. The subvertical scarp faces locally display smoothened surfaces (e.g., *Risco Liso*, *Pared de Roberto*) in comparison to other sections of the headwall displaying irregular relief. The headwalls locally display indentations and small embayments formed by piecemeal collapses and continuous foundering, revealing unweathered volcanic successions (Fig. 1.2.7). Volcaniclastic deposits, up to 200 m thick (e.g. Roque de la Viña, extend up to 1 km outward from the amphitheatre walls. They have accumulated below conspicuous source indentations and have been previously interpreted as rock avalanche deposits [*Navarro and Coello*, 1993]. These deposits have been further dissected by fluvial erosion.

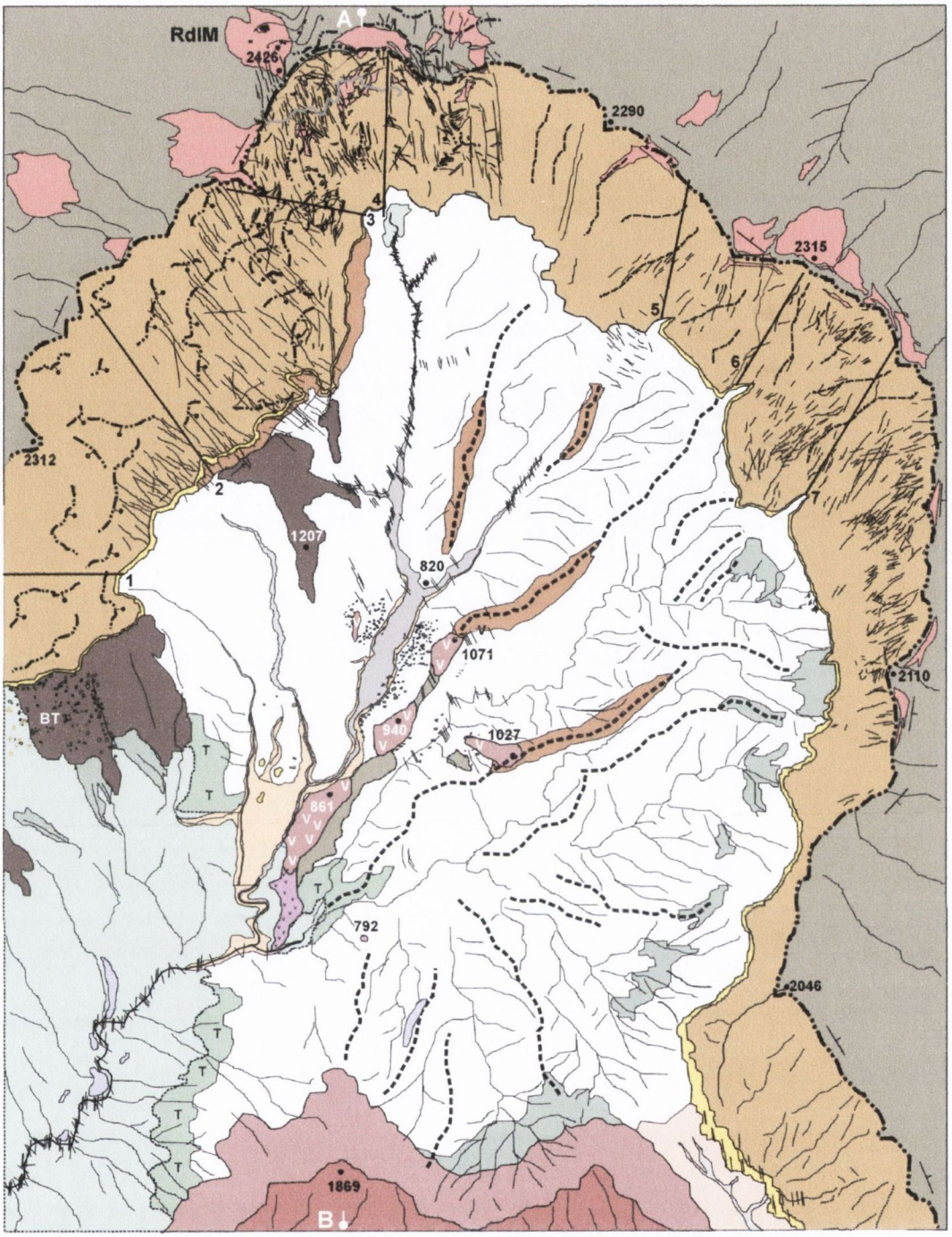


# Caldera de Taburiente, La Palma

## Geological Map

N
W
E
S

Bejenado
- TOREVAS REMNANTS
- SCORIA / SPATTER AND LAVA SUCCESSIONS
- LAVAS AND PYROCLASTS

Taburiente
- SCORIA CONES
- SCORIA / SPATTER AND LAVAS
- AMPHITHEATRE BENCH ZONE

- UNDIFFERENTIATED INTRUSIVE ROCKS AND VOLCANICLASTICS
- T SUBMARINE EXTRUSIVES AND SHEETED INTRUSIONS

2 km

- GRAVELS / BOULDERS
- EMBANKED ALLUVIALS
- ROCK AVALANCHE DEPOSITS
- SEDIMENT STACKS (EL TIME)
- TCB TECTONIZED VOLCANICLASTICS
- TCBm ALTERED VOLCANICLASTICS
- LC METAMORPHOSED VOLCANICLASTICS

SPOT HEIGHT (m) • 2046

- STRIKE / DIP OF LAVAS
- DIKE (STRIKE)
- PHOTOLINEARS (DIKES)
- MAJOR CANYON APEX
- CANYONS AND CHASMS
- AMPHITHEATRE SCARP (ball on down thrown side)

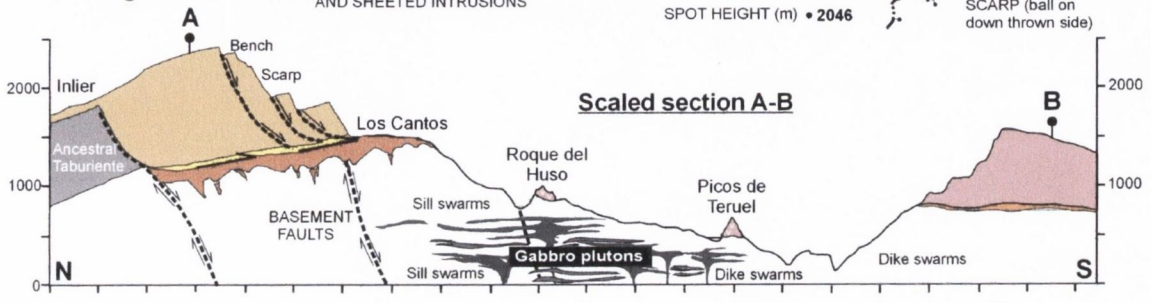


Scaled section A-B

**Fig. 1.2.6.** (previous page) Geological map and scaled interpretive section of the Caldera de Taburiente. Galerías are numbered as follows. 1. Risco Liso, 2. Bombas de Agua, 3. Los Cantos I, 4. Los Cantos II, 5. Verduras Afonso, 6. Bco. de Los Guanches, 7. Altaguna. The area marked BT, south of Risco Liso shows large accumulations TCB boulder trains.. The oblique normal fault systems are shown having a steep inward dip; consistent with their outcrop characteristics within the amphitheatre – but not on the periphery where they are markedly less inclined.

**Fig 1.2.7.** No basal volcaniclastic unit! The discordance between the intrusive core and the overlying subaerial lavas at Bco. Verduras de Afonso. The wooded ridge (Lomo Murmurado) is constructed of 80-90% dikes. At the angular discordance with the shield volcanics the density of dikes decreases to ~15%. A small collapse indentation (arrowed) can be seen undercutting the base of the shield volcanics..

The discordant contact between the intrusive core and the subaerial edifice is visible for over 3 km, in a sector between Los Cantos and Verduras Afonso. The discordance is characterised by an abrupt change in the density of dikes, from up to 100% in the intrusive core to around 15% in the subaerial edifice. The discordance is irregular in geometry (Fig. 1.2.7) and it appears to dip radially by up to 40° to the north and northeast. The volcaniclastic substratum which is typically exposed at the base of the Taburiente edifice is difficult to distinguish in this sector from either helicopter observations or from high resolution ground-based photographs. However, the map of *Navarro and Coello*, [1993] indicates the presence of the correlative "*agglomerado*" unit. Nevertheless, in the geological map the unit designated as the TCB (see Chapter 2.1), is not present between the galerías at Verduras Afonso and Los Cantos II. The omission of this unit in this particular sector is supported by the hydro-geological report of *Bravo and Coello* [1979] which indicates that the correlative "*agglomerado*" unit is either absent, poorly distinguished or only inferred to exist beneath this sector of the Caldera.

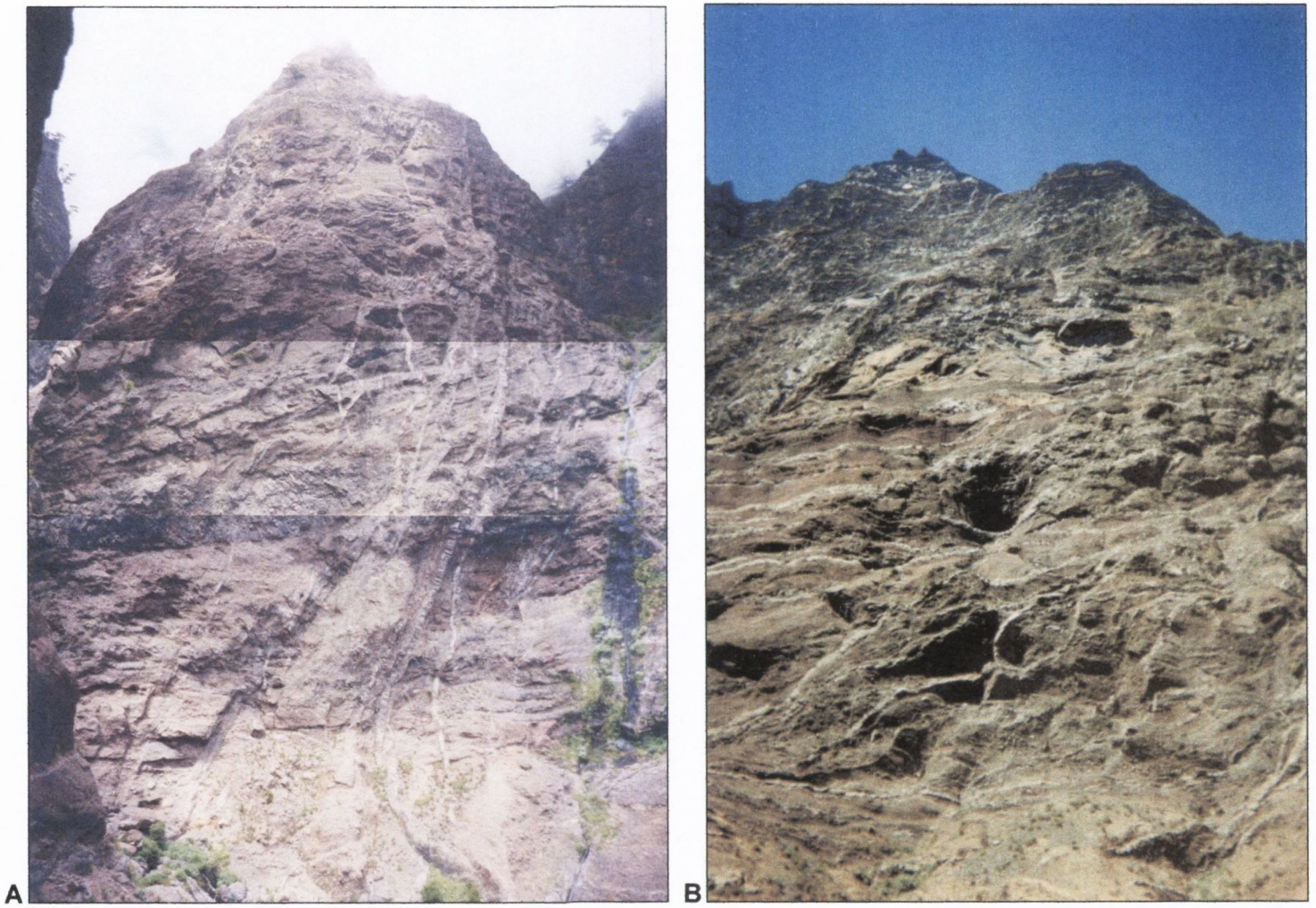


**Fig. 1.2.8**. *A.* The lower part of the amphitheatre wall at the NW part of the Caldera. The photo-mosaic shows dikes inter-laced with sill and laccolith-shaped bodies that intrude the lava and scoria-based volcanic successions. Location: Hoyo Verde. *B.* The lower scarp of the Caldera at Barranco de los Cantos.

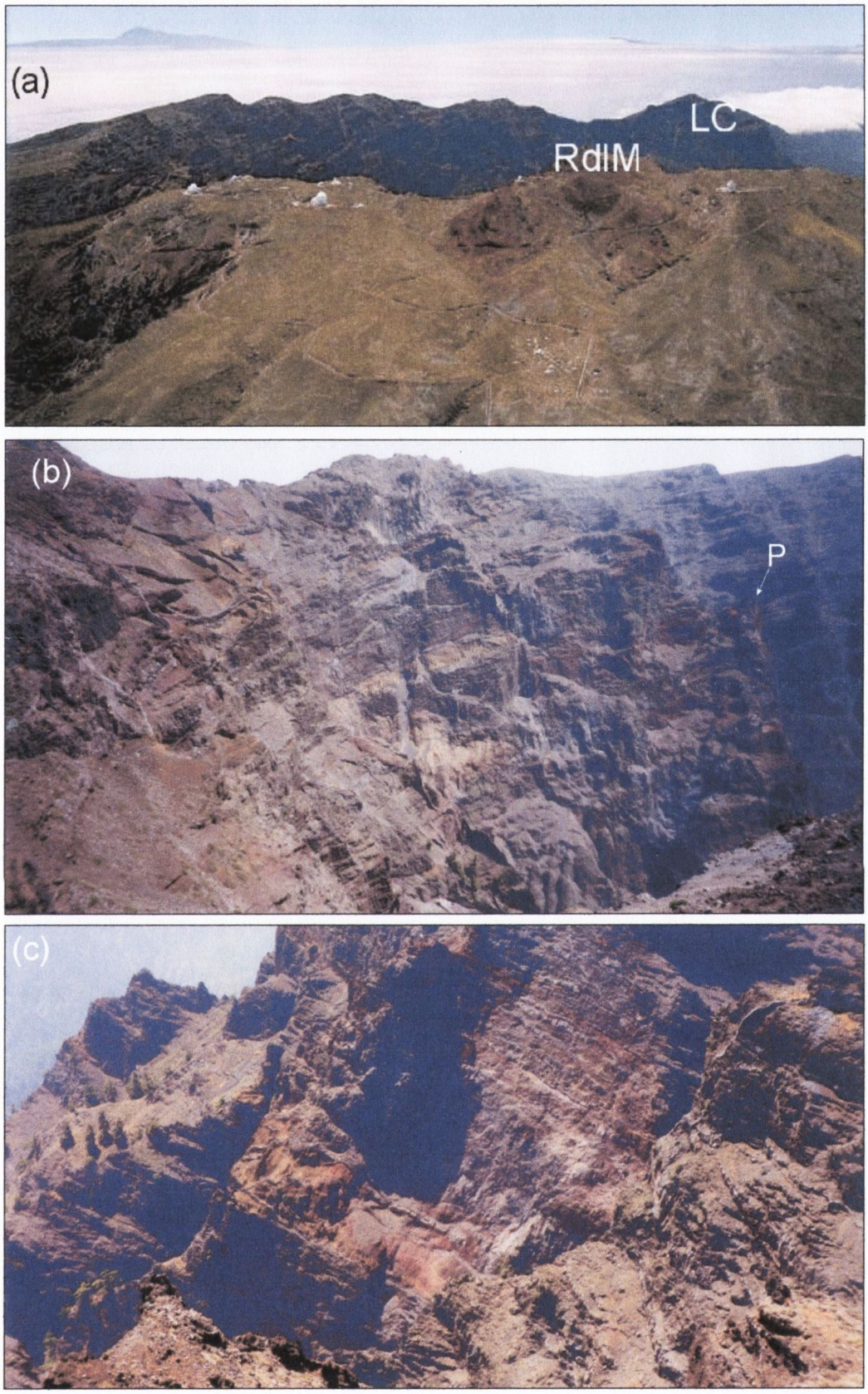


**Figure 1.2.9.** (a) View east across the rim of the Caldera towards La Cumbrecita (LC). The deeply weathered brownish-red scoria cone of Roque de los Muchachos (RdlM) is discernible in the foreground. Tenerife is 74 km in the distance. Image sourced from www.ing.iac.es. (b) The amphitheatre walls extending east from Roque de los Muchachos. Bench and scarp topography and an example of a protrusion (marked P). (c) Segment of the amphitheatre wall below Roque de los Muchachos showing sub-horizontal lavas, dikes, orange/yellow and rust-coloured scoria layers and sparsely vegetated scree slopes along the amphitheatre benches

### 1.2.5 The interior of the collapse amphitheatre

The principal geological features of the Caldera's interior are as follows

(1) an intrusive core comprising a dense plexus of sheeted intrusions and small gabbroic stocks.

(2) Thick sequences of breccia that are intruded by sheeted dike swarms. These volcaniclastic units can be differentiated by the presence or absence of hydrous alteration mineralogy into submarine and subaerial breccias.

(3) toreva remnants (relic landslide blocks) derived from the collapse of the north flank of Bejenado volcano [*Roa*, 2003].

(4) boulder trains that extend down-slope from the base of the Cumbre Nueva escarpments (Ch. 2.1).

(5) epiclastic units comprising rock avalanche and alluvial channel and embankment deposits [*Roa*, 2003].

The interior of the Caldera has been accessed as far as the upper reaches of Bco. de Los Cantos (Fig. 1.2.8b), to a position where the canyon narrows very close to the base of the amphitheatre headwalls. At this point outcropping pillow fragment breccias, which are ubiquitous on the middle to lower course of the Bco. de las Angustias, are observable as screen-like bodies between densely packed dikes. Other 3$^{rd}$ order canyons such as the Bco. del Diablo and Bco. Verduras del Mato are impenetrable, making field studies at the base of the amphitheatre escarpment impossible.

#### 1.2.5.1 The intrusive core

The bedrock geology of the amphitheatre floor consists of dense swarms of vertical, subvertical and interlacing dikes and stacks of sheeted sills up to 350 m thick. This is typical of a coherent intrusive complex as described by *Walker*, [1986; 1992] from Koolau volcano, O'ahu, Hawaii and from other oceanic island volcanoes. The geological structure of the intrusive core is identical to the basal complex of Fuerteventura in terms of the very high density of sheeted intrusions and the mineral assemblages diagnostic of a hydrous metamorphic overprint [e.g., *Stillman*, 1987; *Schiffman and Staudigel*, 1993]. Exposures of layered gabbro (1.2.10c) are interspersed throughout the amphitheatre floor and it has been suggested that these rocks form stock-like intrusions that connect at shallow depths to crystallised magma bodies [*Staudigel and Schmincke*, 1984: *Gee et al.,* 1993]. However, the margins of these supposed stocks are difficult to distinguish from the dense plexus of dikes that cross-cut them. *Staudigel and Schmincke* [1984] indicate that the stocks are some tens to hundreds of meters across, whereas the maps of *De la Nuez* [1983] and *Navarro and Coello* [1993] show kilometre-scale zones of alkali gabbro, albeit in differing positions. Meta-trachytic rocks representing intrusions or dome-like flows, outcrop in upper portion of the seamount sequence [*Fernández et al.*, 2002].

When observed from the lowest stratigraphic interval, level with the canyon floors (see Fig. 1.2.11a), the rock mass is composed entirely of sheeted intrusions (100% outcrop). The intrusion density locally decreases with stratigraphic height to around 20% at the level of exposure along the canyon apices (Fig. 1.2.11c), otherwise the % dilation is between 95-100% until the contact with the shield volcanics Individual dikes are between 0.25 and 1.5-m wide although there are numerous exposures where a petrographically or texturally distinct planar intrusion has been injected medially into an existing member, widening the intrusive body. The dikes are typically non vesicular or poorly so; although the medial and peripheral zones of some dikes are vesicle-rich or amygdaloidal.

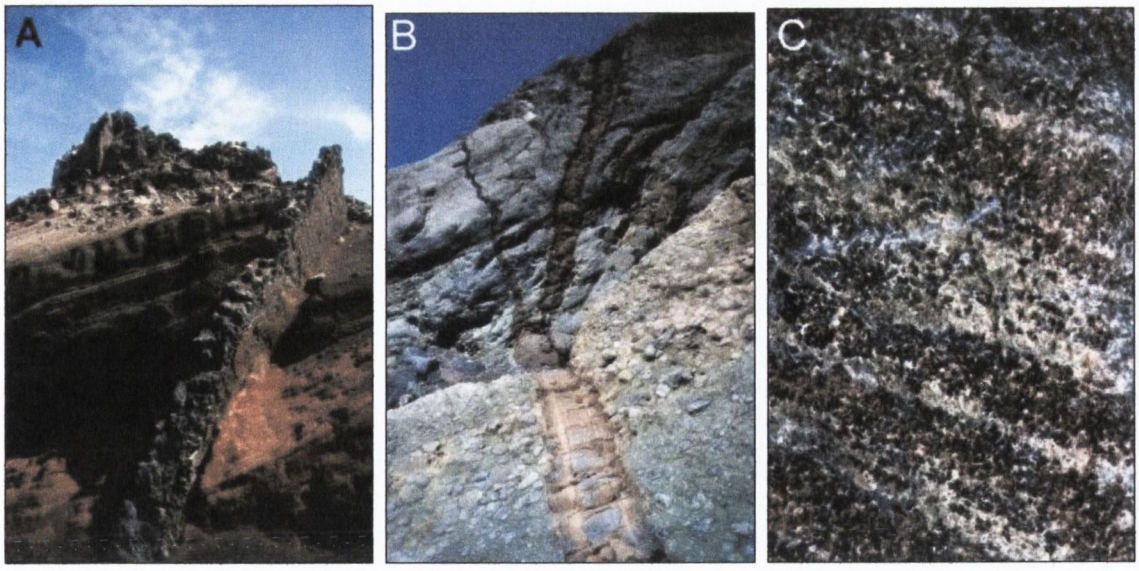


**Fig. 1.2.10.** (a) A dike eroding out of loose tephra deposits near Roque de los Muchachos. (b) A hydrous metamorphosed dike penetrating pillow fragment breccia deposits in the Pliocene seamount series. (c) Layered alkali gabbro from boulder deposits in the Bco. Las Angustias.

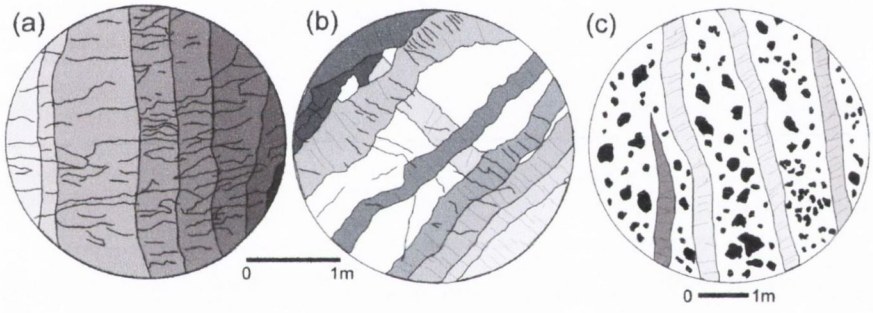


**Fig.1.2.11.** Field sketches of sheeted intrusions from the exhumed basement (a) Dikes comprising 100% of the rock mass, an example of a coherent inrusion complex (Bco. Almendro Amargo). (b) Interlacing dikes cutting metatrachyte and leukogabbro (southwest of Dos Aguas). (c) Dike swarms cutting the TCBm volcaniclastic units (see text) along the canyon apex of Morro Negro. See also Fig. 1.2.12.

There are other less distinct geological characteristics of the Caldera's interior. Hydrothermal mineralization (chalcendony, calcite, siderite), occupying millimeter to centimeter thick veinlets and stockworks, occurs sporadically around the periphery, becoming more frequent towards the center of the amphitheatre. Fossil sinter deposits, some of which have been extracted by small trench mining operations (perhaps early $20^{th}$ century), are exposed around the periphery of the intrusive core (e.g., at Roque de las Ramas). Iron-laden waters that emanate from effervescing springs at Dos Aguas, produce the discoloration in the canyon waters whilst sulphate sublimates are locally exposed in the chasms that incise the lower reaches of the Caldera walls (e.g., Bco de Los Guanches). Finally, the air temperatures inside some of the galerías measure between 17°C and 28°C [*Bravo and Coello*, 1979], an indication perhaps of residual geothermal activity within the intrusive core.

### 1.2.5.2 The amphitheatre volcaniclastics

Volcaniclastic deposits are abundant within the Caldera and along the entire course of the Bco. de las Angustias. *Ancochea et al.* [1994], *Vegas Salamanca et al.* [1999] and *Roa* [2003] summarize the characteristics and significance of a number of spatially and temporally distinct volcaniclastic sequences. There are several basic sub-divisions in the volcaniclastic stratigraphy outlined in table 1.2.1.

| Group | Name / classification | Characteristics | Thickness (m) | Age range (Ma) |
|---|---|---|---|---|
| F2 | Basinal epiclasticss | Unaltered, some pyroclasts | 40 – 200(?) | 0.55 - Holocene |
| F1 | Intra-caldera epiclastics | Unaltered epiclastics | 30-170 | Holocene |
| E | El Time fan delta | Unaltered, intercalated lavas | 370 | 0.41-0.44(?) |
| B | Bejenado (relic debris) | Unaltered, base of torevas | 1-2 | 0.44(?) |
| C | Cumbre Nueva (breccia) | Unaltered, 1-2% dikes | 100 | 0.55 |
| TCB | Ancestral Taburiente | Unaltered, 5-20% dikes (Tectonized) | 100-350 | 1.2 |
| TCBm | Ancestral Taburiente | Partially metasomatized, 20-30% dikes | 100-200 | 1.2 |
| H2 | Submarine - debris | Hydrous metamorphosed, many dikes | 400(?) | Pliocene |
| H1 | Submarine – clastics | Hydrous metamorphosed, many dikes | 3000(?) | Pliocene |

Table. 1.2.1. Basic grouping of volcaniclastic units in northern La Palma. Taken from *Roa* [2003].

The geologic maps of *De le Nuez* [1990] and *Navarro and Coello* [1993] show large tracts of what they refer to as "*chaotic breccia*" and "*basaltic breccia*" respectively; exposed predominantly within the confines of the Caldera. Although the mapped distribution of these breccias differs considerably, there is sufficient spatial overlap to suggest that each study has described and differentiated each geological unit.

*A. Unit TCBm*

Undifferentiated sequences of volcaniclastics, here designated as TCBm, are exposed along the canyon interfluves that extend towards the base of the amphitheatre headwalls (e.g., Morro Negro – Fig. 1.2.12 and Lomo El Negrito). These form a part of the volcaniclastic unit generically termed as "agglomerates" in the descriptions of *Gastesi et al.* [1966], *De La Nuez* [1983] and *Ancochea et al.* [1994]. They are between 400 and 750 m thick and are exposed almost exclusively within the confines of the Caldera. Volcaniclastic successions identical to the TCBm unit are also exposed on either side of the amphitheatre at Hoyo Verde, Los Cantos, El Escuchadero and Bco. de Los Guanches. The geological map in Fig. 1.2.6 does not completely represent the overall distribution of this unit since the terrain is restrictive for outcrop-scale observations.

In essence, the TCBm volcaniclastics are composed of angular to subangular blocks (between 0.2 and 4 m wide) and clasts (0.01-0.2 m) composed of dense olivine basalt, ankaramite, trachybasalt with lesser amounts of gabbro, pyroxenite and scoria. These coarse/oversize components are suspended in a moderate to well indurated brown to light rust-brown polymict matrix composed of scoria lapilli, crystals and subangular pebble-sized fragments of basalt. Hydrous alteration selvages are present within the basal part of the TCBm rock mass, diminishing with stratigraphic height. Dikes, rising from the intrusive core, are interspersed within the TCBm, decreasing in density with stratigraphic height. There are no structural-stratigraphic breaks throughout the TCBm hence the crude alteration intensity with depth appears to be the only discriminating geologic criterion. Fig. 1.2.13 is a schematic section through the Caldera illustrating the depositional setting and the structural/stratigraphic relationships with the TCB/toreva remnants.

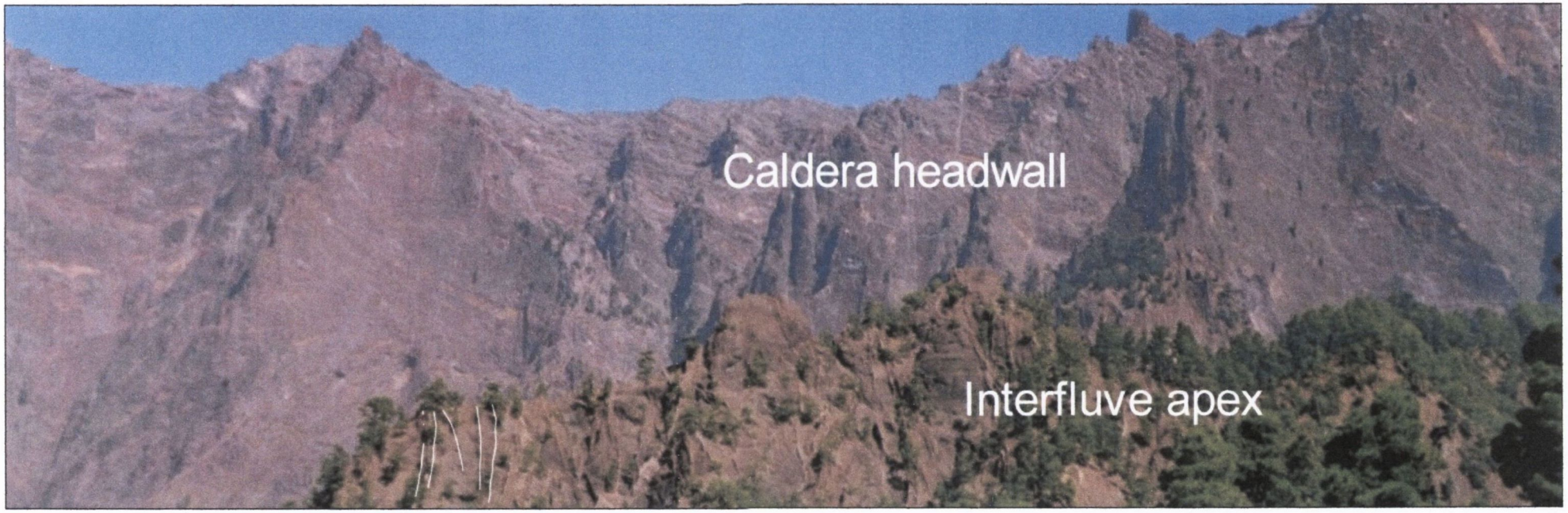


**Fig 1.2.12.** A panoramic photo looking NW toward the Caldera headwalls. The interfluve (Morro Negro) in the foreground is constructed of TCBm volcaniclastics with interspersed dikes. See Fig. 1.2.11c.

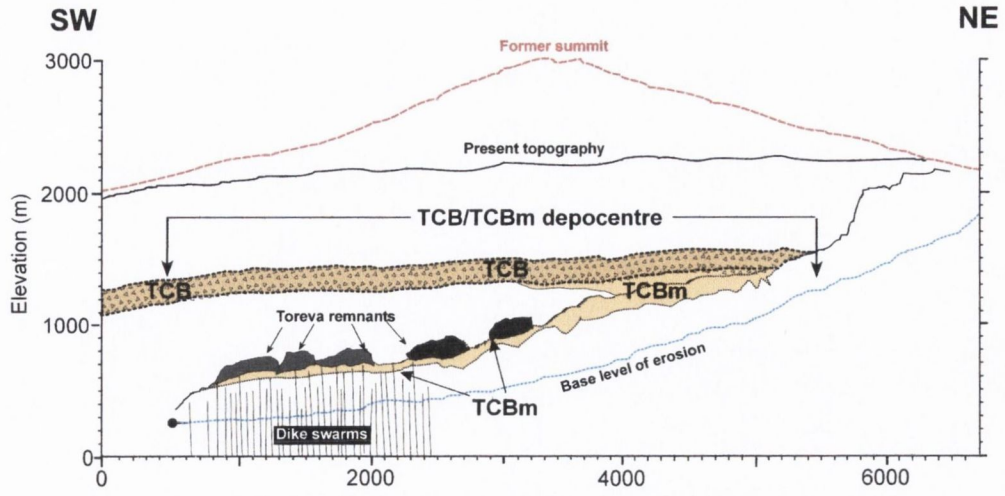


**Fig. 1.2.13.** Scaled section through the interior of the Caldera illustrating the intimate spatial relationship between the TCB/TCBm units. The ridge of Morro Negro is in the foreground.

*B: La Cumbrecita Group (H2)*

Thick and structureless sequences of hydrous metamorphosed volcaniclastics appear as screens between dikes around the upper reaches of the amphitheatre floor in the southeastern and western parts of the Caldera. These poorly to moderately consolidated and clast-supported volcaniclastic accumulations form a locally extensive stratigraphy especially around La Cumbrecita, Bco. de Las Traves and Lomo Cumplido. Collectively designated in this work as 'La Cumbrecita group volcaniclastics', these units are not to be confused with the hydrous metamorphosed pillow fragment breccias and re-worked volcaniclastic deposits exposed along the walls of the Bco. de las Angustias [see *Staudigel and Schmincke*, 1984]. La Cumbrecita group have been interpreted from previous studies as breccia accumulations derived from de-constructive events associated with the pre-emergence stage of the Pliocene seamount [*Ancochea et al.*, 1994]. Again, the narrow and unstable canyon apices prohibit correlative exposure-scale observations, therefore the unit designated in the geological map as undifferentiated intrusives and volcaniclastics (Fig. 1.2.6) only serves as a proviso for the total extent of both the TCBm and La Cumbrecita groups. The spatial distribution of these units, and others within the amphitheatre, may become easier to define in the future when high resolution Landsat imagery of spectral reflectance, and alteration intensity become available.

### 1.2.5.1 Subaerial pyroclastic deposits

Subaerial pyroclastic deposits, typically composed of scoria and/or lapilli, are locally exposed along the road cuts following the steep ridges leading up to the Cumbre Nueva escarpment and Caldera headwalls. Although often masked by sub-alpine vegetation and subjected to epicalstics processes (large-scale remobilization) and often intense argillic alteration, these pyroclastic deposits are indicative of residual volcanic activity subsequent to the major sector collapse of Bejenado Volcano.

## 1.2.6. The origin of the Caldera de Taburiente

### 1.2.6.1 The diversity of caldera-type landforms

The term "*caldera*" describes most elliptical landforms or near circular depressions (generally >>1 km wide) with a prominent topographic rim, forming the summit regions of many types of volcanoes. The term can be used to describe either a relic morphological feature or an active volcano-tectonic structure. Calderas sometimes dominate the morphology of an edifice, largely due to their expansive diameters (e.g., Cerro Galan, Chile: 35 km x 25 km, and Valles Caldera, New Mexico:- 22 km wide).

The formation and structural development of calderas are controlled by at least three intrinsic processes, (1) magmatic evolution, (2) plumbing system geometry and (3) regional/local stress fields [e.g., *Acocella et al.*, 2002: *Stix et al.,* 2003]. The development of caldera's on basaltic volcanoes involves relatively passive vertical subsidence or flexural downsag of the summit region along concentric ring faults (the piston-type caldera) [e.g., *Walker*, 1984; *Munro and Rowland*, 1996]. This occurs during attendant volcanism or magmatism/seismogenesis. Typical examples include the downsag calderas of Mokua´weo´weo and Kĭlauea, Hawai´i and the exceptionally deep (1.1 km) Fernandina Caldera on the Galápagos Island of Isabella (Fig. 1.3.17).

A second style of Caldera formation, operative on both basaltic and silicic volcanoes, involves vertical collapse and later resurgence subsequent to the withdrawal of magma from an under-pressured magma reservoir (e.g., Ambrym in Vanuatu and Tejeda on Gran Canaria) [*Robin et al.*, 1993; *Schmincke and Sumita*, 1998]. A third mechanism is the cataclysmic collapse of over-steepened and/or unstable volcano summits/flanks (e.g., Las Cañadas - Tenerife, Cha das Caldeiras - Cabo Verde and Lihir - Papua New Guinea), the "avalanche or collapse calderas". Some workers suggest that the processes leading to the formation of such landforms can be initiated by volcano/seismic activity causing the collapse of gravitationally unstable flanks [*Martí et al.*, 1997; *Hurlimann et al.*, 2000]. The type example is the crater that formed during the eruption of Mt. St Helens Volcano (Washington State, USA) in May 1981, which can be classified in the morphological sense as a collapse amphitheatre. It formed as an erupting dacite cryptodome blasted laterally through the collapsing north flank of the stratocone [*Christiansen and Peterson*, 1981]. The scaled plan view shapes of a number of collapse amphitheatres are illustrated in Fig. 1.2.14

Another landform found on volcanoes, both oceanic and continental, is described as an "*erosion caldera*"; a large depression that develops primarily through prolonged fluvial erosion, undercutting and piecemeal collapses [e.g., *Karátson et al.,* 1999, *Paris and Carracedo*, 2001]. However, this term is too general to adequately distinguish between a large morphological depression formed by the intrinsic processes described above and one formed by extrinsic processes. For instance, *Szakács and Ort*, [2001] and *Karátson and Thouret*, [2001] have, amongst other authors, debated how a caldera-type structure can be identified or inferred subsequent to the erosive processes that have heavily modified its primary form. Therefore, in scenarios where the input of fluvial erosion as the root landform-shaping mechanism is under question, one could remove the word "caldera", due to the genetic implications of primary processes, or simply replace the noun with an adjective in cases of exceptional pleading (i.e., an eroded caldera or an eroded collapse amphitheatre). Examples of the latter may include the cirque-like features on Piton des Neiges (Fig. 1.2.13a,b), the eroded shield volcano forming the northern part of Réunion Island in the Indian Ocean. Here the island morphology is dominated at its centre by three coalesced amphitheatre-shaped depressions that constrict down-slope along steep-sided valleys (Fig 1.2.15a).

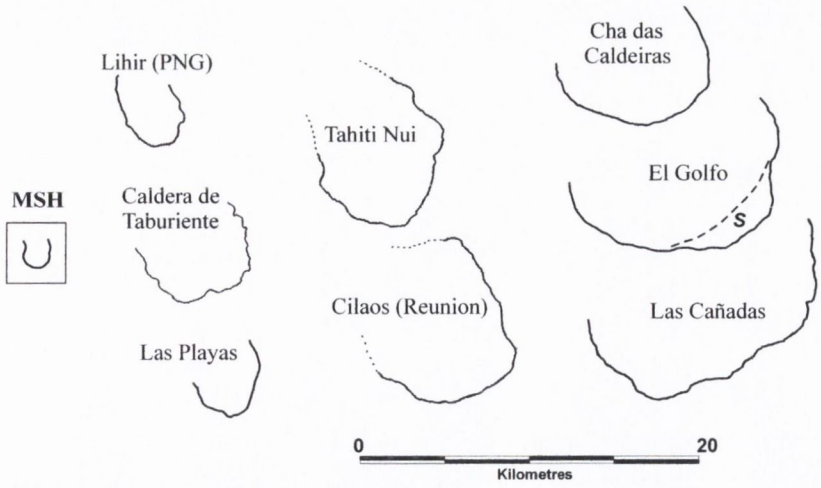


**Fig. 1.2.14.** The shapes of collapse calderas from various oceanic island/arc volcanoes compared with the Mount Saint Helens collapse amphitheatre (abbreviated MSH). The abbreviation S denotes a seondary scarp.

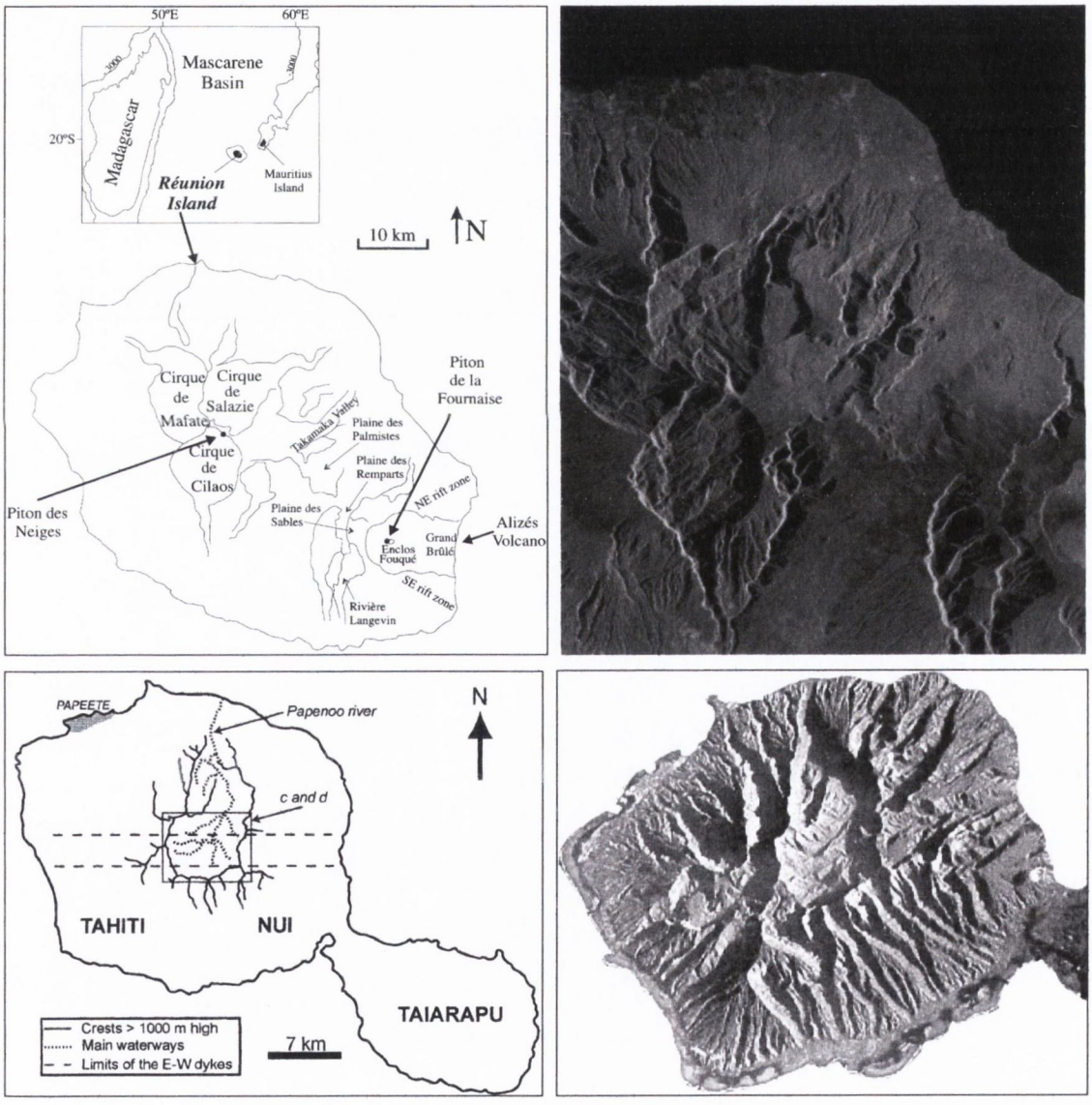


**Fig. 1.2.15.** Oceanic island volcanoes with large central depressions. (a). Piton des Neiges (Réunion). Location map sourced from *Malengreau et al.* [1999]. (b) RADARSAT-SAR image of the northern part of Reunion Island showing the relief that developed subsequent to the collapses of the formerly active Piton de Neiges Image sourced from *Toutin et al.* [1998]. (c) Tahiti Nui (Society Islands). Map by *Clement et al.* [2002]. (d) The near vertical shuttle image (lower right) shows in detail the array of deep canyons that emanate from the central depression of the island. Image sourced from www.volcano.und.edu.

Large submarine debris avalanche deposits have accumulated at the outlet of each cirque, leading some authors to suggest an origin through giant landslides [*Bachelery et al.,* 1996]. A similar example, illustrated in Fig. 1.2.15b, is the central depression of Tahiti Nui in the Society Islands, the scarp-like form of which, together with the occurrence of epiclastic deposits on the floor region, supports the interpretation of an origin through giant landslides - between 0.57 and 0.39 Ma ago [*Clement et al.*, 2002].

Early studies on the namesake Caldera de Taburiente suggested an origin due to fluvial erosion [*Lyell*, 1855], a hypothesis that has been carried forward by numerous authors [*Middlemost*, 1971; *Navarro and Coello*, 1993; *Carracedo*, 1994; *Carracedo et al.*, 1999a,b, 2001, *Paris and Carracedo*, 2001]. However *Ancochea et al.* [1994] indicate that, in terms of processes, fluvial erosion has played a less significant role in comparison to giant landsliding in shaping the Caldera. Instead, they propose that the location and geometry of the Caldera, and more specifically the direction of landsliding, were structurally controlled by the topography of the Ancestral Taburiente collapse caldera; the buried rim of which is nested outside of the present Caldera. Before discussing the alternative model, further consideration is given to the influence of fluvial erosion on the morphology of oceanic volcanoes and how this is governed by regional climate trends and by island-wide micro-climatic variations. Following this, the succinct arguments behind and weaknesses of the "erosion caldera" hypothesis will be addressed.

### 1.2.6.2 The erosion of oceanic volcanoes

The salient geomorphologic characteristic of post-shield* oceanic island volcanoes is the serrated high-relief terrain that develops by fluvial erosion, undercutting and piecemeal collapses. In this stage of their morphological evolution, the volcano slopes are characterized by deep gulches, sharp ridges and isolated pinnacles that often merge upslope towards large central depressions. Examples include the post-shield volcanoes of Tahiti Nui, Piton des Neiges and West Maui Volcano in Hawaii where the original shield volcano profiles are still well preserved. The effects of erosion are less distinct on active shield-building volcanoes where volcanic activity overwhelms the rate of erosion. Examples include Mauna Loa (Hawaii), Fogo (Cabo Verde) and Fernandina in the Galápagos Islands. However, once the frequency of volcanic activity declines, the equilibrium between construction and degradation is offset, enabling fluvial processes and piecemeal mass movements to re-shape the volcanic landform.

The majority of oceanic island volcanoes are located in the tropical / subtropical latitudes where high rates of precipitation prevail on a seasonal basis. Precipitation in the Canaries is modulated by a high atmospheric pressure system called the Azores High [*Gallego et al.*, 2000]. The typically stable and dry weather conditions are due to a prevalent subsidence inversion layer found at altitudes between 600 and 1500 m [*Graham*, 2003]. As the prevailing wind flows across the cool Canaries sea current, low cloud often develops and laps onto north-facing coasts. The top of this low-cloud is usually coincident with the inversion layer. When the Azores High is offset by Atlantic low pressure systems, particularly during the winter months, the resultant cyclonic weather systems can be severe, as was the case during February of 2002 on Tenerife. For comparison, the Hawaiian Islands and surrounding waters are generally affected by the strength and position of the Eastern Pacific Subtropical High. In winter the Subtropical High is in its southernmost and weakest position and mid-latitude disturbances and fronts move into the region [*METOC*, 2003].

*The post-shield stage is characterised by a lull in volcanic activity and accelerated canyon develepment, although the shield profile is still well preserved.

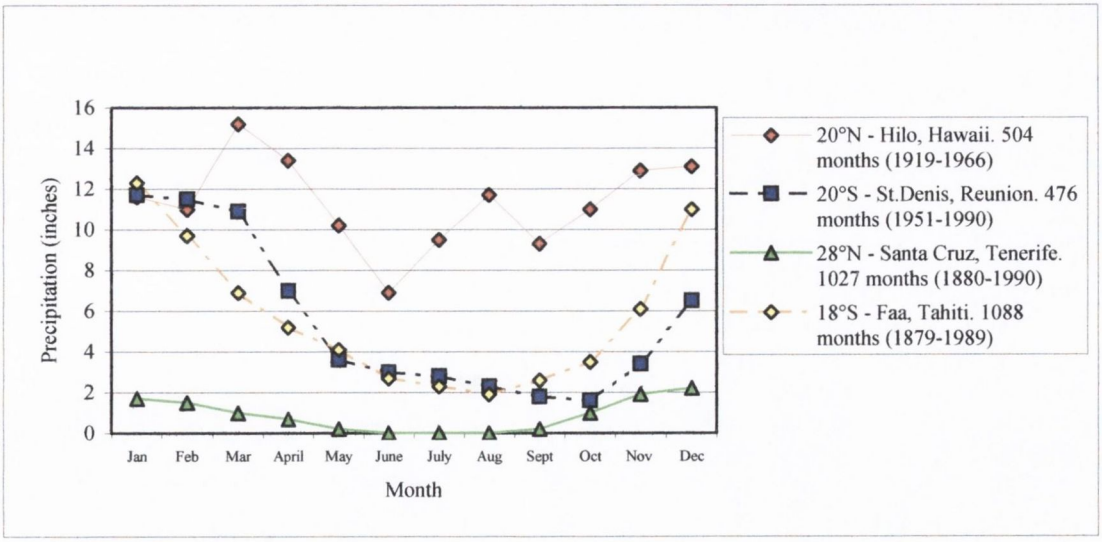


**Fig 1.2.16.** Precipitation statistics from oceanic island environments. Data sourced from www.worldclimate.com.

For example, 1 m of rain fell in south-eastern Hawai'i in the nine days leading up to the November 2000 aseismic slip event of Kilauea volcano [*Cervelli et al.*, 2002]. Fig. 1.2.16 graphs the seasonal variation in rainfall for a number of oceanic islands, illustrating the differences in time-averaged precipitation in sub-tropical (e.g., Tenerife) and tropical latitudes (e.g., Hawai'i). Although it is based on observations taken over periods of up to 110 years, the graph fails to reflect on the influence of aspect in the distribution of rainfall. This is an important climatic parameter since precipitation and fluvial erosion are consistently concentrated on windward-sloping flanks. For instance, the heavily eroded northern and eastern flanks of Gran Canaria have developed under the influence of the north-easterly trade winds that have persisted in this direction since the Miocene; consequently, the thickest epiclastic deposits have accumulated in this sector [*Schmincke and Sumita*, 1998]. The greater width of the offshore abrasion platform to the north of Anaga (NE Tenerife), together with steeper subaerial slopes on the north side of Tenerife are also consistent with a stable trade winds direction and powerful sea-swell from the northeast [*Mitchell et al.*, 2003]. In similarity, the post-shield volcanoes of La Gomera (Canaries), Kohala, Haleakalā and Kaua'i (Hawaiian Islands) exhibit a distinct contrast between the depth and distribution of canyons that are more prolific and far deeper on the northeast-facing windward slopes. Furthermore, there is a clear contrast in the distribution of vegetation on most oceanic islands from lush or well-wooded windward slopes to partially desertified or dissimilarly vegetated leeward slopes.

Some oceanic shield volcanoes reach altitudes in excess of 3 km above sea level, influencing the zonation of micro-climates over short vertical intervals along the volcano slopes. For example, during the last ice age, glacial sheets enveloped the summit region of Mauna Kea, Hawai'i (4205 m) above the 2800 m contour [*Wolfe and Morris*, 1996]. The summit region of Teide volcano (3718 m) was, to a lesser extent, glaciated during the same period [*Albay and Marti*, 2000]. Glacial activity resulted in the incision of deep summit-region bluffs and the deposition of moraine-like deposits around the upper flanks of the volcanoes, both of which are snow-capped during winter months. Perennial snow cover above the 2100 m contour is not uncommon on northern La Palma. In fact, *Navarro and Coello* [1993] have mapped what they interpret to be peri-glacial deposits limited within the small v-shaped bluffs radiating downslope from the Caldera's rim. As previously mentioned the windward slopes of La Palma are commonly enveloped by orographic clouds between altitudes of 600 and 1500 m AMSL. The images in Fig. 1.2.17, illustrates how the morphology of the island influences the distributions and patterns of cloud cover when the subsidence inversion layer is stable.

Fig 1.2.17a is a false colour infra-red image showing how the lush sub-tropical vegetation and cloud forest are preferentially distributed along the northern and eastern slopes. It follows that the largest gulches and ravines on La Palma are concentrated in the same sector – in the influence of the northeast trade winds. The gulches often coalesce upslope into broad v-shaped canyons that expose the uppermost stratigraphic units of Ancestral Taburiente (particular on the northern slopes). This is in contrast to the leeward, western slopes where ravines and canyons are markedly less developed; the exception being the leaf-shaped Bco. del Jieque upslope from Tijarafe.

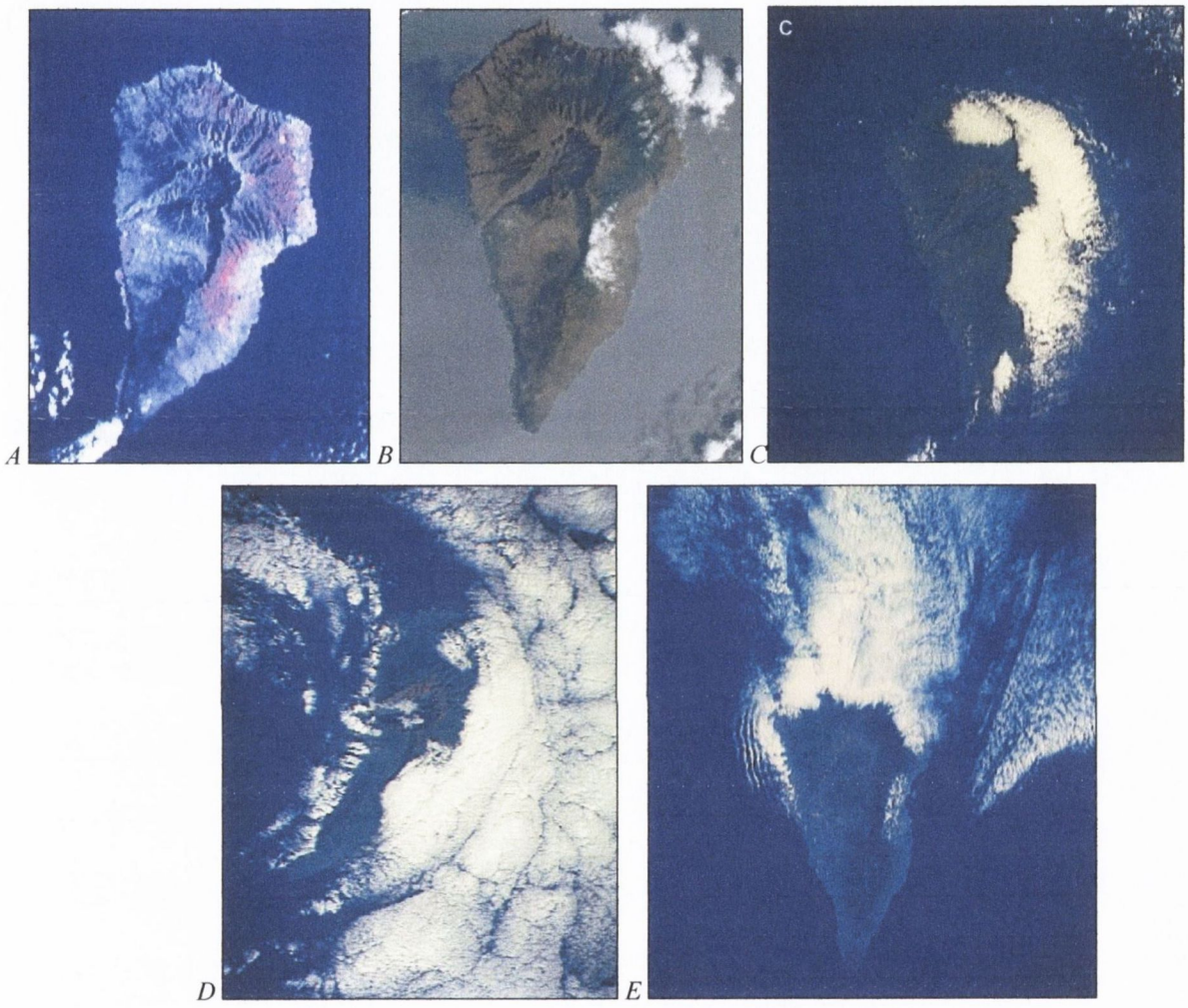


**Fig. 1.2.17.** Images of La Palma taken from Earth orbit showing the effects of island morphology on the distribution of cloud cover and its impact on erosion and vegetation. A. STS-050-105-033. False colour image showing the extent of lush sub-alpine cloud forest and sub tropical vegetation (tones of dark purple and red) on the N and NE island flanks. B. STS047-085-092. Near azimuth image of true colour contrast to correlate with image A. C. STS-052-20086309At azimuthal image showing discrete cloud banks engulfing the east flank of La Palma. D. STS-056-92-39. Contrasting cloud formations on leeward and windward La Palma. North is to the top right. Azimth image of cloud streaming from the NE (trade winds direction) towards the northern slopes of Taburiente. Image ID unknown. Images sourced from www.jsc.visiblearth.com

The remaining narrow gullies on the western slopes are typically between 80 and 110 m deep, and they are separated by greater distances. The eastern slopes, flanking the Cumbre Nueva escarpment, are incised by deep gulches that are infilled towards the south by Holocene lavas sourced from the northeast rift zone of Cumbre Vieja. The cut-away shaded relief images in Fig's. 1.2.18 and 1.2.19 show the contrast in the topography between the windward and leeward slopes. Most of the constructional surfaces have been stripped away with the exception of the prominent scoria cones preserved along the low elevation flank protrusions.

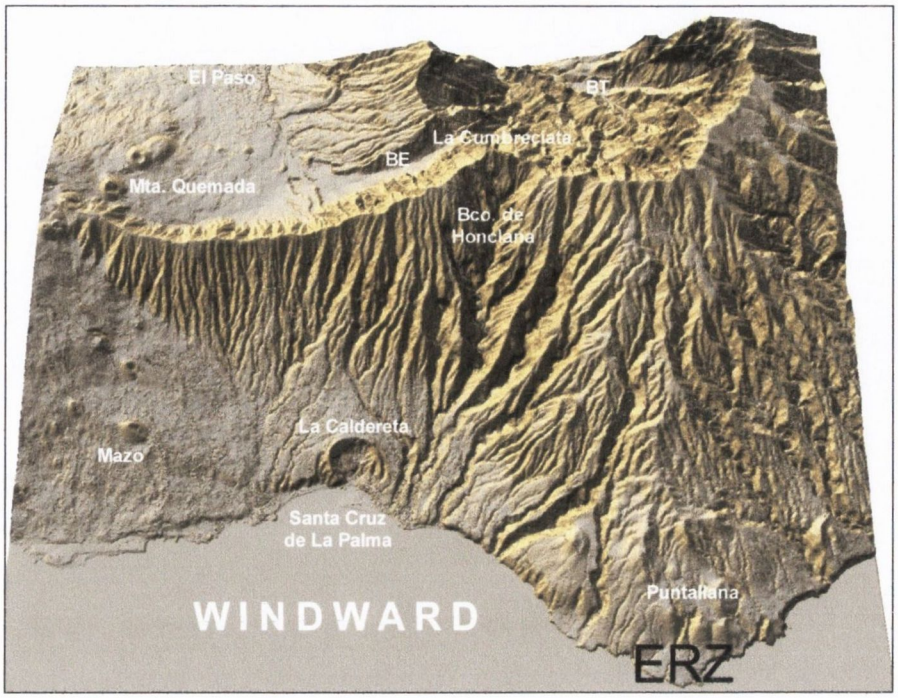


**Fig. 1.2.18.** Low oblique shaded relief image looking due west, showing the canyon terrain on the west flank of northern La Palma. The view is 18.4 km, north to south. Compare with Fig. 1.2.19 below. Holocene-historic lavas from the NE and NW rift zones of Cumbre Vieja have enveloped the southern part of the Cumbre Nueva headwall. The abbreviations BE and BT denote Bejenado embankment and the Barranco de Taburiente.

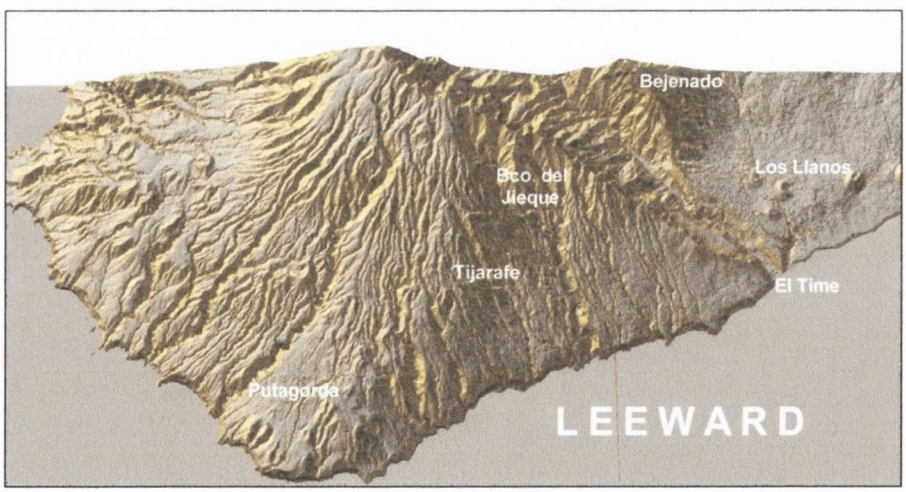


**Fig. 1.2.19.** Shaded relief image of north-western La Palma (north is to the left, the image is 24.5 km across). When compared with Fig. 1.2.18 this high oblique east-looking image shows the contrast in the scale of erosion between the windward and leeward slopes.

### 1.2.6.3 The erosion caldera hypothesis

In 1855 *Charles Lyell* hypothesised that the Caldera had formed as a consequence of fluvial erosion; a supposition in contrast to the uplifted crater (craters of elevation) theory put forth by *Von Buch* [1825]. *Lyell's* "erosion caldera" hypothesis has been embraced by numerous authors (e.g., *Middlemost*, [1971]; *Navarro and Coello* [1993]; *Carracedo* [1996]; *Paris and Carracedo* [2001]; *Hildenbrand et al.* [2003]*. In the model of *Carracedo et al.* [1999a], the Caldera extends for 15 km along a northeast-southwest trend, incorporating the linear wall of the Cumbre Nueva embayment as part of a southwest constricting structure that is bounded to the south by the dismantled north flank of Bejenado Volcano. These authors suggest that the Caldera was "*initiated*" by a tectonic event (the Cumbre Nueva lateral collapse). The subsequent entrapment of a drainage system (the forerunner to the current Angustias catchment area) led to the rapid "*headward erosion*" of the northern segment of the embayment and the development of the Caldera's relief by under-cutting and collapses. This drainage system ran between the linear side-wall of the embayment and the developing stratocone of Bejenado. The resulting depression subsequently enlarged through time and extended by "*erosional retreat of the embayment walls*" [*Paris and Carracedo*, 2001]. Fig. 1.2.20 illustrates the conceptual development of the Caldera under this regime of accentuated fluvial erosion. Despite the popularity of the erosion caldera hypothesis there are several important weaknesses in terms of climatology, morphology and temporal constraints on its formation.

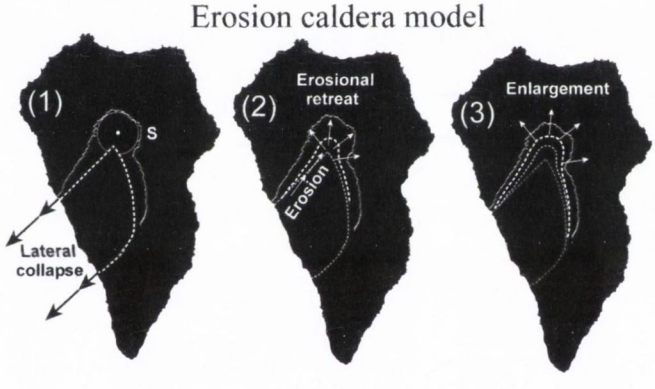


**Fig. 1.2.20.** Models for the genesis of the Caldera de Taburiente, an 'erosion' caldera caused by differential fluvial erosion of the walls of the Cumbre Nueva embayment towards the summit (marked as s) in the leeward side of the prevailing trade winds.

#### A: Volume, symmetry and relative age

First, the erosion caldera hypothesis falls short in explaining how a volume of material incorporating the edifice centre and summit region of Taburiente Volcano (~30 $km^3$) was undercut and removed in a remarkably symmetrical fashion by gradual fluvial erosion, while the adjoining Cumbre Nueva escarpment underwent retrogressive erosion to a lesser extent. This is in spite of the fact that the Caldera and the much larger Cumbre Nueva escarpment are both open to the west. If fluvial erosion and retrogressive undercutting of the summit region are the main landform-shaping mechanisms, one would expect a more irregular exotic terrain of inter-linked canyons as exemplified by the interior regions of La Gomera, Gran Canaria and Kaua'i (the latter is in Hawaiian Archipelago). However, the topography of these islands has developed since the Miocene and Pliocene, and this is a critical factor to consider since the canyon terrain of Taburiente, a Pleistocene-age volcano, has not developed to the same extent.

* These authors also imply uplift as an enlarging process for the Caldera.

Therefore, does the amount of missing mass signify that the greater altitude of the summit region facilitated an accelerated rate of denudation relative to the more uniform erosion of the Cumbre Nueva escarpment along lower elevations? (see Fig 1.2.21). It is difficult to grasp this notion especially when one compares the Caldera on a morphological basis with the Plio-Pleistocene volcanoes of Tahiti Nui and northern Reunion. Both localities experience significantly higher rates of time-averaged precipitation when compared to the Canary Islands (Fig. 1.2.16). Furthermore, it is important to recall the evidence that large amphitheatre-shaped central depressions have developed on Tahiti and Reunion primarily by giant landslides [*Bachelery et al.,* 1996; *Oehler et al.*, 2003; *Clement et al.*, 2002]. The central depression of Tahiti Nui faces into the trade winds, and, as a consequence, the associated amphitheatre rim has developed a more serrated relief compared to the Caldera de Taburiente.

Subaerial Tahiti Nui developed between 1367 ± 16 and 187 ± 3 ka [*Le Roy*,1994], whilst the oldest dated lavas on Piton de Neiges are 2.08 Ma old [*McDougall*, 1971]. Both volcanoes reached elevations of up 3000 m above sea level [*Malengreau et al.,* 1999; *Clement et al.*, 2002], similar to the summit elevation (inferred here) of Taburiente prior to its Quaternary deconstruction. The radiometric data from the relic debris avalanche deposits exposed inside the central depression of Tahiti Nui suggest that they accumulated between 570 and 390 ka [*Clement et al.*, 2002], an age similar to that of the Cumbre Nueva collapse (i.e., 550 ka [*Guillou et al.*, 2001]). Data for the temporal development of the central depressions of Reunion, suggest that that they formed during the shield stage*, prior to the emplacement of the alkaline differentiated lavas (dated between 330 and 12 ka) [*Deniel et al.*, 1992]. Nevertheless, one may stipulate on the basis of relative ages, morphology and climate contrast that the Caldera, which has very similar dimensions to the collapse amphitheatres found on Tahiti Nui and Reunion, originated in a related manner.

### B: The scale of differential erosion.

The second inconsistency in the erosion caldera hypothesis is the scale of differential erosion between the windward and leeward slopes of northern La Palma. As demonstrated in section 1.2.5.2, erosion in the Canary Islands has been concentrated along the northern and eastern flanks of the islands in the influence of the trade winds. This is further illustrated in Fig. 1.2.21 by sections of the island slopes along the leeward and windward sides. The shape of the Taburiente summit cone is extrapolated using two criteria.

- The existing volcano slopes as a basic frame of reference for the convergence of a simple cone.
- The occurrence of differentiated lavas (trachytes and phonolites) at higher elevations on Taburiente, [*Carracedo et al.,* 2001], that by way of their higher viscosity relative to alkali basalt, may have \ steepened the upper cone.

The original topography of the windward flank (Fig. 1.2.21b) is extrapolated using the interfluve apices as the closest approximation to the Quaternary palaeo-surface of Taburiente. *Mitchell et al.* [2003] use a similar method of terrain re-construction for the Miocene relief of Anaga Volcano on Tenerife. These authors assume that elongate volcanic peaks remain after erosion has deeply incised the flanks. Relic scoria cones and spatter ramparts preserved along the higher parts of the La Palma interfluves further define the palaeo-surface position. Fig. 1.2.21b illustrates how the scale of differential erosion implied by *Carracedo et al.* [1999a,b] conflicts with the observed erosional regime that has developed the islands' relief throughout the Pleistocene. Clearly the scale of the Caldera's relief is over an order of magnitude larger than any of the individual canyons on the windward slopes.

* Shield–stage volcanoes in the Canaries and Hawaii are, because of their frequent volcanic activity, particularly prone to large-scale slope failure due to the accelerated accumulation of mass.

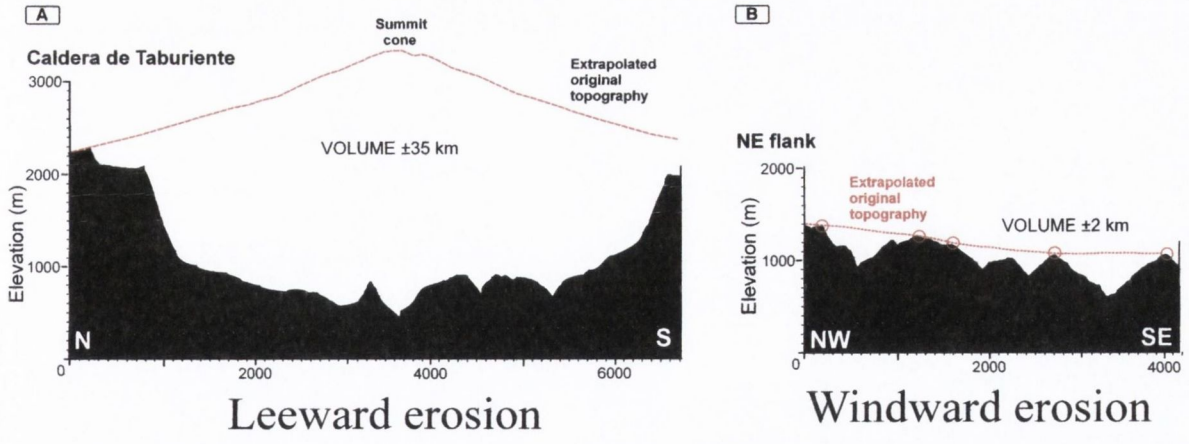


**Fig. 1.2.21.** The differences in the scale of fluvial erosion implicit in the erosion caldera hypothesis. In B, the volcanic peaks are highlighted by circles to define the closest approximation of the palaeo-surface.

C: Time and space considerations for the development of Bejenado volcano.

Another inconsistency with the "erosion caldera" hypothesis is that it is difficult to integrate the development of Bejenado Volcano into the concept of gradual erosional retreat. *Carracedo et al.* [1999a] imply that "*since the Caldera deeply dissects Taburiente and Bejenado, it must therefore post-date the formation of both*". However, if the Caldera had formed by gradual erosion, then what became of the associated epiclastics? The relict volume of detritus at El Time is too small (<2 $km^3$) to be associated with a prolonged period of erosion, rather the disposition, facies architecture and volume of the El Time deposits can been attributed the shunting of volcaniclastic associated with the flank collapse of Bejenado Volcano [*Roa*, 2003].

According to the erosion caldera hypothesis the proto-Angustias catchment area developed during the growth of Bejenado with "*linear incision rates in excess of 1 m/ka and headward 'erosion' rates exceeding 3 m/ka, with the highest values at the boundaries of the collapse*" [*Paris and Carracedo et al.*, 2001]. These estimations entail that the rate of erosion was higher than the rate of magma production; otherwise Bejenado Volcano would have overwhelmed the flow regime of the proto-Angustias catchment area and essentially blocked the development of the purported erosion caldera. This discrepancy in terms of timing and space constraints is unresolved due to a lack radiometric data for the El Time volcaniclastics and the asociated toreva remnants. It has been suggested that the toreva remnants are a source of evidence that the Caldera already existed prior to the development of Bejenado [*Roa*, 2003]. If for instance the torevas were derived from the Cumbre Nueva headwall (during collapse), this would conflict with the evidence for toreva slip from elevations higher in the present Caldera. The basal slip surfaces together with the extent of basement rock comminution underlying the toreva remnants is an indication that slip occurred from areas higher up along the canyon apices within the Caldera, perhaps from within 2 km or less of the amphitheatre headwalls. By process of elimination, if the toreva remnants were sourced from the collapse of the summit region of Taburiente Volcano, how could they have remained intact subsequent to envelopment by the north flank of Bejenado Volcano? The deductions put forth by *Roa*, [2003] place simple constraints on the origin of the toreva remnants and, to this end, suggest that the Caldera had been in existence in order to have accommodated the growth and subsequent collapse of the north flank of Bejenado (discussed further in Ch. 3.2.4.1).

### 1.2.6.4. The collapse amphitheatre model

Erosive sedimentary flows are an important landform-shaping process on oceanic island volcanoes and their submarine flanks [*Clague and Moore*, 2002; *Mitchell et al.*, 2003]. However, there are several lines of evidence indicating that a single giant landslide has superseded the processes of subaerial fluvial erosion and piecemeal collapses in shaping the Caldera de Taburiente. Paramount among these is the preserved symmetry and the scale of the Caldera; comparable to older and more recent collapse structures on Tahiti Nui and Cabo Verde. The ramp-like profile of the main interfluves, together with the overall cuspate geometry of the Caldera (Fig. 1.2.5) are reconcilable with the base of the collapse amphitheatre in its near primitive position.

*Ancochea et al.* [1994] suggest that the present Caldera mimics the geometry of the buried escarpments generated by the partial deconstruction of Ancestral Taburiente. This is, in their view, an important factor that influenced the geometry, volume and the direction of failure of the summit region. This type of structural control on the scale and geometry of successive or 'nested' flank collapses has been described from many other volcanoes where collapse structures have broadly similar eccentricity. The scenario involves the growth of an embayment-filling volcanic edifice that eventually develops sector instability and ultimately undergoes slope failure in the approximate direction of the ancestral collapse(s) [e.g. *Masson et al.*, 2002]. This synoptic view of a common source region for successive debris avalanche deposits is exemplified by the geometrically similar landslides that took place on the NW flank of Stromboli (Italy) in the last 13 ka [*Tibaldi*, 2001] and on the NE flank of the Miocene Teno Volcano on western Tenerife [*Walter and Schmincke*, 2002]. In both scenarios the direction and scale of flank failure has been influenced by the orientation and geometry of bounding rift zones. Other examples from strato volcanoes include Shiveluch Volcano on the Kamchatka Peninsula which underwent several large sector collapses in the last 10,000 years, each event recurring within the confines of repeatedly failed flanks [*Belousov et al.*, 1999]. In Ecuador, Sangay Volcano is constructed within the collapse amphitheatres of at least two ancestral volcanoes (Sangay I and II) that underwent eastward-directed sector collapses [*Monzier et al.*, 1999]. *Friant et al.* [2003] describe recurrent large-scale collapse events affecting the development of the southeast flank of Montagne Pelée in the Lesser Antilles. Fig 1.2.22 illustrates, for most of these locations, how flank instability has developed preferentially within the confines of dismantled flank sectors under the influence of the near field stress (or edifice stress).

The hypothesis of structural control on the shape, symmetry and opening direction of the Caldera is reconcilable with the morphology, sub-structural geology and the time frame for the erosion of northern La Palma to its present state. The spatial extent of the escarpments generated by the collapse of Ancestral Taburiente have been partially delineated from the hydro-geological studies of *Bravo and Coello* [1979], *Coello* [1987], *Navarro and Coello* [1993]. It lies at a circumference of up to 1.8 km outside of the rim of the Caldera, enclosing and essentially supporting the amphitheatre bench zone. Based on the outcrop pattern of substratum beneath the Caldera and Cumbre Nueva escarpment, it is possible to elaborate on the total extent of the ancestral collapse structure. It should extend southwest along the linear side-wall (virtually in parallel with it) as far as the upper reaches of the El Time sequence and east of the Caldera towards the southern part of Puntallana. There is no evidence that it extends offshore from the bathymetric data of *Urgeles et al.* [1999].

The summit region of Taburiente was founded upon the same volcaniclastic substratum (the thick "agglomerates" described by *Gastesi et al.* [1966] and *De la Nuez,* [1983]) as the eastern and western flanks. One may stipulate therefore on the basis of this common substratum that both the flank and summit region were influenced by a similar stress field the magnitude of which may have been intensified by the SW tilted basement. It is proposed therefore that the summit region destabilized following the development of a southwest-facing deviatoric stress field that was initiated by the Cumbre Nueva lateral collapse.

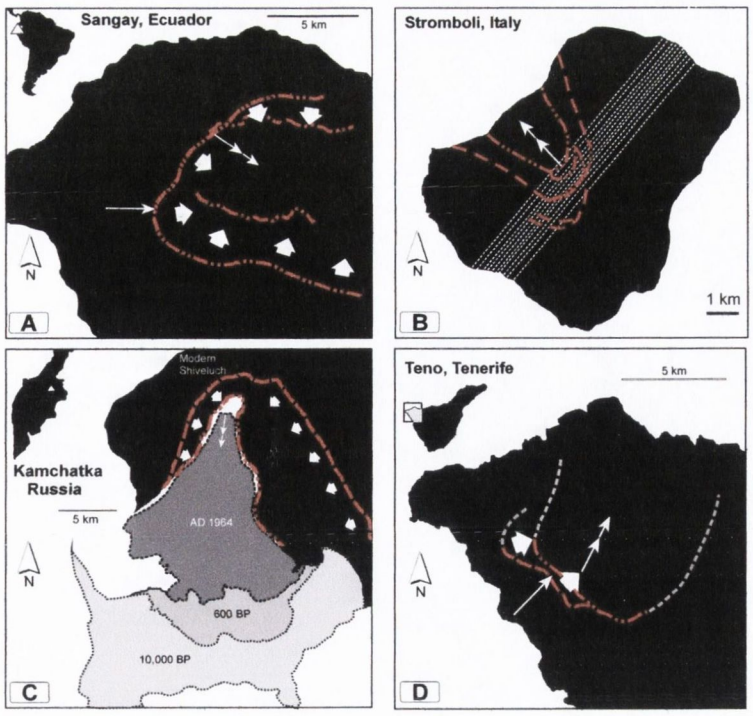


**Fig 1.2.22**. Examples of geometrically self similar (nested) collapse escarpments. A: The eastward-directed collapses of the composite Sangay Volcano, the southwesternmost active volcano in Ecuador [*Monzier et al.*, 1999]. B: North-westward-directed flank collapses (several chronologically separate events) on Stromboli Volcano, Aeolian, Arc, Italy; in each case the landslide was directed normal to the direction of dike injection (white stipple). [*Tibaldi*, 2001]. C: Successive, southward-directed debris avalanche deposits of Shiveluch Volcano, Kamchatka Peninsula, Russia [*Belousov et al.*, 1999]. Northeastward collapses of the Miocene Teno edifice, Tenerife, Canary Islands. [*Walter and Schmincke*, 2002]

Loading around the rim of the ancestral collapse caldera, as illustrated in Fig. 1.2.23, may have led to the development of SW-directed deviatoric stress, relieved in part by gravitational spreading of the western and eastern flanks. One possible scenario is that upon collapse of the west flank, the effects of lithostatic unloading left the summit region unbuttressed and critically unsupported towards the southwest as the stress levels became accentuated around the northern part of the new void space (i.e., the Cumbre Nueva embayment. Therefore, once the west flank began its momentum of failure, the un-supported summit region responded by decompressive collapse, scalloping the northeast segment of the Cumbre Nueva embayment. An alternative scenario, discussed further in Ch. 3.2, is that the summit collapse occurred synchronously with that of the west flank.

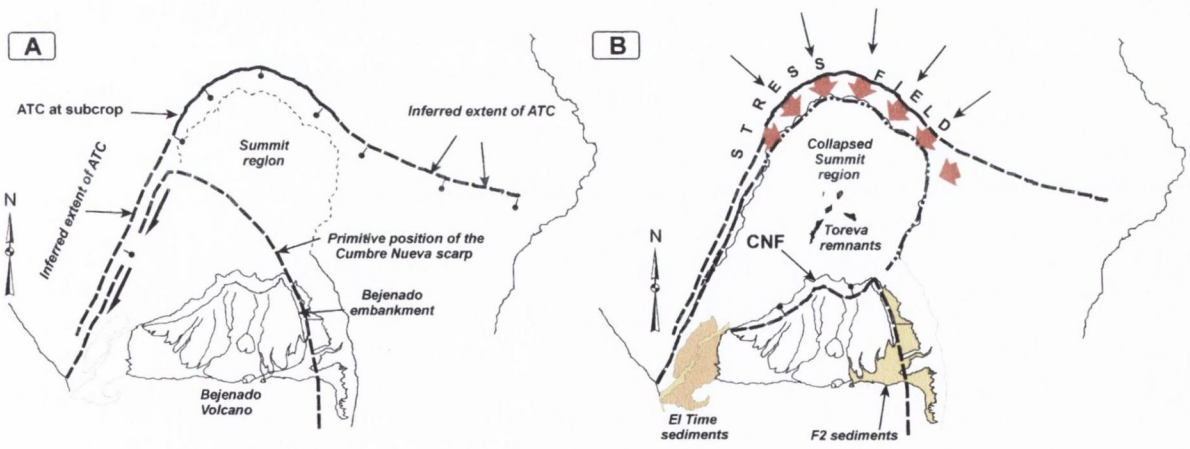


**Fig 1.2.23**. Structural elements inferred to have controlled the geometry and direction of summit region collapse. (A) Geometric relationship between the Ancesteral Taburiente collapse structure (ATC) and the Cumbre Nueva escarpment. (B) Suggested mode of formation of the Caldera de Taburiente. The circumferential stress field enables the unsupported summit to collapse southwestwards. The abbreviation CNF denotes the collapsed north flank of Bejenado Volcano.

The water table around the dismantled summit region subsequently experienced instantaneous draw-down to a new level that was subsequently over-run by an intra-collapse edifice (Bejenado stratocone). The extant drainage system developed subsequent to the collapse of the north flank of the stratocone inside the Caldera, possibly in the last 0.4 Ma [*Roa*, 2003]. Subaerial components of a debris avalanche deposit may exist beneath Bejenado Volcano, including toreva remnants from the Cumbre Nueva escarpment [*Roa*, 2003]. However the main body of the debris avalanche deposit was removed throughout the incision of the Angustias catchment area and remoblised offshore.

### 1.2.7. Conclusions

Amphitheatre-shaped landforms, that develop primarily by giant landslides (measuring between 5 and 10 km wide), are particularly common in the central parts of many oceanic island volcanoes in the Canaries, Reunion and Tahiti. The eponymous Caldera de Taburiente is perhaps a type-example of such a landform, owing to its geometry, symmetry, size and age relationships with the Cumbre Nueva escarpment and Bejenado Volcano. Here it is argued that the formation of the Caldera involved the collapse of the unsupported summit region of Taburienete Volcano, hence the deeply dissected inter-Caldera canyon terrain is merely a facet of post-collapse erosion since around 0.4 Ma. While erosion and associated epiclastic processes have clearly contributed significantly to the morphology and geology of northern La Palma, the alternative concept of an "*erosion' caldera*" is difficult to reconcile with the erosive regime that has prevailed in the islands' morphological development throughout the Quaternary.

The summit region of Taburiente developed within the confines of a pre-existing collapse structure upon the same volcaniclastic substratum that is exposed beneath the Cumbre Nueva escarpment. The geometry, location and, more specifically, the direction of the summit collapse appears to have been structurally controlled by the bounding headwalls of this ancestral collapse structure, and perhaps, by the load-bearing capacity of the substrate. This model of geometrically self similar (nested) collapse structures is comparable with volcanoes in contrasting tectonic settings. Further support for a collapse origin is drawn from comparisons, on the basis of erosional morphology (by fluvial processes) and relative age with the post-shield volcanoes of Tahiti Nui and northern Reunion (Indian Ocean), where large central depressions of equivalent dimensions have developed by giant landslides [e.g., *Clement et al.*, 2002; *Bachelery et al.,* 1996].

# 1.3 The Rift Zone Morphology of La Palma

Rift zone volcanism; be it a facet of the subaerial evolution or an inherited trait from the Pliocene seamount stage has had a paramount influence in the morphological development of La Palma. An excursus is presented on the implications of volcanism and tectonics in the evolution of the rift system.

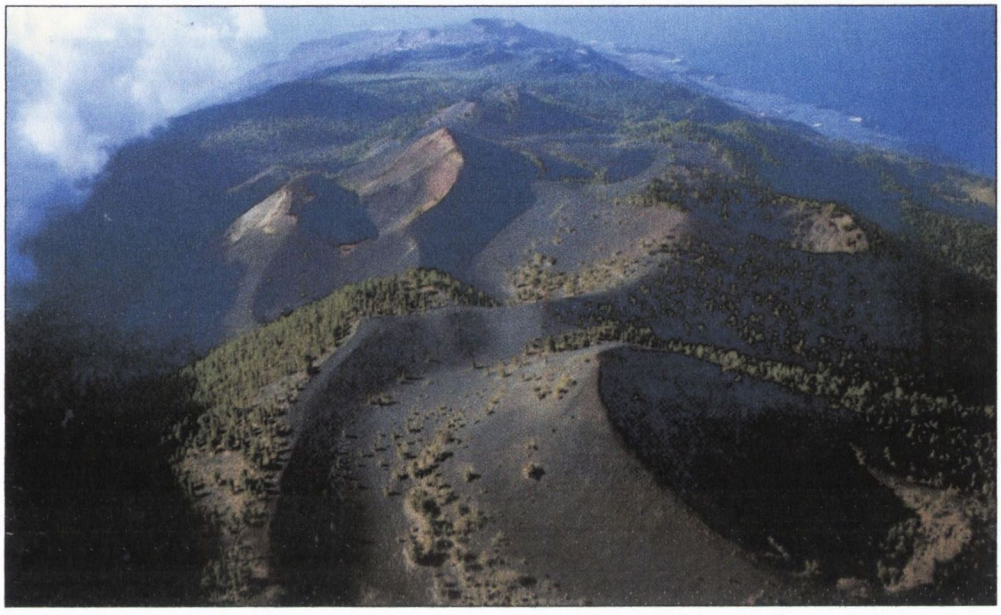

**Fig. 1.3.1.** View south along the ridge of Cumbre Vieja Volcano, showing the archetypal surface of a Canarian rift zone; compact groups of scoria cones, all Holocene to historic in age, are clustered along the N-S axis of the rift zone. Photo by Juan Socorro.

## 1.3.1 Introduction

La Palma is the emergent part of a large submarine volcanic complex that rises 4 km from the Atlantic Ocean floor [*Urgeles et al.*, 1998; 1999]. This section investigates the range of processes that may have influenced the morphological development of the subaerial volcanoes, particularly Taburiente/Cumbre Nueva, and how they should relate to the evolution of the submarine foundations. This primarily concerns the structure of the rift zones, the orientations of which control the shape of the volcanic complex. The rift zones vary in morphology from an array of 'fan-shaped' rifts in the north (Taburiente), to what remains of a 'coherent rift zone' (in the sense of *Walker* [1992]) - the Cumbre Nueva rift - in the south. It has been implied through radiometric/palaeomagnetic and structural studies that the rift zones were initiated late in the subaerial evolutionary history of La Palma (at around 0.8 Ma), overprinting a radial configuration of fissures [*Guillou et al.*, 2001; *Carracedo et al.*, 2001]. However, the bathymetric data indicate that the NW rift zone of Taburiente is the subaerial component of a much larger constructional feature [*Urgeles et al.*, 1999; *Masson et al.*, 2002]. Here it is proposed, on the strength of the available bathymetric data, together with GIS data on the subaerial morphology, and field data on the structure and configuration of dikes in the exhumed Pliocene basement, that the northern rift zones should be an inherited feature from the Pliocene seamount stage. This is in agreement with observations from seamount volcanoes throughout the ocean basins that develop from simple early conical shapes, later to more complex stellate morphologies at or around the 3 km height interval [*Mitchell*, 2001]. Since sediments form an important component of the pre and syn-volcanic stratigraphy of the Canary Basin [e.g., *Schmincke and Sumita*, 1998; *Urgeles et al.*, 1998; *Steiner et al.*, 1998], it is possible that hot-spot related crustal thickening has been influenced to some extent by loading and deformation of the various pre and syn-volcanic substrates. This is known to occur in Hawaii [e.g., *Morgan and Clague*, 2003] and possibly Reunion [*De Voogd et al.*, 1999], and has been inferred for Tenerife using analogue modelling [*Walter*, 2003].

### 1.3.2. Rift zones, rifting and gravitational spreading; general aspects

Rift zones form the structural framework and influence the morphological development of many oceanic island volcanoes [e.g., *Guest et al.*, 1999; *Eakins et al.,* 2003]. They act as a conduit for the episodic intrusion and storage of magma from various levels in the crust [e.g., *Clague and Delinger*, 1994; *Hansteen et al.*, 1998], and ultimately they convey magma to the surface. A coherent rift zone develops by the repetitive emplacement of planar intrusions, localized along elongate axes that are narrow with respect to the length of the volcanic edifice (e.g., Kĭlauea, Hawai'i [*Walker*, 1992] and Taveuni, Fiji [*Cronin*, 2001]). Side-by-side clustering of intrusive sheets is observable at outcrop from the exhumed "coherent intrusive complexes" of La Palma, Fuerteventura and Koolau Volcano, on the Hawaiian island of Oahu [*Staudigel et al.*, 1986, *Stillman*, 1987; *Walker*, 1986; 1992]. Observations at this level imply that significant extension must occur within a volcanic edifice and its supporting crust in order to spatially accommodate the many thousands of dike members that constitute a rift zone [e.g., *Marinoni*, 2001].

Rift zones display salient contrast in topography, curvature and aspect ratio, often in the same edifice, exerting a strong control on overall structural development parameters. The along-axis variation in morphology and structure has prompted much research into how the strain of repetitive dike intrusions is distributed in space and time, and how the deformation is accommodated during volcano growth [e.g., *Delaney et al.*, 1998; *Owen et al.*, 2000]. Part of the solution comes from multi-disciplinary studies such on seismicity, ground deformation, bathymetric/submersible surveys and numerical simulations [e.g., *Borgia*, 1994; *Owen et al.*, 2000; *Lipman et al.*, 2001]. On Hawai'i, specifically the adjacent shield volcanoes Kĭlauea and Mauna Loa, the deformation is taken up by seaward gravitational spreading of the flanks along deep-seated decollements with cooperative slip along arrays of listric normal faults upslope [*Delinger and Okubo,* 1995; *Morgan and Clague,* 2003]. Displacement along these structures accommodates most of the expansion and migration of the rift systems through episodes of seismic and aseismic slip [*Borgia and Treves*, 1990; *Delaney et al.*, 1998; *Cervelli et al.*, 2002]. As the south flank of Kĭlauea and the west flank of Mauna Loa are driven seaward by their own gravitational momentum, they undergo shortening at the toe of the edifice and uplift of the frontal bench located offshore, accreting and deforming volcaniclastic strata in the process [*Lipman et al.*, 2002, *Morgan and Clague*, 2003]. The balance between vertical accretion of extrusive rocks and their counterpart intrusions (loading) and lateral mass transfer (spreading) is thus maintained by extension of the summit and compression around the base during and after episodes of rifting [*Borgia*, 1994]. This concept of gravitational or volcanic spreading presents a unified perspective on how rifting, flank deformation and giant landslides are orchestrated in space and time [*e.g., Lipman et al.*, 2002].

At a lithospheric scale, the localization and orientations of the rift zones on the Canary Island volcanoes have been controlled by regional stress regimes namely 'African and Atlantic' [*Hernandez Pacheco and Ibarrola*, 1973; *Anguita and Hernan*, 2000] (discussed later). However, the existing bathymetric and seismic data have not delineated structures that are diagnostic of gravitational spreading in other island groups (e.g., frontal benches, sediment accretion, deep-seated decollements), where rift zones exist upslope [*Mitchell et al.*, 2002]. Nevertheless, some workers have modelled how gravitational spreading might be an important element in the development and migration of rift zones, given the abundance of pre and syn-volcanic sediment in the Canary basin, and how these could deform through loading [*Walter*, 2003].

Geometrically, the Canarian rift zones are configured along triple junctions (e.g., El Hierro and Tenerife [*Navarro and Farrujia,* 1989; *Anguita and Hernan*, 2000]), or as structures with a prominent linear trend, as observed from the exhumed basement complexes (i.e., Fuerteventura, [*Stillman*, 1987]). On the younger western islands' the rift zones are observed to bound large embayments, formed by lateral collapses of the flanks [*Carracedo et al.*, 1999b; *Gee et al.,* 2001a].

Evidently, there is a limit to the amount of gravitational stress, rift zone dilation, seismic shock and other phenomena that a mobilized flank can facilitate, before critical dis-equilibrium and edifice failure occurs [*Ellsworth and Voight*, 1995; 1996; *Iverson*, 1995; *Day*, 1996].

### 1.3.3 The morphology of La Palma

#### 1.3.3.1. Offshore data.

The shape of La Palma rising from the sea floor is that of a flattened double cone, between 80 and 95 km in basal diameter and nearly 7 km in elevation (Fig. 1.3.2). The salient constructional features of the submarine superstructure are the north-western slopes, and the narrow southern ridge that forms the submarine continuation of Cumbre Vieja Volcano [*Urgeles et al.*, 1999, *Mitchell et al.*, 2002]. Herein these features are referred to as the 'Puntagorda Rise' and 'Fuencaliente Ridge' respectively (Fig. 1.3.2). Dimensional analyses of these features show steepening upward profiles, with the median slope values showing a non-linear variation with depth, reflecting variable curvature of the flank profiles [*Gee et al.*, 2001b; *Mitchell et al.*, 2002] (Fig. 1.3.4a). The topography of the Puntagorda Rise extends for 43 km, merging upslope onto the subaerial NW rift zone of Taburiente Volcano [*Urgeles et al.*, 1999; *Masson et al.*, 2002] a theme that is addressed in Ch. 3.2.

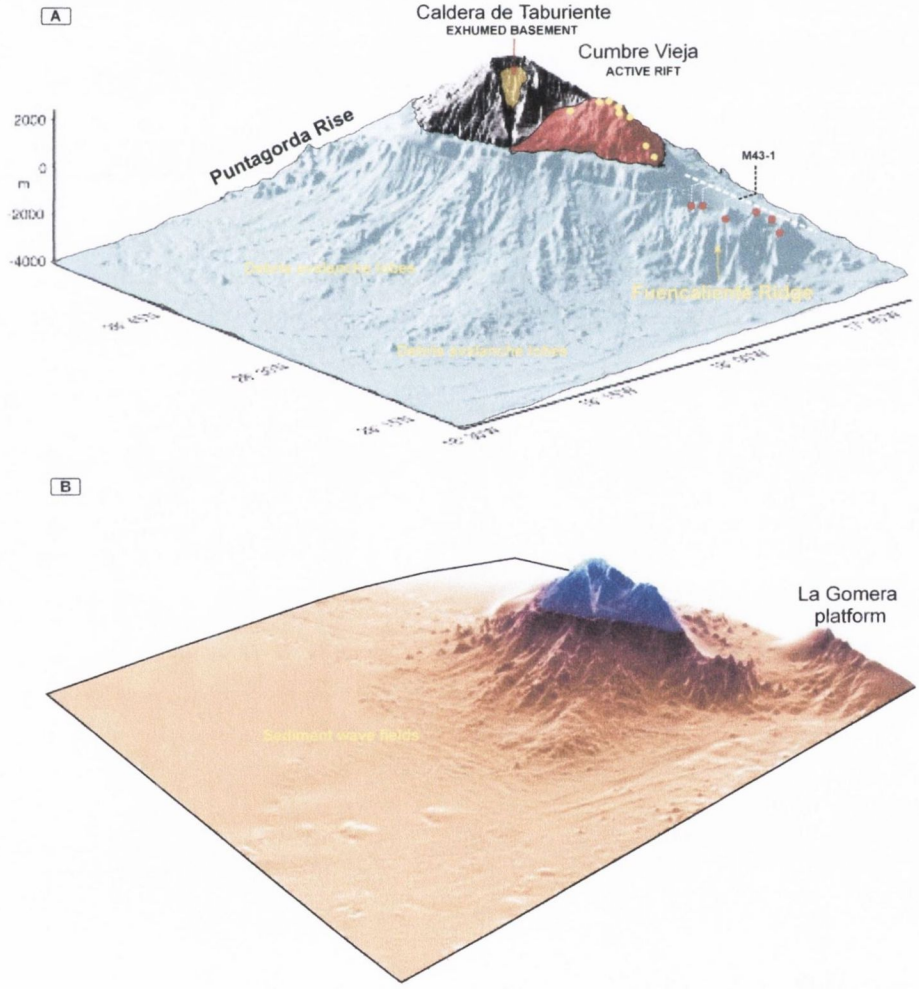


**Fig. 1.3.2**. Perspective images of La Palma and its submarine construct. A: View of the mass wasted western flank and the lobate debris avalanche deposits below it. Viewed from the southwest, from an elevation of 20° and illuminated from the north. Abbreviation: CdT, Caldera de Taburiente. Vertical exaggeration = 6. Red dots are dredge sample sites during cruise M43-1. Stippled line is the axis of bathymetric mapping during the first leg of the cruise. Yellow dots are historic eruption vents. Modified from *Urgeles et al.* [1999]. B: Distant perspective of La Palma's volcanic system showing the proximity of the La Gomera platform and the sediment wave field around the insular edfice. Modifed from *Urgeles et al.* [2000].

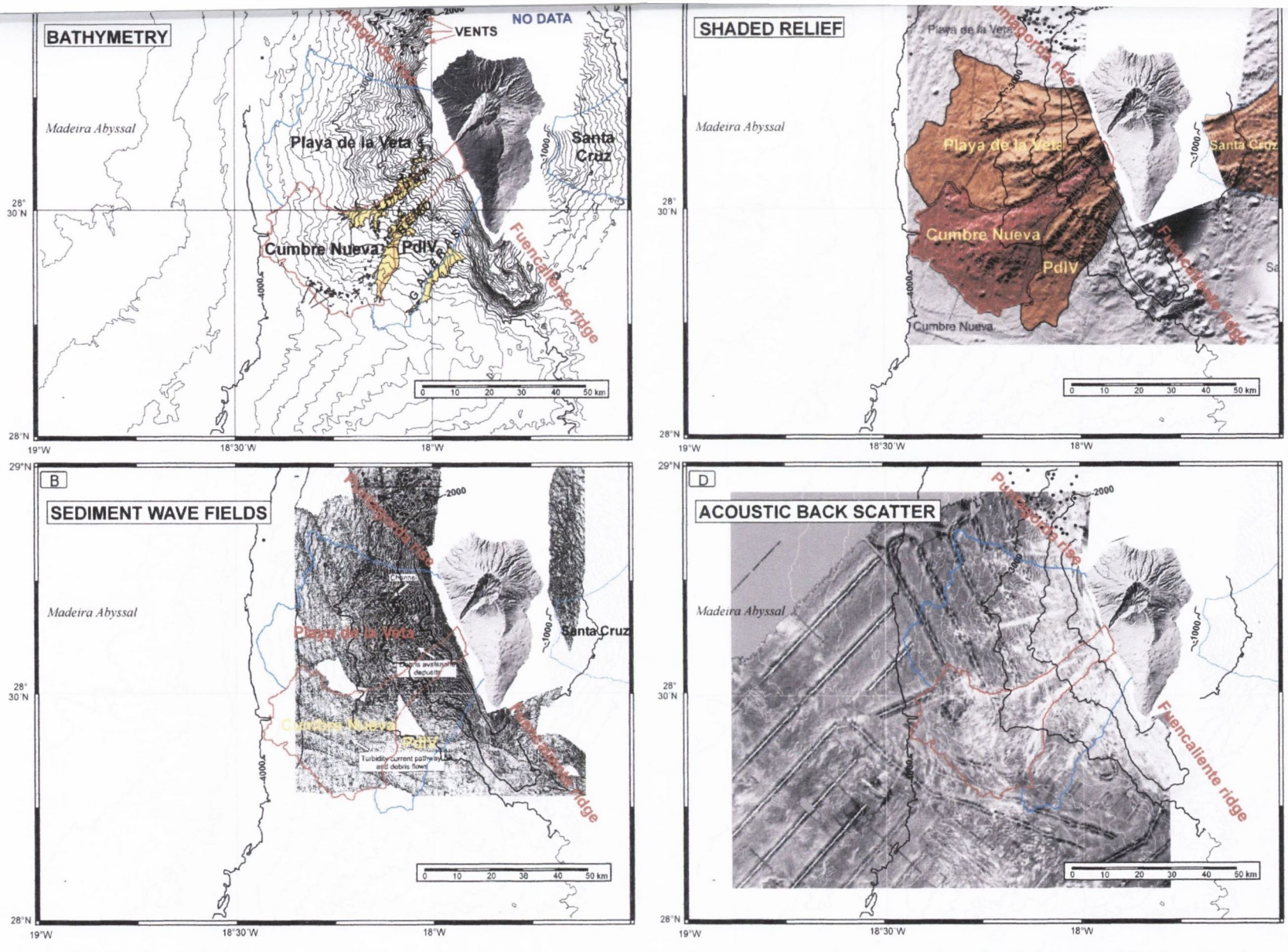


**Fig. 1.3.3**. Compiled bathymetric and seismic data from around La Palma A. Bathymetry with major constructional ridges and debris avalanche lobes. Modified from *Urgeles et al.* [1999]. Bathymetry provided by *D.G. Masson.* B. Sediment wave fields around La Palma [*Wynn et al.*, 2000]. C. Shaded relief image of the submarine slopes and major debris avalanche deposits. Modified from *Masson et al.* [2002] D: acoustic back scatter showing drainage systems. Modified from *Urgeles et al.* [1999] Shaded relief image of La Palma provided by *J.C.Carracedo.* Abbreviation PdlV: Playa de la Veta.

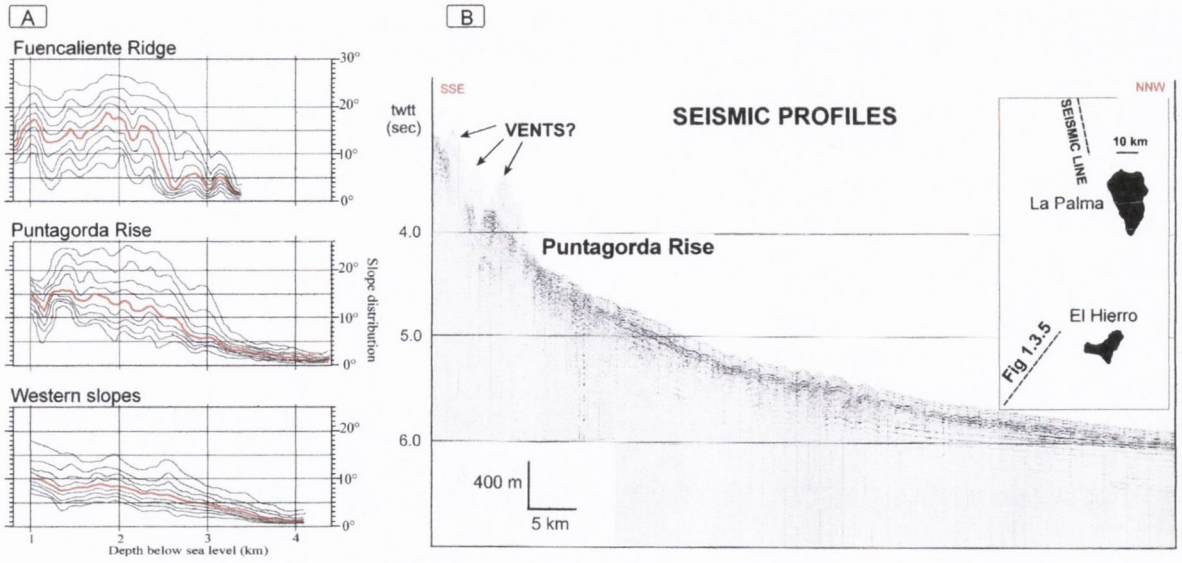


**Fig. 1.3.4.** A: Slope distribution graphs for the submarine slopes off La Palma. The lines show slopes corresponding to various percentiles of the distribution: red lines are the 50% level (median slope). The grey lines are successive 10% levels. Modified from *Mitchell et al.* [2002]. B: Seismic profile of the NW submarine slopes Modified from *Wynn et al.* [2000].

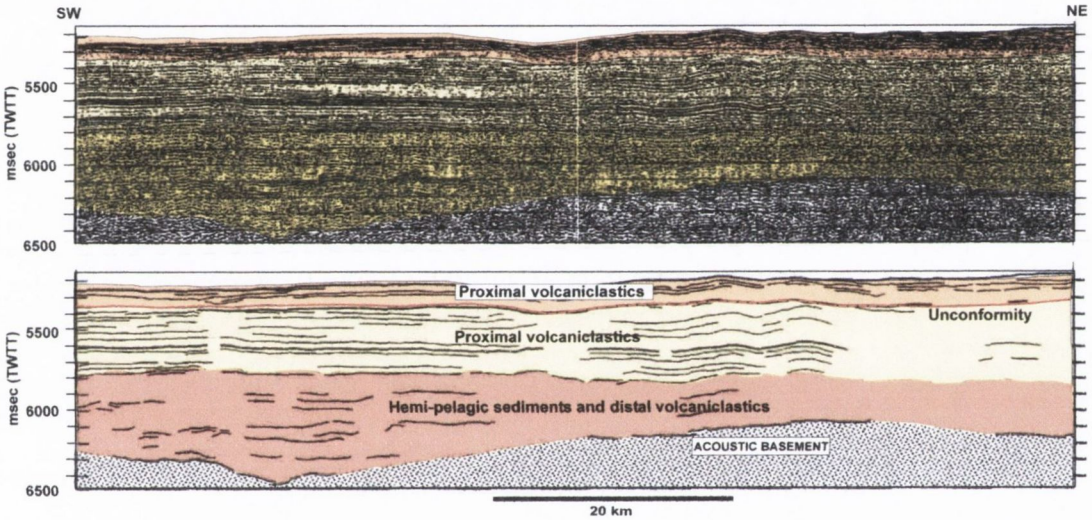


**Fig. 1.3.5.** Seismo-stratigraphic section west of El Hierro with interpretation based on the amplitude of reflections. Modifed from *Urgeles et al.* [1998]. See Fig. 1.3.4 for location of section.

The submarine construct around La Palma constricts southward (above the –2000 m contour), eventually narrowing to around 14 km along the steep-sided and locally embayed Fuencaliente Ridge. The ridge itself inflects eastward for a total of 20 km before descending onto the ocean floor at around -3900 m. Conical-shaped features, 71 in total, are distributed along the broad slopes of the Puntagorda Rise and have been previously interpreted as aligned vents [*Mitchell et al.*, 2002] (Fig. 1.3.3a). Fuencaliente Ridge is also surfaced by clustered conical-shaped features (identified during Meteor cruise M43-1 [see *Abratis et al.*, 2002]). Dredge hauls from the ridge (Fig. 1.3.2) during cruise M43-1 were frequently coated in layers of globular manganese between 3 and 5 cm thick, possibly indicative of suppressed volcanic activity relative to subaerial Cumbre Vieja. The rocks are alkali basalts and basanites with lesser amounts of tephrite, hawaiite, trachyte and phonolite and their altered equivalents [*Abratis et al.*, 2002].

Giant debris avalanche deposits, estimated to encompass a surface area of around 2000 km$^2$, extend onto the lower west flank from the direction of the land-slipped subaerial sectors, and also from the eastern submarine slopes [*Urgeles et al.*, 1999; *Krastel et al.*, 2001] (Fig .1.3.3a).

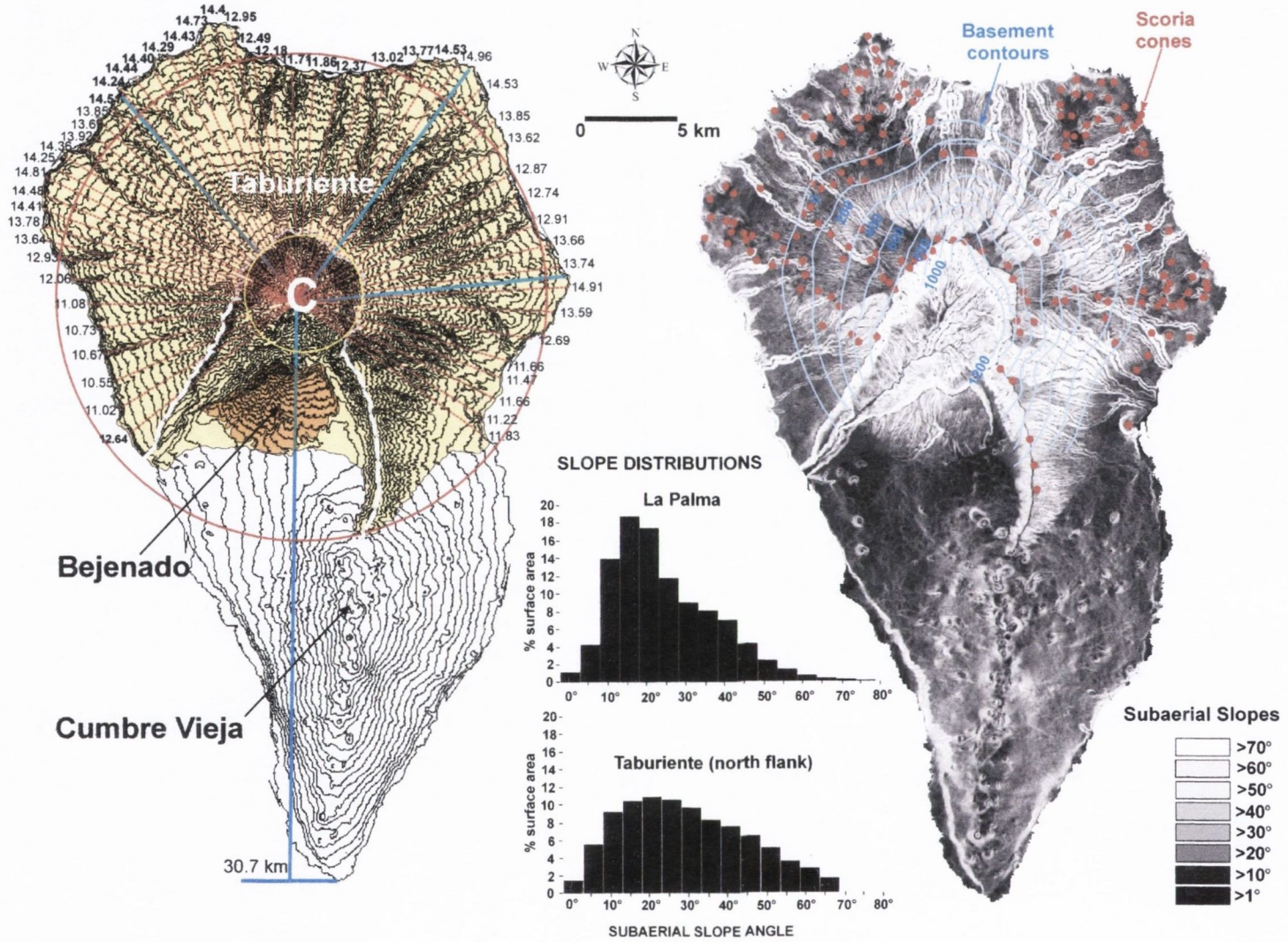


**Fig. 1.3.6**. A. Topographic map of La Palma showing the mean radius of Taburiente Volcano relative to the centre of the Caldera (marked C). The red circle marks the average radius of La Palma (13.12 km). Yellow circle is the partial circumference of the Caldera. The contour interval is 100 m. The flank length variation is plotted in Fig. 2.1.7b. The blue lines are the principal elongation axes of the island while the stippled white line is the relic Cumbre Nueva escarpment. B. Basement contours [*Bravo and Coello,* 1979] and relic scoria cones with a base map of slope distributions.

Other features along the western submarine slopes include well-developed flat-floored channels (previously named channels A, B and C [*Urgeles et al.*, 1999]), that are herein referred to as channels Laguna, Remo and Galeras from localities on the coastline. The 11 km thick oceanic crust underlying La Palma is of Jurassic age (145 to 148 Ma) [*Roest et al*, 1992], and is overlain by numerous seismo-straigraphic sequences over 1 km thick, interpreted as pelagic sediments and later shield-stage volcaniclastics (Fig. 1.3.5) [*Urgeles et al.*, 1998]. Expansive sediment wave fields, covering ~20,000 km$^2$, extend north and northwest of La Palma (Fig. 1.3.3b) [*Wynn et al.*, 2000]. Piston cores recovered from surficial sediments draping the lower submarine slopes in this sector contain volcaniclastic turbidites and pelagic/hemipelagic sediments.

### 1.3.3.2. Onshore/GIS data

The island of La Palma has an elongate roughly triangular shape measuring 45.6 km (N-S) and has a maximum east-west width of 27.5 km. The island measures 45.6 km north to south and is 27.5 km wide and encompasses a planimetric area of 784.168 km$^2$, a surface area of 904.554 km$^2$ and a volume of 594.5Km$^3$. The northern part, forming Taburiente Volcano, has an average radius of 13 km, although the lower flanks extend along three sectors (E, NE and NW); each protrusion measures around 14 km in length (Fig. 1.3.6 and 1.3.7b). In profile, the shape of subaerial Taburiente and the on-lapping Cumbre Nueva edifice resembles a composite shield/strato-cone, made incomplete by the decapitated summit region (Fig. 1.1.6). The island slopes are exceptionally steep, with 37% of the surface area >30°, a result in part of the high relief generated by catastrophic slope failures and accentuated canyon development since the termination of the shield-building stage (Fig. 1.3.6). The relatively smooth-surfaced Cumbre Vieja Volcano shows a southward increasing aspect ratio with the value of $\Pi_1$ reaching as high as 0.44. The arcuate segment of the Cumbre Nueva escarpment, located inland, forms a topographic saddle between Taburiente and Cumbre Vieja.

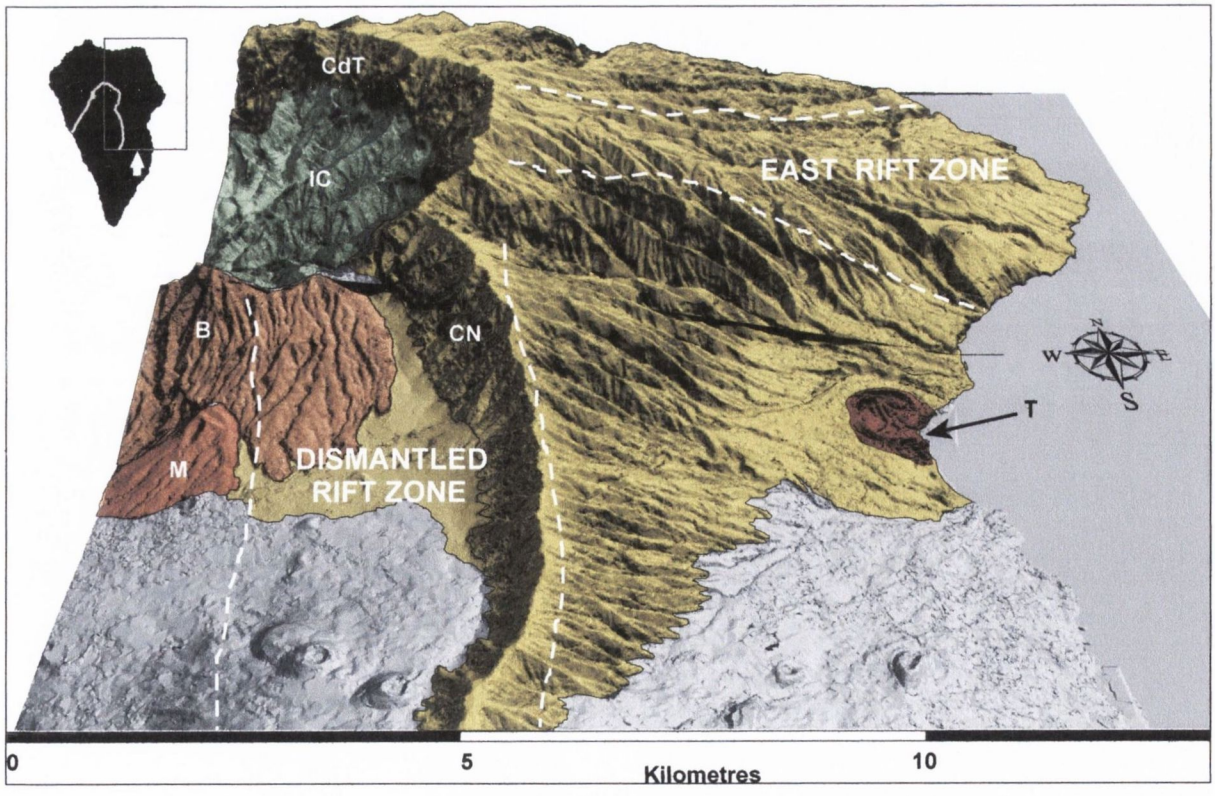


**Fig. 1.3.7**. Shaded relief image of the northwestern side of La Palma showing, in white stipple, the inferred width of the dismantled south rift zone (Cumbre Nueva edifice), and the protruding morphology of the east rift zone. Abbreviations: B: Bejenado Volcano. CdT: Caldera de Taburiente, CN: Cumbre Nueva escarpment, IC: the exhumed intrusive core , M: Montaña la Hiedra, a parasitic vent of Bejenado. T: La Calderata, a phreatomagmatic tuff cone at the port of Santa Cruz de la Palma – dated at around 1 Ma [*Carracedo et al.*, 2001]. Cumbre Vieja lavas and vents are in the foreground.

The eroded west-facing walls of the escarpment are quite steep (inclined at around 47°), and are enveloped by Cumbre Vieja lavas and pyroclasts at an elevation of 1453 m above sea level, at a distance of 12.45 km from the centre of the Caldera. The cut-away shaded relief images (Figs. 1.3.7 and 1.3.8) show this prominent morphological feature together with the rift zones and the relief variation between the deeply dissected northern shield and the relatively smooth-sloped ridge of Cumbre Vieja.

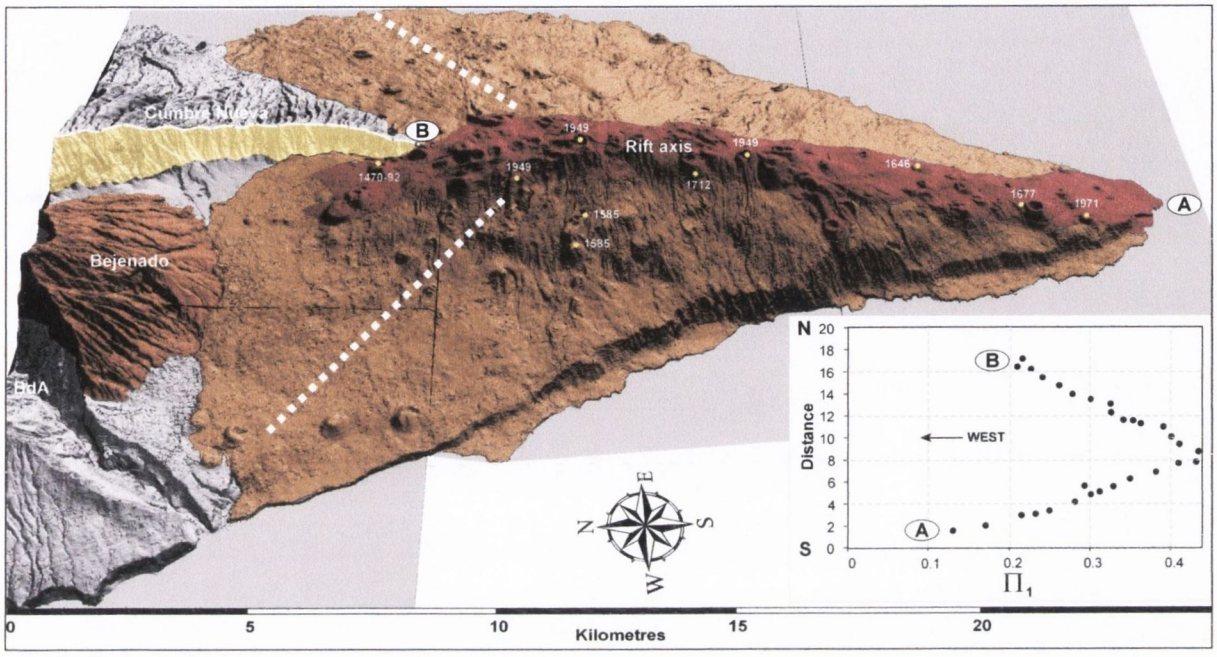


**Fig. 1.3.8.** Shaded relief image of southern La Palma. Stippled white lines represent subordinate rift zones of Cumbre Vieja that have been apparently inactive for the last 7000 years [*Guillou et al.*, 1998]. Historic vents in yellow. The inset graph depicts the north to south aspect ratio $\Pi_1$ distribution across the Cumbre Vieja rift axis.

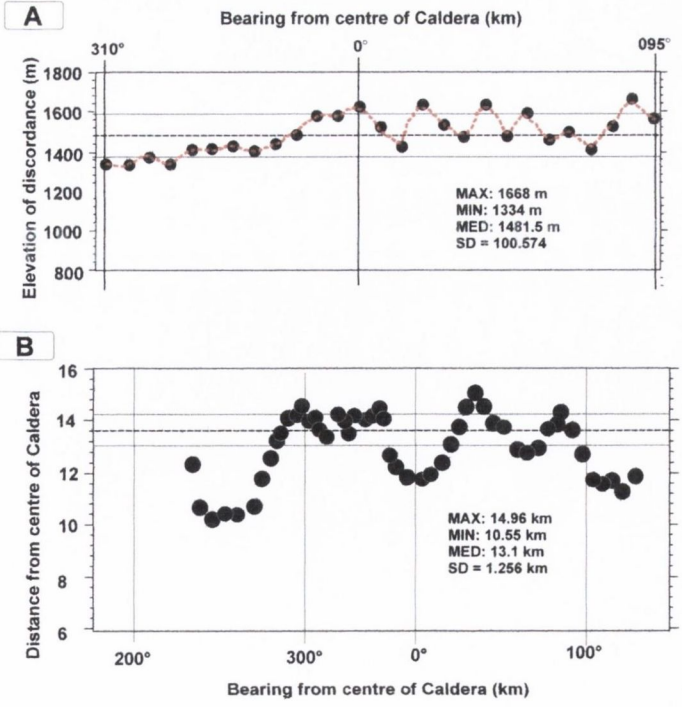


**Fig. 1.3.9.** A: Topography of the discordance between the intrusive core and the shield volcanics in an area that is largely inaccessible. B. The flank radius of Taburiente Volcano between bearing 234°W and 128°E. See Fig. 1.3.6 for construction lines.

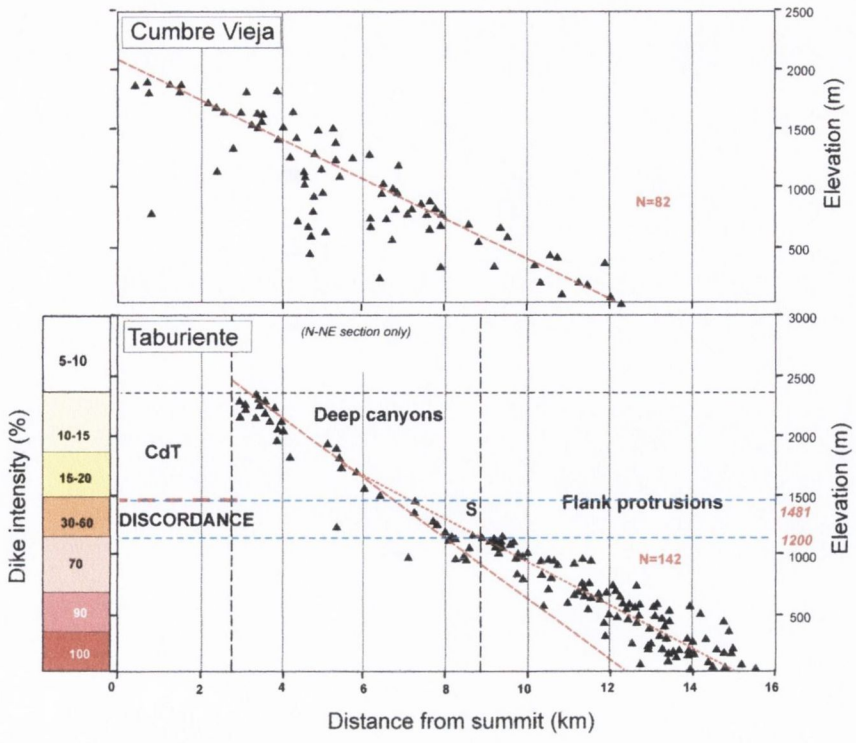


**Fig 1.3.10.** (a) Plots of elevation above sea level versus radius for the Holocene vent population of Cumbre Vieja and the relic vent population of Taburiente with interpolated lines of best fit. The vent positions were acquired by analysing digital elevation models, and aerial photographs and existing geological maps [*Carracedo et al.*, 2001]. A total of 142 vents were identified. See also Fig. 1.3.16.

Over half of the elevation of northern La Palma is taken up by the uplifted seamount basement (Figs. 1.1.4 and 1.3.2). The irregularity of the discordance separating the high-level intrusive core and the overlying shield is plotted in Fig. 1.3.9a. Emission centres are clustered below the 1200 m flank contour, where the slope of the subaerial cone inflects and shallows towards the protruding lower flanks. Fig 1.3.10 is a comparative plot of the distribution of cones versus their elevation for Cumbre Vieja and Taburiente. For the latter the mean stratigraphic height of the discordance is included. The cone distribution data for Taburiente have a tendency to reflect on the NW rift zone (where vents are most abundant) whereas the slope inflection is not as well developed on the NE and E rift zones.

### 1.3.3.3. Dikes in the intrusive core and the subaerial shield.

Dikes record the passage of magma from various levels in the crust, propagating in directions and along inclinations that are controlled by the stress field in the country rock, and by the magmatic pressure gradient throughout the length of the intrusion [e.g., *Walker*, 1989; *Gudmundson et al.*, 1999]. The plane of dike/sill propagation is often perpendicular to the direction of the minimum principal compressive stress ($\sigma_3$) [*Anderson*, 1937]. Quantitative analyses of dike orientations and other major structures (e.g., normal faults, shear zones and folds) have been used to constrain the direction of rift extension and the palaeostress evolution of the older, dismantled Canarian volcanoes through different geological periods of rift development*. In active volcanoes, the distributions of vents can be studied to make inferences on magmatic processes, since vent distributions/elongations are the surficial expression of a volcano's intrusive structure and can be used as a proxy for the stress field orientation [e.g., *White and Schmincke*, 1999; *Mazzarini and Armienti*, 2001, *Bosworth et al.*, 2003].

The dikes on northern La Palma are exposed at two distinct structural/stratigraphic levels: the shield and the unroofed intrusive core. Correlations between the directional maxima of dikes, the distribution of flanking scoria cones, together with the morphology of the edifice, can be used in conjunction with age data to make inferences on the temporal development of the rift zones. Quantitative analysis of dikes and normal faults on Taburiente suggests that the stress field (between 1.7 and 1.2) was controlled by radially compressive (volcanic) and by regional tensile stresses of tectonic origin [*Fernandez et al.,* 2002]. Four temporally and structurally distinct groups of planar intrusions have been recognised in the exhumed basement complex, on the basis of their structural relationships and by the relative ages of a population of 1200 intrusions [*Staudigel et al.*,1986; *Fernández et al.,* 2002]. The seamount feeder dikes of group 1 (hereafter G1) were emplaced between 4 and 2.9 Ma and were later tilted to their present inclinations due to differential uplift caused by inflation of the seamount [*Staudigel and Schmincke*, 1984]. Sills (hereafter G2) coeval with or younger than G1 were emplaced parallel to the extrusive layering in the seamount, prior to the onset of subaerial volcanism (>1.6 Ma) [*Staudigel et al.*, 1986]. The vertical continuity of G1 and G2 is disrupted abruptly at the interface between the intrusive core and the overlying shield volcano (the discordance in Fig. 1.2.7). Vertical to subvertical dikes, correlated with the subaerial shield (hereafter G3), bisect G1 and G2.

From these and other studies it has emerged that volcanism on northern La Palma developed through radial eruptive fissures [*De la Nuez*, 1983; *Féraud et al,* 1985*; Staudigel et al.*, 1986], with a prominent extension to the south (Cumbre Nueva), later recognised as a dismantled rift zone, forming a discrete volcanic edifice [*Navarro and Coello*, 1993; *Ancochea et al.*, 1994] (Fig. 1.3.9). Island-wide mapping, with structural observations from galerías and radiometric/palaeomagnetic cross-correlations, were used by *Carracedo et al.* [2001] and *Guillou et al.,* [2001] to temporally constrain the development of volcanism on La Palma. These studies revealed the development of diffuse rift zones, extending to the northeast and to the northwest (Fig. 1.3.9d), late in the evolution of the subaerial shield, roughly coinciding with the Matuyama-Brunhes polarity transition (0.779 Ma) (Fig. 1.3.9). By this rationale, the transition in dike configuration from radial fissures to rift zone volcanism took place over 0.4 Ma after the partial collapse of Ancestral Taburiente (dated ~1.2 Ma [*Ancochea et al.*, 1994]).

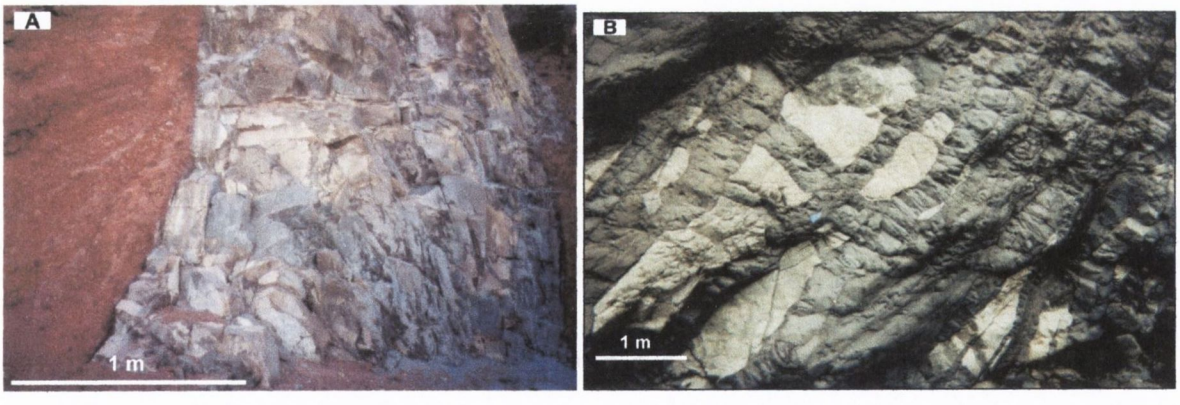


**Fig. 1.3.11.** (a) An obliquely truncated dike penetrating and deforming stratified scoria at the summit region of Taburiente; Locality: Road cut approaching Roque de Los Muchachos. (b) Dike plexus cutting meta-trachytes in the seamount series. Location: Upper course of the Bco. De Las Angustias.

*For Fuerteventura, $\sigma_3$ is reported to have been orientated E-W then WNW-ESE from the Late Oligocene to Early Miocene [*Stillman*, 1987; *Fernandez et al.*, 1997]. For the Miocene of Tenerife $\sigma_3$ was orientated NE-SW [*Marinoni and Gudmundson*, 2002] and, for the Plio-Pleistocene of La Palma, NW-SE [*De la Nuez*, 1983]. In Lanzarote, $\sigma_3$ varied from WNW-ESE (Miocene to Pliocene) to NNW-SSE in the Late Pleistocene-Holocene [*Marinoni and Pasquare*, 1994].

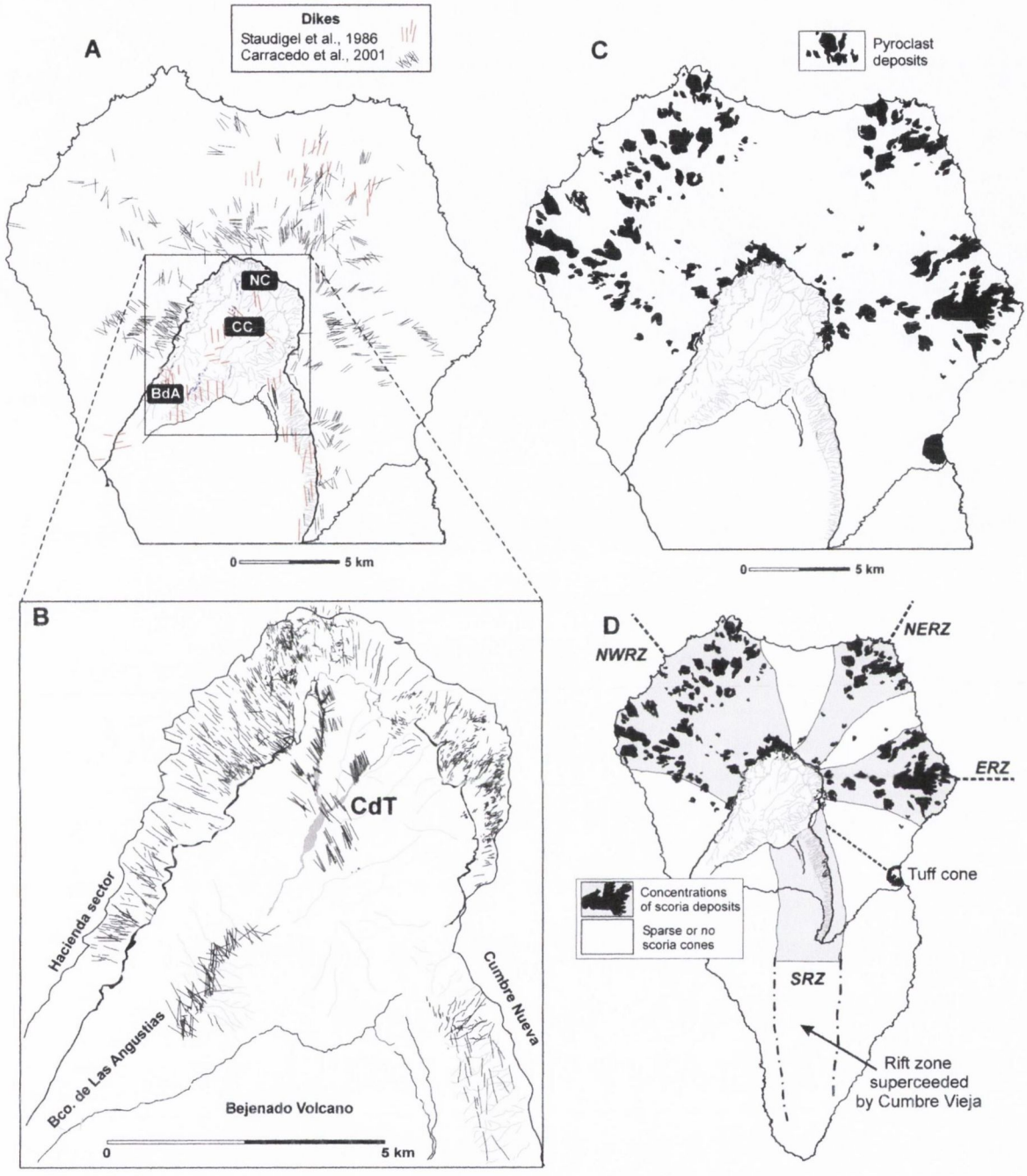


**Fig. 1.3.12.** Summary of dike orientations and pyroclasts distributions on northern La Palma. A. Dike orientations from *Staudigel et al.* [1986] *Carracedo et al.*, [2001]. Datasets were geo-referenced in MAP INFO 7. Abbreviations: BdA – Bco. De Las Angustrias, NC – north Caldera and NCC – north central Caldera. See rose diagrams in Fig. 1.3.11. B. The distribution of pyroclastic deposits on northern La Palma [*Carracedo et al.*, 2001]. C. Tracing of dikes from 1:5000 ortho-photo's and 1:15,000 aerial photos. D. Interpolated zonation of rift zones on La Palma with the speculative continuation of the Cumbre Nueva or South Rift Zone (SRZ). The abbreviations ERZ, NERZ, NWRZ refer to the east, northeast, and northwest rift zones.

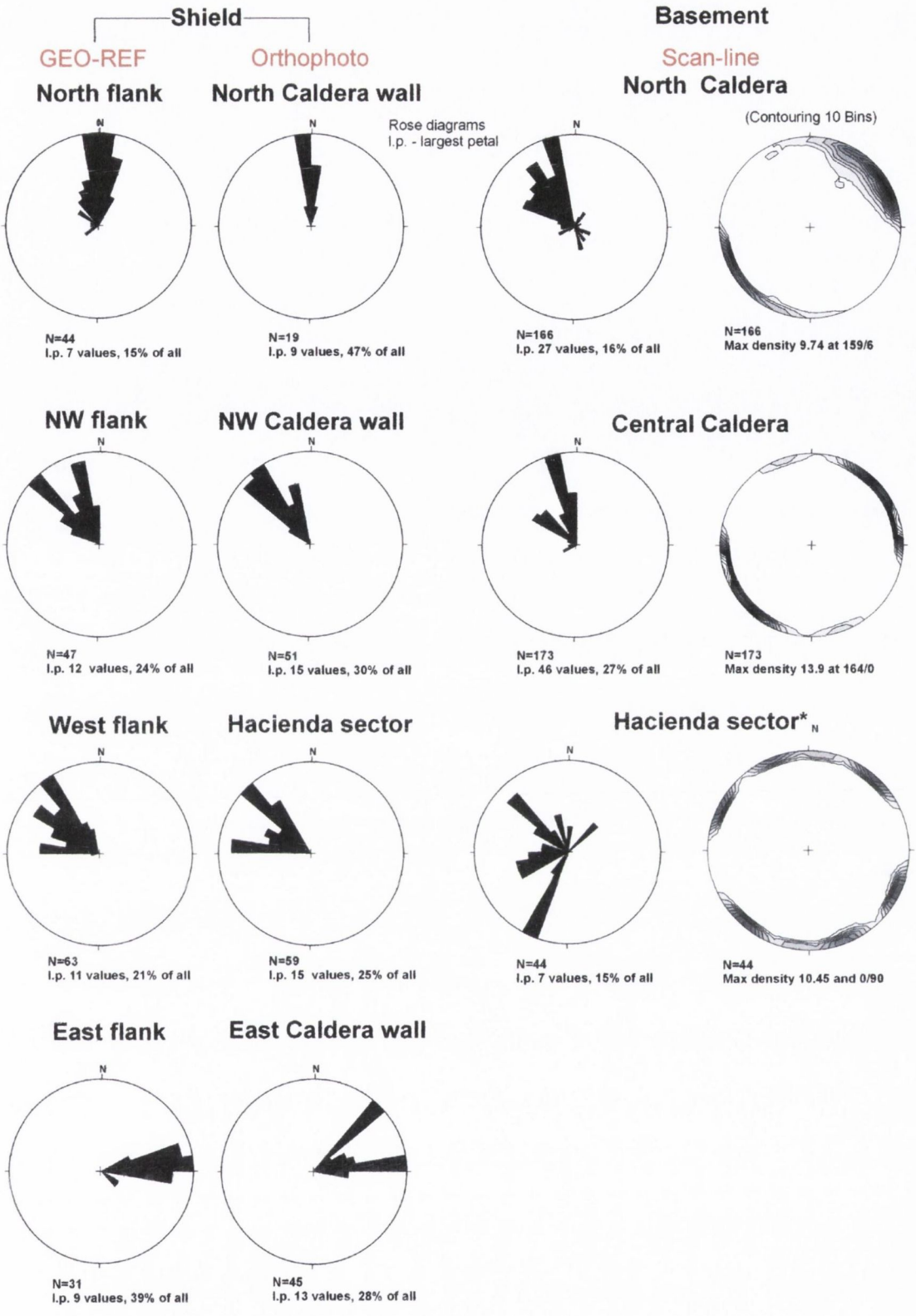


**Fig. 1.3.13**. Rose and contour diagrams (poles to planes, Schmidt - equal area lower hemisphere projection.). GEO-REF are dike orientation data geo-referenced in MAP INFO 7 from *Staudigel et al.* [1986] and *Carracedo et al.* [2001]. Orthophoto represent linear features interpreted from 1:5000 aerial images. Scanline represents field measurements.

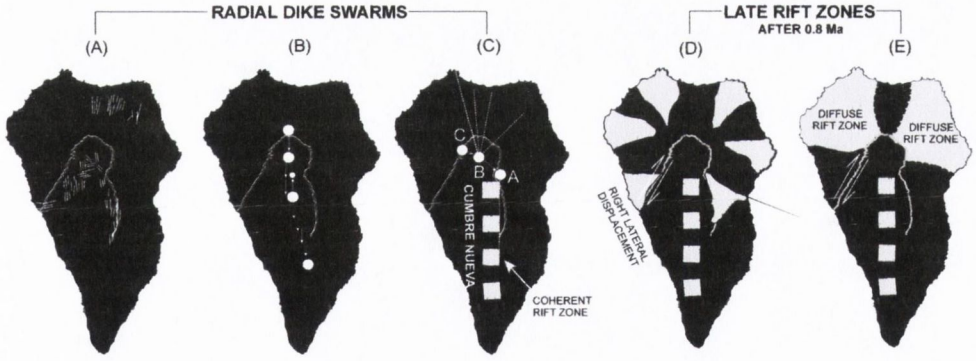


**Fig. 1.3.14.** Studies of dike orientations on La Palma. (A) White lines are dikes. Data from *Staudigel et al.* [1986]. (B) Southward migrating volcanism. Data from *Navarro and Coello* [1983]. (C) Volcanic centers and the southward migration towards rift-centred volcanism [*Ancochea et al.,* 1994]. (D) Late multi-axial rift zones overprinting a radial configuration [*Carracedo et al.*, 1999b]. (E) Broad, rift zones diffusing from the summit region [*Carracedo et al.*, 2001].

The orientations of dikes in the subaerial sector, delineated stereoscopically from paired images and from ortho-photos, together with compilations from previous studies, are illustrated in Fig. 1.3.10a. In the western part of the Caldera, sections of the intrusive core were measured along scan-lines, with the results plotted in Fig. 1.3.11. The subaerial dikes (Fig. 1.3.9a) are typically sub-vertical often displaying sinuous, jagged trajectories and are often observed to cross cut and inter-lace with other sheeted intrusions.

In the intrusive core, dikes and equally abundant sills are tightly packed at outcrop (100% rock mass), invariably metamorphosed [*Staudigel and Schmincke*,1984] (or metasomatized), and have a maximum width of 2.2 m and a minimum of 0.09 m (i.e., as apophyses and stringers). The dike plexus in Fig. 1.3.11b is on the periphery of the intrusive core. In the central, north and north-western part of the Caldera (the localities of Playa de Taburiente, Bco. Almendro Amargo and Bco de los Cantos) the prevailing dike orientation is NW and NNW, conforming with the observations of *De la Nuez* [1983]. This trend is further reflected by the dikes that transect the shield volcanics, visible from the Caldera walls and outboard of the Caldera (Fig. 1.3.12a,b). Detailed dike orientation data from the eastern part of the Caldera were not recorded[T] and precise correlations between dike orientations are difficult. However, dikes in the eastern and north-eastern parts of Caldera wall, and the adjacent flank, trend toward the east or northeast. Well-preserved scoria cones are concentrated on the protruding eastern and north-eastern flanks, suggesting a structural link with feeder dikes, at least in the subaerial section. Each cluster of scoria cones is separated from the other by flanking lavas where vents are rare or absent (Fig 1.3.10c,d). The Cumbre Nueva escarpment reveals a stratigraphy of eastward tilted lavas, bisected by swarms of N-S orientated dikes. *Carracedo et al.* [1997; 1999b] suggest that the axis of the dismantled Cumbre Nueva rift zone was positioned a kilometre or so to the west of the present escarpment which is the peripheral part of the former rift zone. In their initial evaluation of the rift configuration of northern La Palma, *Carracedo et al.* [1999b] define a multi-axial array of rift zones along each protruding flank (Fig. 1.3.14d). In a later evaluation, the rift system is broader, more diffuse, encompassing the entire NW and NE sectors [*Carracedo et al.*, 2001] (Fig. 1.3.14e).

### 1.3.4 Origin and evolution of the rift zone architecture

A three-part approach is used to address the rift zone evolution of La Palma. First among these is the timing of rift formation and how the relationship between morphology and structure can be used with data on seamount/shield evolution in general, to re-evaluate spatial and temporal parameters. Second is tectonics, both local and far-field, and how this has influenced rift localization and orientation. This section ends with a concise overview of the substratum and basement architecture and their potential implications for morphological development of La Palma.

#### 1.3.4.1. Late or inherited rift zones?

The rift zone configuration of La Palma combines an active high aspect ratio rift zone in the south with an array of divergent (or diffuse) rifts in the north with comparatively subdued morphology; the latter have been inactive since around 0.4 Ma [*Guillou et al.*, 2001]. The ridges that bifurcate either side of the arcuate Cumbre Nueva escarpment are subordinate rift zones (of Cumbre Vieja) and have been inactive since around 7 ka [*Guillou et al.*, 1998]. There is no succinct explanation for the observable structural contrast in rift architecture since the bathymetric coverage north of La Palma is incomplete, and there are no submersible observations or age determinations reported from rocks on the submarine slopes. The seismic and acoustic backscatter data have defined a profusion of conical-shaped features aligned NW-SE along the Puntagorda Rise ('vents?' in Fig 1.3.3) [*Urgeles et al.*, 1999; *Mitchell et al.*, 2002; *Wynn et al.*, 2000], which, given the position below the vent-clustered subaerial slopes, could plausibly represent the vent regions of the extant rift zone. The constructional morphology of the rise extends for 38 km from the –3700 m bathymetric contour, nearly three times the length of the subaerial NW rift zone.

If the development of rift zones is a facet of the late-stage subaerial development of Taburiente [*Guillou et al.*, 2001; *Carracedo et al.*, 2001] then the question remains as to what caused the shift these authors propose from radial to rift-centralised volcanism. The interpretation of late rift zones seems to lack a correlation with the morphology and structure of La Palma's submarine construct. For example, on the neighbouring island of El Hierro (Fig. 1.3.15), where the bathymetric coverage is complete, the morphological disparity, between a coherent rift (in the south) and divergent rift zones (in the north), is also evident. The broad constructional slopes to the NW and NE of El Hierro are around 20 km in length and have an irregular morphology. To the south, an elongate steep sided arcuate ridge with a prominent saddle, extends for nearly 40 km [*Gee et al.*, 2001a, *Mitchell*, 2001]. The 'divergent' rift zones forming the NW and NE slopes are interpreted to have developed by either a wide area of constructional dike activity, or a bifurcation of the onshore rift zones seaward [*Gee et al.*, 2001a]. The contrast in rift morphology is interpreted by these authors to reflect different ages and origins, although no age data exist to support this hypothesis.

The seamount pedestals of oceanic island volcanoes form between 90 and 95% of the mass of each volcano in the Canary Archipelago [*Urgeles et al.*, 1998; *Schmincke and Sumita*, 1998; *Krastel and Schmincke*, 2002] and every other oceanic island [e.g., *Lipman et al.*, 2002]. Given this volumetric consideration, there is a significant probability that the rift zone configuration in the subaerial section of an oceanic volcano is an inherited aspect of the seamount stage, since the deductions made on subaerial data are only marginally representative of the entire volcanic system [e.g. *Lipman et al.*, 2002; *Devey et al.*, 2003]. From a statistical perspective therefore, can it be said that all rift-centred oceanic island volcanoes should have prominent submarine continuations of their rift system? What geometries should the rift zones have?, and, if no correlation exists between the subaerial and submarine sections, then what is the underlying cause of this discrepancy?

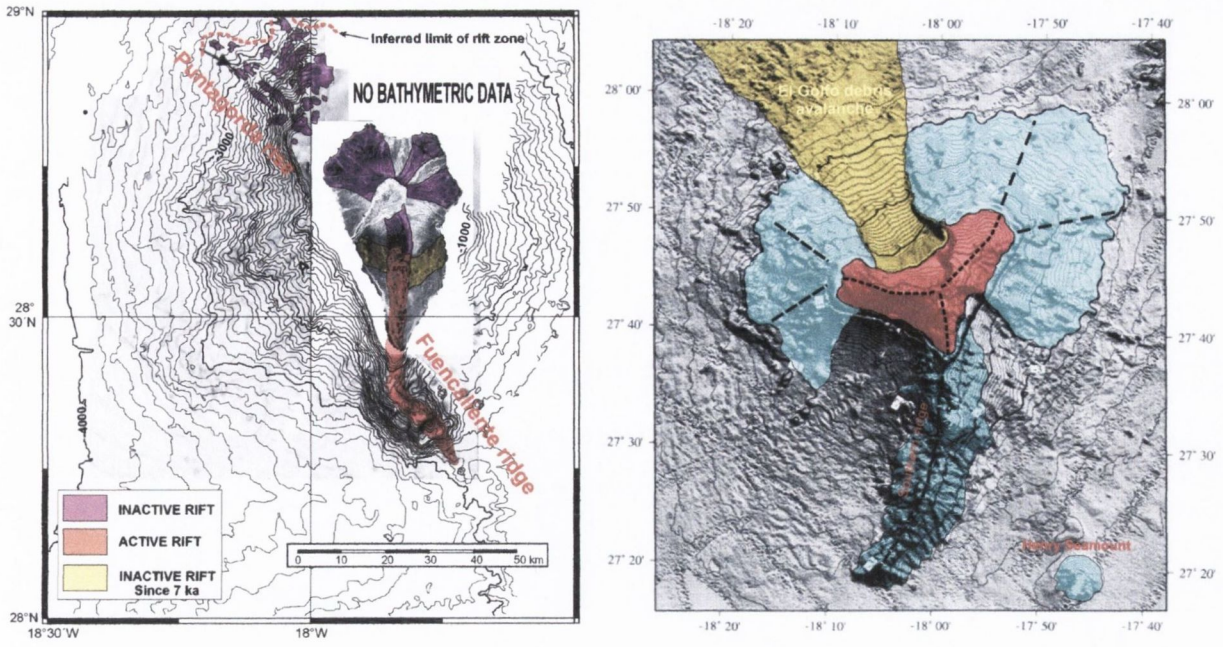


**Fig. 1.3.15.** Comparisons of rift zone architecture between La Palma (left) and El Hierro (right). Background bathymetric DTM of La Palma extracted from *Mitchell et al.* [2002]. The shaded relief bathymetric image of El Hierro shows the subaerial edifice in red and the submarine rift zones in blue, modified from *Mitchell* [2001]. Stippled lines are rift axes [*Gee et al.*, 2001a]. El Golfo debris avalanche from *Gee et al.* [2001b].

These questions have been addressed to an extent by statistical analyses of the morphology of 141 seamount volcanoes throughout the ocean basins [*Mitchell*, 2001]. It emerges that seamount volcanoes undergo a gradual transition in morphology from conical to stellate forms due to the innate effects of rift zone localization and flank collapses [*Vogt and Smoot*, 1984 *Mitchell,* 2001]. In theory, the morphological transition from simple (conical) to large and complex forms (rifted/collapsed) occurs at around the 3 km growth interval from the base of the edifice, as magmas rise higher into the cone [*Mitchell*, 2001]. At high levels of neutral buoyancy in a large volcanic edifice, magmas are fed more efficiently into flanking rift zones than from magma reservoirs lower in the crust (Fig. 1.3.16).

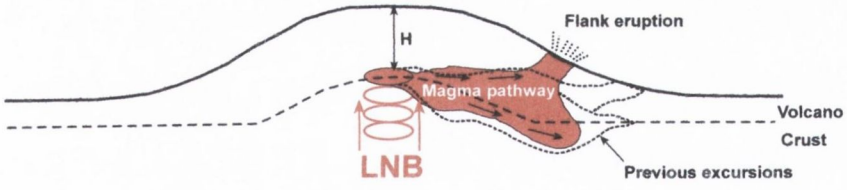


**Fig. 1.3.16.** The path of a dike from a high level magma body, illustrating the efficiency of lateral dike propogation relative to the level of neutral bouyancy LNB in a large volcano. H is the height of volcano. Modified from *Mitchell* [2001].

Furthermore, lavas erupted from the summit region must ascend through an additional 1 or 2 km of the volcanoes carapace while lavas erupted from a vent and conduit system on the lower flanks have less head. The latter is the deduction of *Naumann and Geist* [2000] for the structural development of Cerro Azul volcano on the Galápagos Island of Isabella. Volcanism on Cerro Azul is dispersed through radial fissures on the flanks, and through concentric vents along the summit calderas; linear rift zones are absent [*Naumann and Geist.*, 2000].

Diffuse rift zones are interpreted from clustered vent alignments on the NW, NE and southern parts of Wolf Volcano located to the north of Cerro Azul on Isabella Island [*Geist et al.*, 2003]. A prominent east rift zone is located to the east of the dissected caldera of Ecuador Volcano (also on Isabella) [*Geist et al.*, 2002].

Morphologically, the western Galápagos Volcanoes take the form of inverted soup plates with gently inclined lower slopes abutting steep upper slopes (around 35°) that encircle the outer edge of summit platform [*Munro and Rowland* 1996, and references therein]. The reason for the abrupt slope differentiation is related to the additional driving forces necessary to raise magma to higher elevations within the volcano [*Naumann and Geist* 2000]. Fig. 1.3.17 shows scaled cross sectional detail of two of the Galápagos shields, Fernandina and Cerro Azul, compared with sections across northern La Palma. The position of the slope inflection is marked, and in the case of Taburiente, the median level of the shield/intrusive core discordance is included. The similarity in slope inflection could indicate that magmas at high levels of neutral buoyancy have a tendency to feed flank eruptions at the expense of summit eruptions. In the case of the Galápagos shields, none of the basement complexes are exposed since fluvial erosion is suppressed by the arid climate [*Naumann and Geist,* 2000]. On La Palma the exhumed basement extends to a height interval above the level of the slope inflection with significant topographic relief in the intrusive core. Fig. 1.3.8 shows the clustering of vents along the lower flanks relative to the slope inflection and the discordance.

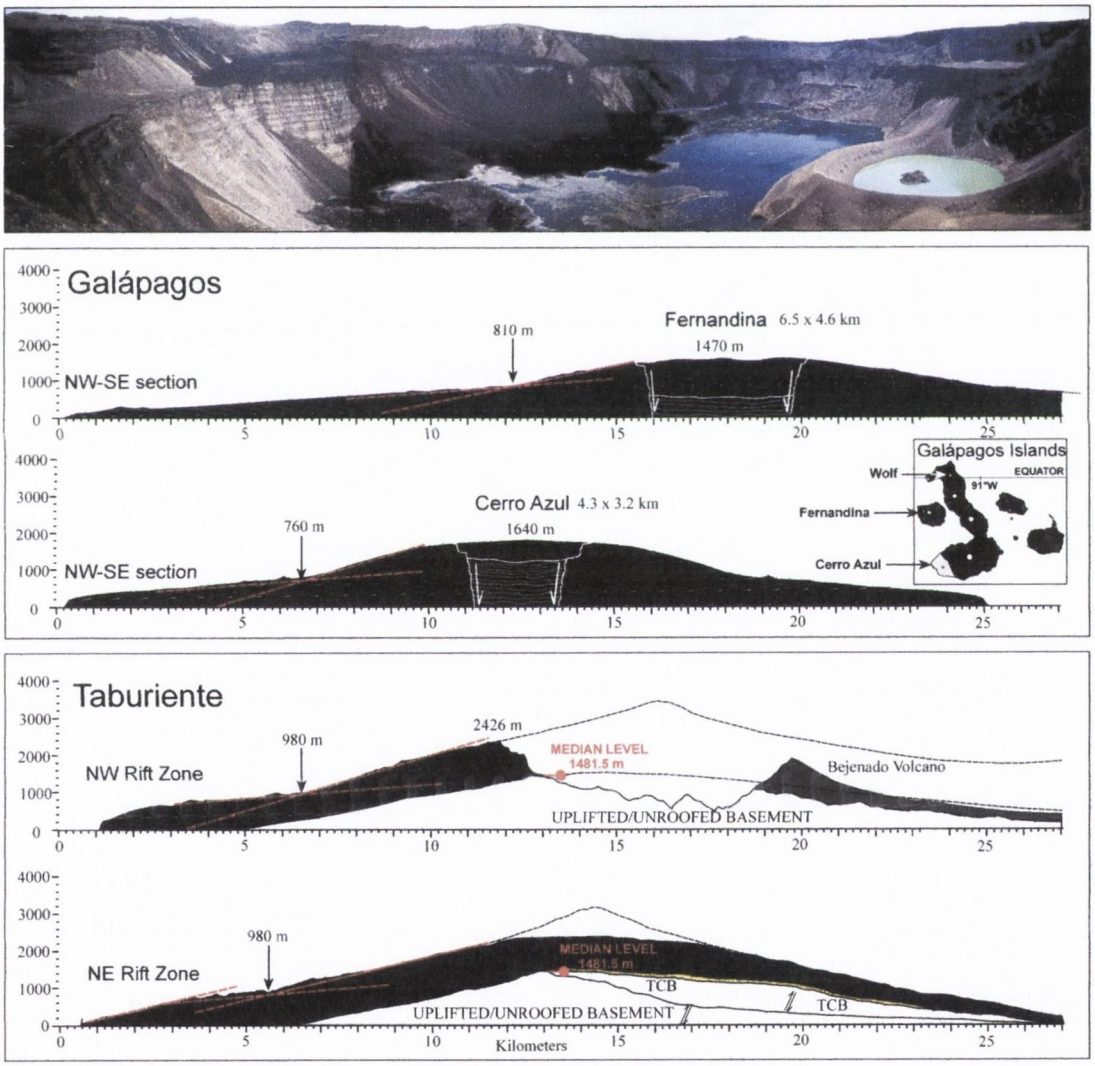


**Fig. 1.3.17.** Comparisons of the relic topography of Taburiente and the Galápagos Volcanoes, Fernandina and Cerro Azul. Modified from For each volcano the slope inflection point is marked with a vertical arrow, with the flank height interval. Abbreviation: TCB, Tenerra Collapse Breccia (see chapter 2.1). No vertical exaggeration. The photograph shows the lake, tuff cone and draping lavas inside the caldera of Cerro Azul. Extracted from *Naumann and Geist* [2000].

*Cerro Azul flank eruptions are more voluminous than the summit eruptions [*Geist et al.,* 2000].

When illustrated with the profile of the Puntagorda Rise (Fig. 1.3.18) it would appear that the change in slope of the subaerial edifice is related directly to the peak level of neutral buoyancy once attained by magmas in the uplifted basement. The observed clustering of vents along the lower flanks and along the slopes of the Puntagorda Rise, could therefore indicate continuity of the NW rift zone across the submarine/subaerial section. The absence of vents between the main protruding axes of the island (Fig. 1.3.12d), could indicate that vent clustering was controlled by enhanced fracture connectivity along the rift axes and by gravitational stresses in the edifice, similar to Wolf Volcano [*Geist et al.,* 2003] and perhaps Mt. Etna [*Mazzarini and Armienti*, 2001]. With the opening question in mind; (should the processes that effect the submarine development of an oceanic volcano reflect in the subaerial?), the wealth of observational data from a deep undersea perspective [e.g., *Hekinian et al.*, 2002, *Lipman et al.*, 2002, *Eakins et al.,* 2003; *Devey et al.*, 2003] are supportive of this theory. Therefore, the northwest rift zone could plausibly represent the subaerial/uplifted component of a much larger and earlier structure inherited from the seamount (Fig. 1.3.18). As the seamount was elevated or 'jacked up' above sea level, perhaps by the development of a giant sheeted sill complex, magmas ascended to higher levels of neutral buoyancy. It has been suggested that uplift may have been augmented by the development of La Palma on the flexural arch of Tenerife/Gran Canaria [*Urgeles et al.*, 1998]. The high-level magmas efficiently fed rift eruptions, in a now large edifice (i.e. >3 km high), through sills and/or dikes (Fig. 1.3.18). Recall that sheeted sills, occurring in stacks up to 350 m thick, are observed at outcrop in the intrusive core (Ch. 1.2).

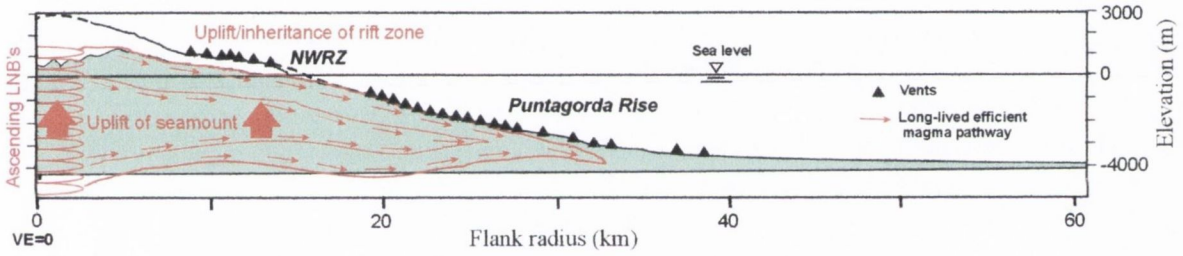


**Fig. 1.3.18.** Scaled section through the NW rift zone/ Puntagorda rise (submarine profile is UF2 from *Masson et al.*, 2002]). Magmas ascend to increasing LNB's, sustaining rift zone eruptions throughout the uplift and inflation period.

The slope inflection could also be a result of the contrasting viscosities of lavas erupted from summit and flanking vents; again this structural/rheological relationship is inferred for the morphology of Cerro Azul [*Naumann and Geist* 2000]. The alkalic lavas of Taburiente are an intrinsic part of the shield-building phase, not part of the volumetrically minor alkalic cap stage which is a facet of volcanism in Hawaii [*Wolfe and Morris*, 1996; *Nikogosian et al.* 2002]. The latter authors relate the alkalic character of Taburiente lavas to extreme clinopyroxene fractionation in the upper mantle at pressures >10 Kbar, such that a significant proportion of the primary magmatic input is not erupted, but under-plated as cumulates. Based on fluid inclusion studies of xenoliths and phenocrysts, *Hansteen et al.* [1998] suggest that magmas pond at depths of between 7 and 11 km beneath La Palma. The differentiation trends seen in La Palma lavas appear to have been consistent through each constructive phase of volcanism (i.e. basanite to phonolite) from Ancestral Taburiente to modern Cumbre Vieja (Fig. 1.3.19) [*Carracedo et al.,* 2001]. Moreover, *Carracedo et al.* [2001] observe that the most differentiated rocks (i.e. phonolites, tephri-phonolites and trachytes) occur higher up in stratigraphy of the island. This could indicate that the slope inflection itself occurred late in the development of the volcano, brought about, in part, by explosive centralized volcanism (as these authors advocate), erupting blocky lavas and steep-sided domes with limited subaerial coverage. If further bathymetric coverage to the N and NW of La Palma can reveal a pronounced continuity of rift/ridge-like structure, this might further vindicate the inherited rift zone hypothesis advocated here.

Fig. 3.1.20 synthesises the observations and deductions set forth in this section regarding the possible temporal evolution of the northern rift system. The south rift zone (Cumbre Nueva) edifice is treated separately.

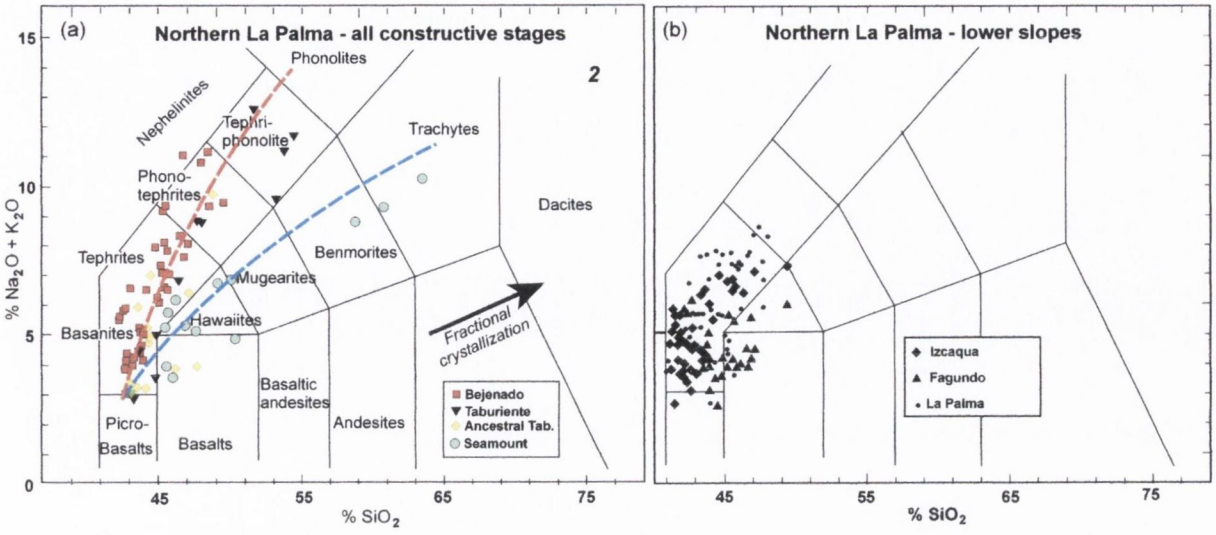


**Fig. 1.3.19.** Total alkali-silica classification diagrams with whole-rock compositions for La Palma. (a) Differntiation trends observed from each constructive stage and stratigraphic height: submarine - blue stipple, subaerial - red stipple. From *Carracedo et al.*, [2001]. b. Samples predominantly from the lower northern slopes of Taburiente (Barranco Izgagua and Barranco Fagundo). From *Nikogossian et al.* [2002].

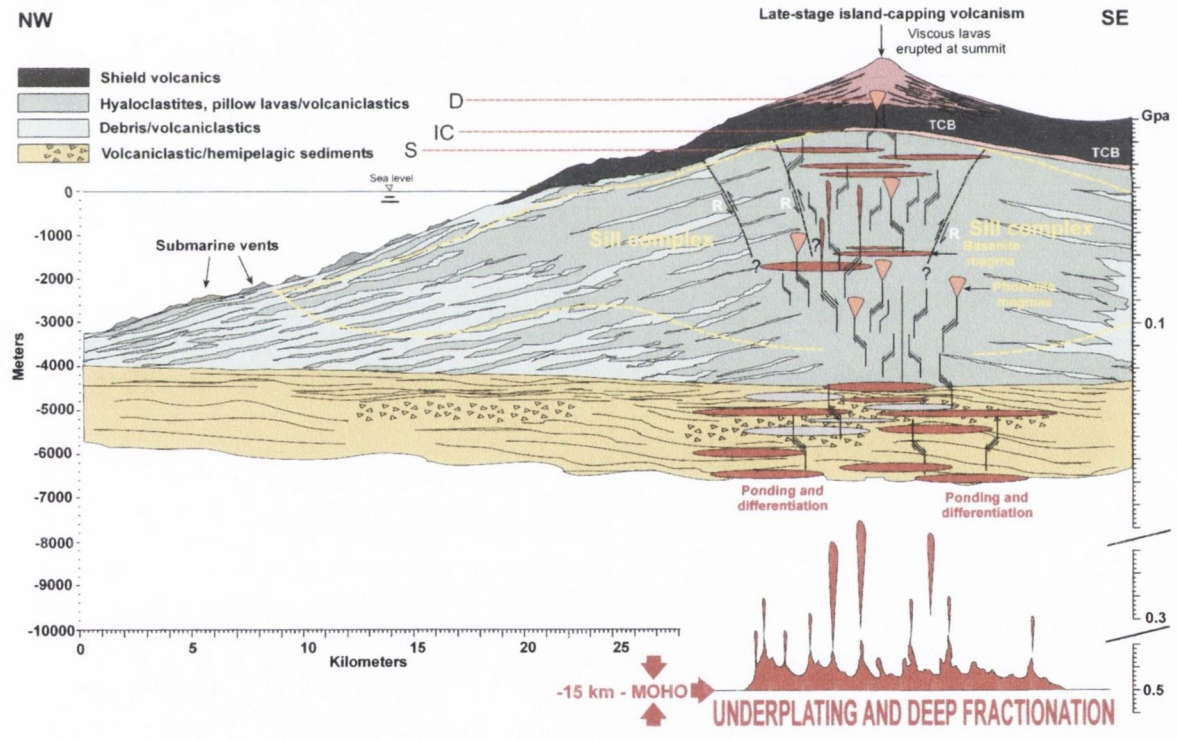


**Fig. 1.3.20.** Section of the subaerial/submarine and crustal structure of La Palma (VE=2). Reverse faults (R) accommodate uplift/inflation of the seamount caused by the construction of an extensive sill complex. Phonolitic and other differentiated magmas rise vertically, mafic magmas are able to move laterally into the rift system. Abbreviations: D: Level of decapitation (summit collapse). IC – Mean level of the intrusive core. S: slope inflection. TCB: Subaerial landslide breccias (see Ch. 2.1).Submarine slopes based on profile UF-2 [*Masson et al.*, 2002]. Crustal pressures from *Hansteen et al.* [1998]. Seamount architecture concept from *Schmincke and Sumta* [1998] and *Lipman et al.* [2002], Sediment thickness from *Urgeles et al.* [1998]. Underplating concept from *Nikogossian et al.* [2002]. Reverse faults previously defined by *Navarro and Coello* [1993].

### 1.3.4.2 The Cumbre Nueva conundrum

The dismantled and partially overlapped Cumbre Nueva edifice presents a conudrum in the scheme of the rift zone evolution of La Palma. In particular it is unclear as to why, given the radiometric and palaeomagnetic data [*Guillou et al.*, 1998; 2001], it only appeared after 0.8 Ma. The period of Cumbre Nueva activity is restricted therefore to between 0.8 and 0.55 Ma, the latter age representing the lateral collapse of the west flank and adjacent surficial rift zone [*Ancochea et al.*, 1994; *Carracedo et al*, 1999a,b; *Guillou et al.*, 2001]. In order to have sustained this rift activity, and the causal flank destabilization (as implied by *Carracedo et al.* [1999a,b]), a significant shift of thermal energy must have occurred in the upper mantle in order to have constructed the rift-centered Cumbre Nueva edifice, while residual volcanism continued on the diffuse rift zones of Taburiente. Furthermore, subsequent to the Cumbre Nueva collapse a small but significant magma budget remained in the north of La Palma for the construction of Bejenado Volcano. Fig 1.3.21 illustrates the spatial and temporal migration in the constructional foci of La Palma.

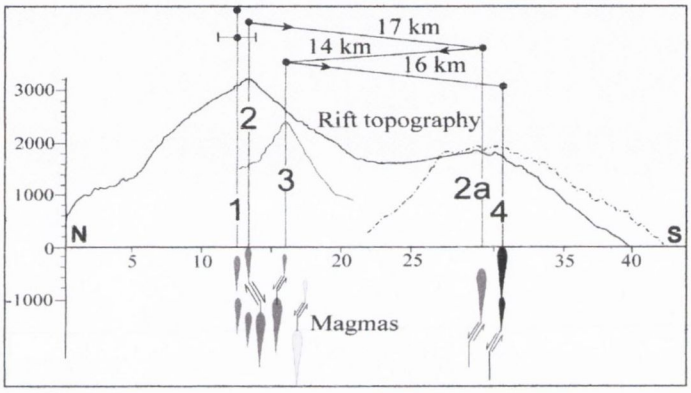


**Fig. 1.3.21.** North-south profile of La Palma (VE=5) showing the apparent migration of the centroid of magmatism from Ancestral Taburiente (1), Taburiente (2), Cumbre Nueva (2a), Bejenado (3) and Cumbre Vieja (4).

The coalescence of the Cumbre Nueva edifice onto the south flank of Taburiente could only have followed a significant submarine stage of construction, building the forerunner to Fuencaliente Ridge. To what extent therefore does the present morphology and southward extent of Cumbre Vieja/Fuencaliente Ridge reflect in the predecessor Cumbre Nueva edifice? For instance, did Cumbre Nueva develop similarly to Cumbre Vieja, as a relatively high aspect ratio coherent rift zone, narrowing southwards?

The southward increasing aspect ratio, together with the morphologically un-complex structure of the submarine slopes west of Cumbre Vieja [*Urgeles et al.*, 1999] could be an indication that gravitational spreading may not have occurred to a significant extent during the growth of the predecessor rift. It is possible therefore that the balance between vertical growth and lateral mass transfer of the flanks along Cumbre Vieja/Fuencaliente Ridge had been hindered since its inception, perhaps by the lack of deformable substrates. To this end, the Cumbre Vieja edifice is implied to mimic the morphology of its predecessor - Cumbre Nueva - as a high aspect ratio topographic rift zone. Why therefore should a disparity exist in terms of rift structure - ie., divergent rifts in the north and a single coherent rift in the south? The conundrum gains weight by the aforementioned age constraints for the onset of rifting (in the face of the inherited rift hypothesis proposed in section 1.3.4.1) and remains un-resolved by any contemporary studies of the islands' geology. Based on analogue modeling, *Walter and Troll* [2003] conjecture that southward migration towards rift volcanism was a consequence of the unstable and creeping southwestern volcano sector.

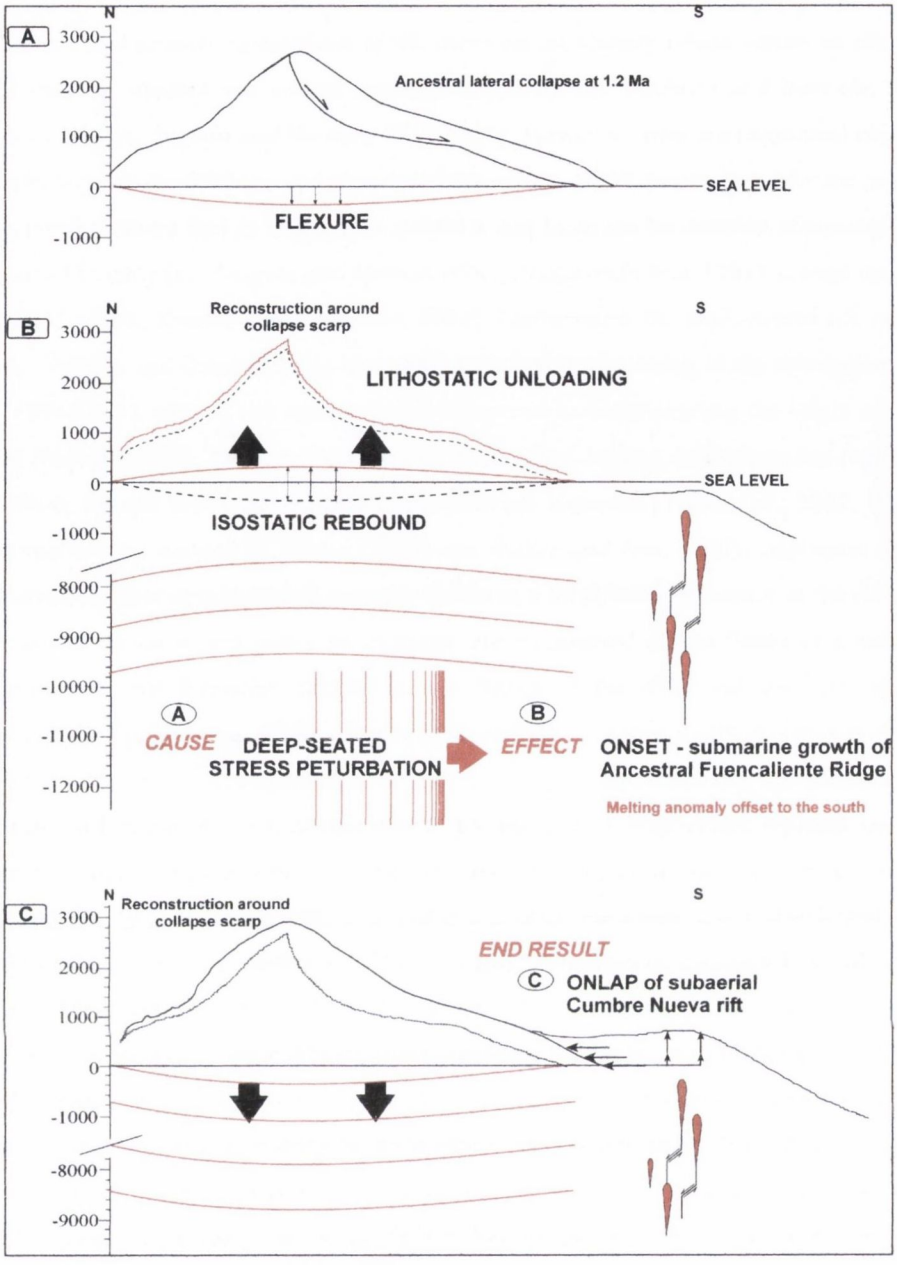


**Fig. 1.3.22.** Schematic representation for the onset of the Cumbre Nueva rift zone incorporating flexure of the lithosphere (amount exaggerated) as a causal mechanism for deflecting the position of the melting anomaly.

Alternatively, rather than being a response to surficial gravitational spreading of the subaerial flanks, it is possible that the underlying reason for the development of the Cumbre Nueva rift zone was caused by deep-seated processes related to extensional stress perturbations in the upper mantle following the removal of lithostatic load during the partial collapse of Ancestral Taburiente. One might expect that the sudden catatclysm brought about by gigantic sector collapse(s) might have had an effect on the magmatic plumbing system. Such an event may have induced flexure of the lithosphere, prompting the southward shift of hot-spot activity (Fig. 1.3.22). The ancestral sector collapse(s) may have perturbed the plumbing system in a way that enabled magmas to ascend along different pathways – promoting the development of a coherent rift. Clearly, the existing models are highly speculative owing to the lack of tangible data and future research is warranted to constrain this important period in the Plio-Pleistocene evolution of La Palma.

### 1.3.4.3 Rift orientations: the influence of regional tectonics.

The localization and primary orientations of rift zones on the Canary Island volcanoes emulate both local and far-field tectonic stresses and crustal anisotopies [*Hernandez Pacheco and Ibarrola*, 1973; *Stillman*, 1987; *Carracedo*, 1994, *Anguita and Hernan*, 1975, 2000]. However, there are theoretical objections to some of the proposed tectonic mechanisms and physical phenomenon of rift development for the insular volcanoes. For example, some workers find no evidence or reason to implicate the localization of structures related to the Atlas Mountains Orogeny [cf. *Anuguia and Hernan,* 1975; *Araña and Ortiz,* 1991], toward the Canary Islands [*Carracedo et al.*, 1998; *Krastel and Schmincke*, 2002]. Furthermore, the triple-armed rift systems observed on El Hierro, Tenerife and Cumbre Vieja may not be the result of doming in the lithosphere, as implied by *Carracedo* [1994;1996], and are not regarded as fundamental to understanding the origin of the archipelago [*Anguita and Hernan* [2000]. Analogue models that employ the doming concept do not replicate the triaxial rift configuration, instead radial and concentric fractures are observed [*Troll et al.*, 2002; *Walter and Troll*, 2003]. The experimental outlook of *Walter* [2003] and *Walter and Troll* [2003] implicates the role of older volcanoes, buried collapse structures and creeping flanks as a modulating influence in the rift configuation of oceanic volcanoes. Hawaiian volcanoes for example, are constructed on the flanks of a neighboring shield that facilitates linear rift formation parallel to the flanks of the older volcano, and spreading in the unbuttressed direction [*Geist et al.,* 2000, *Lipman et al.*, 2002].

The position of the Canary Archipelago in a region of complex neo-tectonism has nourished much debate as to the nature and origin of the Canarian mantle plume, and to what extent regional and local tectonic stresses have influenced the distributions, elongations and deformation histories of the volcanic sytems [e.g., *Anguita and Hernan* 1975, *Stillman*, 1987, *Féraud et al.*, 1985, *Fernandez et al.*, 1997, 2002]. The regional tectonic framework comprises a number of highly dynamic components, summated as follows; (1) the E-W orientated Atlas Mountain belts and the NE-SW orientated Mid Atlas Mountains [*Seber et al.*, 1996a], (2) the Rif-Betic Mountains and the adjacent Alboran Basin (western Mediterranean) [*Seber et al.*, 1996b], (3) the N-S and NE-SW orientations of the West African dike swarms and other lineaments [*Bertrand,* 1991], (4) the NE-SW ridges and other oceanic islands in the northeastern Atlantic [e.g., *Schmidt and Schmincke*, 2002], and finally and perhaps most importantly (5) the Mid Atlantic Ridge and the associated E-W fracture systems.

The Atlas Mountains form part of the orogenic belt that includes the Alps, Appenines, the Betic Cordillera (southern Spain), and other mountain chains traceable through Turkey towards the Zagros Mountains of Iran. These mountain belts began to form around 70 million years ago, when the Tethys Ocean (for-runner to the Mediterranean basin) started to close as the African Plate collided into the Eurasian plates [*Seber et al.,* 1996a, *Beauchamp et al.*, 1999]. Shortening during orogenesis accommodated between 17% and 45% of the total African-Eurasian plate convergence since the early Miocene [*Gomez et al.*, 2000]. According to these authors, large inherited crustal structures (elements of the Early Mesozoic rift system) acted as weaknesses that facilitated deformation. The majority of the plate convergence is accommodated in the Rif-Betic-Alboran region, where the geophysical evidence suggests that the continental lithosphere is delaminated [*Seber et al.*, 1996a,b] (Fig. 1.3.23). Compressional features dominate the Atlas fold belt (Fig. 1.3.24), although extension is manifested by widespread mid to late Quaternary alkali volcanism [*Gomez et al.,* 1996; *Anguita and Hernan*, 2000 and references therein]. It is important to bear in mind that the duration of magmatism in Morocco dates back at least to the Oligocene [*Lancelot and Allegre*, 1974]. In continental West Africa, dike swarms and crustal fractures are predominantly orientated N-S and NE-SW.

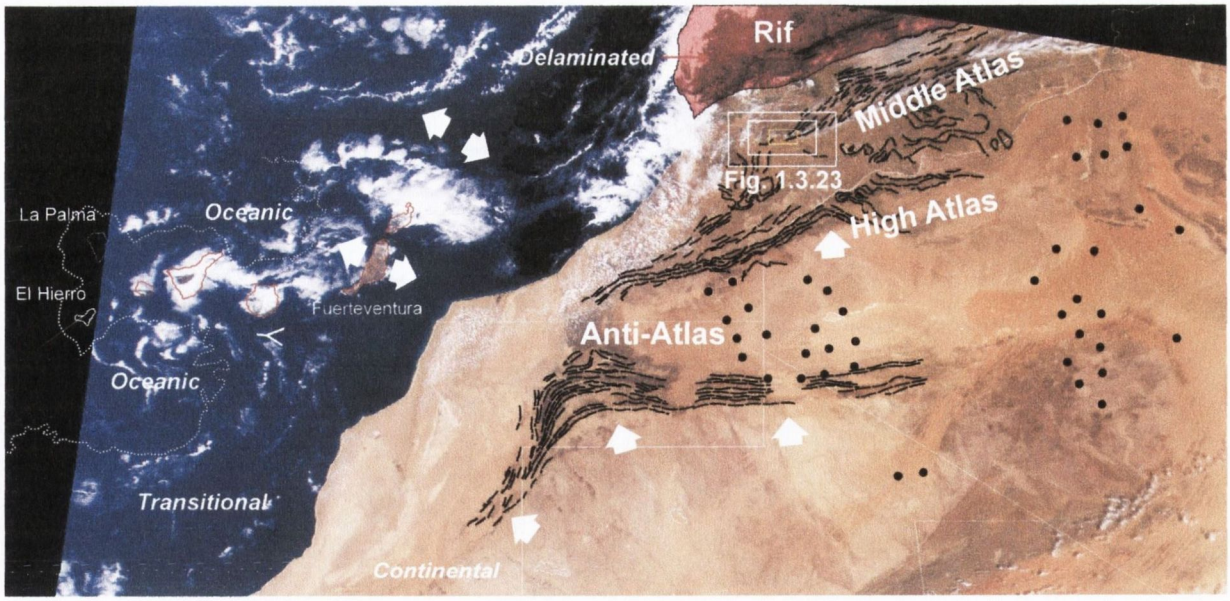


**Fig. 1.3.23.** Shuttle image of West Africa showing prominent parts of the Atlas fold belts (in black tracing) and the approximate dilation axis of Fuerteventura and Concepcion Bank. The distribution of alkaline volcanic centres (black dots) is from *Anguita and Hernan* [2000]. Southern extent of lithospheric delamination from *Seber et al.* [1996a]. STS-056-011-987D Image source: www.visibleearth.nasa.gov

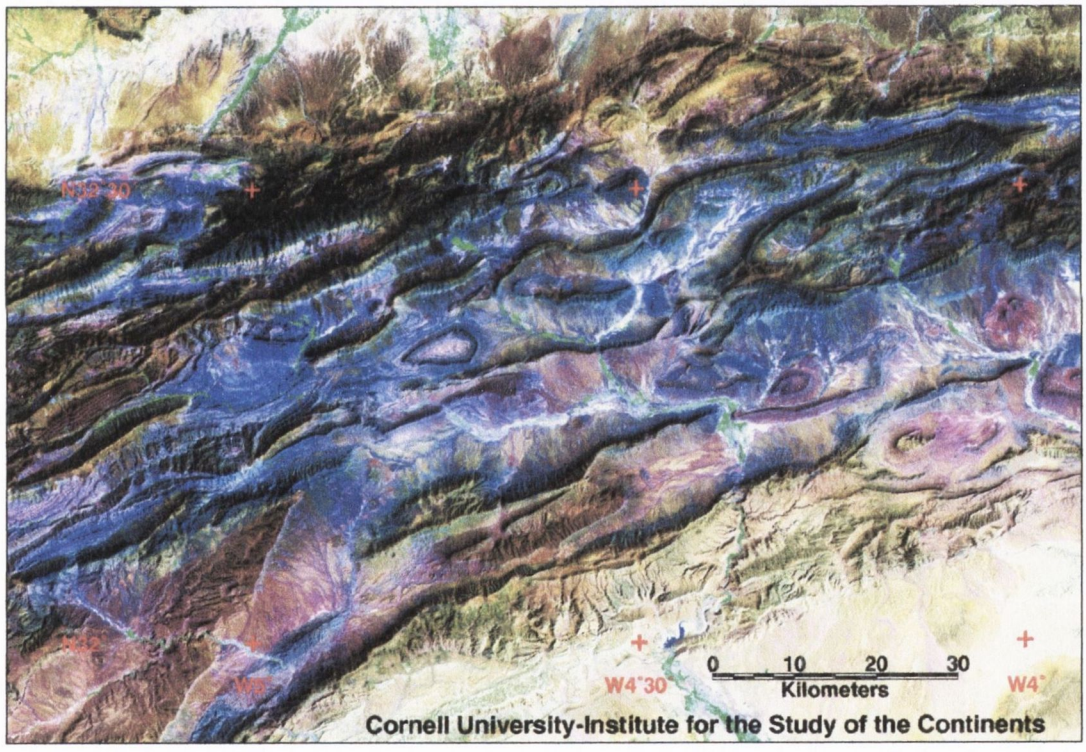


**Fig. 1.3.24.** Landsat scene of the Middle Atlas fold belt in northern Morrocco. See Fig. 1.3.23 for location. Source: http://.atlas.geo.cornell.edu/morocco.html.

These orientations relate to the opening of the Central Atlantic [*Bertrand,* 1991], while other long-lived lineaments (orientations N-20°E, N50°-70°E, N130°-150°E) have been activated during several rifting episodes in the Phanerozoic [*Kampunzu and Popoff*, 1991]. Fig. 1.3.23 shows the proximity of the Canary archipelago to the Atlas/Anti-Atlas tectonic system and the nature of the crust in between.

In their unified model of Canary Island tectonics, *Anguita and Hernan* [2000] regard the present Canarian plume to be a relic of, or a diversified manifestation of a plume that has been active throughout Atlas Mountains Orogeny. In their view, the uplifted basement complexes (visible in four of the Canary Islands) resulted from transpressive shears related to the tectonics of West Africa, not from reverse faults initiated at local scales.

Following this notion, *Hildenbrand et al.* [2003] suggest that La Palma has undergone uplift throughout the subaerial stages of construction as a consequence of far-field stress related to the Atlas Orogeny. They further implicate the aforementioned doming concept and flexure of the lithosphere subsequent to lithostatic stress relaxation due to giant landsliding.

Further afield from the continental tectonic regimes of northwest Africa, the spreading centres along the Mid Atlantic Ridge (MAR) represent the most dynamic aspect of the regional tectonic framework of the Canary Archipelago. The nearest segment of the MAR to the islands is located west of the Azores Platform, over 1600 km to the NW of La Palma (Fig. 1.3.25). The axial zone of the MAR is characterized by exposed mafic and ultramafic rocks where buoyant asthenosphere exerts a lateral stress along the segmented and faulted ridge, causing it to spread apart at a rate of 23 mm/yr [*Cannat et al.*, 1995; *Sandwell et al.*, 2001, *MacLeod et al.*, 2002]. The ridge push force ($F_R$ in Fig. 1.3.25) arises from the buoyancy effect of the asthenosphere that carries energy from the core and the upper mantle (the Earth's geo-dynamo), and is undoubtedly a major force on a global tectonic scale [*Vine and Kearey,* 1996]. Ridge push force is a long term source of renewable stress acting on a plate.

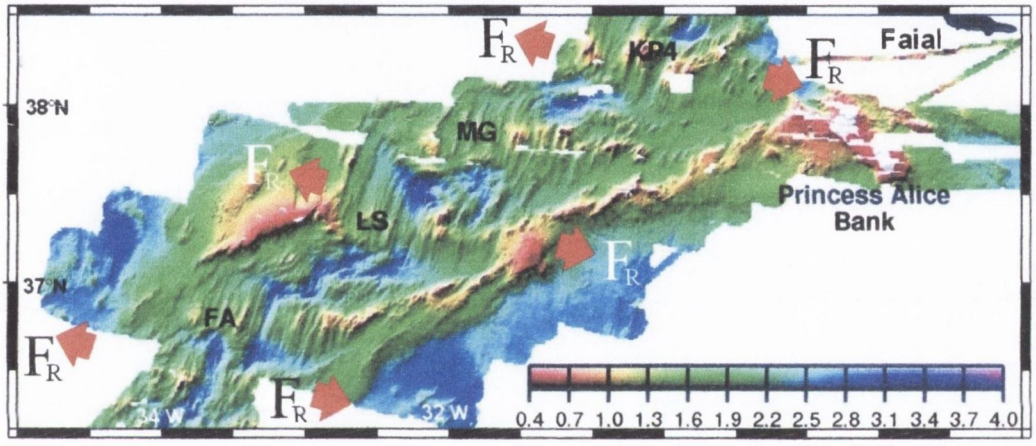


**Fig. 1.3.25.** Bathymetry of the MAR spreading center in the vicinity of the Azores Platform. The Azores island of Faial is included for reference. Abbreviations: MG: Menez Gwen, LS: Lucky Strike, FA: Famous, are segments of the axial ridge. The arrow abbreviated $F_R$ represents the ridge push vector. Modified from *Cannat et al.* [1999].

MORB-type oceanic crust has been detected from xenoliths from all the islands in the archipelago; therefore, each island is founded on some of the oldest (Jurassic) oceanic crust in the Atlantic [e.g., *Schmincke et al.*, 1998; *Neumann et al.*, 2000]. Oceanic crustal fractures are known to control the primary orientations of rift zones in the Azores [*Cannat et al.*, 1999; *Guest et al.*, 1999] and some of the oceanic islands in the Pacific (Hawaii, Tahiti) [*Binard et al.*, 1991; *Eakins et al.*, 2003]. In the Canary Islands the rift zones do not show a clear-cut primary (i.e., localization) relationship with the predominantly E-W fracture systems that penetrate the oceanic crust. However, a correlation in rift orientation does exist with first order structures such as the numerous NE-SW ridges (e.g., Concepción Bank, Madeira-Torre Rise) and the MAR itself. The dikes and lineaments in West Africa (related to the break-up of the Atlantic) also display a sympathetic relationship with some of the insular rift orientations. This may suggest partial inheritance of oceanic structures and associated anisotropies in the trend of Canarian rift zones. Fig. 1.3.26 illustrates how each of the opposing/interacting tectonic stresses correlate with the overall Canarian rift fabric. This includes 18 measurements of individual segments of the MAR between latitudes 27° and 38° N, and 20 measurements of the east-west crustal fractures, at areas immediately adjacent to the MAR. Other structural features in the crust include NW-SE alignments of parasitic vents and an inferred reverse fault in the channel between Tenerife and Gran Canaria [*Romero-Ruiz et al.*, 2000] (Fig. 1.3.26).

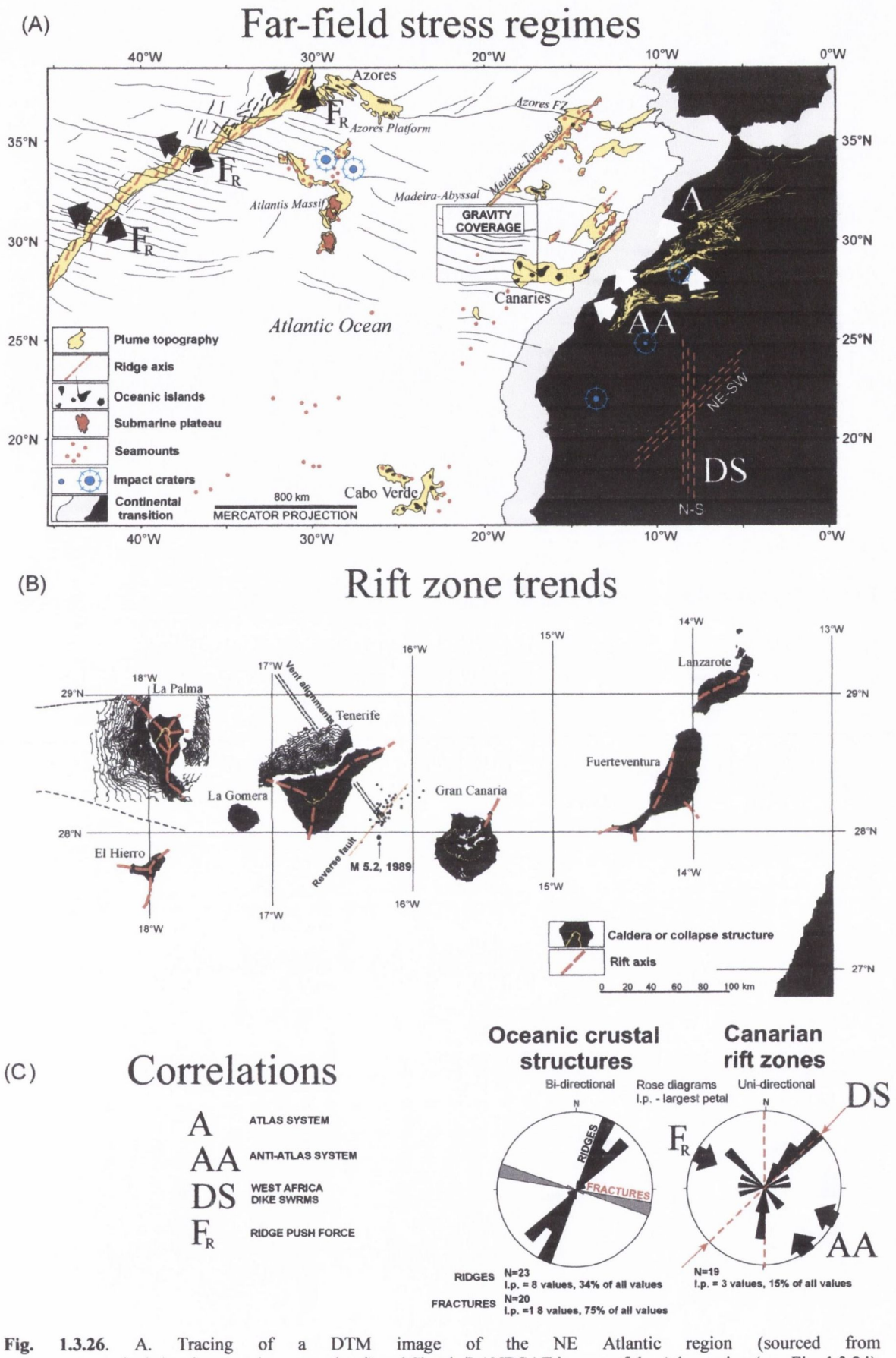


**Fig. 1.3.26**. A. Tracing of a DTM image of the NE Atlantic region (sourced from www.topex.ucsd.edu/marine_topo/mar_topo.html) and Shuttle/LANDSAT images of the Atlas region (e.g. Fig. 1.3.24). Gravity coverage – showing oceanic fractures NW of La Palma from *Ranero and Reston* [1999]. West Africa impact craters from *Simkin et al.* [1994]. Suspect impact craters are marked at the Atlantis Massif. B. Rift zone and other structural orientation of the Canary Islands and supporting crust. Data sourced from *Stillman* 1987; *Urgeles et al.* [1999], *Albay and Marti* [2000], *Romero-Ruiz et al.* [2000] *Gee et al.* [2001a], *Krastel and Schmincke*, [2002], *Mitchell et al.* [2002]. In B the location of the 1989 M5.2 earthquake is marked between Gran Canaria and Tenerife after *Jiménez and Garcia Fernandez* [1995]. C. The rose diagrams in c shows the orientation of rift axes with respect to the centre of each volcanic edifice. Not corrected for rift zone migration.

### 1.3.4.3. Substratum/basement architecture; an influence in morphology?

A phenomenology has developed regarding the evolutionary cycle of shield-building Hawaiian Volcanoes [*cf Borgia,* 1994]. Lateral displacements of the flanes along low strenght layers underlying the volcano, facilitate the reduction of horizontal edifice stresses thereby enabling focused intrusions of magmas along linear rift axes [e.g. *Borgia and Treves*, 1992; *Delaney et al.*, 1998]. Gravitationally driven spreading of the massive flanks away from the rift zones equilibrates the flank length with respect to the edifice height [*Lipman et al.*, 2002; 2003]. However, there are numerous elongate, high aspect ratio rift-centred oceanic island volcanoes (e.g. Cumbre Vieja, Taveuni, Karthala). where this relationship is unbalanced. In these examples the tendency has been towards the construction of high relief rift zones with the capacity for lateral displacements impeded. The reasons why coherent rift zones should develop in such disparate manners is not known at present. Perhaps the difference between low and high aspect ratio (often occuring on the same edifice), relates to the frictional resistance to sliding along the basal detachment(s), or the under-development of a through-going slip surface(s) that facilitates flank displacement. *Borgia et al.* [2000] suggest that volcanoes may 'spread' by sector collapses and by superficial wasting processes if they rest upon strong, intact rocks, lack basal decollements, and possess a high degree of internal strength.

Continental volcanoes that are constructed upon less dense or mechanically weak materials (e.g., lake sediments, ignimbrites), can undergo complex and inter-related changes in magmatic evolution, eruptive styles and structural configuration that can be pertinent to the stability of an edifice [*van Wyk de Vries and Borgia*, 1996; *Borgia and van Wyk de Vries,* 2003; *van wyk de Vries and Francis*, 1996; *van Wyk de Vries et al.*, 2001; *Clavero et al.,* 2002]. Oceanic volcanoes typically interface with the supporting oceanic crust along contiguous layers of pelagic sediment and subaerial/submarine volcaniclastics, generated through volcanism and mass wasting of neighbouring volcanoes [*Urgeles et al.,* 1998; *De Voogd et al.*, 1999; *Lipman et al.*, 2002]. Major structures (e.g., normal faults, penetrative detachments, crustal fractures and pre-existing seamounts) are also present in the upper realms of the oceanic crust, contributing to its intrinsic roughness and structural complexity [*Crough* 1984; *Reston et al.*, 1996; *Ranero and Reston*, 1999] (Fig. 1.3.27). In the Canary Basin, the sedimentary layer overlying the oceanic crust is significantly thicker in comparison to the isolated Hawaiian Archipelagic region [*Mitchell et al.*, 2002], although there is no evidence reported of major gravity-driven deformation structures from around the insular edifices. Efforts to detect major slump-like structures from the bathymetric data (e.g., mid-slope benches, sediment accretion, frontal thrusts), have been inconclusive [*Mitchell et al.*, 2002; *Masson et al.*, 2002], while seismic data, so far, only indicate subsidence due to load-induced flexure of the crust and thickening of sediment drape in the flexural moat [*Watts et al.*, 1997; *Canales and Dañobeitia,* 1998] (Fig. 1.3.28).

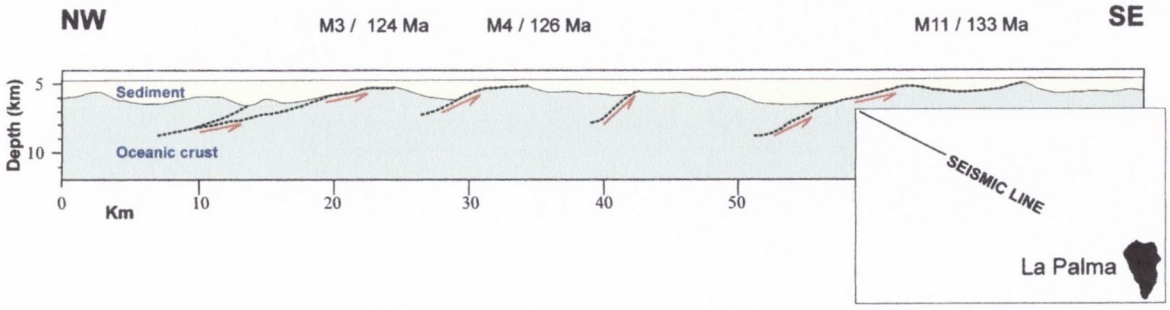


**Fig. 1.3.27**. Depth-migration interpretation of a segment of the oceanic crust centered 230 km NW of La Palma showing the topography of the oceanic basement and detachment faults along the inside corner lithosphere. Modified from *Ranero and Reston* [1999].

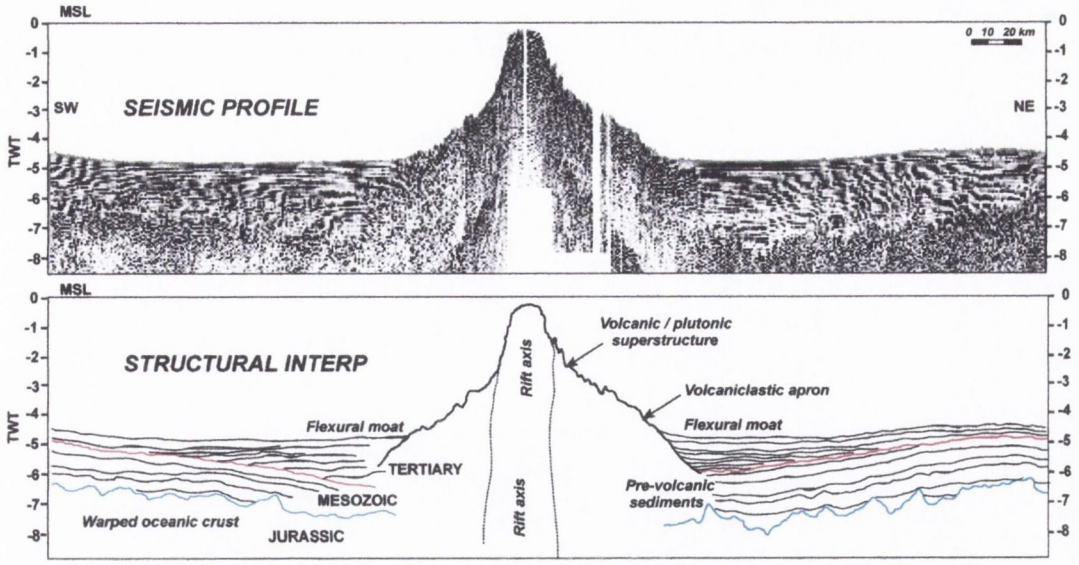


**Fig. 1.3.28.** Structural interpretation of a seismic profile shot along NW submarine slopes off Tenerife, showing the structure and relationship between the relative thicknesses of the pre and syn-volcanic sedimentary sequencing around the flexual moat. Modified from *Watts* [2001].

However, since Canarian volcanoes grow at a rate that is an order of magnitude lower than those of the Hawaiian archipelago [e.g., *Hornle and Schmincke*, 1993; *Dañobeita and Canales*, 2000] (Fig. 1.3.29), the associated deformation features may not be alike and are perhaps more subtle.

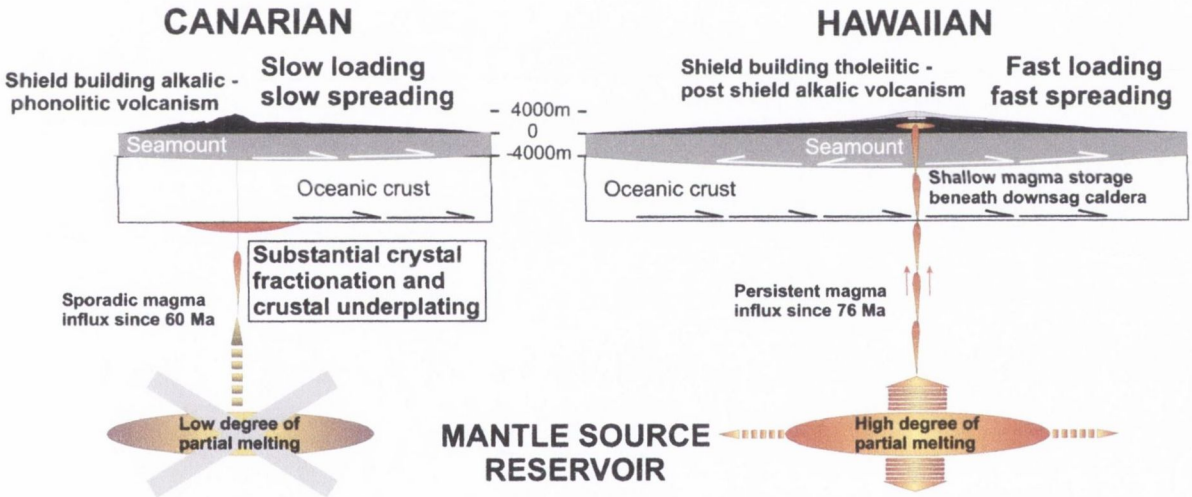


**Fig. 1.3.29.** Scaled sections of the largest volcanoes of the Canary and Hawaiian Archipelagos. Teide (Las Cañadas edifice) nests between 3 older and heavily eroded shield volcanoes while the huge shield of Mauna Loa is partially constructed on the flanks of alkalic stage volcanoes, with Kĭlauea onlapping at the centre of the axial hot-spot.

The sedimentary architecture of the Canary Basin, comprising pelagic and continental-derived sediments intermingled with ash layers and volcaniclastics [*Delius et al.*, 1998; *Schmincke and Sumita*, 1998], is under-studied from a geotechnical perspective, although its hydrocarbon prospectivity is under increasing evaluation. Large amounts of methane-rich gas (between 2000 and 40,000 ppm), were intersected at ODP Site 955, southeast of Gran Canaria, originating from organic-rich sediments derived from the African continental margin [*Schmincke and Sumita*, 1998]. Seismic bright spots following the sedimentary bedding across the southern part of the basin may be indicative of low-permeability sequences as hydrocarbon reservoir seals that flank a series of diapirs [*Müller et al.*, 2000].

Negative pore fluid pressures (between 0 and -85 Pa) were recorded from free-fall penetrometer devices (4 m penetration) around the western submarine slopes of La Palma [*Urgeles et al.*, 2000]. The "abnormal" downward fluid flow is interpreted by these authors to signify a hydrothermal cell generated by thermal buoyancy around La Palma's active geothermal system. Carbonate-rich sediment, recovered in cores, again from La Palma's western submarine slopes, indicate that the surficial sediment drape is heavily to lightly over-consolidated [*Roberts and Cramp* 1996]. Geotechnical tests of clays drilled from the oceanic-continental transition (West Iberia, 619 m depth), indicate high pore-fluid pressure in these basal sediments [*Ask*, 2001]. The intense fracture/vein development in these clays suggests that the pore-fluids originate from deeper sections in the basement.

Like La Palma, the volcanic system of Tenerife, 84 km to the east, is founded upon thick successions of pre and syn-volcanic sediments, only thicker (>3.5 km) due its closer position to the continental slope and rise of West Africa [*Schmincke and Sumita*, 1998; *Urgeles et al.*, 1998]. Seismic reflection profiles show that Tenerife's flexural moat is infilled with sediments that dip towards the edifice interior (Fig. 1.3.28), stratigraphically onlapping the underlying Mesozoic sediments [*Watts*, 2001; *Mitchell et al.*, 2002]. Volcanism on Tenerife spans over 11 Ma, with the construction of three Miocene shields, and a rifted central volcano, Las Cañadas, over-lapping the older shields [*Albay et al.*, 2000]. Consolidation of the underlying sediments under loading, and a tendency toward a balance between volcano growth and erosive processes, may have suppressed slump-like deformation of the volcanic superstructure [*Masson et al.*, 2002]. Conversely, *Walter* [2003] suggests that load-induced deformation of the sedimentary sequences facilitated edifice spreading and triaxial rift development. Using a substrate of PDMS*, simulating the sedimentary layer, *Walter* [2003] modelled the structural evolution of Tenerife. Three sand cones (simulating the Miocene shields) were allowed to settle upon the PDMS, opposite or in mutual contact with each other, forming the basic shape of Tenerife. A larger cone was later placed in the middle, partially overlapping the older cones. Circumferential expansion of the cones resulted in the formation of summit grabens, the configurations of which resemble the triaxial rift orientations of the Las Cañadas edifice.

Given the ever-presence of normal and reverse faults, detachments, folds, fractures and alteration zones in the subaerial rock mass of the archetypal Canarian volcano e.g., [*Pérez-Torrado*, 1992; *Marinoni and Gudmundson*, 2002; *Fernandez et al.*, 2002; *Walter and Schmincke*, 2002], how best can the deep-seated substrates be characterized in terms of structures and pressure/temperature conditions? Flexure of the oceanic crust confirms that the pre-volcanic sediments are warped downwards (for Tenerife) [*Watts et al.*, 1997] (Fig. 1.3.28), while the oceanic crust itself is altered (by vigorous hidrotermal processes) [*Ye et al.*,1999] and often underplated [*Nikogossian et al.*, 2002; *Dañobeitia and Canales* 2000]. It is rational to assume therefore that the substrate must accomodate an immense lithostatic load during crustal thickening, alleviated slightly during reccurent mass wasting events. Finite element models of the hydrogeological evolution of the Canary, Hawaiian and Marquesas Islands and their substrates indicate a growth-stage variation in fluid flow which is dependant on edifice construction and sedimentation rates, edifice size and lithospheric flexure [*Christiansen and Garven*, 2004]. For the Canaries, these authors hypothesize that the lower pore pressures along the substrate-edifice interface (compared to Hawaii) may explain the lack of evidence for (deep-seated?) edifice spreading. As previously stated however, the criteria for deep-seated gravitional spreading may be different to Hawaii but this does not neccessarily relegate the evolutionary process involving gravitacional spreading.

At the centre of each edifce (at the base), heat flow must be high since the magma plexus feeding the central vent or rift systems obviously penetrates the sediment layer underwhich it connects to a cumulate prism anchored in the upper crust.

*PDMS is a 65%vol component of Silly Putty™ [*Cambridge Research Group*, 2002].

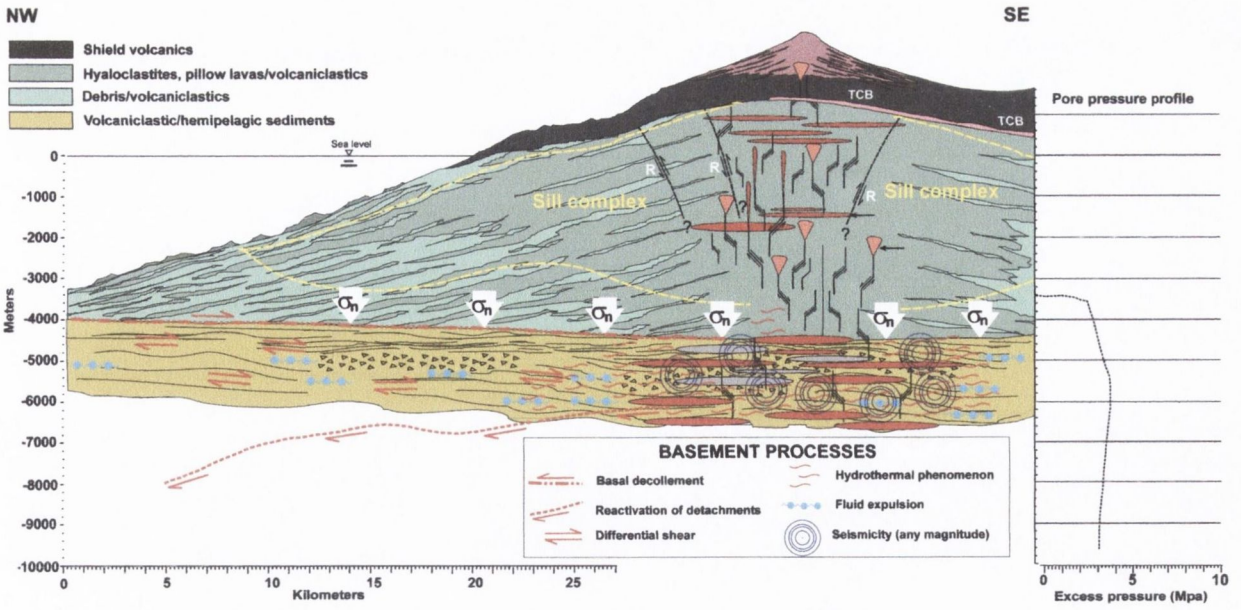


**Fig. 1.3.30.** Section of La Palma's volcanic system illustrating the range of phenomenon and structural condictions that may have influenced the development of the volcanic pedestal. Modelled pore pressure profile from *Christiansen and Garven* [2004]

*Fernandez et al.* [2002] suggest that the reactivation of structures in the oceanic lithosphere, such as the hypothetical prolongation of the fracture zones toward the Canary Archipelago, may have had an important influence in the development of the archipelago. The same could be said for the detachment faults abounding in the oceanic crust (Fig. 1.3.30). In addition to these large scale structures it is theoretically possible that compression, dewatering, hydrothermal phenonena, diagenetic effects (including hydrocarbon generation) and devolatilzation of magmas, occur along the substrate. Such activity could influence the development and magnitude of fluid pressures and associated deformation as illustrated schematically in Fig. 1.3.29. One can only speculate that such processes had influenced the morphological development of La Palma's volcanic system by enabling differential gravity-driven spreading with suppressed outward displacement of the flanks. In this manner equilibrium is preserved between vertical growth and lateral mass transfer of the submarine superstructure.

## 1.3.5. Conclusions

The observations and deductions reported here, although they preclude estimations of the temporal development of the Cumbre Nueva rift zone or its structural relationship with the contiguous divergent rift zones of northern La Palma, nevertheless provide a set of arguments that place reasonable constraints on the morphological development of subaerial La Palma and its larger submarine construct. One of the most important deductions is that the Puntagorda rise is a rift zone, or a large part of one, that has developed during the Pliocene seamount stage. This deduction is based on the paradigm that the processes intrinsic to the magmatic and structural development of the subaerial volcanoes should reflect on the larger, older submarine pedestals. The preferred interpretation therefore is that multi-axial rift zone activity was well established before the subaerial stage of Taburiente volcanism, although radiometric data of submarine rocks together with complete high resolution bathymetric imaging is needed to qualify this assumption. The slope differentiation observed on the subaerial slopes was induced at a late stage in the evolution of Taburiente, resulting from eruptions of differentiated rocks (phonolites/trachytes) more viscous than alkali basalts that typify the shield stage of volcano growth. As yet it is difficult to unambiguously determine if the sediment layers underlying La Palma have influenced the morphology and structural evolution of the volcanic system.

# CHAPTER 2

# VOLCANO-TECTONIC UNITS AT THE BASE OF THE CALDERA & CUMBRE NUEVA ESCARPMENT

Note: The symbol [T] at the end of a sentence is used to denote unstable and/or inaccessible terrain.

# 2.1 The Tenerra Collapse Breccia

A volcaniclastic substratum, between 60 and 350 m thick, is exposed at the base of the Quaternary collapse escarpments. It is well-consolidated and compositionally heterogeneous, containing an important component of juvenile pyroclastic material (20-40% volume). Introducing the Tenerra Collapse Breccia (TCB) as the first of two fundamental tectono-stratigraphic units on La Palma.

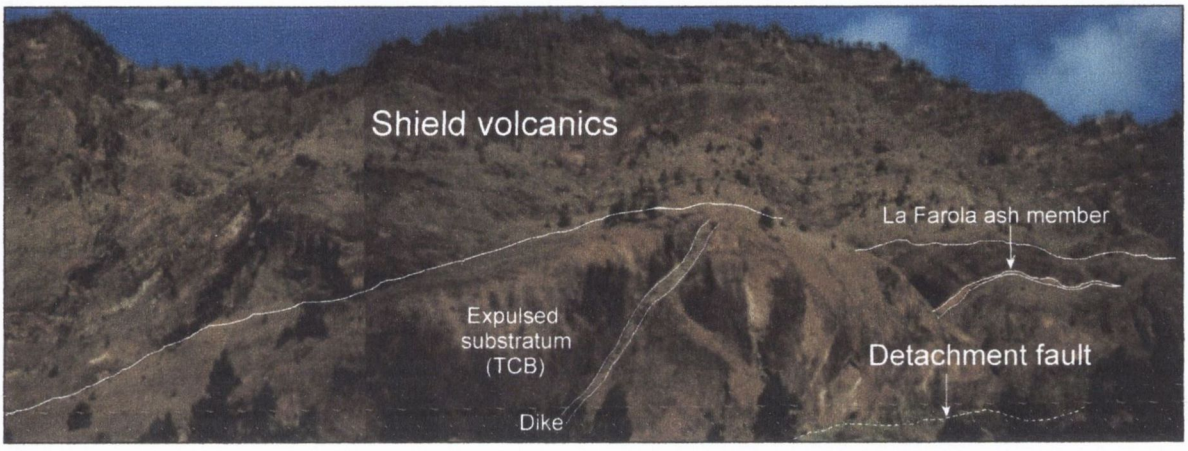


**Fig. 2.1.1.** Photo-mosaic showing a longitudinal segment of the TCB (Tenerra Collapse Breccia) at Hacienda del Cura.. The detachment fault is part of the Cumbre Nueva detachment. Compare this image with Fig. 2.1.23, a profile view of this locality taken 2 km to the NE.

### 2.1.1 Introduction

This section describes the distribution, characteristics and significance of the volcaniclastic/pyroclastic substratum outcropping at the base of the Quaternary collapse escarpments (Fig. 2.1.1), the so-called 'agglomerates' mentioned in previous works on the geology of La Palma [e.g., *Gastesi et al.*, 1966; *Navarro and Coello*, 1993]. Henceforth this substratum is referred to as the "Tenerra Collapse Breccia" or "TCB". The importance of the TCB in the stratigraphic framework of the island can be viewed from two distinct perspectives; volcanological and structural. It accumulated during the southward-directed lateral collapse of Ancestral Taburiente at around 1.2 Ma, and was subsequently buried by Taburiente Volcano [*Ancochea et al.*, 1994]. The TCB is well consolidated and highly heterogeneous in terms of the constituent clast, block and matrix petrography and type. Several of the compositional and structural characteristics of this unit have eluded detection by contemporary studies, foremost among which is the profusion of juvenile materials and the evidence of localized deformation in the interior of the constituent ash members. The ash members are formed by laterally persistent sheet-like deposits up to 20 m thick. More abundant 'ash bands' also show evidence of localized deformation in the form of attenuated clasts and shearing of matrix. This section also explores the volcanological aspects of the TCB in terms of its mode of accumulation, depositional structures and important parts of its structural evolution since 1.2 Ma. It presents evidence that the TCB underwent ignimbrite-like rheomorphism and solidification after accumulating during a powerful volcanic eruption, concurrent with the partial collapse of Ancestral Taburiente. Further discussion is presented on the post-Cumbre Nueva collapse (i.e., 0.55 Ma) behavior of the TCB in response to lithostatic unloading.

### 2.1.2 The location and geometry of the TCB from outcrop and subcrop studies

The TCB outcrops at the base of the Quaternary landslide escarpments along a distinct break in slope between the seamount series/intrusive core and the overlying shield volcanics. It is traceable discontinuously for nearly 20 km, is between 60 and 350 m thick, and characteristically protrudes out from the base of the escarpments. The protruding or overthrust surface presents SW orientated slickensides, the significance of which is discussed in Ch. 2.2. The position of the TCB relative to the uplifted basement and the conformably overlying shield volcano is illustrated in Fig. 2.1.2. The aerial photograph in Fig. 2.1.3. illustrates the three main sectors (1) the Hacienda sector, forming the right lateral fault-controlled northern limit of the embayment (as defined by *Carracedo et al.*, 1997; 1999a), (2) the arcuate Cumbre Nueva sector (forming the headwall region of the Cumbre Nueva landslide) and (3) the Guanche sector which is exposed below the east wall of the Caldera. No data were acquired from below the headwall of the Caldera[T] (labeled 'La Pared' – the wall).

#### 2.1.2.1. The Hacienda sector.

The field investigations were focused on the most accessible 'Hacienda sector' from where the Cumbre Nueva Detachment outcrops in its most pristine form (Ch. 2.2). The remarkably linear escarpment bounding the Hacienda sector (Figs. 2.1.4 and 2.1.5a) extends for 9 km, sloping at angles between 5° and 17° southwestward, from stratigraphic intervals ca 1400 to 640 m above sea level. The escarpment has been identified from previous studies as a right-lateral detachment-like structure that facilitated the collapse of the west flank by wrenching it away from the stable northern slopes [*Carracedo et al.*, 1997; 1999a]. Field observations from the NW wall of the Caldera are included in this sector. The TCB is intermittently obscured by steep rock avalanche and piedmont alluvial fan deposits and by thick scrub vegetation. The seaward end of the linear escarpment is obscured, over a distance of 4.5 km, by successions of volcaniclastics (the El Time sediments and lavas) between 200 and 370 m thick.

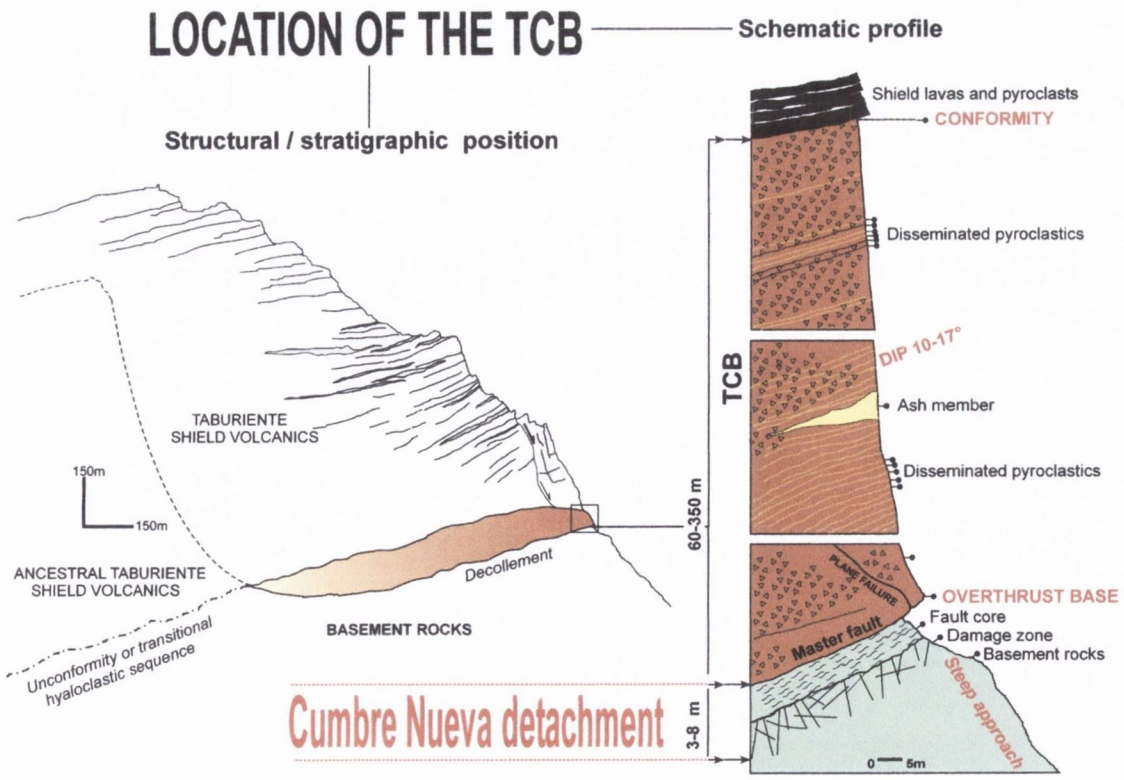


**Fig. 2.1.2.** Scaled section and schematic profile of the TCB and the underlying detachment fault. The scaled section shows a NW-SE transect through the SW-striking Hacienda sector (see text).

Fig. 2.1.2 (cont). The section is based, in part, on the hydro-geological reports [*Bravo and Coello,* 1978; *Coello,* 1984] that show scaled cross-sectional detail of the hangingwall breccias and their conformable relationship with the shield volcanics and the intrusive core. Note the overthrust base of hangingwall.

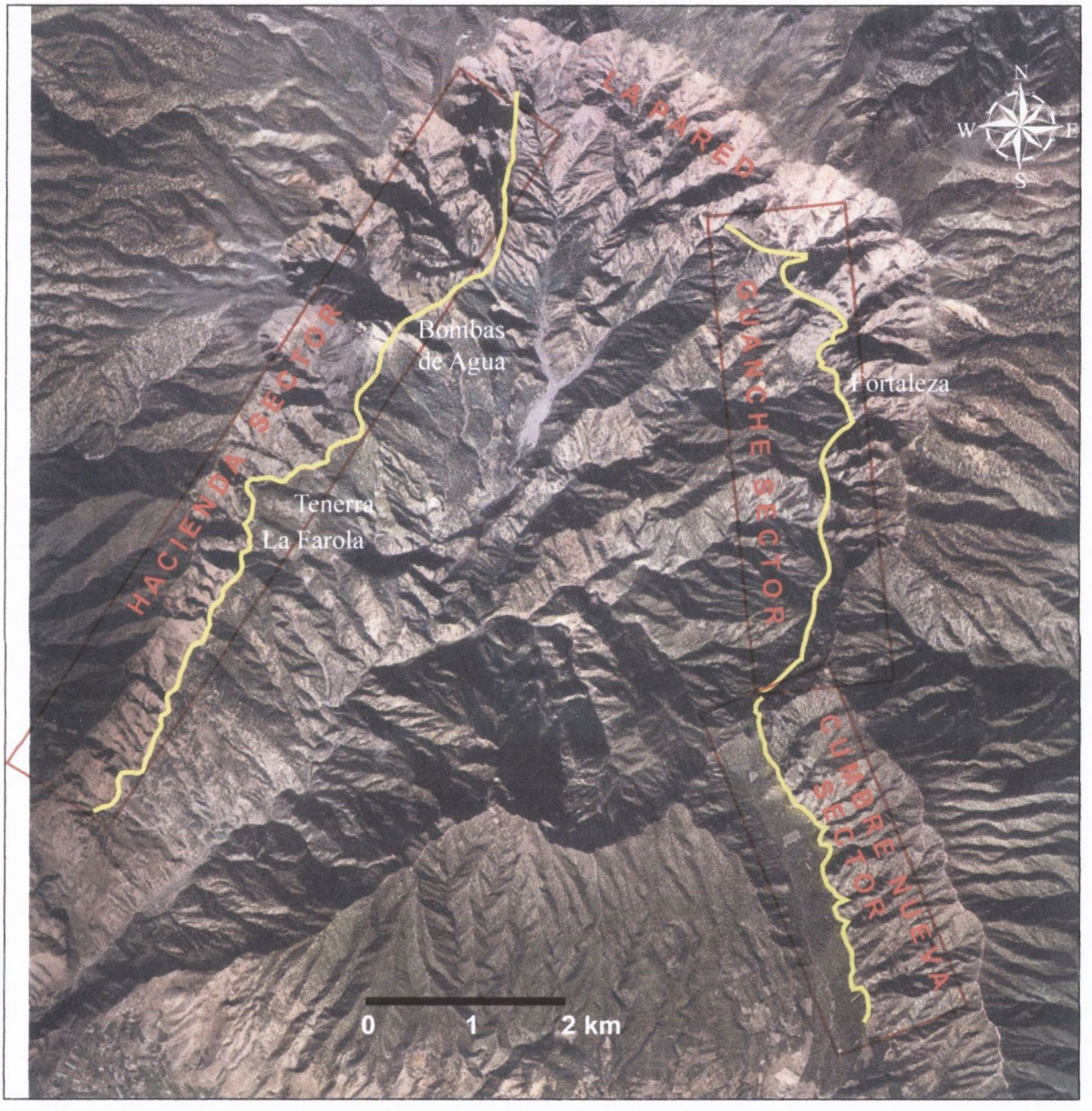


**Fig. 2.1.3.** Aerial photo showing the extent to which the TCB (in yellow) has been exhumed by the lateral collapse structures. The trace of the detachment is outlined in yellow. La Farola, Bombas de Agua and Fortaleza are localities from where ash members are exposed (see text). Image source – GRAFCAN, 2001.

**Fig. 2.1.4**. a. Photo-mosaic of the straight-walled Hacienda sector. The collapsed north flank of Bejenado volcano is visible on the left. b. Clouds cascading over the arcuate segment of the Cumbre Nueva escarpment. Note the topography of the NW rift zone of Cumbre Vieja The abbreviation V is a vent of Cumbre Vieja. c. Box cut and decline near El Paso (March, 2001) for the Cumbre Nueva tunnel highway TF-812 linking Santa Cruz and Los Llanos. d. The southern end of the escarpment where it is enveloped by Cumbre Vieja volcano. The scoria cone (Montaña Quemada) and lavas are possibly late 15$^{th}$ Century AD.

### 2.1.2.2. The Cumbre Nueva sector

Along the Cumbre Nueva sector, the TCB is exposed below the south-striking arcuate Cumbre Nueva escarpment (Fig. 2.1.4b), the southward continuation of which is buried beneath Cumbre Vieja volcano. The TCB is exposed along this sector, albeit incompletely, beneath the northernmost segment of the 11 km long escarpment, dipping to the east, between 5° and 11° (measurable from the volcaniclastic layering). Towards the south, the exposure gives way to vegetated alluvial fan deposits and lava flows (Holocene/sub-historic) vented from the northern segment of the Cumbre Vieja rift zone (Fig. 2.1.4d).

Small (Holocene?) rock avalanche deposits, generated by escarpment foundering, have also locally obscured the exposure. However, the galerías in this sector penetrate a substantial thickness of TCB materials. Furthermore, tunneling operations underneath the escarpment (Figs. 2.1.5c and 2.1.6), have, according to the site engineers' reports, been excavated through thick sequences of TCB-like materials, lavas and dikes. The initial excavation is supported within several hours of each advance by a 2 cm thick lining of shotcrete with rock/cable-bolt and mesh reinforcement. This made it impractical to conduct site studies at the cutting face. Where it is exposed, the TCB protrudes outward from the base of the escarpment, in some areas up to 150 m laterally.

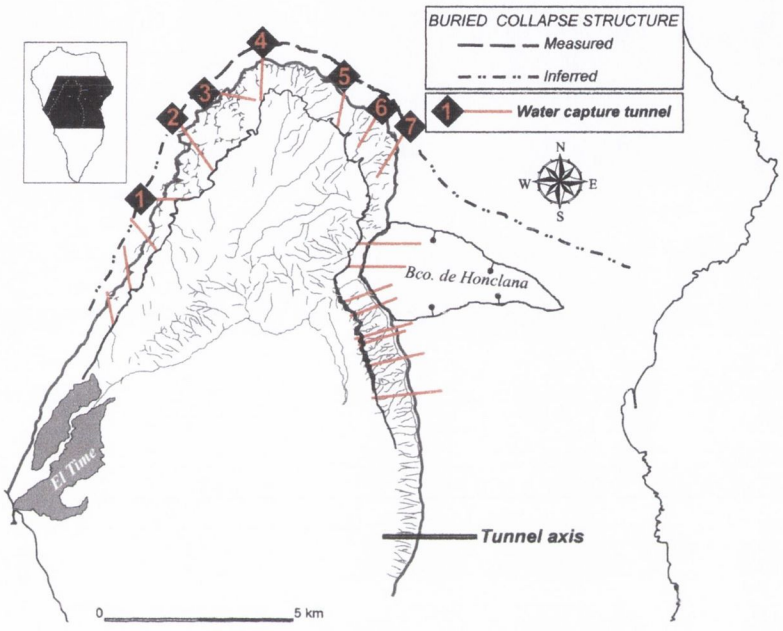


**Fig. 2.1.5.** Map showing the geometry of the Caldera/Cumbre Nueva escarpment in relation to the Ancestral Taburiente collapse structure and Bco. de Honclana. The trace of the buried collapse structure has been ascertained from hydro-geological studies [*Bravo and Coello,* 1978; *Coello,* 1984]. The axis of the Cumbre Nueva tunnel is shown. Numbers denote the galerías in Fig 2.3.6.

### 2.1.2.3. The Guanche sector

The Guanche sector (Fig. 2.1.3) extends for over 7 km northward from La Cumbrecita to Bco. Verduras Alfonso, and has not been investigated in detail [T]. The TCB was observed at outcrop in the vicinity of the galería at Bco. de Los Guanches. Further south, the striated surfaces of boulder train blocks (Ch. 2.3) and talus fan clasts give an indirect indication that the TCB is also spatially associated with this sector.

## 2.1.3 The geology of the TCB

### 2.1.3.1 Volcaniclastic deposits

The volcaniclastic constituents make up the bulk of the TCB, influencing its colour (often light brown to yellowish brown at a distance). In terms of the depositional structure, there are at least two distinct varieties, (1) a rhythmically layered type and (2) a massive structureless type; the relationship between the two is unknown[T]. Summary logs showing the components and volcaniclastic fabrics are illustrated in Figs. 2.1.9 and 2.1.10. Stratigraphic profiling at outcrop was supplemented by structural and petrographic observations of the large boulder train blocks and slabs which have accumulated in the ravines leading from the outcropping TCB down to the floor of the Caldera/Bco. de Las Angustias. The boulder trains are sourced from all stratigraphic intervals of the TCB, giving an invaluable insight into its depositional structure and its compositional variation. Ravines and perrenial cascades, incised into the TCB, offer further three-dimensional exposure at outcrop.

A polished section of the TCB (Fig. 2.1.6) shows the characteristic hand-specimen colouration and the diversity of petrographic components and clast sizes typical at outcrop scale. In bulk, the TCB is composed of matrix-supported blocks (i.e., >0.5 m) and clasts (i.e., <0.5 m) that account for between 50 to 68 vol% of the rock mass composition. Crystals are between 5 to 15 vol% while the juvenile pyroclastic matrix (discussed separately), ranges between 10 to 30 vol%. In the matrix-supported units the clast are dispersed or equi-distanced at centimetre scales.

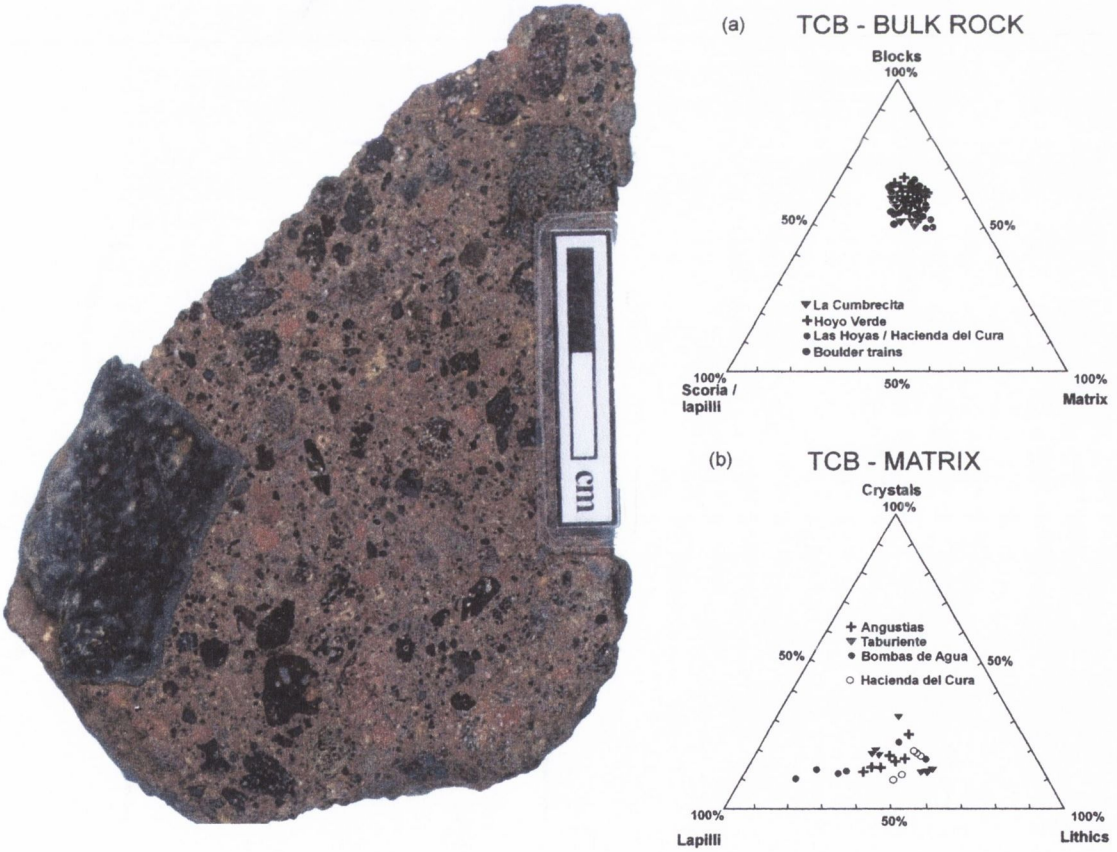


**Fig. 2.1.6.** Polished hand specimen (character grab) of the TCB from Hacienda del Cura. Note the abundant particles of scoria and lapilli (red, orange and yellow) >5%Vol. The material characteristics of the TCB based on visual estimations of (a) bulk rock and (b) matrix components. Note: In (b) the observations from the Bco. de las Angustias, Bco. de Taburiente and Bco. Bombas de Agua are from boulder trains. Those of Hacienda del Cura are in situ observations.

The closed framework units comprise clasts and blocks in mutual contact or separated only at millimetre scales. The coarse to fine sand-sized matrix is composed of lithic fragments and relic crystals, mixed with substantial amounts of juvenile scoria and lapilli (see section 2.1.4.2). The latter components produce vivid oxidation colours (red, orange, purple etc.,) made more intense by a banded appearance. In terms of grain shape, the pebble and sand-sized lithics and cinders are equant, hackly and elongate.

Unlike the TCBm units (subjacent to the TCB), there is no trace of metasomatic alteration in either the clasts/blocks or the matrix. However, occasional angular clasts and shards of hydrous metamorphosed basement rock are entrained within 1 to 2 m of the base. The constituent clasts/blocks are petrographically highly heterogeneous, ranging from ankaramite, basanite, gabbro, phonolite, aphyric, etc. However, there are innumerable laterally persistent layers where the clastic components are petrographically homogenous. The colour contrast in the clasts/blocks is typically grey, bluish grey, red, yellow, purple, etc. Oxidation halos and selvages, between 0.2 and 5 cm wide, infiltrate the matrix surrounding some of the blocks. The clasts/blocks show substantial variation in dimension, density and size, ranging from 1 to 3 m wide tabular sections of jointed dike, 0.3 to 2 m wide sections of jointed, dense lava flow core, to irregular 10-60 cm clasts of scoria, lapilli and highly vesicular lava. No toreva remnants have been observed in the TCB. The block and clast surfaces are embayed, hackly, equant and curvaceous, locally displaying evidence for through-going fracturing and incipient break-up and comminution in the same plane as the volcaniclastic layering. Other blocks and clasts show reticulate and jigsaw fractures.

One of the most characteristic features of the TCB is its hardness. Some sections are exceptionally lithified and even appear silicified, thus making granulometric analyses impractical. The hardened surface is often curvaceous and bulbuous at outcrop, with large-scale tension fractures penetrating the rock mass. The fracture spacing is around 10 to 60 m. The aperture widths (see Profile 5 in Fig. 2.1.8) along the fracture planes are a few millimeters to tens of centimeters wide. The wider apertures correlate with boulder-sized segments (often slab-like in geometry and up to 60 m high) that are in the process of detaching and collapsing away from outcrop (Fig. 2.1.10b).

Other characteristics of the TCB include the rhythmically bedded, sorted and occasionally well graded arrangements of the constituent clasts/blocks and matrix. This ordered structure contrasts with an equally abundant (perhaps even more dominant) structureless variety. Evidence exists, particularly in the matrix, of particle disaggregation and clast stretching/flattening, particularly among the layered scoria-rich horizons (see profiles 1,2 and 3 in Fig 2.1.10). The frequency of sheeted intrusions that transect the TCB is low along the SW end of the Hacienda sector, between 1 and 10 dikes per hundred meter interval, but this increases north-eastwards towards the interior of the Caldera, where the density of sheeted intrusions is between 1 and 10 intrusions per 20 m interval.

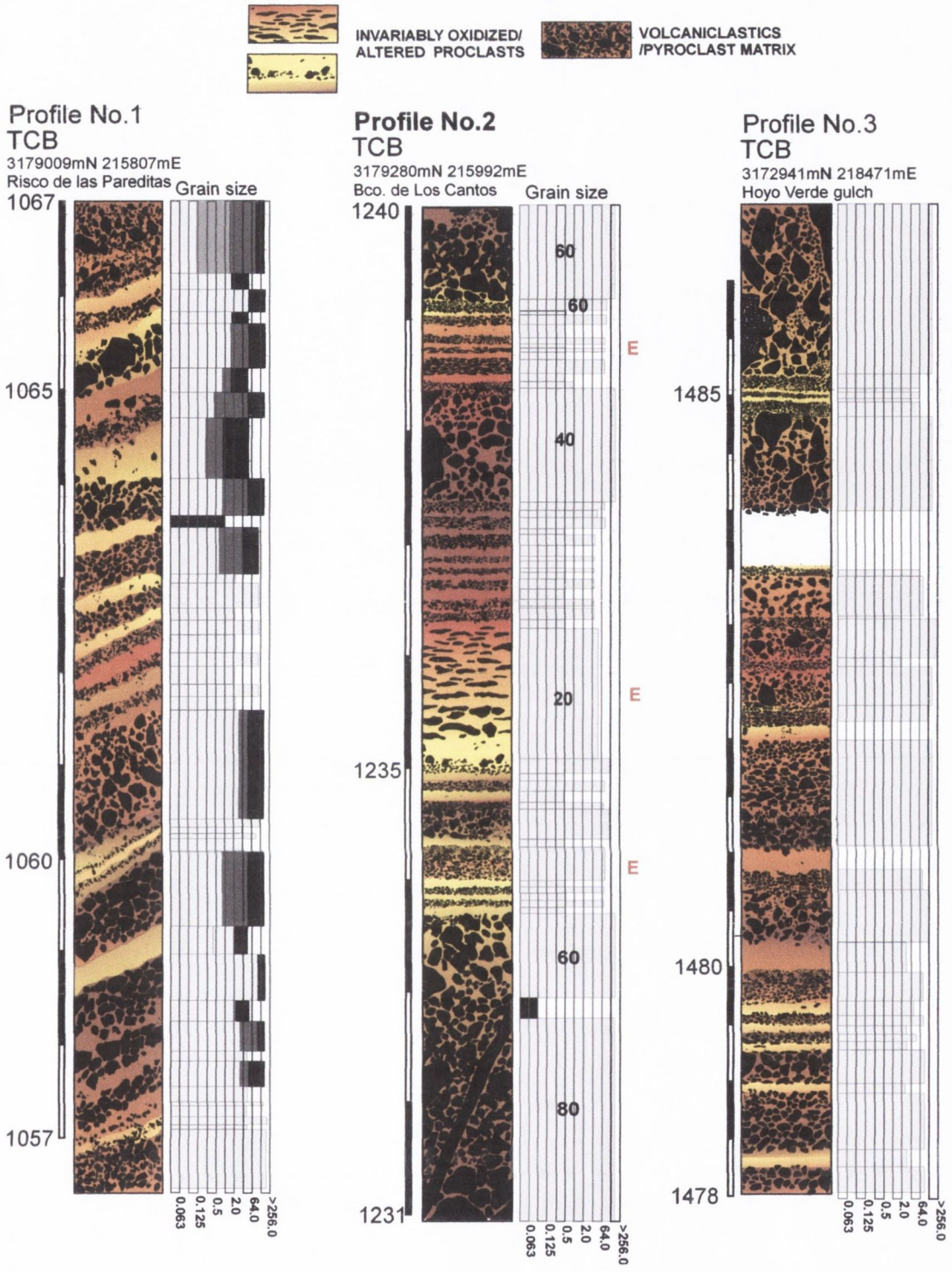


**Fig. 2.1.7.** Scale variant stratigraphic profiles of the TCB. All heights are in meters. The colour intensity is exaggerated to enhance volcano-stratigraphic sequencing..

Profile No.1. Dip is 243°SW. The profile illustrates a layered fabric of blocks/clasts and ash bands.

Profile No.2. Layering of large dense blocks of basalt and scoria, segregated by thin ash bands The interval between 1235 and 1236.3 is displays a eutaxitic (E) texture.

Profile No.3. Veneering of juvenile-rich blocky layers and discrete ash bands.

# Tenerra Collapse Breccia

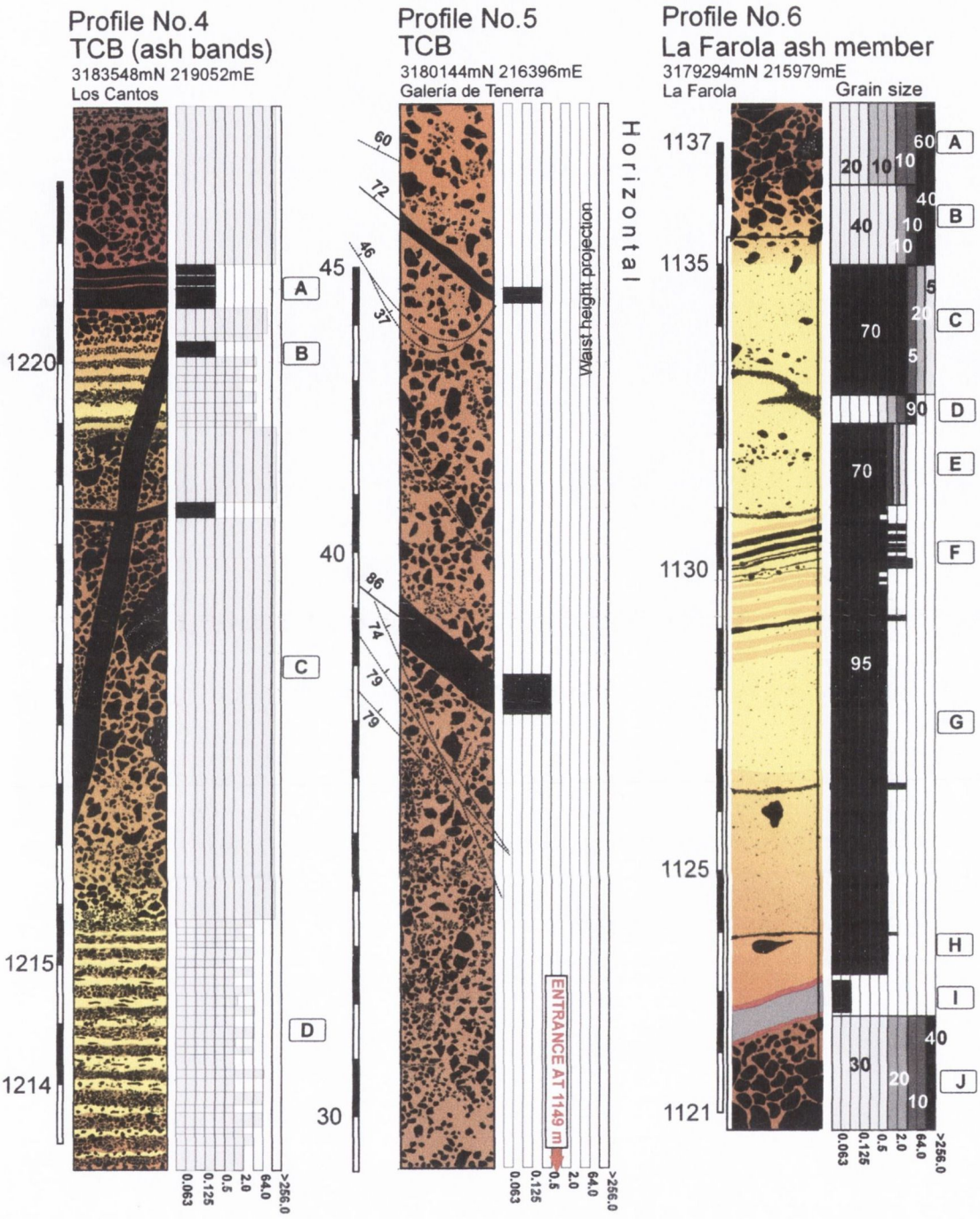


**Fig. 2.1.8.** Scale variant graphic profiles of the TCB. All heights are in meters.

Profile No. 4 A and B. Aphyric sills. C. Poorly sorted multilithic volcaniclastic unit D. Ash bands with flattened and attenuated scoria (eutaxitic texture) and crystal laminations.

Profile No. 5 A sub-horizontal traverse through a TCB unit with no discernible layered structure. Joint planes between 0.1 and 2 cm wide are heavily oxidized and show significant seepage.

Profile No.6. A. $TCB^2$ volcaniclastics with 15% disseminated lapilli and scoria. B. Lapilli and scoria with occasional lithic blocks. A thermal aureole is present in the region of lithic blocks. C. Scoria layer with basaltic bombs. D. Cpx - lapilli seam. E. Pale-yellow cinders and lapilli with Cpx rich scoria clots and bombs. F. Couplets of cpx and lapilli. G. Pale-yellow cinders and lapilli with cpx rich scoria clots and bombs. H. Progressive darkening of scoria toward base of sequence. I. Cpx-ol phyric dyke (2-3% crystals) with 2 cm chill margins. J. TCB1 volcaniclastics speckled with altered lapilli bands.

**Fig. 2.1.9.** (a) A late-stage feeder dyke traversing part of a 200 m succession of lithified TCB at Los Frailes (north of Tenerra). A baked contact is seen in the upper part of the photograph. The tape is extended to 1 m. (b) An arrangement of dense plagioclase-phyric lava blocks, ankaramite clasts and fractured aphyric dike fragments suspended in a structureless open framework, comprising 5-10% juvenile lapilli matrix. Location: Las Hoyas.

**Fig. 2.1.10.** (a) A slab of TCB material detaching from primary outcrop along a wide aperture tension fracture. (b) Boulder train accumulations inside Bco. Bombas de Agua leading up to the escarpment at Risco Liso. Person (circled) for scale. See also Fig 2.1.25.

### 2.1.3.2 Pyroclastic components

Pyroclastic materials form an integral component of the TCB, occurring as three distinct deposit types, (a) laterally extensive scoria/lapilli horizons up to 20 m thick (herein referred to as ash members), (b) centimeter-wide scoria and lapilli layers (herein, ash bands) and (c) disseminated scoria and lapilli.

#### a. The ash members

The ash members are formed by sheet-like deposits, up to 2 km long, composed of altered yellow scoria/lapilli and bombs. Three ash members were observed along the Hacienda and Guanche sectors; the map and section in Fig. 2.1.11 illustrates their spatial distribution. Here they are named :

(1) the La Farola Ash Member

(2) the Hoyo Verde ash member

(3) the Fortaleza ash member.

The ash members are between 0.2 and 30 m thick and often display a pronounced internal fabric characterized by dark, banded crystal/lapilli formations, tens of centimeters in thickness. These darker formations are termed couplets. Included in the deposits are various amounts of ballistic bombs, slabby lava drapery and scoria and other accidental clastic fragments and large blocks of the type described in section 2.1.3.1.

The ash members are strata-bound within the enclosing TCB volcaniclastic deposits, displaying sharp contacts with the scoria/lapilli-rich TCB matrix, with diffuse thermal aureoles up to 2 m thick. The bulk of the observations regarding the stratigraphy, internal structures and regional significance of the ash members are based on the sections exposed at La Farola, Roque de la Fortaleza, Bco. Bombas de Agua/Hoyo Verde.

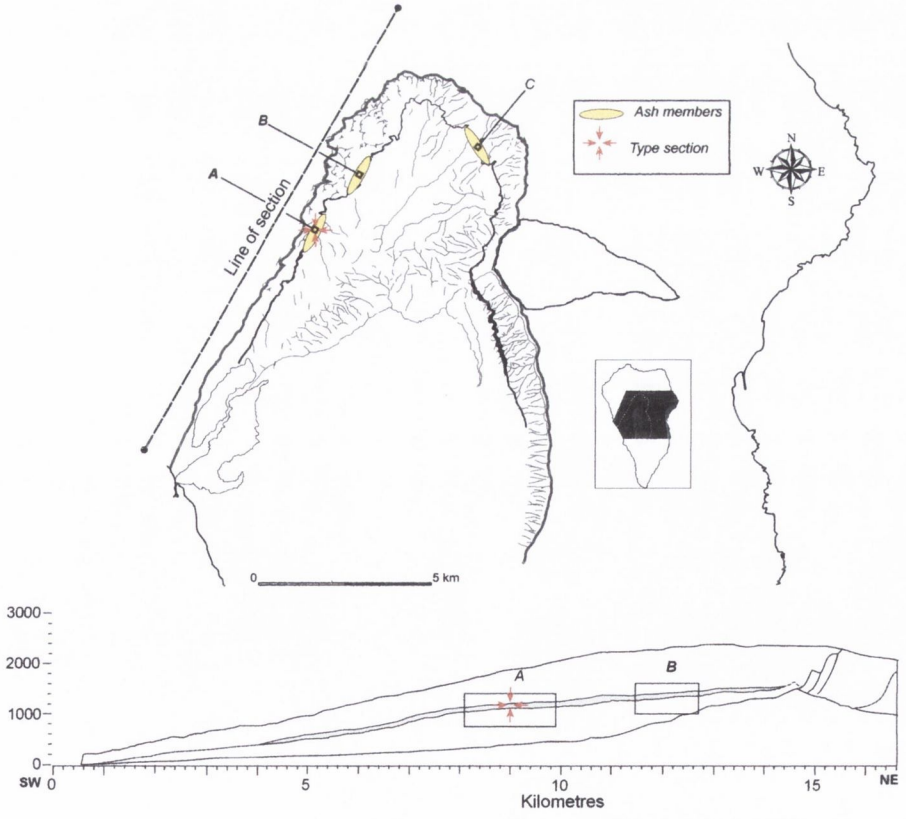


**Fig. 2.1.11.** Map and section illustrating the structural / stratigraphic positions of the main ash member depo-centres. A. La Farola. B. Hoyo Verde/Bombas de Agua C. Roque de la Fortaleza.

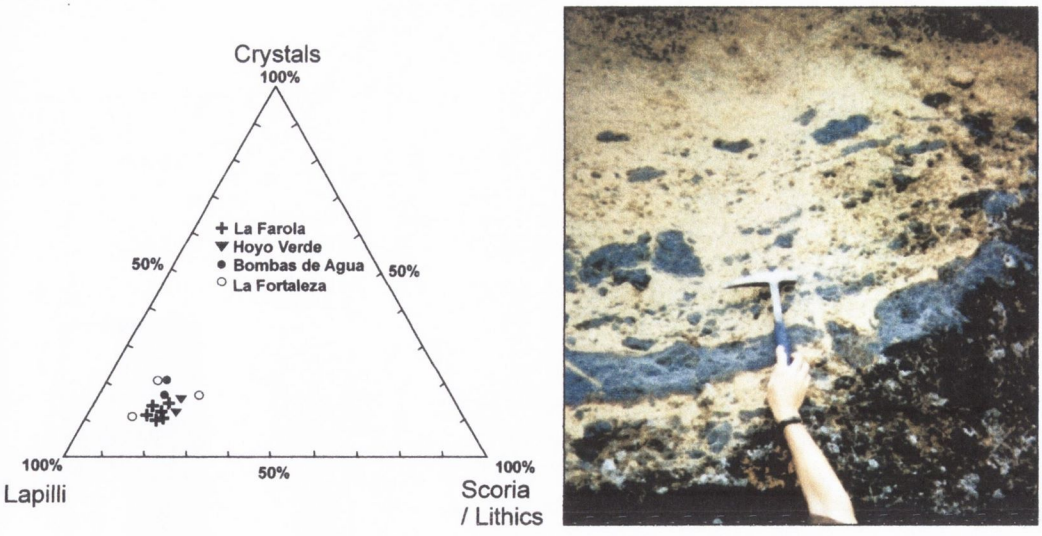


**Fig. 2.1.12.** Grain composition plot for the ash members. The image right shows part of the Hoyo Verde ash member showing palagonitized scoria/lapilli with ol/cpx-phyric slabby lava drapery and spatter. Location:- Hoyo Verde

The La Farola Ash Member* is up to 25 m thick, extends laterally for ~2 km, from stratigraphic intervals ca 800 m to 1350 m AMSL. The type-section at La Farola, illustrated in Profile 6 (Fig 2.1.8), is located around 80 m above the base of the escarpment,. dipping 16° towards the NW. The La Farola deposits conformably overlie a 70-300 m thickness of volcaniclastics (herein $TCB^1$) as described above and then by 60-80 m of compositionally equivalent volcaniclastics (herein $TCB^2$). Included in the deposit are dense lava blocks and fragments of petrographically diverse vesicular basalt (e.g., ankaramite, cpx-rich, olivine rich). The entrained basaltic boulders are between 0.5 and 1 m wide and display well-developed thermal aureoles where they have been enveloped by the uppermost part of the ash member. Internally, small ballistic bomb sags are quite common (Fig. 2.1.15a) while large 'rip up clasts' and scour trails are well exposed along the base of the ash member and from sections of the Bombas de Agua ash member.

The main body of the La Farola Ash Member is invariably composed of 60-80% coarse-grained lapilli, 10-70% free crystals (exclusively cpx), 5-10% juvenile scoria, bombs with cow-pat spatter, slabby lava drapery and between 15 and 35% accidental lithics. Cut sections of the La Farola Ash Member are presented in Figs 2.1.13 and 2.1.14 illustrating the different concentrations of the constituent crystals. The lapilli and cpx crystals form the well-developed stratification, defined by the banded couplets, between 2 and 15 cm thick (Fig. 2.1.15a) especially in the core of the formation, where locally they appear heavily deformed. Fig. 2.1.15b shows the core of a SW verging recumbent fold with parasitic M-shaped folds on the hinge of the anticline. The limb region displays well-developed chevron folds with sharp hinges and straight limbs (Fig. 2.1.16a). Polyclinal folds, located beneath the recumbent folds, are in close proximity to flame-like diapiric structures arranged as linked sets up to 40 cm high and 40-60 cm in wavelength (Fig. 2.1.16b ). At the base of the formation, clinopyroxene crystals (0.5-1% by volume) show a pronounced flattening and shearing in plane with the stratification. The dark cpx/lapilli banding is also locally contorted around impact sags (see Fig. 2.1.16 a and b).

* The La Farola type-section is accessed from the dirt track leading to the overlook at Los Brecitos. There is a storage hut in open ground, about 1 km before the overlook, this marks the waypoint. Roque de la Fortaleza is accessed via Bco. Verduras Afonso and then by ascending a steep-sided, partially collapsed ridge leading up to the NE wall of the Caldera. The latter two sections are accessed along steep talus fans that drop off into the amphitheatre chasms.

**Fig. 2.1.13.** Cut section of the La Farola Ash Member exhibiting a centimeter-scale wavy banded texture and around 15% augite crystals. Left hand part of scale card is graduated in centimeters.

**Fig. 2.1.14.** Cut section of the La Farola Ash Member showing 70% augite crystals.

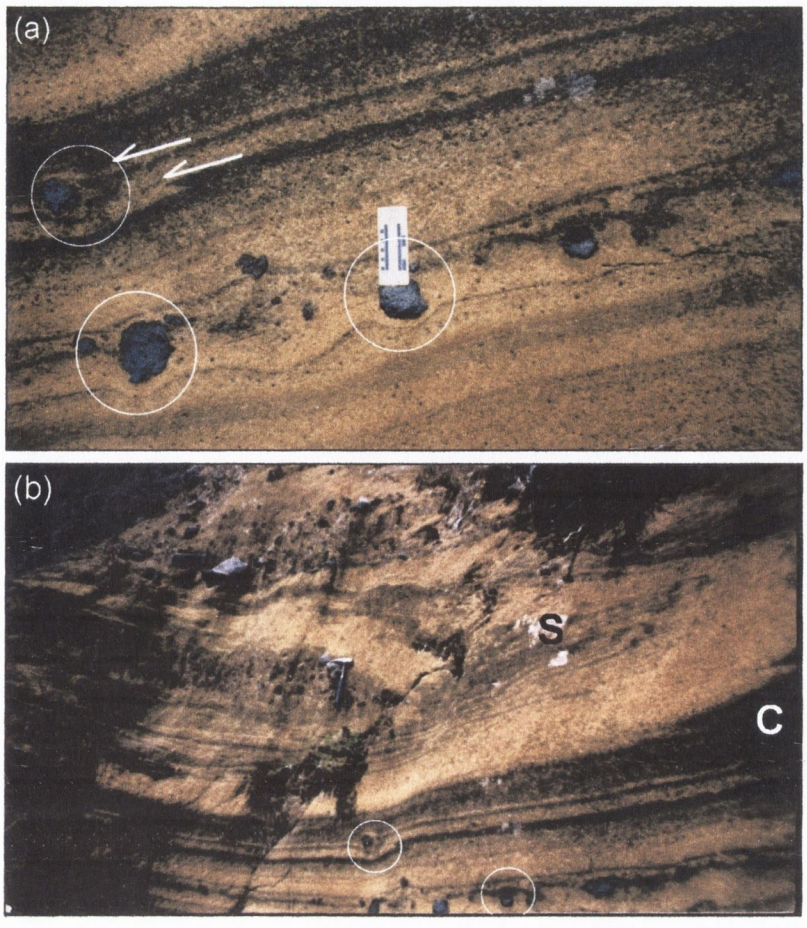


**Fig. 2.1.15.** (a) Impact sags (circled) and deformed couplets (shear symbols). SW-NE from left to right. b) The core of a recumbent fold with parasitic chevron folds (marked C) and M-shaped folds on the hinge region. Note the warped impact sags (circled) and basalt blocks (upper left).

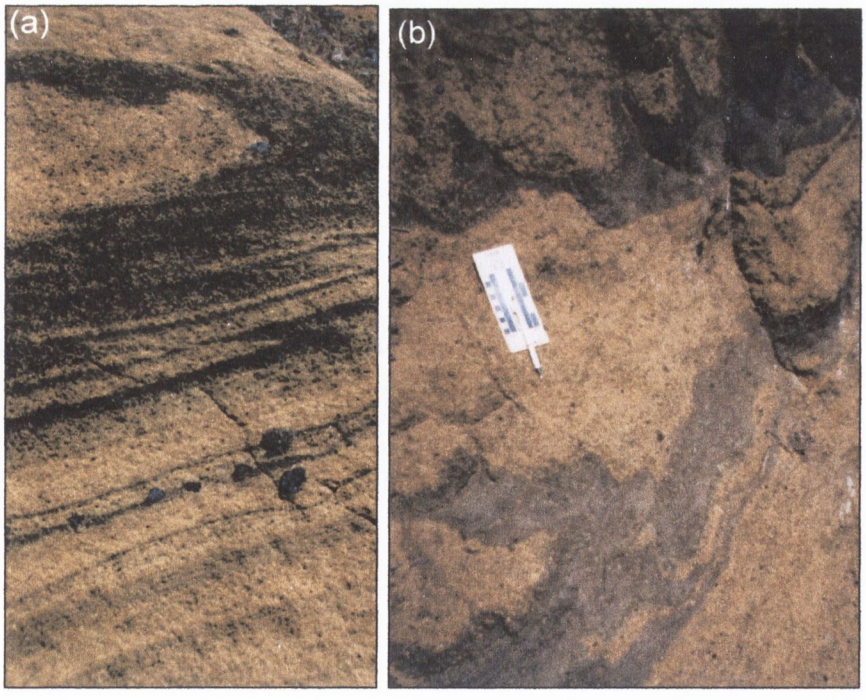


**Fig. 2.1.16.** Deformation structures in the core of the La Farola Ash Member. SW-NE from left to right. (a) Parasitic chevron folds on the limb of a small recumbent fold. The main "Z" is 4.5 cm thick. (b) Polyclinal folds underlying flame-like diapiric structures. Both are exposed around 20 m NE of and 10 m below the main recumbent fold.

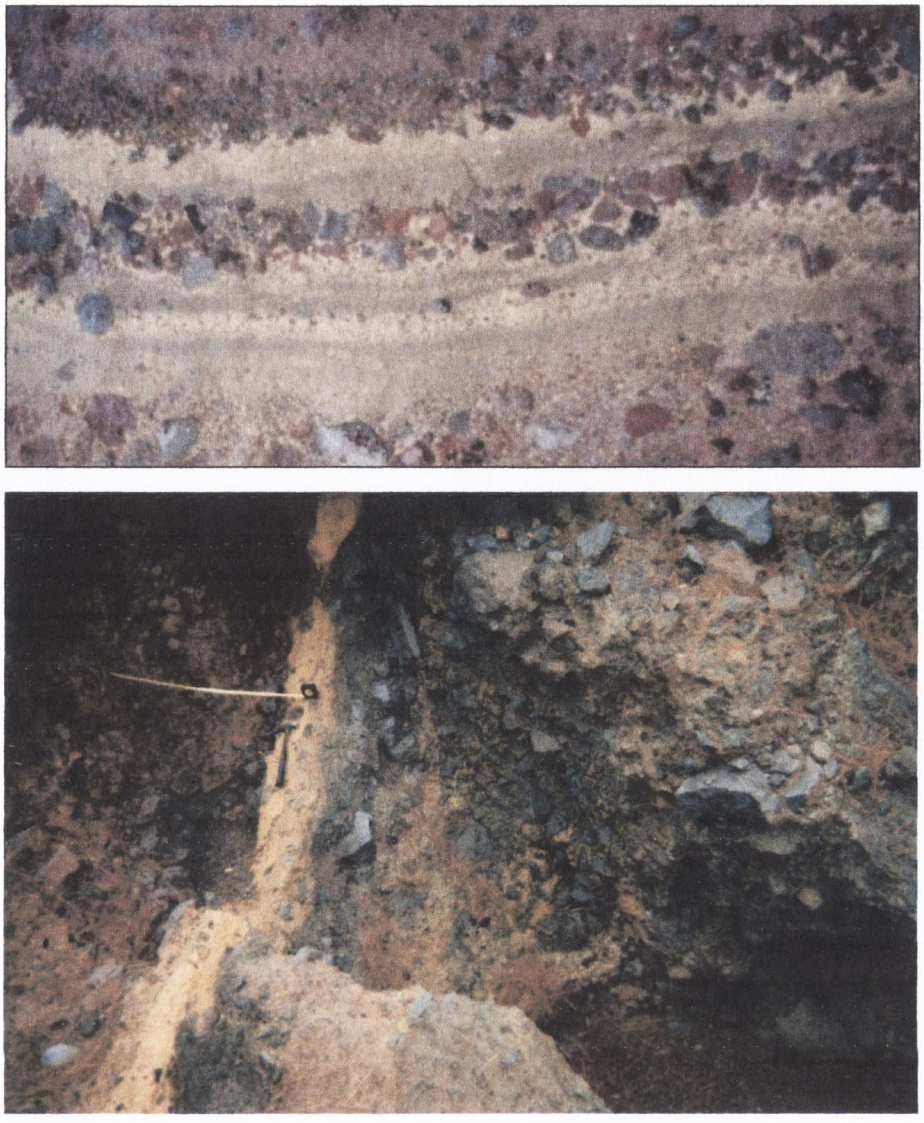

**Fig. 2.1.17. (a)** A 22-24 cm thick pale yellow ash band exposed from a boulder train block inside Bco. De las Piedras Redondas. (b) A large slab of TCB material exposed in an ephemeral ravine, exhibiting a distinct yellow ash band with pyroclast rich matrix in the surrounding TCB. The tape measure is extended to 1 m. Location: Bco de Las Traves.

### b. Ash bands and patches

The ash bands are defined by layers of medium to coarse grained scoria and lapilli that are associated with larger abundant fragments of oxidized scoria. The ash bands are between 5 cm and 60 cm thick and are typically pale or bright yellow, often with darker margins. They are prolific along the Hacienda sector, occurring singularly or as multiple sets (couplets). The ash bands often display flattened and attenuated fragments of scoria (profiles 2, 3 and 4 in Figs. 2.1.8 and 2.1.9). Other cm-m scale scoria layers with highly diffuse contacts occur as seemingly patchy concentrations are termed ash patches.

### c. Disseminated ash

Particles of scoria and lapilli are disseminated at different concentrations throughout the TCB, becoming more concentrated towards the interior of the present Caldera. The grab sample in Figure 2.1.6 is an example of the concentration of juvenile scoria within the TCB encountered along the southwestern part of the Hacienda and Cumbre Nueva sectors.

## 2.1.4. Discussion

### 2.1.4.1. The subsurface distribution of the TCB

The surface upon which the TCB originally accumulated (the seamount platform) was largely destroyed during the Cumbre Nueva lateral collapse. Therefore, to reconstruct the geometry of the failure surface representing the partial deconstruction of Ancestral Taburiente would require detailed structural investigations from the array of galerías on La Palma; logistically this task was not possible. The southern limits of TCB accumulation are impossible to detect or extrapolate and this is highly problematic for the analysis of instability domains (Ch. 3.2.2). Hydro-geolgical surveys have been undetaken in order define the structural controls on the geomerties of La Palma's aquifers and the associated flow rates [*Bravo and Coello,* 1978; *Coello,* 1984]. These studies neccessitated the delineation of major volcano-stratigraphic units, particular among which is the subaerial/submarine contact that acts as a major aquifer boundary. Basement contour data from these surveys indicate a domal basement structure, controlled by the uplifted/inflated seamount foundations.

It is reasonable to assume therefore that the sub-surface distribution of the TCB should emulate the morphology of the basement and the extent of the collapse unconformity generated by the partial deconstruction of Ancestral Taburiente. The hydro-geological data [*Bravo and Coello,* 1978; *Coello,* 1984; *Navarro and Coello*, 1993], summarized in the composite map of Fig. 2.1.18, illustrate the basement contours extrapolated from the galería surveys. These data would indicate that the TCB extends for at least 1 km outward from below the crest of the Caldera along most of its circumference. While the galería at Risco Liso (No. 2 in Fig 2.1.18) traverses a substantial thickness of TCB, the galería at Los Cantos II (No. 4) does not traverse any. Galerías in the Guanche sector begin traversing a thin sequence of TCB from galería Verduras Afonso (No.5) to galería Altaguna (No. 7). South of galería Altaguna the TCB is only detectable from proximal boulder trains[T] but it is exposed underneath the northern part of the Cumbre Nueva sector. Also shown are the distribution of Ancestral Taburiente inliers [*Navarro and Coello*, 1993] which, together with the measured and inferred extent of the ancestral collapse structures [*Coello,* 1987; *Ancochea et al.*, 1994], can be used to define two main subaerial structural sectors – Sector A: undisturbed foundations confined to constructional areas (rift zones and their immediate flanks) and Sector B: foundations upon which multiple or singular collapse events have occurred. By process of elimination, one may stipulate that the TCB should only exist at sub-crop in sector B, forward of the buried ancestral collapse headwalls. The total extent of the TCB is impossible to determine, since the northern part of Cumbre Vieja volcano has overlapped a large part of sector B (south of the map area in Fig. 2.1.18).

*Ancochea et al.* [1994] suggest that the shape of the unconformity between Ancestral Taburiente and the succeeding Taburiente edifice reflects a SSW orientated depression with a west-dipping basal detachment, (their Fig. 6B). This model indicates closure of the collapse depression to the east when one would expect a correlation between the spatial distribution of the TCB/TCBm units (at outcrop and subcrop), and the geometry of the ancestral collapse structure into which they accumulated. *Navarro and Coello* [1993] illustrate a broader structure which is more open to the east, but they interpret this structure as an erosional landform generated essentially by fluvial processes.

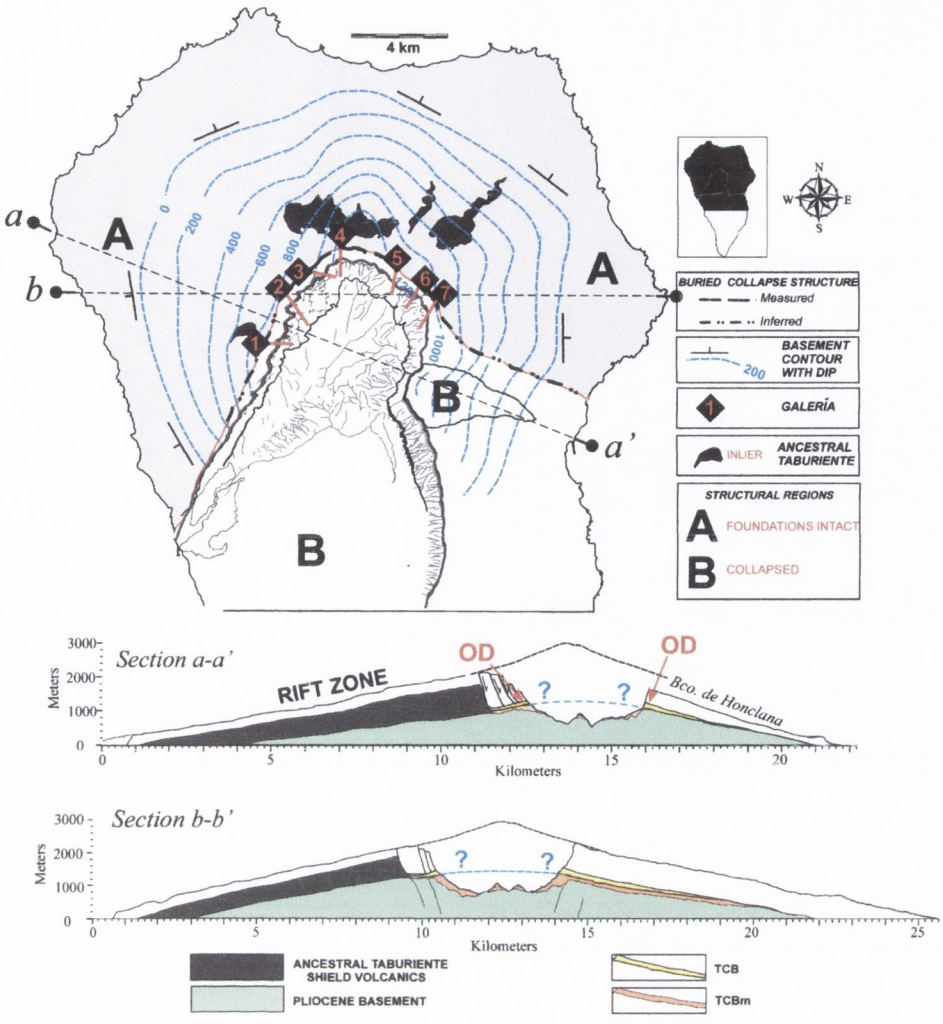


**Fig. 2.1.18.** Composite map of northern La Palma showing the basement contours in relation to the collapsed and intact sectors of Taburiente volcano. The abbreviation OD signifies the overthrust base of the TCB. Basement contours and substructure data from *Bravo and Coello* [1978]. Inlier positions from *Navarro and Coello*, [1993]. Blue stippled line is an extrapolation of the palaeo-surface.

### 2.1.4.2 The volcanological and structural significance of the TCB

The compositional, depositional, and stratigraphic characteristics of the TCB reveal new and important insights into the structural and volcanological evolution of northern La Palma. These data are interpreted from two distinct perspectives.

(1) the mode of origin of the TCB relative to the partial destruction of Ancestral Taburiente

(2) Substratum expulsion and subsidence of the amphitheatre bench zone.

#### 2.1.4.2a Origin of the TCB

It is well established that the development of Ancestral Taburiente Volcano was interrupted by major sector collapse event(s) dated at around 1.2 Ma [*Ancochea et al.*, 1994; *Carracedo et al.*, 1999a; *Guillou et al.*, 2001]. When integrated, the onshore and offshore data (i.e., field descriptions, radiometric analyses, bathymetry and their correlations) demonstrate the recurrent nature of sector collapses in the evolution of subaerial Taburiente and its submarine pedestal [*Staudigel and Schmincke*, 1984; *Ancochea et al.*, 1994; *Urgeles et al.*, 1999; *Masson et al.*, 2002] as is well documented from oceanic/arc volcanoes in various tectonic environments.

However, there has been no attempt to investigate the nature of the ancestral collapse(s) in terms of the mode(s) of failure and, more specifically, the significance of the intimate relationship between the volcaniclastic and juvenile pyroclastic components of the TCB, a component-characteristic that has been hitherto overlooked. The TCB represents the onshore component of a relict debris avalanche deposit that had spread out from within the spatial confines of the ancestral collapse structure during a significant volcanic eruption. One may further stipulate on the basis of the bathymetric data [*Urgeles et al.,* 1999] and the age constraints available for the emplacement of major debris avalanches, that a substantial part of debris spread onto the submarine flanks around La Palma.

What does the field evidence reveal about the eruption dynamics and the vent configuration during the ancestral collapse? First, the presence of accretionary lapilli, lithic and crystal fragments within the ash members is evidence of pyroclastic fall-out from an eruption column generated at least in part by phreato-magmatic activity. The entrainment of lapilli and scoria within $TCB^1$ demonstrates that an eruption was underway as the TCB accumulated en masse. A volcanic explosivity index (VEI) of between 3 and 5 is inferred for this event(s). Scouring of $TCB^1$, the entrainment of accidental blocks together with the paucity of impact sags around the large blocks, may signify transport and accumulation by laterally expanding and highly energetic pyroclastic surges. The blocks entrained within the core of the La Farola Ash Member may represent pre-existing materials that were dislodged during wall-rock collapse beneath the developing vent region(s) or accidental lithics. The position of the ash members up to 6 km apart suggests that there was more than one eruption centre.

The deposition of the ash members up to 20 m in observable thickness and up to 200 m above $TCB^1$, is indicative of a hiatus in the accumulation of the blocky volcaniclastic components that constitute the main body of the TCB. This can be taken as evidence that the TCB accumulated gradually during the paroxysmal event; it was not emplaced instantaneously in its entirety. In essence, the wide dispersal and relative thickness of the ash members may indicate that the ancestral collapse occurred in discrete stages, two at least. There are two important assumptions conceived for the timing and style of the eruption. First, all the ash members are stratigraphically equivalent, and second, they accumulated over a period of hours or days (hence their thickness). These criteria, together with the absence of observable toreva remnants within the TCB, point to high fragmentation during accumulation. Was the partial collapse of Ancestral Taburiente thus triggered by the coeval eruption and, if so, what volcano tectonic conditions might have prevailed to promote sector instability on such a grand scale? There are several factors that demand consideration, some of which are inter-related.

1: the basement faults and their influence in localized subsidence (i.e., of the ancestral summit region)

2: the apparent thickening of the TCB/TCBm towards a depo-centre – the present Caldera

3: magmas, as sill complexes and/or stocks residing at high levels in the basement

4: a well-developed hydrothermal circulation system

5: the seaward dipping inclination of the subaerial/submarine interface.

6: a low cohesion subaerial/submarine interface

7: the pyroclast-dominated stratigraphy at and below the summit region (centroid of the rift system).

1. Basement faults.

Shallow-angled to steeply dipping faults with tabular assembalges of granular gouge and breccia, up to 0.3 m thick are observed within the seamount basement, particularly within the seamount series (Figs. 1.1.5 and 2.1.19), These prominent faults generally become steeper toward the centre of the intrusive core and have been previously recognised as reverse slip structures [*Navaro and Coello*, 1993]. They have not been observed to penetrate the subaerial stratigraphy and their spatial distribution and frequency have not been determined by this or any other study[T]. One may stipulate that the development of these faults began intitially during uplift and inflation of the basement, accommodating flexural slip along arrays of fault structures, perhaps concentric in geometry, around the seamount super-structure. This may have occurred in order to accommodate the development of the high-level magma reservoir that ascended to increasing levels of neutral buoyancy during the uplift/inflation period [*Gee et al.*, 1993]. The possibility exists that these basement faults accomadated localized subsidence, perhaps under the weight of the dense cumulate magma reservoir and sill complex, or due to the withdrawal of support after magma chamber evacuation. If so, could this subsidence have facilitated the development of a subaerial proto-caldera, not unlike the downsag calderas on the Hawaiian and Galápagos Islands? Alternatively, could the development of a caldera-like structure have been carried foward through the the uplift/inflation period, explaining the tilted aspect of the seamount series volcanics?

The geometry and size of the downsag caldera may have been approximately equal to the cross sectional area of the underlying magma chamber. *Martí and Gudmundsson,* [1999] propose such a spatial/geometric relationship for the formation of the Las Canñadas collapse caldera on Tenerife. These authors propose that the size and geometry of Las Canñadas is related to the partial destruction and migration of the magma chamber after each caldera collapse event. For Ancestral Taburiente, the instability mechanism being considered involves the interaction between vertical tectonics and lateral flank failure, a concept that has been proposed for the development of the Cañadas/Orotava depressions on Tenerife [*Martí et al.*, 1997; *Martí and Gudmundsson*, 1999; *Hurlimann*, 1999; *Albay and Martí*, 2000]. There are several more factors that require attention before entering into a more unfied discussion.

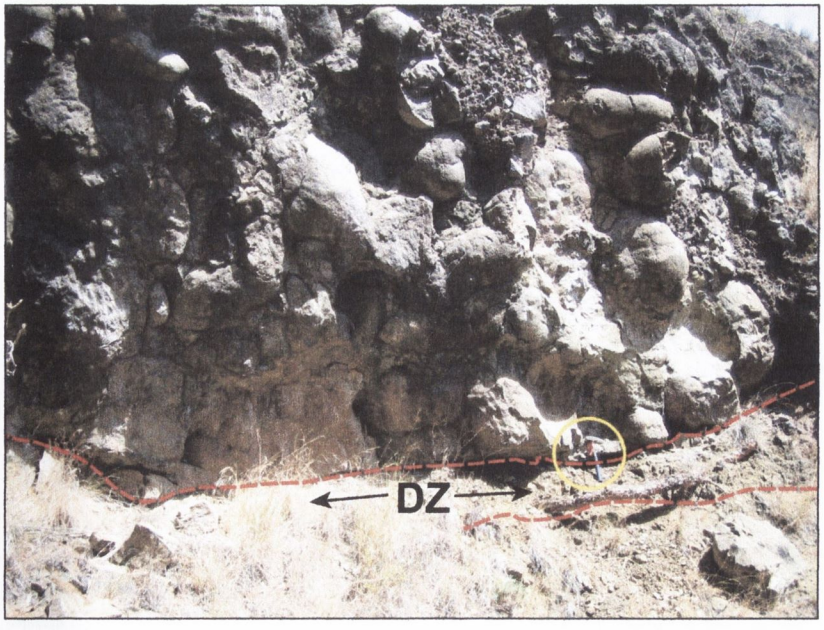


**Fig. 2.1.19.** Sub-horizontal fault zone (kinematics undetermined) with pillow lavas in the hanginwall. Footwall rocks are masked by talus and vegetation. The true thickness of the damage zone (abbreviated DZ) is undetermined but is at least 30 cm (see hammer, circled). SW of Hacineda del Cura.

## 2. Localised thickening of the TCB

Within the confines of the Caldera, the TCB/TCBm units reach a combined thickness of up to 1100 m. Both volcaniclastic units are identical from a petrographic perspective; tectonic facies and metasomatic alteration appear to be the only differentiating criteria. The resemblance and intimate spatial relationship between the TCBm and the TCB, together with the radiometric constraints for the formation of the ancestral collapse stucture(s) [*Ancochea et al.*, 1994: *Guillou et al.*, 2001], make it high probable that both volcaniclastic units are part of the same suberial debris avalanche breccia.

How therefore, could a depo-centre of such thickness (1100 m) have formed at the centre of the ancestral edifice when, around the periphery, the TCB is only 100-350 m thick. The answer, it is proposed, lies in the faults that cut through the basement. As suggested earlier, these faults may have been activated during the withdrawal of roof support underneath or within the magma column. Gross subsidence, centralised below the ancestral summit region, must have occurred relatively rapidly in order to have contained such a substantial thickness of collapse breccia. The approximate amount of subsidence, illustrated in Fig. 2.1.20, should equate to the combined thickness of the TCB/TCBm, i.e., between 600 and 1100 m, deepest at the centroid of subsidence. This illustration shows the divide between the TCBm and TCB. As will be discussed in Ch. 2.2, this is a part of the detachment surface that developed during the reconstruction and substratum deformation of Taburiente.

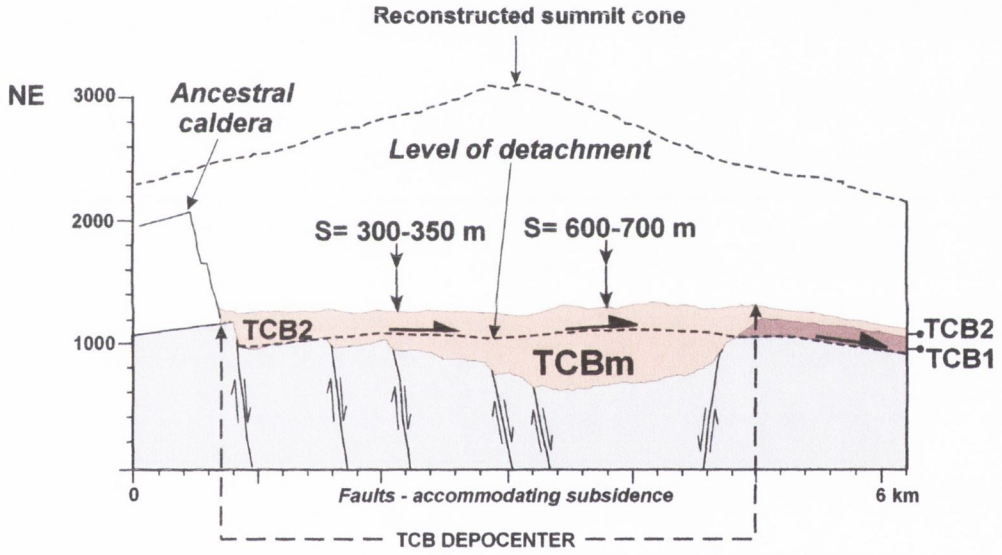


**Fig. 2.1.20.** Illustrative structural/stratigraphic setting and components of the TCB, with inferred subsidence (S) values. The level of detachment and the reconstructed summit cone are aspects of the Taburiente phase of volcano growth (i.e., post 1.2 Ma) discussed in Ch. 3.2.

## 3. The intrusive core and the geothermal system

The TCB depocentre overlies, and is intruded by, a dense plexus of sheeted intrusions and small stock-like bodies of gabbro/syenite (chapter 1.2.5.1). The geothermal system once supported by these magma bodies has important implications for the origin of the metasomatic overprint in the TCBm units. Re-growth of Taburiente led to the burial of the TCBm within the re-developing geothermal system. The volcaniclastic deposits and their surrounding wall rocks were subjected to water–rock interactions and ion exchange between previously metamorphosed seamount-stage rocks. Heat exchange from the intrusive core would have induced hydrothermal circulation of meteoric and juvenile fluids/gasses entering the summit region. Fluid circulation in this environment may have influenced the kinematic evolution of the basement faults as well as promoting localised hydrothermal alteration of the surrounding rocks.

### 4. Pyroclast dominated stratigraphy

One of the most characteristic features of the volcanoes forming the Canary Archipelago is the strong component of pyroclastic materials in the stratigraphic architecture, particularly along the surficial rift zones (i.e., between 1 and 2 km deep) [e.g., *White and Schmincke*, 1999; *Hurlimann*, 1999]. Here the edifice structure is composed of compact groups of scoria cones at surface, merging downwards into nested/overlapping scoria deposits, all meshed together by interlacing dikes that are subjected to hydrothermal phenomena and associated rock mass alteration. In terms of rock mass characterization, this zone is often heavily fractured; the softer pyroclastic materials have a lower rock mass strength, in comparison to stacked lavas and intrusives disintegrating readily during seismic loading and landsliding.

### 5. Strength characteristics and inclination of the interface.

The inclination of the interface between the ancestral edifice and the basement is presently between 3° and 26° since continuous uplift, evidenced in part by the terraced form of the El Time sediments [*Hildenbrand et al.*, 2003], diminished in the Pleistocene. Nevertheless a seaward dipping inclination could have contributed to the destabilizing gravitational forces acting on the flanks, the strength of which may have been intensifed by a mechanically weak substrate, perhaps characterized by relic shoaling-stage hyaloclastites and pillow fragment breccias. It is *Ancochea et al.* [1994] who suggest this sceario such that the ancestral edifice "*de-stabilized due to the presence of a plastic substrate*" (what they refer to as compacted emergent-stage volcaniclastics). In general, detachment can be caused by the density contrasts between interfacing rock strata subjected to gravitational instability forces [e.g., *Kehle*, 1970] especially when faciltated by a dipping basement, even with shallow inclinations [e.g., *Wooller et al.*, 2004].

## 2.1.4.2b. The collapse of Ancestral Taburiente, a new hypothesis.

The eruption and cataclysmic flank collapse(s) of Ancestral Taburiente generated a pyroclast-rich debris avalanche deposit in at least two climactic phases, each one characterized by high fragmentation. The volcanic eruption the accompanied the collapse(s) is herein reffered to as the La Farola eruption. It is proposed that subsidence of the magma column (perhaps due to magma chamber evacuation), led to the withdrawal of support beneath the ancestral summit region. The basement depression generated by the collapse(s) was rapidly backfilled with avalanche debris as the ancestral summit region disintegrated. This scenario provides an explanation for the centralised thickness of the ancestral debris avalanche breccia (i.e., TCB/TCBm) within the confines of an irregular cauldron-shaped body - the vacated downsag magma column. The vertical shear stress ($\tau_v$) generated by the caldera-forming event may have initiated the lateral collapse of the south flank, as the flank eruptions developed through phreatomagmatic, vulcanian, and strombolian phases (stage 3 in Fig 2.1.21). Decompression of the magma chamber (stage 5 in Fig. 2.1.21), associated with the removal of the lithostatic load (the summit region of the edifice), may have lead to a sequence of violent volcanic eruptions. For instance, the removal of a large portion of a volcanic edifice, as a result of slope failure, can destabilize the underlying magmatic/hydrothermal systems, in some cases causing highly energetic eruptions [*Belousov et al.*, 1999 *and references therein*].

Similarities in style can be inferred between the collapse of Ancestral Taburiente with the laterally directed landslide/eruption of Mt. St. Helens (Fig. 2.1.22). The St. Helens flank collapse was preceded by weeks of precursory seismicity, phreatic explosions at the summit craters and, most important, deformation of the north flank, caused by the emplacement of a dacite crypto-dome [*Christiansen and Peterson*, 1981]. The climactic stage occurred during an earthquake that critically destabilized the heavily strained flank [*Glicken*, 1996 *and references therein*].

In similarity to the Mt. St Helens landslide/eruption, it is inferred that the volumetrically larger sector collapse of Ancestral Taburiente involved vigorous magmatic activity. Precursory ground deformation, in the form of rapid subsidence (stage 3 in Fig. 2.1.21), probably occurred around an array of faults – concentric about the summit region. The first debris avalanche deposit accumulated on the failure surface exhumed by the collapsed south flank and spread onto the submarine slopes, perhaps for some tens of kilometres (stage 4 in Fig. 2.1.21). Violent seismic activity continued as the source vents re-located inside the giant collapse depression, close to or on the escarpments. The second debris avalanche formed as the remaining part of the summit caldera foundered, collapsing and disintegrating through increasingly explosive volcanism and seismic upheaval. As mentioned earlier, some days must have passed for the second debris avalanche to have been emplaced as the La Faroloa eruption ensued..

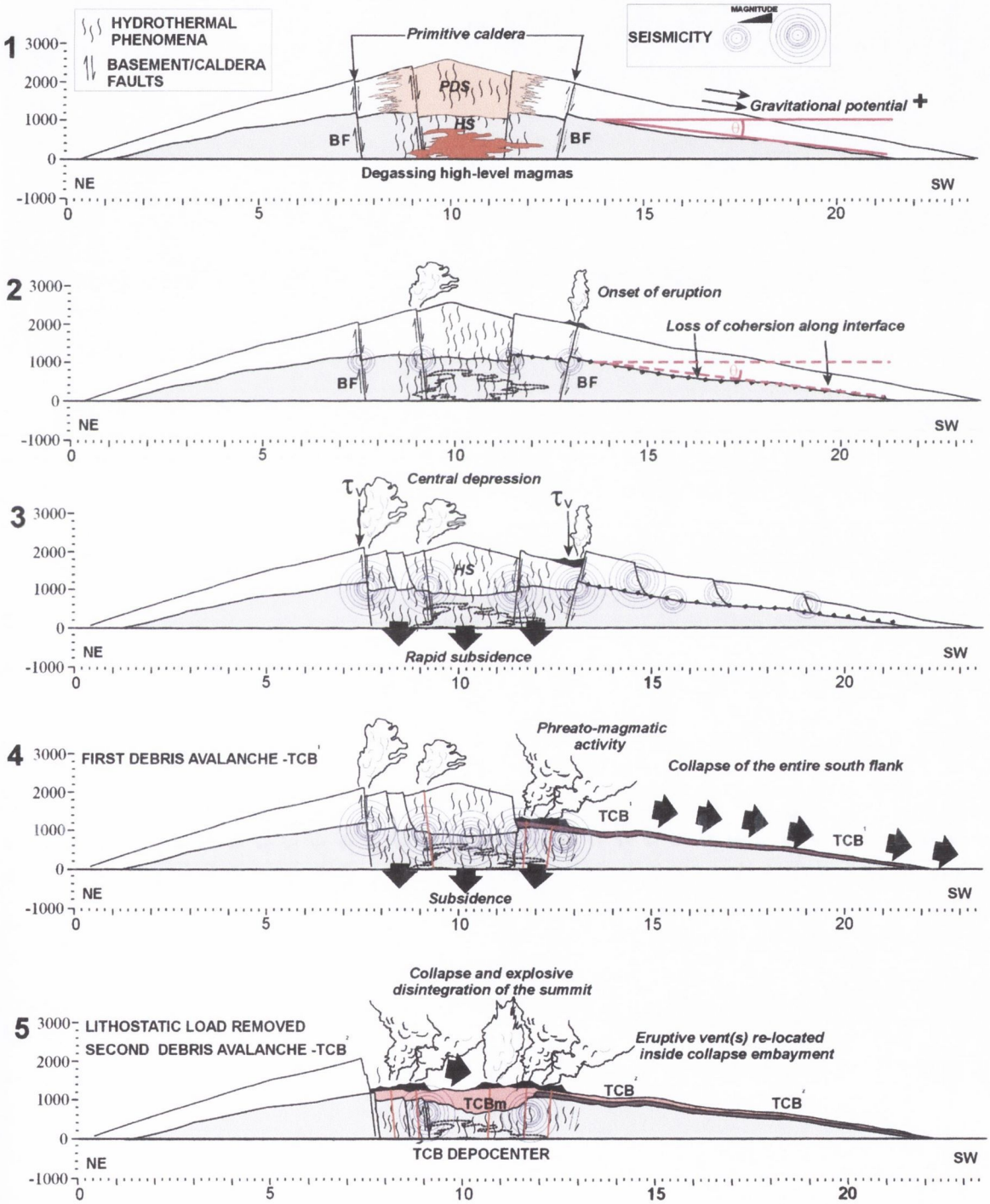


**Fig. 2.1.21.** Conceptual development of the ancestral collapse structures and the deposition of the TCB, illustrated by scaled sections. Abbreviations: BF – basement faults. PDS – pyroclast dominated stratigraphy. HS – hydrothermal system.

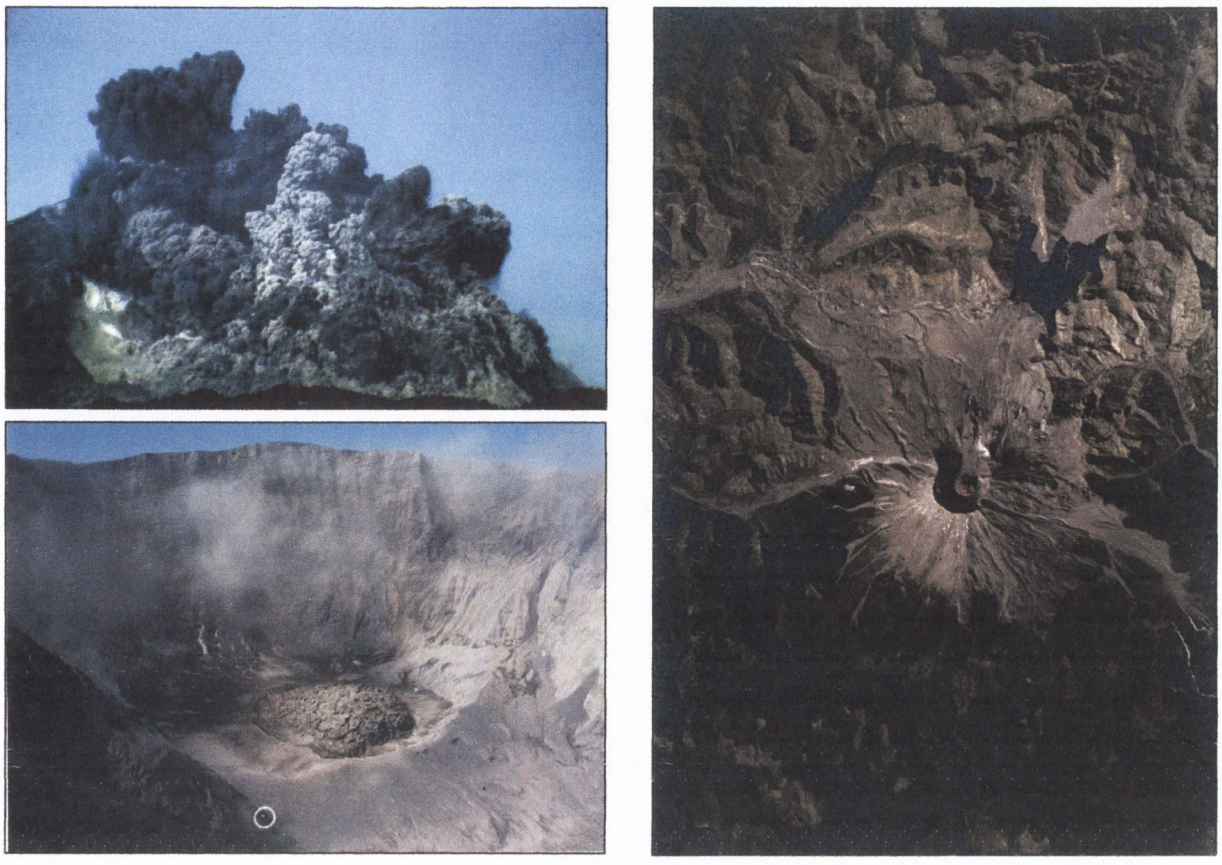

**Fig. 2.1.22.** The landslide/eruption of Mt. St. Helens, May 18th, 1980. The image top left shows the initial seconds of the collapse and lateral blast that destroyed the summit and north flank. Bottom left shows the collapse amphitheatre and central lava dacite dome.Source www.usgs.gov.volc.msh/htm. STS-064-051-025 (right). Shuttle photograph showing the collapse amphitheatre (with lava dome) and the extent of northward directed debris avalanche deposit. Source www.jsc.nasa.gov.

### 2.1.5. Lithificition and substratum expulsion

a. Ignimbrite-like lithification

The hardness of the TCB, together with the extent of deformation structures in the ash members, raises a key question regarding its mechanical characteristics. The stiffness of the material has important implications for the kinematic development of the Cumbre Nueva detachment (Ch. 2.2). What needs to be considered is whether the large volume of entrained juvenile pyroclasts had influenced the consolidation and stiffness of the deposit by fusing it together *in situ.* Rheomorphism and hot-state stiffening are a characteristic of ignimbrites which, in general, show complex vertical and lateral changes in structure and rheology, and this is indicative of differences in compaction and welding intensity both during and long after emplacement [e.g., *Sumner and Branney*, 2002; *Barry et al.,* 2003]. For example, the well indurated, lithic-rich Roque Nublo ignimbrites (Gran Canaria) consolidated while they were still hot, due to the reaction between vitric components and water vapour. The alteration of vitric fragments lead to the formation of secondary minerals that cemented the components together [*Pérez-Torrado et al.,* 1995]. The compositionally zoned 'TL' Ignimbrite (Gran Canaria) aggraded during an explosive eruption in which the composition, eruption style, and intensity of welding varied with time [e.g., *Sumner and Branney*, 2002]. Before coming to a halt, the rheomorphic ignimbrite traveled up to 300 m, undergoing mixing and deformation in the process.

There are a number of indicators of ignimbrite-like solidification and deformation in the TCB, localised within the ash members and the ash bands. The fold structures may have formed under loading and rheomorphic shear as the TCB accumulated *en masse*, not by the subsequent growth and loading by the Taburiente edifice. If the latter were the case one would expect more significance evidence of vertical strain in the TCB, if for instance it had accumulated and remained unconsolidated (i.e., without pyroclastic components). It is suggested therefore that loading and hot-state gravitational slumping had produced the load structures (diapirs, polyclinal folds) and the SW verging folds in the ash members (Fig. 2.1.23). Flattening and attenuation of pyroclasts, together with localized shearing along ash bands further support the evidence of down-slope extension and compression during flow.

The seaward tilted slope of the basement onto which the TCB had accumulated would have facilitated hot-state creeping motion under gravity. Zones within the TCB that appear texturally silicified, may reflect an increasing intensity of welding, perhaps in the presence of meteoric fluids. However, the extent to which fluids, either juvenile or meteoric, were involved in the consolidation process is undetermined. Furthermore, the distance traveled during the inferred state of hot, creep flow is undetermined.

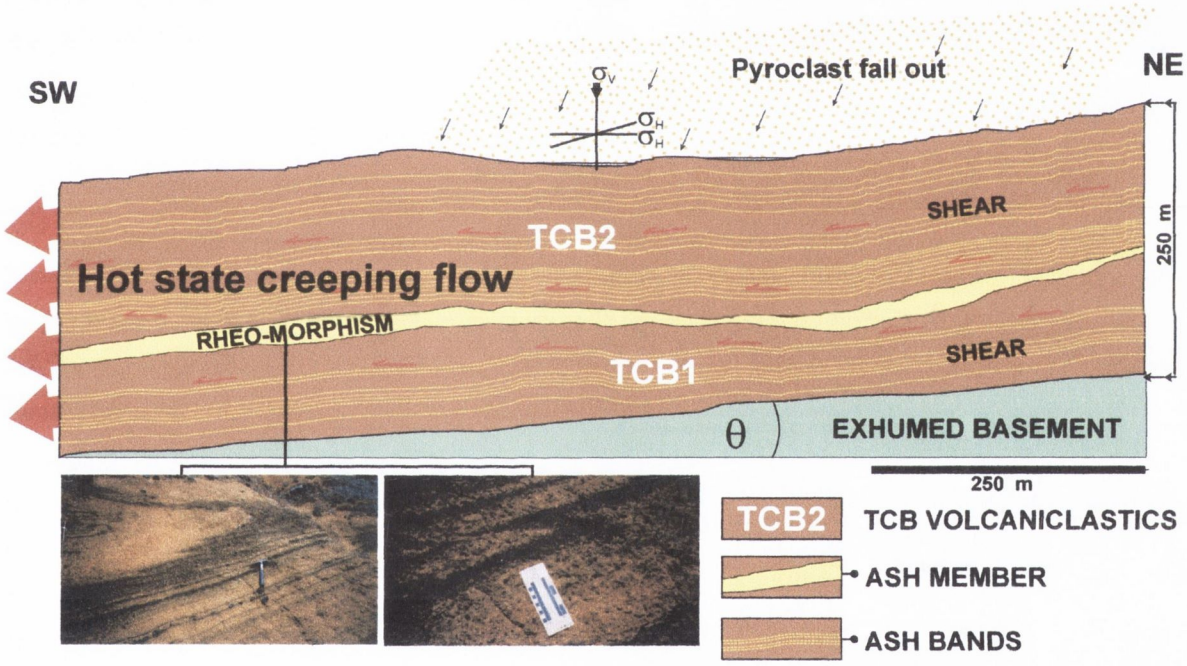


**Fig. 2.1.23.** Longitudinal profile through the TCB (Hacienda secor) showing the depositional structure and proposed model for accumulation and deformations.

b. Substratum expulsion.

The expulsion of substratum occurs due to excessive lithostatic loading on structurally weak or less dense materials forming the basement of volcanoes [e.g., *van Wyk de Vries et al.,* 2001]. This phenomenon is manifest on volcanoes with a prominent mobile (or collapsed) sector, characterized by folding, diapirism and shearing of the substrate, typically along the lower flanks. Field evidence for substratum deformation/expulsion is reported from Mombacho and Concepcion volcanoes (Nicaragua) [*van Wyk de Vries and Francis*, 1996; *Borgia and van Wyk de Vries*, 2003], Mount Etna, Sicily [*Borgia et al.*, 1992] and Socompa Volcano in northern Chile [*van Wyk de Vries et al.*, 2001]. The field evidence from La Palma indicates that the expulsion of the TCB has occurred as a response to collapse-related de-compressive unloading of the edifice and de-stressing of the resultant headwalls along the ABZ. This would explain the conspicuous protruding aspect of the TCB (2.1.23a), the overthrust disposition of the hangingwall (2.1.23b) and the proliferation of boulder train deposits below the TCB; all of these features can be related to a common process. As illustrated in Fig. 2.1.26a, the orientations of the horizontal stresses within the Taburiente edifice have been modified by the gigantic void space created by the Cumbre Nueva collapse. This type of large-scale structural readjustment in the state of stress is analogous to an open pit mining operation where the virgin stress state is altered by excavations. The stresses are forced to redistribute around the pit walls as the pit profile widens and deepens. For the case shown in Fig. 2.1.26a the maximum stress concentrations ($\sigma_v$ . vertical, and $\tau$ - shear stress) will exist at the toe of the de-stressed region where substratum expulsion occurs. The vertical stress is the gravitational load.

The overthrust surfaces define the toes of developing slump sectors along the ABZ, as gross subsidence continues upon the unconfined substratum, forcing it to extrude from the base of the escarpments (Fig. 2.1.24). Substratum expulsion occurs along the detachment fault surface causing the TCB to protrude or bulge) where it has been thrust outwards and upwards. In the chain of events - tension fractures develop as the substratum is overthrust without basal support (Figs 2.1.25a and 2.1.25b). As the fractures widen and deteriorate with continuing substratum explulsion and aperture weathering, the un-supported hangingwall undergoes plane and toppling-type failures. The unstable portion collapses away from primary outcrop and shatters upon impact. The derivative blocks and slabs are gravity fed down slope to form the boulder-train deposits (see Fig. 2.1.26b). High concentrations of boulder train deposits and slabs should reflect areas of pronounced substratum expulsion. There should also be a strong correlation between the zones of expulsion and the smoothness of the overthrust detachment fault. For instance, Fig 2.1.25 illustrates the profile topography of the fault surface as it appears from different sections of the overthrust hangingwall. Two distinct profiles are evident: (1) smoothened and (2) jagged. It is proposed that the smooth profiles are an indication of the most recent increments of slip (overthrusting), while the rough profiles could reflect lapses of overthrust motion due to the locking effect of asperities on the detachment surface.

Boulder trains are prolific beneath both observed overthrust types, but the main implication of the fault surface smoothness is that substratum expulsion is an ongoing process. One would expect evidence for this in the form of damaged footwall and hangingwall contacts where the galerías intersect the detachment fault. Since the oldest tunnels were excavated at the turn of the 20$^{th}$ century, it would be necessary to conduct a survey of each galería that penetrates the Cumbre Nueva detachment in order to substantiate this argument. The amount of slip that has occurred on the de-stressed region (the ABZ) is unquantified. However, based on the size of the source indentations, and from areas of pronounced bench-scarping and substratum expulsion, it is possible that between 0.2 and 0.4 km of escarpment readjustment has occurred since the collapses.

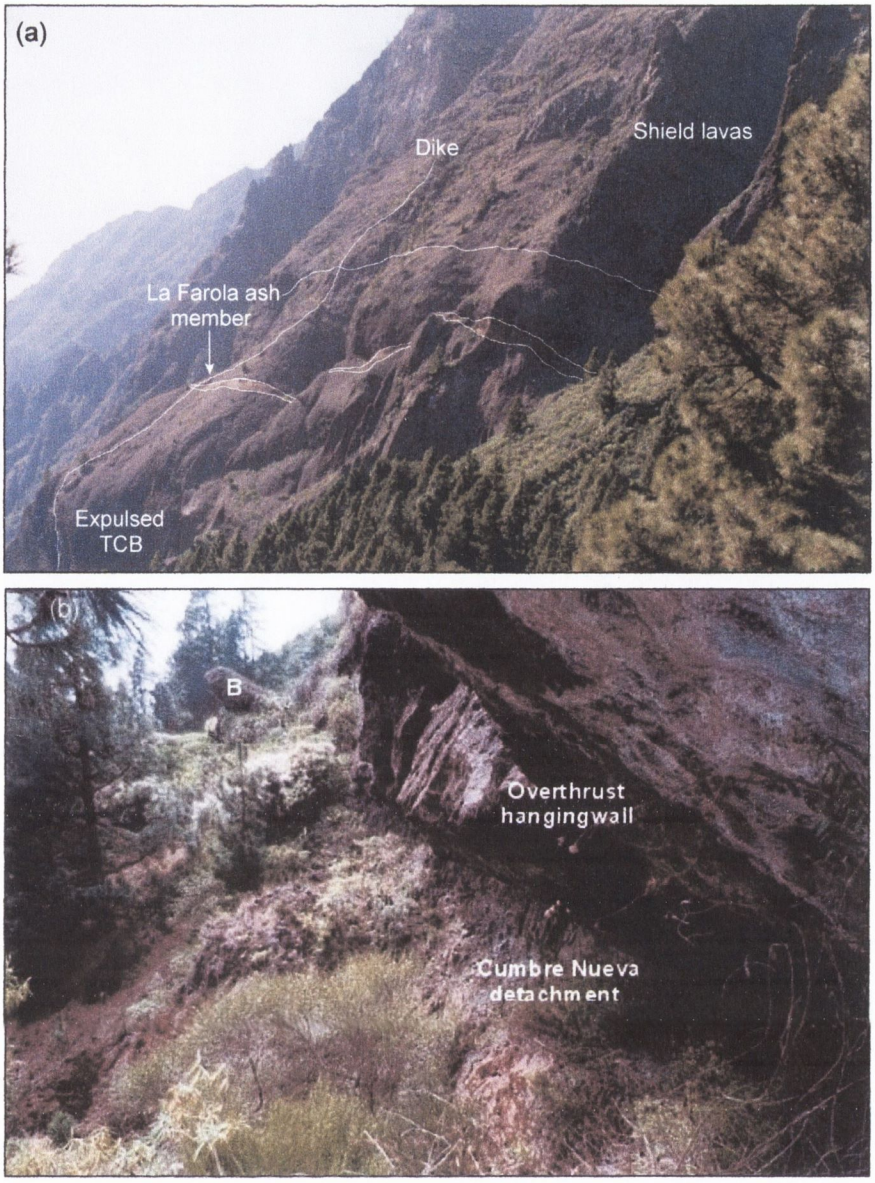


**Fig. 2.1.24.** (a) A segment of the Hacienda sector undergoing pronounced substratum expulsion. The nose-like protrusion of TCB extends outwards from below the escarpment by over 240 m. Location – Hacienda del Cura. (compare with Fig. 2.1.2). (b) A segment of the overthrust hangingwall near Hacienda del Cura. In the foreground overthrusting has occurred without the development of recent fractures, while a large boulder (B) (one of many) indicates recent spall and break-up.

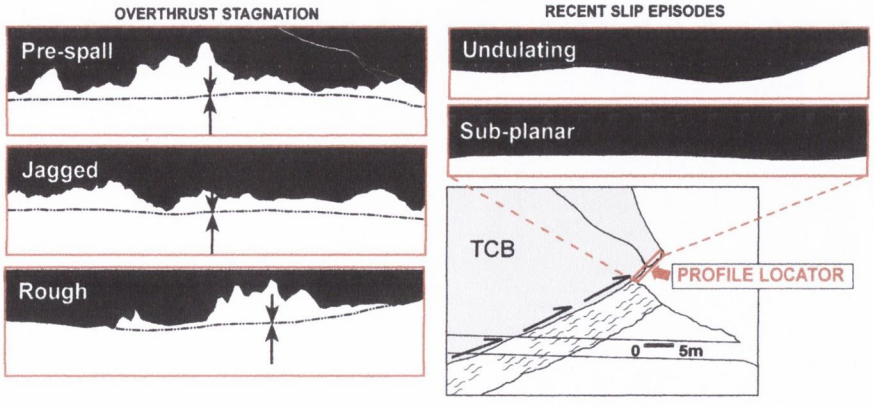


**Fig. 2.1.25.** Stages in the expulsion of TCB, drawn from profiles of the overthrust detachment fault. Two phases of thrust motion are inferred (1) overthrust stagnation relected by irregular to undulose surfaces and (2) recent slip where the fault plane is smooth, sometimes striated.

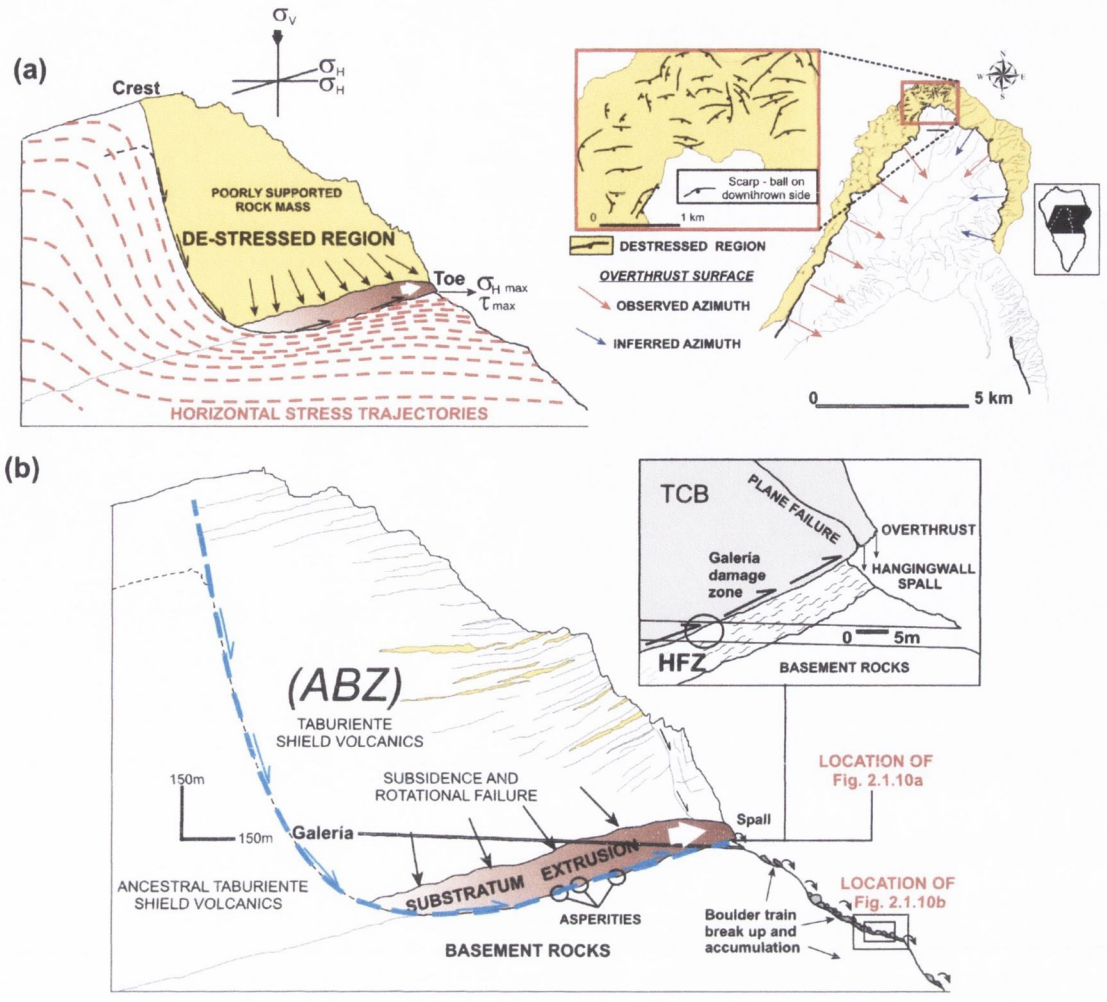


**Fig. 2.1.26.** (a) Two dimensional representation of the redistribution of horizontal stresses around a part of the Hacienda sector. The map outlines the spatial extent of the amphitheatre bench zone (in yellow) and the extrapolated horizontal stress trajectories. (b) Subsidence profile through the Hacienda sector, showing the limits of substratum expulsion and how this relates to overthrusting, spall and the generation of boulder train deposits. Compare with Fig. 2.1.10.

If this assumption is correct, then further foundering of the ABZ can be expected over periods of geological time. For instance, the rock avalanche deposits forming Roque de la Viña and the ridge of Tenerra are located below large indentations in the escarpments [e.g., *Navarro and Coello*, 1993]. The most significant implication of substratum expulsion is that a new episode slip-related expulsion may affect the structural integrity of the Cumbre Nueva tunnel during a volcano-seismic swarm on the northern part of Cumbre Vieja. It is possible that substratum expulsion occurs aseismically, although seismic activity may hasten the rate of expulsion.

### 2.1.6. Conclusions

The climactic stages of the sector collapse of Ancestral Taburiente were associated with a pyroclast-rich debris avalanche deposit, 'the TCB', the proximal part of which accumulated upon the tilted surface of the Pliocene basement. During emplacement the debris avalanche underwent ignimbrite-like deformation before fusing together and halting *en masse*. The high volume of entrained juvenile pyroclastics may signify two alternate collapse mechanisms.

(1) The removal of lithostatic load during slope failure and the subsequent exposure of a high-level magma reservoir/hydrothermal system. The outcome may have led to near instantaneous decompression of the magma chamber causing a flank collapse event reminiscent of Mt. St. Helens in 1980..

(2) The collapse may have been triggered by the replenishment of magma into the high-level reservoir causing flank deformation (flank bulging) and slope failure.

The debris avalanche deposit thickens inside the Caldera de Taburiente, a possible indication of a relationship between centralized subsidence of the basement along well-developed fault zones and accumulation within a down-sag depo-centre. This may further demonstrate the role of vertical tectonics and voluminous pyroclastic flow phenomena as advocated for other Canary Island volcanoes [e.g., *Martí et al.*, 1997].

The Tenerra Collapse Breccia was exhumed by the Cumbre Nueva lateral collapse, and is best exposed beneath the walls of the Caldera/Cumbre Nueva embayment. The inward recline of the amphitheatre bench zone together with the expulsion of the TCB beneath the benches, is interpreted to represent a post-collapse response to unloading of the Taburiente edifice. The protruding disposition of the TCB, together with the extent of derivative boulder trains, indicates that the processes of substratum expulsion and associated subsidence of the overlying headwalls is ongoing.

- Radiometric data of *Ancochea et al.* [1994].

# 2.2 The Cumbre Nueva Detachment

Below a sharp, locally striated fault plane, at the base of the TCB is a zone of chloritic gouge and breccia between 3 and 8 m in thickness. The cataclastic textures within the fault zone do not appear to be randomly distributed; instead an ordered internal structure is observed where particle size distributions are controlled vertically by the distance to the detachment surface and laterally by Riedel slip surfaces. Introducing the Cumbre Nueva detachment fault.

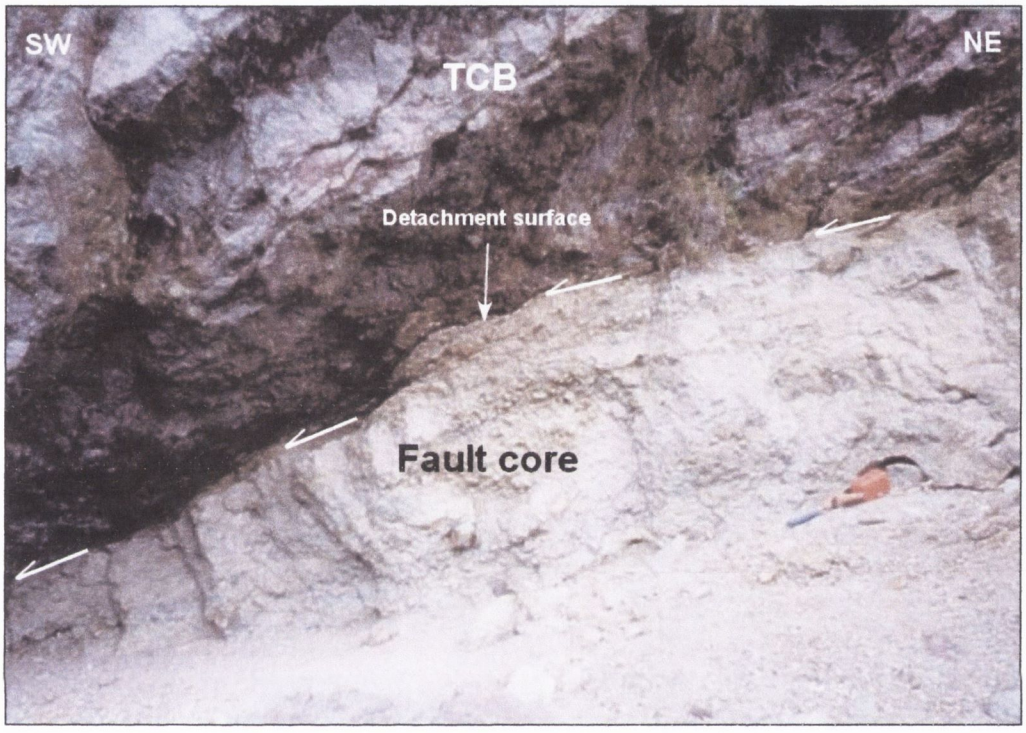


**Fig. 2.2.1**. A section of the Cumbre Nueva detachment showing a light-coloured, crudely foliated chloritic fault gouge and breccia in the footwall of the TCB. A geologic pick and hip chain give scale. Locality: Hacienda del Cura.

## 2.2.1 Introduction

This section presents data on the exhumed detachment fault (herein named the Cumbre Nueva detachment) discovered at the base of the TCB during the course of initial field studies in 1998. The detachment consists of a tabular fault zone, typically 3 m thick, and presents many undulating upper surfaces, with predominantly dip-slip slickenside lineations on the overthrust hangingwall. At its upper bounds it consists of a continuous layer (between 2 and 20 cm thick) of ultra-fine grained (UFG) gouge that parallels the striated base of the TCB. The fault core marks a region of granular and often banded gouge between 1 and 3 m wide. The core is transected by arrays of Reidel (R) fractures and P/Y shears, and it merges vertically and laterally with a damage zone, comprising heavily fractured or brecciated and oxidized basement host rocks. The damage zone merges further downward with hydrous metamorphosed but otherwise undeformed rocks. At outcrop, the fault rock is typically pale chloritic green or white (Fig. 2.2.1), although it is often infiltrated by colour-banded-alteration-zones. Dikes and sills are offset at the detachment surface, while other earlier planar intrusions display conjugate fractures within the damage zone. In the latter, the structural markers are invariably absent from the fault core, or, are difficult to trace laterally. The dangerous headwall conditions preclude an estimation of the partial or total displacement along the fault zone. Instead, a scaling relatonship with normal faults and detachments is investigated.

### 2.2.2 The basic nomenclature and properties of fault rocks

#### 2.2.2.1 Fault core, damage zone, ultra-cataclastite

Most shallow-seated crustal fault zones contain a low-temperature form of cohesive or incohesive fault gouge and breccia and associated shear fractures, that are assumed to be the result of brittle deformation processes, such as cataclasis and granular flow [e.g., *Scholz*, 1990; *Sibson*, 1996; *Morgan and Boetcher*, 1999]. The essential kinematic behaviour in the development of fault zones is their dilatancy and component particle size diversification and reduction [*Chester and Logan*, 1986; *Lockner*, 1995]. The particle sizes evolve by pervassive grain fracturing and grinding, while angular particles resist cooperative rolling and thereby stengthen the granular assemblage [*Morgan and Boetcher*, 1999]. As granular flow accrues during slip, the inter-granular contact stresses, per unit volume, diminish.

Traditionally, fault breccia is composed of >30% visible fragments while fault gouge contains <30% visible fragments [*Sibson*, 1977, *Cladouhous*, 1999a]. Table 2.2.1 summarizes the basic nomenclature and particle size ranges for brittle fault rocks, compiled from studies on exhumed fault zones. This is the adapted classification scheme for the fault rocks along the Cumbre Nueva detachment.

| Fault rock type | Particle size range | References |
|---|---|---|
| Ultra-fine-grained gouge | <0.1 mm | *Scholz*, 2002; *Ben Zion and Sammis*, 2003. |
| Clay gouge | 0.1 – 10 mm | *Cladahous*, 1999a. |
| Granular gouge | 0.1 – 50 mm | *Cladahous*, 1999a |
| Breccia | 0.5 m – 1 mm | *Chester et al*, 1986, *Scholz* 2002. |
| CATACLASTITE | Vol% fine grain matrix | *Brodie et al.*, 2002 (IUGS system). |
| Proto-cataclastite | <50 | |
| Meso-cataclastite | >50 <90 | |
| Ultracataclastite | >90 | |

Table 2.2.1. Range of particle sizes and nomenclature of cataclastic rocks.

Cataclastic rocks can display some form of centimeter-scale preferred linear orientation of mineral grains or larger scale flow banding and shape preferred orientations* (SPO) of survivor clasts [e.g., *Chester and Logan*, 1986; *Seront et al.*, 1998; *Cladouhos*, 1999a,b]. It is assumed that flow structures are formed by steady creeping granular flow in fault zones, involving particle size reduction through inter-particle grinding and fracturing (among many other intrinsic processes) [*Magloughlin et al.*, 1996; *Morgan and Boetcher*, 1999].

Fault zones normally consist of two distinct hydro-mechanical units; first - a fault core (the interval with the highest concentration of deformation), and second - a damage zone (the peripheral interval with weaker deformation), both of which are bounded by relatively undeformed host rocks [*Gudmundsson*, 2001, *Shipton and Cowie*, 2001]. The damage zone is intrinsically related to the mechanical development of the fault core although the strain relationship between the two may span some orders of magnitude [*Chester and Logan*, 1986; *Seront et al.*, 1998]. There is unanimous agreement that displacement in fault zones is accommodated within the fault core [*Ben Zion and Sammis*, 2003]. Sometimes this occurs along thin layers of ultra-fine grained fault rock known as ultra-cataclastite. An example is the Punchbowl Fault in southern California, an abandoned strand of the San Andreas strike-slip system that accommodated most of 40 km of displacement along a continuous layer of ultra-cataclastite <1 m wide [*Chester and Chester*, 1998, *Chester*, 1999]. Comminution of this nature, confined to narrow tabular zones, is also reported along the Turtleback Detachment Fault (Death Valley, California), where slip has concentrated in the finest grained material, a 10-30 cm wide zone of flow banded or foliated gouge, adjacent to the hangingwall [*Cladouhos* 1999a]. In similarity, the Glarus overthrust in Switzerland, accommodated ~40 km of displacement along a single layer (albeit mylonitic), between 20 and 200 cm wide [*den Brok and Oliver Jagoutz*, 2000].

### 2.2.2.2 Riedel shears

In addition to granular flow, deformation within fault zones is commonly localized along sets of ephemeral and long-lived shear fractures that develop under evolving grain structure, fabrics and shear strain conditions [*Morgan and Boetcher*, 1999; *Ben Zion and Sammis*, 2003]. Reidel shear fractures form a specific geometric pattern within fault zones (Fig. 2.2.2) that include relatively short *en échelon* slip surfaces that are linked to form a through-going principal shear zone [*Cladouhos,* 1999b; *Ahlgren*, 2001]. Laboratory experimentation of simulated gouge have shown that synthetic Riedel (R) shears (Fig. 2.2.2) form during the early stages of fault development although they do not accomodate large amounts of slip [*McKinnon and Garrido de la Barra,* 1998; *Morgan and Boetcher,* 1999]. By convention, R shears lead to thickening whereas P shears lead to thinning of the constituent fault gouge [pers com. *J.J. Walsh*]

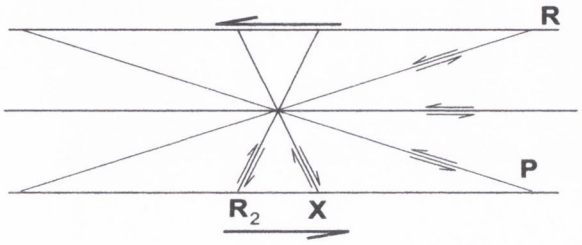


**Fig. 2.2.2.** Fracture array and geometric relations in fault gouge during triaxial compression, after *Ahlgren* [2001].

With strain increase, Y shears begin to develop at various levels within natural and experimental gouges, parallel to the boundaries of the shear zone [*Scholz,* 1990]. Whereas the amount of slip on R shears is limited by their geometry, Y shears can accommodate substantial amounts of slip [*Scholz,* 1990].

## 2.2.3. Structure of the Cumbe Nueva detachment fault

The general structure of the Cumbre Nueva detachment is that of a shallow-seated, seaward-dipping fault zone (Fig. 2.2.4), dipping to the southwest along the Hacienda sector, and to the northeast along the Guanche sector. The fault zone separates the TCB and the super-adjacent shield volcanics from the Plio-Pleistocene basement rocks and is geographically limited to the west and to the northeast by the buried collapse escarpment of Ancestral Taburiente; the southern and eastern bounds are undetected. The discontinuously exposed fault has a trace length ($L$) of <10 km along the Hacienda sector, although the expected fault length is around 14 km since the seaward end of the detachment is obscured by or truncated just ahead of the El Time sediments [*Roa*, 2003]. Along the Hacienda sector the fault zone dips between 3 and 5° to the southwest, between Los Cantos and Tenerra. The dip increases to between 7° and 24°, between Tenerra and Hacienda del Cura, becoming less inclined further southwest (between 4° and 11°), ahead of the Amagar embankment. The fault width ($W_f$), i.e., the total process zone = damage zone + fault core, is between 3 and 8 m. The ratio of fault width to fault length ($W_f$ /L) falls within the order of $10^{-4}$ (0.0002 – 0.0006), which compares favourably with other fault zones (Fig. 2.2.3).

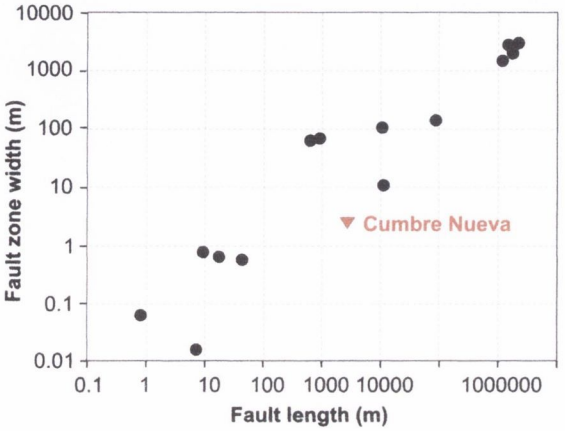


**Fig. 2.2.3.** Plot of process zone (fault width) versus fault length for the Cumbre Nueva detachment with published data from *Janssen et al.* [2002] and references therein.

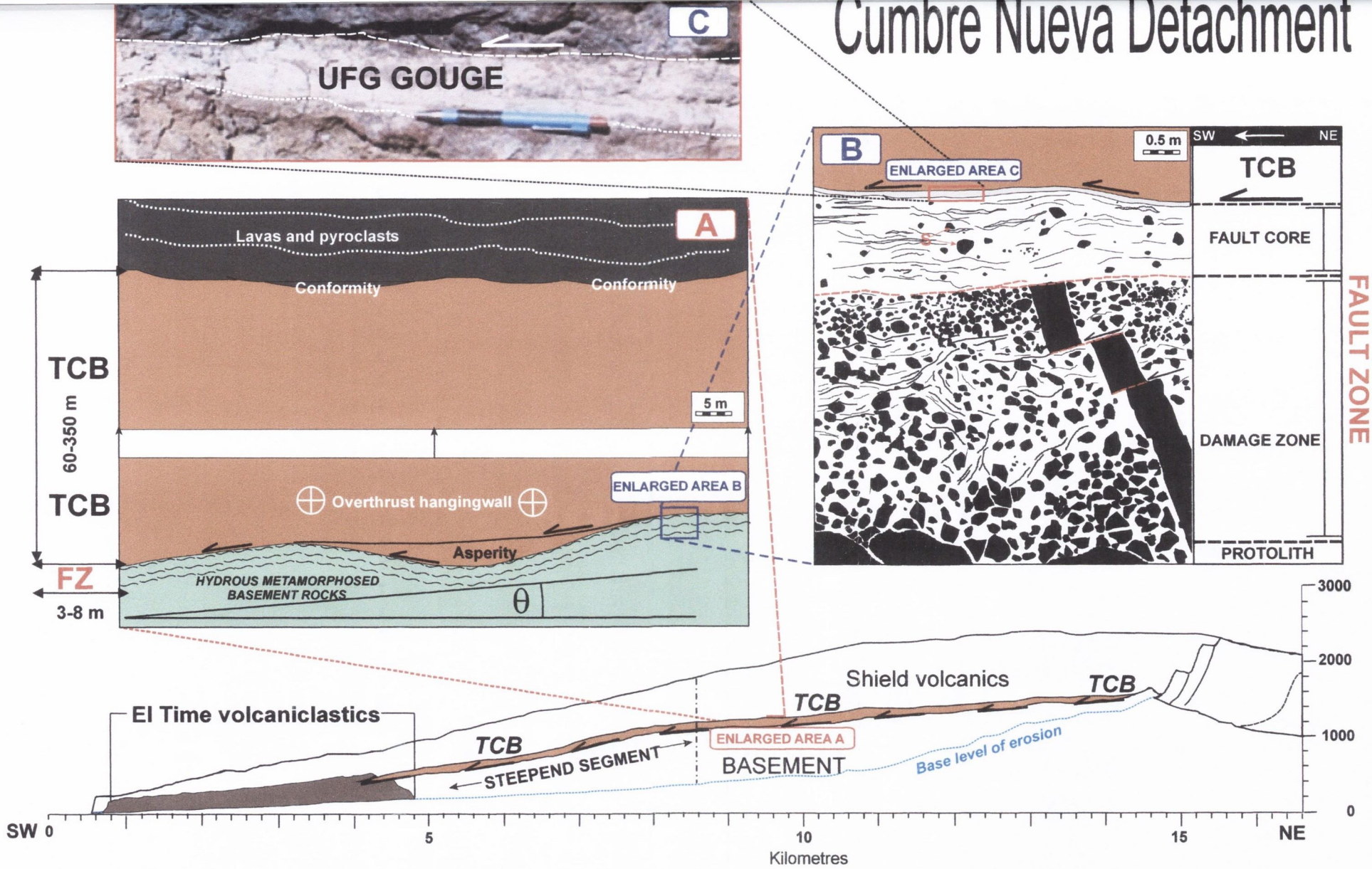


**Fig. 2.2.4.** Components of the Cumbre Nueva detachment illustrating its position and dip variation along the Hacienda sector and its relationship with the TCB. B. Schematic representation of the components of the fault zone. The abbreviation S indicates survivor clasts (see text). C. A seam of ultra-fine grained fault gouge at the hangingwall contact, extracted from Fig. 2.2.10d. Abbreviation FZ – fault zone.

The clay-smeared surface of the overthrust fault plane (Fig. 2.2.10a) is irregular in geometry, with manifold asperities visible from the hangingwall. The steep and unstable terrain affords good 3-D exposure of the fault zone that is otherwise obscured by rock avalanche deposits, talus and thick vegetation. In general, the fault rocks are not coherent enough to sample due to effects of weathering on the already hydrous metamorphosed rocks. However, there are numerous sections at Hacienda del Cura, La Farola and Bombas de Agua where the fault rock mass is solid, and granular flow/shear structures are pristine. Samples were collected from Hacienda del Cura and La Farola for petrographic and XRD analysis. Some of these samples were strenghtened with epoxsy resin before being removed from outcrop.

### 2.2.3.1. Host rocks

The host rocks adjacent to the Cumbre Nueva detachment are composed of hydrous metamorphosed seamount-stage rocks (in the footwall) and subaerial landslide breccias (TCB/TCBm) in the hangingwall. Both are incorporated into the fault zone, with a clear predominace of seamount rocks (perhaps 95% composition) along the Hacienda sector. The seamount stratigraphy is formed by pillow lava pods (decreasing in size with stratigraphic height), hyaloclastites, bedded and non-bedded hyalo-tuffs (Fig. 2.2.5) and dikes that increase in abundance toward the intrusive core [*Staudigel and Schmincke*, 1984; *Staudigel*, 1987]. The hydrous mineral assemblages (e.g., epidote, smectite, albite etc.) are characterized by a continuous series of mineral zones (Fig. 2.2.5), between zeolite and greenschist facies [*Gee et al*, 1993]. The zonation defines a fossil geothermal gradient in the order of 200-300°C/km vertically [*Schiffman and Staudigel,* 1994]. Toward the interior of the Caldera the host rocks are predominatly composed of the TCB/TCBm units. These volaniclatic deposits contain a considerable component of subaerial dikes (i.e., un-metamorphosed dikes traceable upward into the shield stratigraphy). As indicated in Ch. 2.1, the landslide breccias thicken toward a depocentre inside the present Caldera.

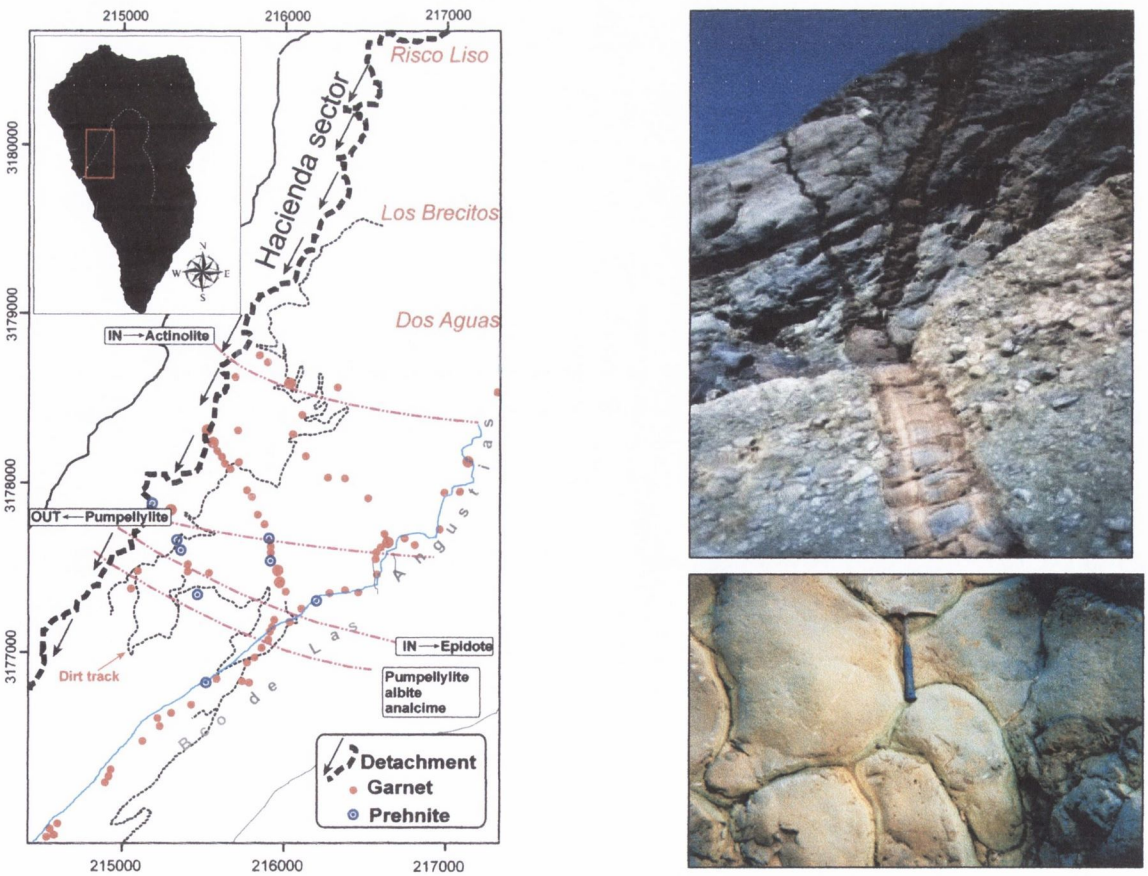


**Fig. 2.2.5.** A map showing the distribution of mineral zones in the Seamount Series. Modified from *Schiffman and Staudigel* [1995]. Upper right: A branching seamount dike, transecting hyalocalstites and pillow fragment breccias (Bco. de las Angustias) Lower right: Hydrous metamorphosed pillow lavas. (Bco. de las Angustias).

### 2.2.3.2. Structure of the fault core

The fault core has been mapped in detail both vertically and horizontally at several widely spaced localities. The map quadrants in Fig. 2.2.6 shows the extent and types of observations along the detachment. At its upper bounds, the fault core is marked by a fault plane with lustrous striations preserved on overthrust segments of the detachment fault. A chip sample in Fig. 2.2.7 shows the characteristic surface topography etched in the base of the TCB. Many overthrust surfaces are devoid of striations due to hangingwall spall. Striations are also visible on the boulder-train blocks (Fig. 2.2.7) and talus fan clasts that fringe the detachments. Talus fans draping the east wall of the Caldera at La Cumbrecita contain delicate rock fragments with striated surfaces. Although they are of no direct kinematic value, their presence dictates an origin in common with their parent fault that is either obscured by talus or is not directly accessible. A composite plot in Fig 2.2.8 illustrates the how the striations are orientated relative the emabyment/amphtitheatre walls. Crude striations directed normal to the Hacienda sector are visible on most overthrust surfaces.

In terms of its basic internal structure, the fault core is composed of coarse breccias (with very angular rock fragments) and a variety of gouges with distinct particle size distributions (i.e., clay gouge, ultra-fine grain gouge, granular gouge, banded gouge). All of these fault rocks are present in a relatively narrow 0.2 to 3 m wide zone with hybrids of each fault rock type forming the lateral continuity. The intensity of comminution increases towards the detachment plane a basic relationship illustrated by profiles 7 and 8 (Fig. 2.2.9), however, it is important to emphasize that lateral changes in particle size distributions are also evident were Reidel shears compartmentalize the fault rock types (Fig. 2.2.11).

The fault breccias, comprising coarse and highly angular fragments, often form a dense mesh-like fabric that mingles laterally with other fault rock fabrics that display a moderate concentration of coarse fragments. The breccias display a crude foliation, defined by lenses and slivers of footwall rock and aligned fractures but they are often observed to be structure-less at outcrop scale.

A continuos layer of texturally homogenous ultra-fine grained gouge (UFG gouge), between 10 and 30 cm thick, is present at the upper part of the fault core, buffering it from the detachment surface (Figs. 2.2.4c,d, 2.2.5). This layer is ubiquitous, except where undeformed subaerial dikes cut across the detachment. The boundaries between the UFG gouge and surrounding cataclastites are sharp. The UFG gouge is locally well consolidated but it is undetermined if this reflects cementation or case-hardening. Layers of inter-mingled clay gouge and granular gouge run parallel with the boundaries of the fault core, forming sinuous lenticular bodies, irregular veinlet-like networks and thicker ponded clay gouge bodies. Clay gouge often occurs between assemblages of granular gouge/breccia in proximity to the detachment. A discontinuous foliation is defined by a sometimes remarkably banded fabric of chloritic green granular gouge separated by paler layers of clay gouge.

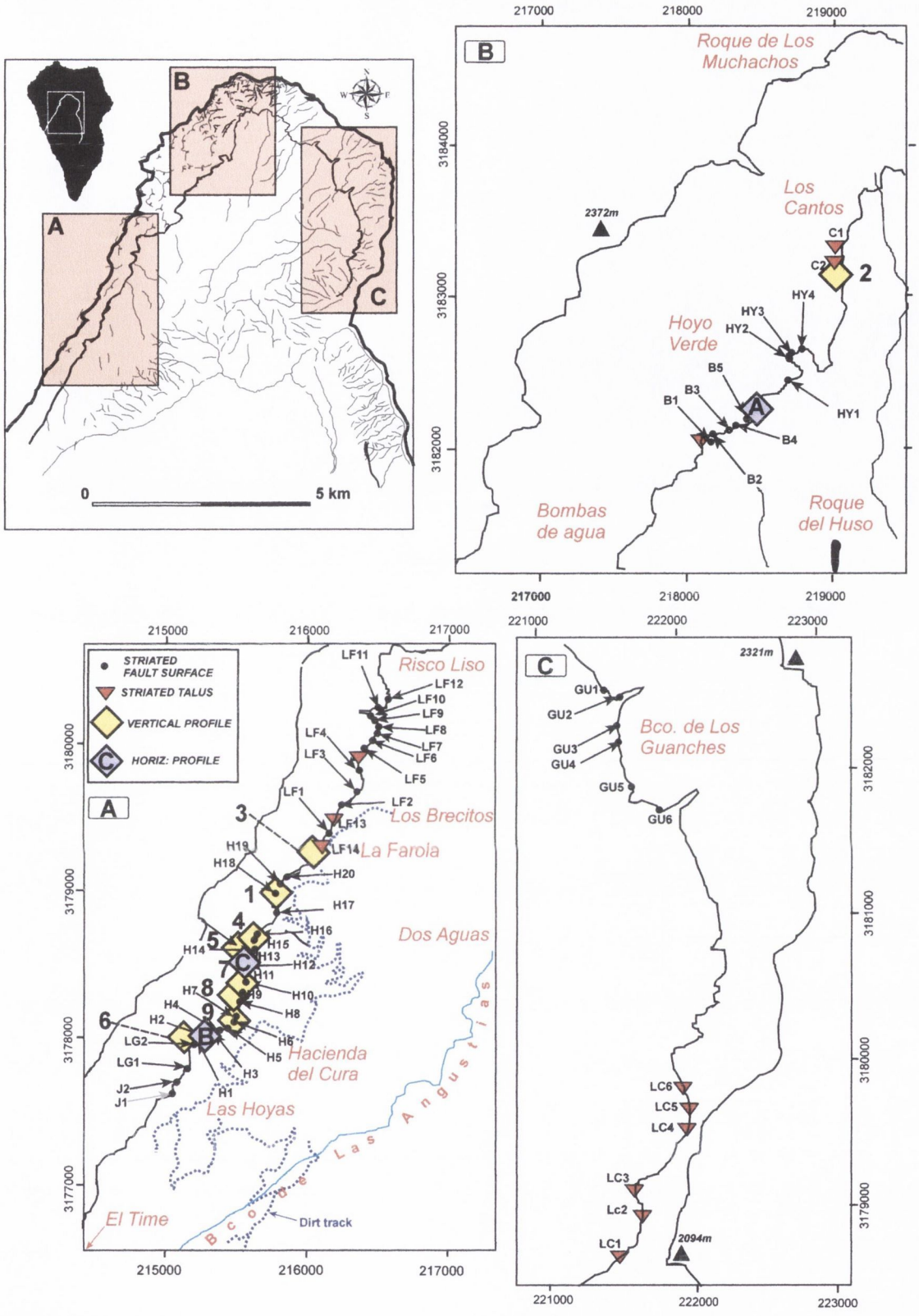


**Fig. 2.2.6.** Map quadrants showing locations of stratigraphic profiles/sections and orientation data points. The horizontal profiles (purple diamonds) are shown in Fig. 2.2.11.

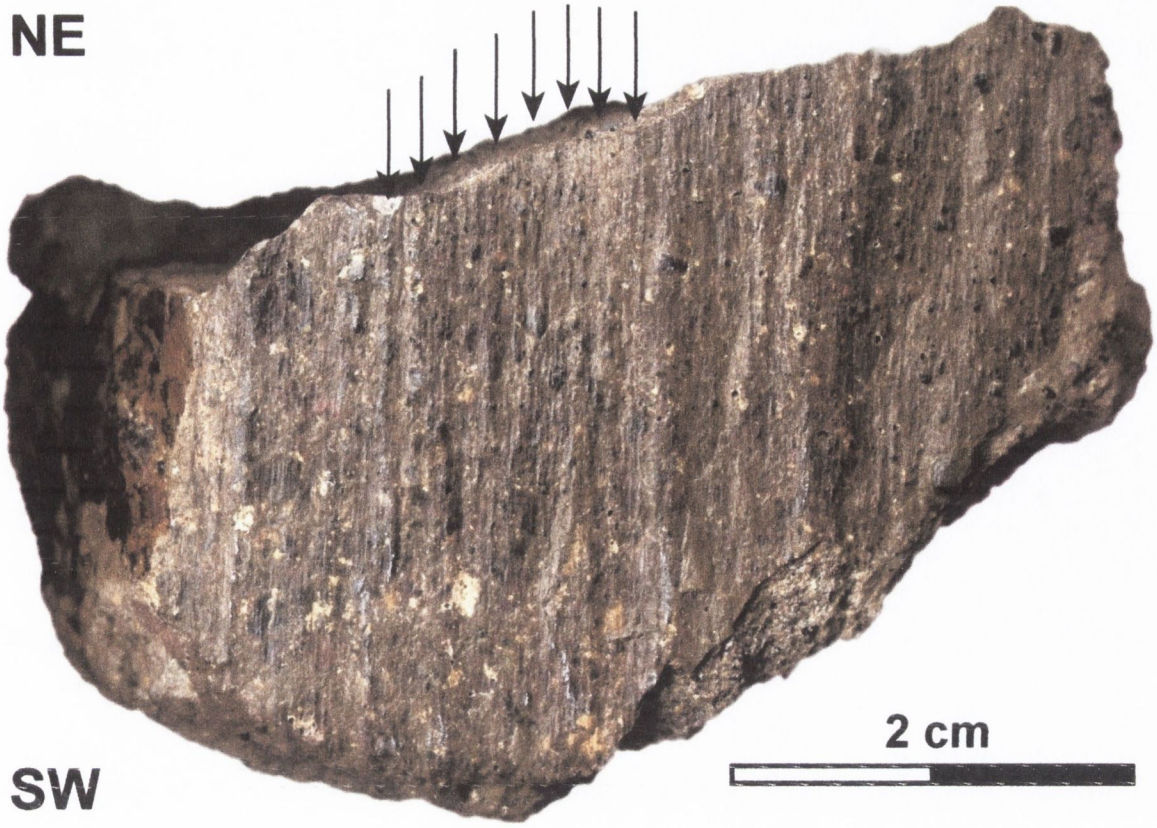

**Fig. 2.2.7. (Top)** Orientated chip sample from the inner (expulsing) part of the corrugated fault surface (base of TCB) showing lustrous striae. Yellow and orange speckles are juvenile pyroclastic materials: Locality - Tenerra.

Right: striated fault plane exposed from an overturned spall block. Locality: Los Brecitos. Scale card at centre of block is 16 cm long.

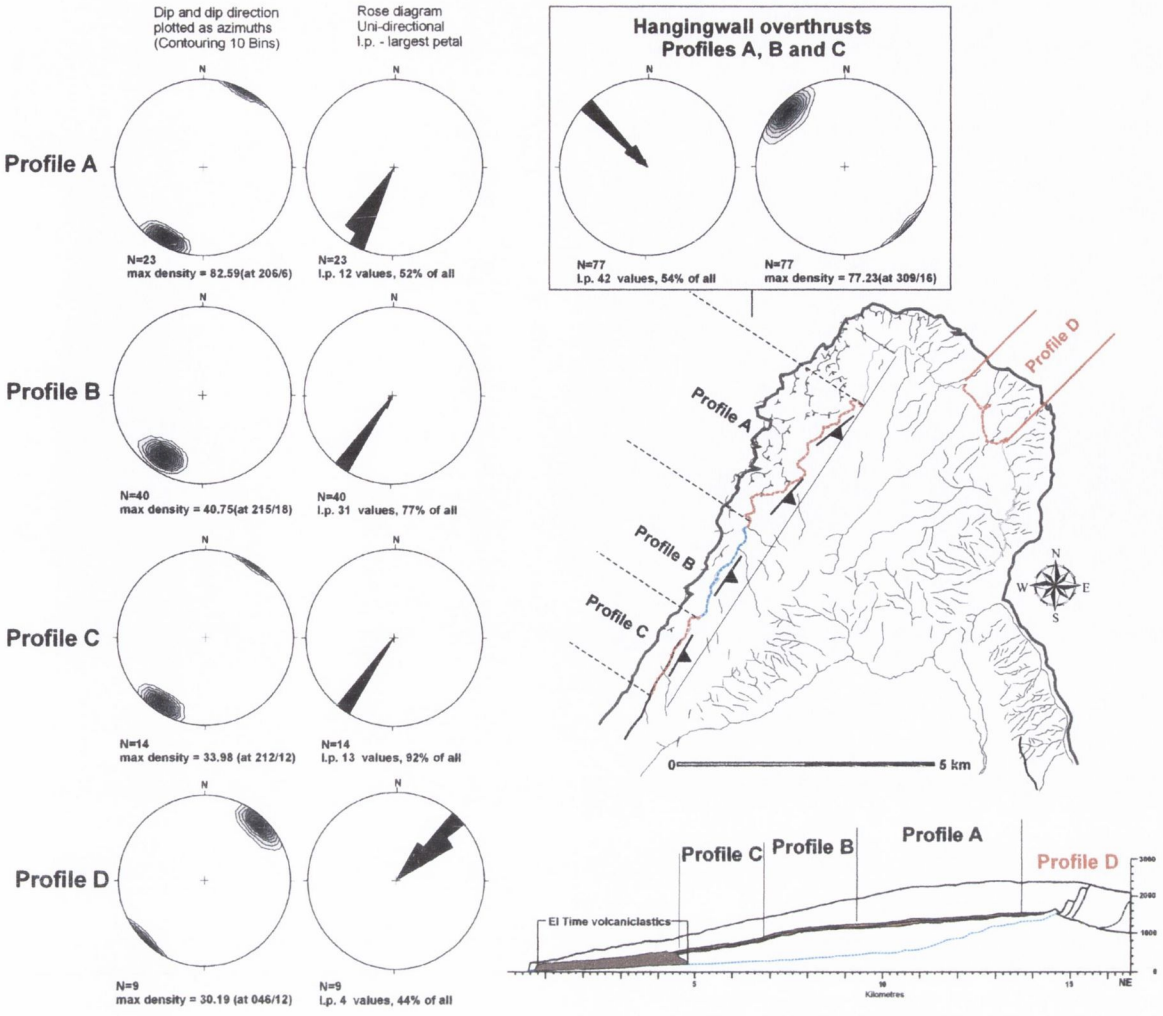


**Fig. 2.2.8.** Schmidt projections, rose and contour diagrams for slickensides at the base of the TCB. The overthrust symbols along the Hacienda sector denote post-collapse substratum expulsion.

Centimetre-thick banding and clay-scale foliaton are locally well developed around asperities where shear fractures tend to congregate. Heavily comminuted seamount-stage rocks and hangingwall breccias are juxtaposed along through-going P-shear fractures, particularly where large asperities exist. Where P shears step into the hangingwall (Fig. 2.2.11c), the basal part of the TCB is comminuted to a pale purple (Fig. 2.2.10c) or darker purple-brown colour often forming granular and clay gouge. Although occassional clasts of basement rock are visible at the base of the TCB, there is no widespread mixing between the juxtaposed gouge components. The UFG gouge is charateristically palest green or greyish white at outcrop, while the surrounding pale chloritic green gouge is often infiltrated by colour banded alteration zones displaying sharp inter-band margins (Fig. 2.2.10b). The alteration zones are well developed along spring-lines and around bissected and undeformed sheeted intrusions. They are typically dark brown, dark blue, green and pale purple and consist of cohesive scaly clay minerals.

Dikes that cut across the fault zone are frequently truncated at the detachment surface (Fig. 2.2.12a,b), however many subaerial feeders are un-deformed especially at outcrop inside the Caldera de Taburiente. Lateral tracing of dikes along the hangingwall has not been accomplished with any success[T], Metamorphosed or metasomtized dikes, that display conjugate offset within the damage zone, are completely absent within the fault core and un-traceable or irreconcilable even with reasonable lateral work space.

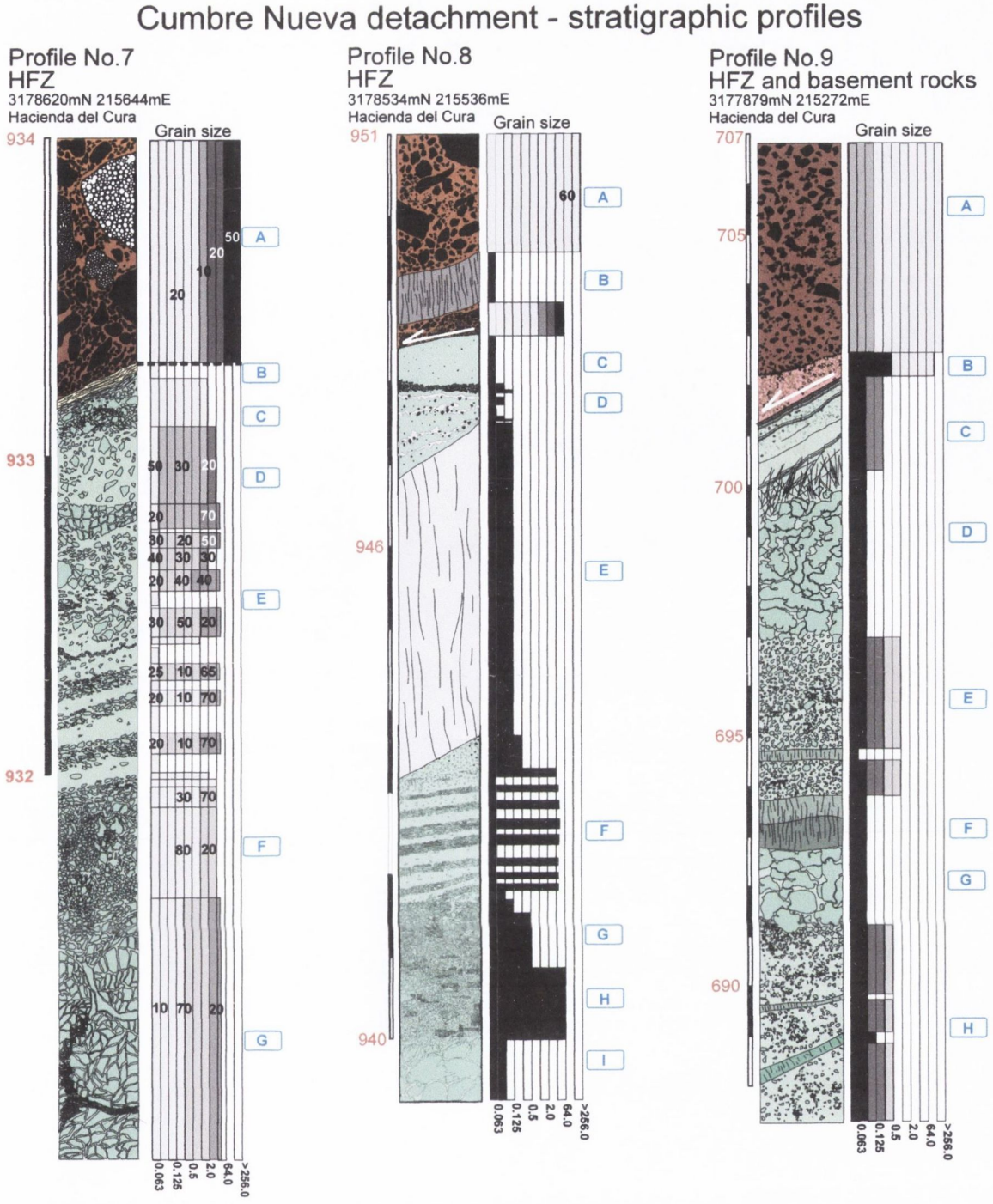


**Fig. 2.2.9.** Stratigraphic profiles through the CND and the basement lithologies

Profile 7. A. TCB1. B. Ultra-fine grained gouge. C. Granular gouge. D. Coarse aggregates and clay-sized matrix. E. Layers of granular banded gouge and UFG gouge with pervasive color banding. F. Coarse aggregates with no recognizable protolith fabric. G. Coarse aggregates with crude pillow lava geometries.

Profile 8. A. TCB1. B. Aphyric sill (heavily fractured). C. Clay gouge with minor survivor clasts. D. Clay gouge with color banding. E. Ol-cpx phyric dyke (20% crystals). F. Rhythmic seams of banded gouge and clay gouge. G. Coarse aggregates with no discernible protolith fabric. H. Pillow lavas in incipient states of disaggregation. I. Fractured pillow lavas (1-3% ol).

Profile 9. A. TCB1. B. Granular gouge in the basal part of TCB1. C. Fault core and mergent damage zone. D. Small pillow lava pods showing incipient disaggregation at 698.5 m. E. Indurated pillow fragment breccia suspended in hyaloclastite matrix. No comminution. F. Sheeted sills with transverse fractures. G. Ol phyric pillow pods. H. Pillow fragments and shards suspended in hyaloclastite matrix – disperse, thin sheeted intrusions.

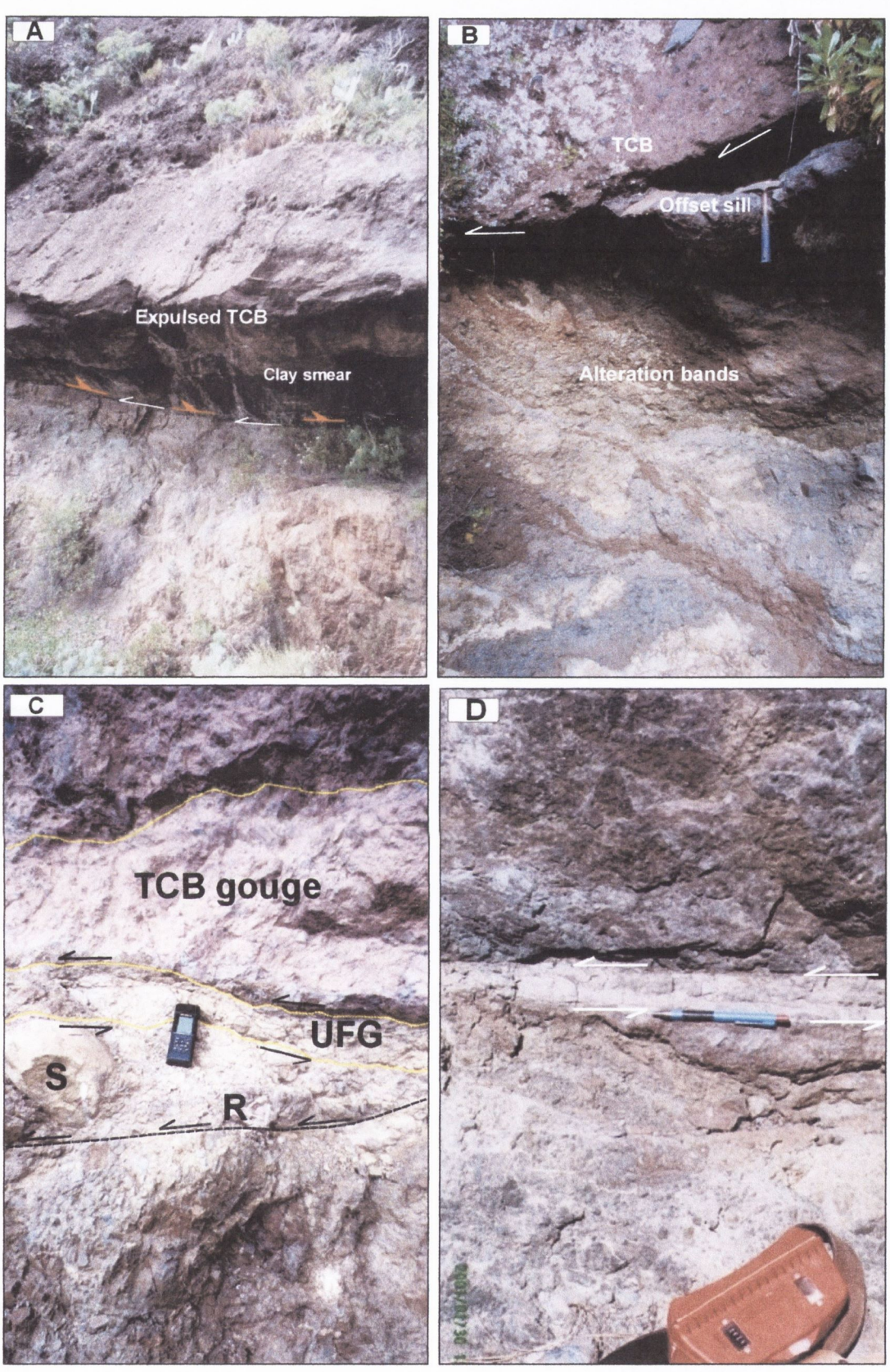


**Fig. 2.2.10.** Outcrop appearances of the Cumbe Nueva detachment fault along the Hacineda Sector.

A: Overthrust hangingwall with clay smear and, at the inner portion, survivor striations dipping to the southwest (shear symbols). The orange coloured thrust symbols denote the direction of substratum expulsion. Locality Near galeria – Hacienda del Cura. B. Colour banded alteration zones in the fault core with a sill offset at the fault contact (not traced laterally due to dense vegetation). Locality, about 1 km southwest of La Farola. C. UFG gouge between 11 and 25 cm thick with a Riedel fracture (R) dipping under a large survivor clast (S). The survivor clast is suspended in granular gouge. Note the pale purple granular and clay-rich gouge in the hangingwall. Location: near Tenera. D. A pale layer of UFG gouge with subjacent granular gouge (see Fig.2.2.3c). Location:- near Los Brecitos.

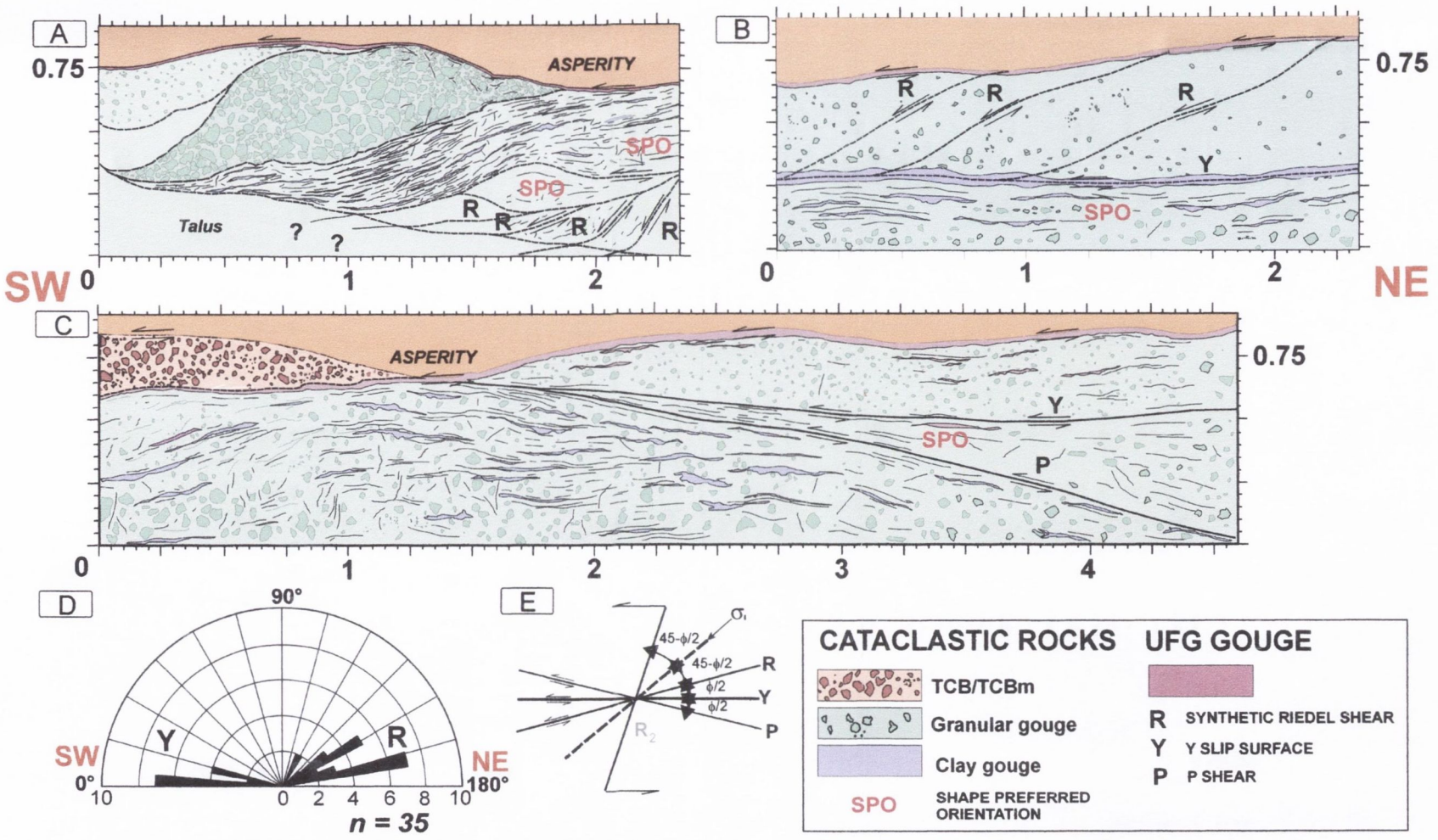


**Fig. 2.2.11.** Scaled sections of shear fracture geometries and particle size distributions along the Cumbre Nueva detachment. **A** Set of close-spaced R fractures conregating at an asperity, with a pronounced deflection of the granular fabric and well developed SPO inclined to the shear planes. (Locality: Hoyo Verde). **C** Intersection of Y and P shears forming a lenticular hangingwall (HW) gouge patch (Las Hoyas). **D.** Measurements of shear fracture orientations along the Hacienda sector with respect to the horizontal. E. The common elements of a Riedel shear system. R – synthetic Riedel shear. $R_2$ – antithetic Riedel shear (not observed at Cumbre Nueva). P – synthetic thrust shear. Y – displacement parallel shear. Modified from *McKinnon and Garrido de la Barra.* [1998].

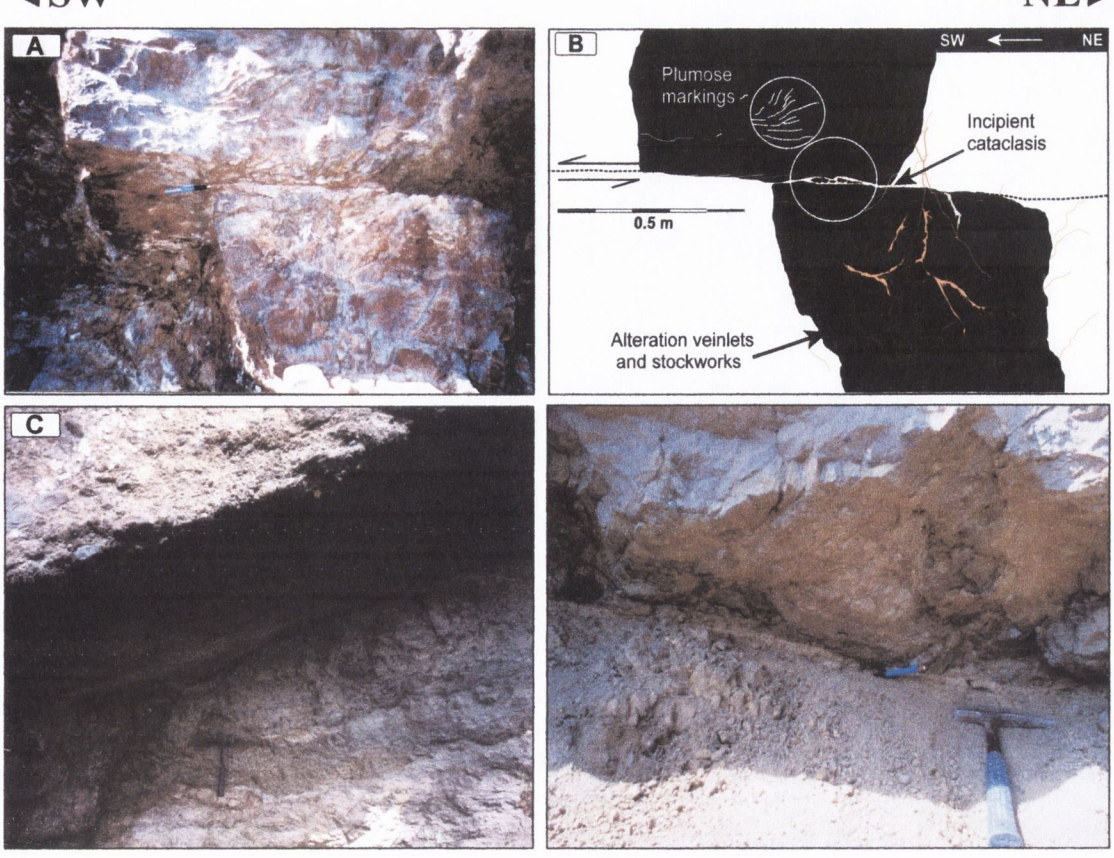


**Fig. 2.2.12.** A: Dike bisected at the detachment surface. Offset 33 cm. Locality between Los Brecitos and Tenerra. B: Tracing of dike in A showing structural features. C: Granular banded gouge and lenticular clay gouge. Clay smeared hangingwall is overthrust 1.7 m (see Fig. 2.2.13 for detailed section map). D: decomposed/weathered gouge. The UFG gouge seam is still discernable (at pencil). Note the faint southwest-directed striations. Locality: Las Hoyas.

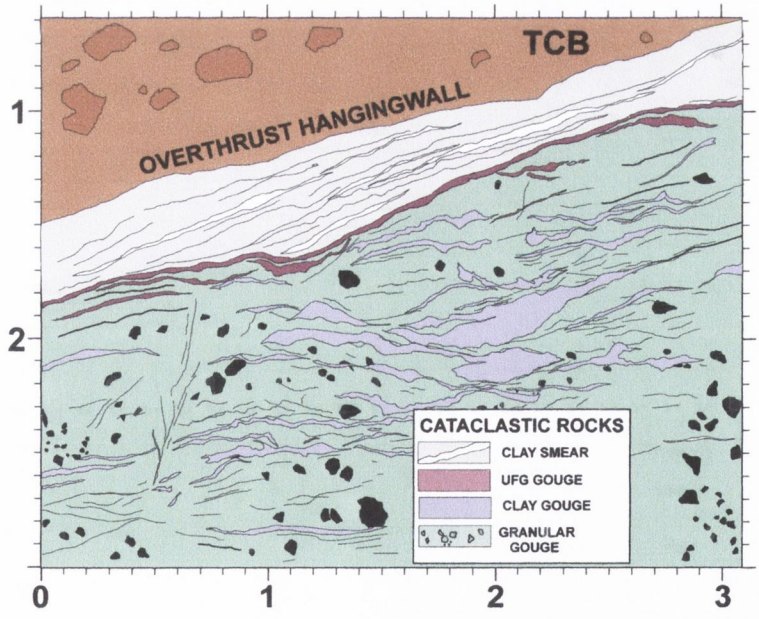


**Fig. 2.2.13.** Distribution of particle sizes through a section of the fault core in Fig. 2.2.12c.

Large, isolated, subrounded to very well rounded clasts (Figs. 2.2.10c and Fig. 2.2.13), between 20 and 50 cm wide, are observed throughout the fault core, suspended in matrices of different particle shapes and concentrations. These are survivor clasts, a term used by *Cladouhous* [1999a] to distinguish clastic components that escaped grinding and fracturing during the formation of gouge along the Turtleback detachment in Death Valley, California. The Cumbre Nueva survivor clasts are sometimes fractured/embayed but not pervassively so.

In similarity to the Death Valley detachments, shape-preferred orientations of survivor grains/clasts are observed in assemblages of Cumbre Nueva granular gouge, where the long axes are aligned into non-random orientations. Along the Cumbre Nueva detachment, the most pronounced shape prefferred orientation of grains is observed between the arrays of shear fractures that develop around asperities.

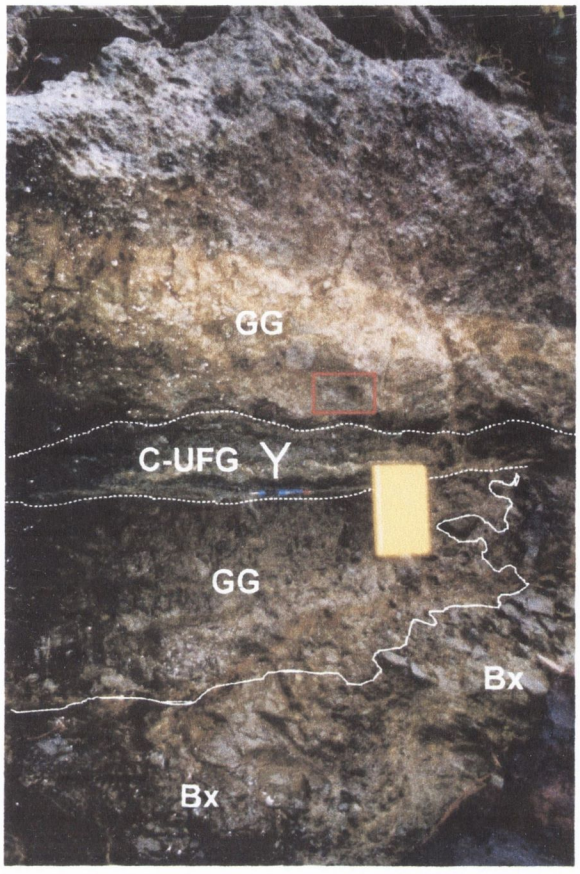


**Fig. 2.2.14.** Section of the fault core showing mingled clay and UFG gouge along a Y shear. The red box is a petrographic/XRD sample site. The notebook is 19 cm long. Abbreviations: Bx: breccia, C-UFG: mingled clay and UFG gouge, GG: granular gouge. Rust coloured talus in the lower left are TCB clasts. Location: galleria entrance at Hacienda del Cura.

Along the Cumbre Nueva detachment there are localities were the fault core is poorly developed over lateral intervals between 7 and 15 m, and is instead characterised by a predominantly very crude breccia, more reminiscent of the damage zone. In such instances, the seam of UFG gouge adjacent to the detachment surface prevails, but the core *(sensu strictu)* is only a few centimetres thick. Conversely, there are areas where the fault core is exceptionally thick apparently, at the expense of the damage zone. Again this often occurs where R fractures occur in thickened fault rock mass, typically around asperities.

Several types of Riedel shear fracture are distinguished within the fault core, primarily by their geometric relationships with respect to the northeast-southwest sense of down-dip slip. These fractures have produced a composite fabric of R, Y and P slip surfaces. As well as compartmentalizing the fault zone (in terms of particle size distributions), the slip surfaces sometimes gently deflect the prevailing foliation away from the master fault especially around asperities.

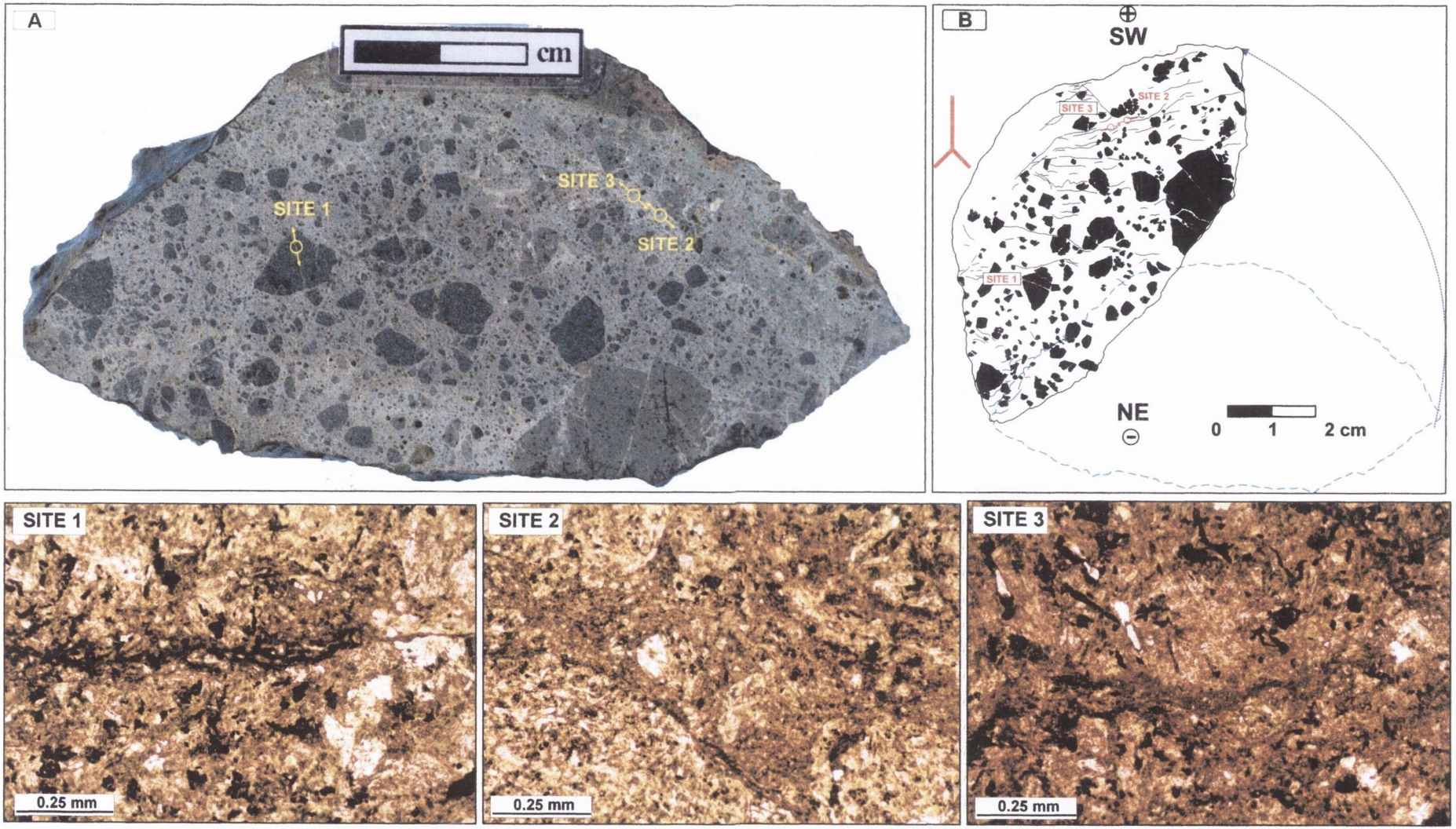


**Fig. 2.2.15.** A Orientated specimen of chloritic gouge from the fault core at Hacienda del Cura showing abundant fractured and disintegrating grains and veinlets of clayey matrix. B. Virtual orientation of the specimen showing intact grains and grains with intergranular fractures. Southwest (with the + symbol) is towards the observer, northeast (-) is into the page. PPL photomicrographs of fractures (SITE 1) and veinlets (SITES 2 and 3).

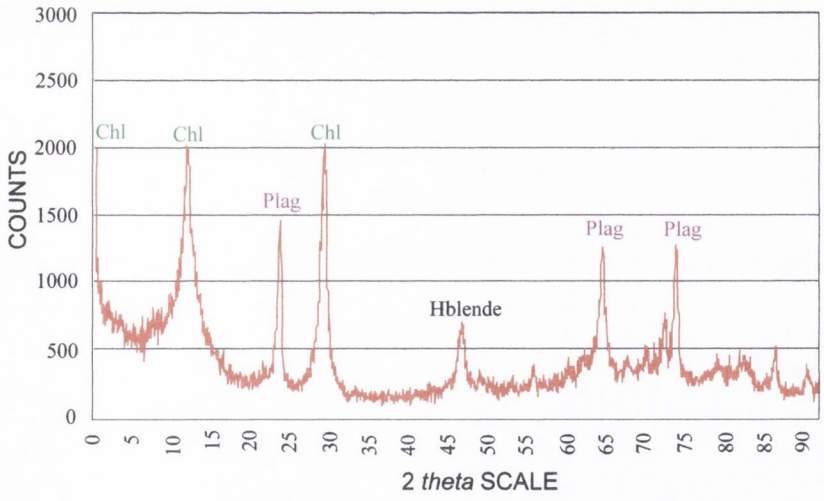


**Fig. 2.2.16.** XRD analysis of the sample in Fig. 2.2.11.
Analysis courtesy of *Kirsten Hetfield.*

An orientated chip sample of dark chloritic granular gouge was taken from just above a Y shear (Fig. 2.2.14) in order to investigate its mineral chemistry and petrographic characteristics. The hand-specimen structure is shown in Fig. 2.2.15a and b, specifically the grain-scale fractures and intra-granular fabric; the later is characterized by millimetre-scale anastomosing veinlets, typically paler than the surrounding matrix. The predominantly sub-angular grains are in various states of dissagregation but are rarely in mutual contact. Chlorite (Chl), that is relatively iron rich, creates well-defined XRD peaks (Fig. 2.2.16), and dominates the mineralogy of the examined clay fraction. The only two other minerals identified were plagioclase (Plag) and hornblende (Hblende). No diagenetic minerals (e.g., smectite, illite) were detected from XRD or petrographic analysis, although both are ubiquitous in the seamount host rocks as recrystallisation products of glass and palagonite and as amygdale linings [*Schiffman and Staudigel*, 1995; *Staudigel*, 1997]. XRD analyses of 2 μm samples form the fault core at La Farola identified montmorillonite/chlorite as the dominant clay minerals with plagioclase and gypsum (see Fig. 2.2.17), again with no trace of smectite or illite. The sample in Fig. 2.2.1.5 was taken from an outrcop with excellent preservance of fault textures and structures while those of Fig. 2.1.17 are more weathered.

### 2.2.3.3 The damage zone

Moving downward from the fault core there is a zone of heavily fractured, brecciated and moderatley indurated fault rocks, tabular in geometry, and often with iron and manganese-stained surfaces. This is termed the 'damage zone' (in the sense of *Chester and Logan* [1986] and *Seront et al.* [1998]). In this interval of the Cumbre Nueva detachment the clasts are between 0.5 and 25 cm in size and they comprise 70-95% of the fault rock mass. At its lower bounds, pillow lavas in the incipient stages of dissagregation can often be distinguished from an otherwise disfigured rock mass often composed of very coarse crush breccias (with <5% matrix) traversed by close-spaced fractures. Dikes, with and without hydrous or metasomatic overprints display conjugate offsets were they cut through the damage zone. The transition between the damage zone and the fault core is detectable from the change in fracture intensity (being more random and heterogeneous in the damage zone) and matrix content. The transition with the protolith is marked by a decrease in fracture intensity that makes the contact difficult to precisely locate and is made even more indistinct due to the effects of weathering, talus and thick scrub vegetation cover.

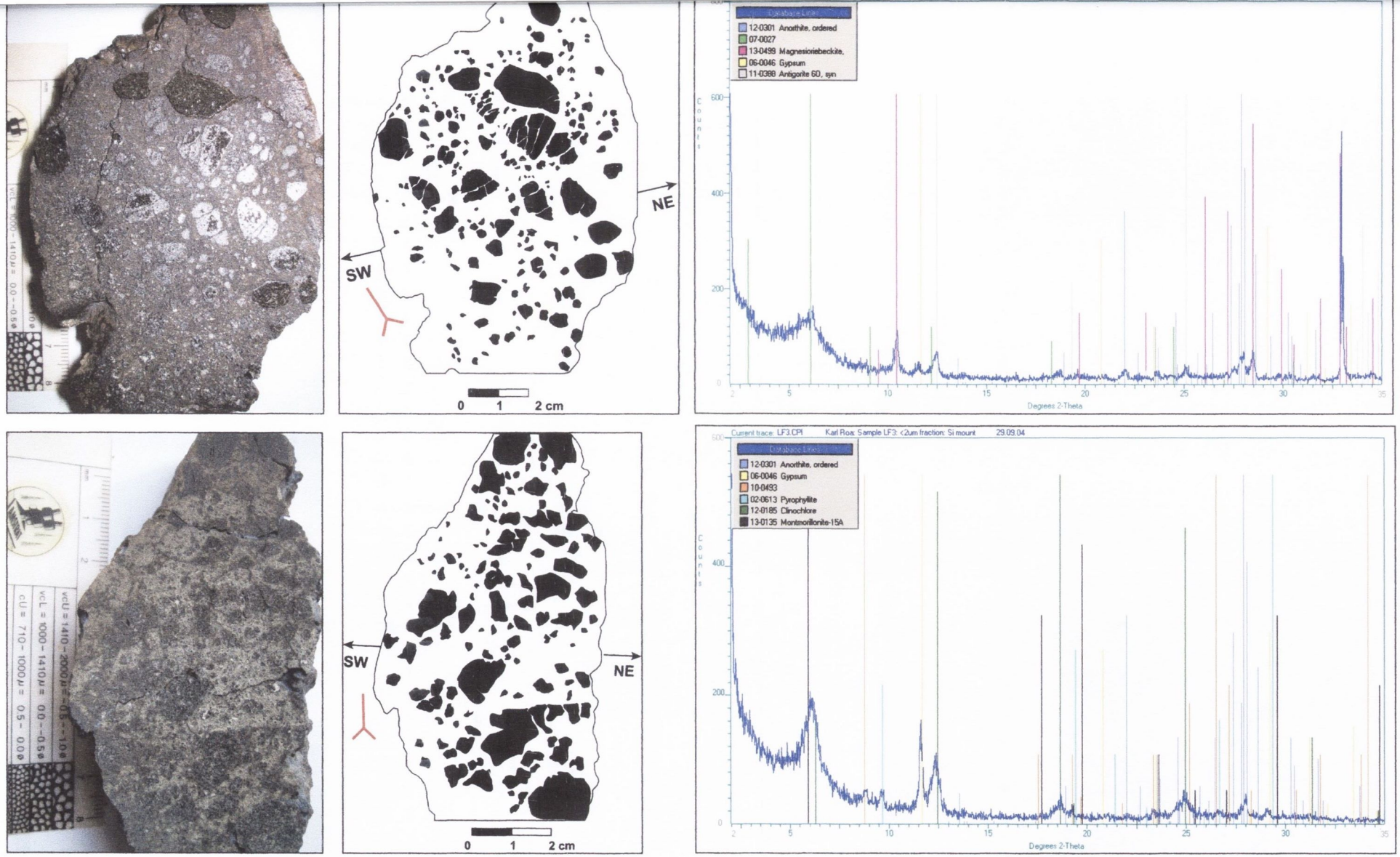


**Fig. 2.2.17.** Orientated chip samples form the fault core with XRD traces and interpretations of the <2μm fraction (glycolated). The polished split samples have been scanned to produce the black & white graphic maps so as to acentuate grain-scale fracturing where visible. Location: La Farola. XRD analyses courtesy of Robbie Goodhue.

### 2.2.4 Synthesis of the structural data

#### 2.2.4.1. Gravitational spreading

The field kinematic data from the fault zone indicate that the large parts of the western and eastern flanks of Taburiente/Cumbre Nueva were mobile prior to the Cumbre Nueva lateral collapse. This invokes the process of gravitational spreading illustrated in conceptual stages of development in Fig. 2.2.18. Detachment of the flanks from the uplifted basement resulted in the development of a focal southwest-facing slump sector, with an ancillary slump sector projected toward the east and remaining in place to this day. The northern part of the edifice, overlaping Ancestral Taburiente, is assumed to have been immobile Duch that it acted as a butress to the mobile sectors (Fig. 2.2.18). It is proposed that the onset of detachment was brought about by a density/rock mass competancy contrast between the base of the stiffened TCB and the uppermost seamount successions. Stiffening and synchronous compaction of the TCB facilitated a higher shear strength relative to the seamount rocks favouring bulk slip in the footwall. This was augmented by persistent uplift and steepening of the proto-detachment interface. For gravitational spreading to begin, the differential stress that gravity induces must exceed the yield strength of the basement rock [see *Schultz-Ela,* 2001].

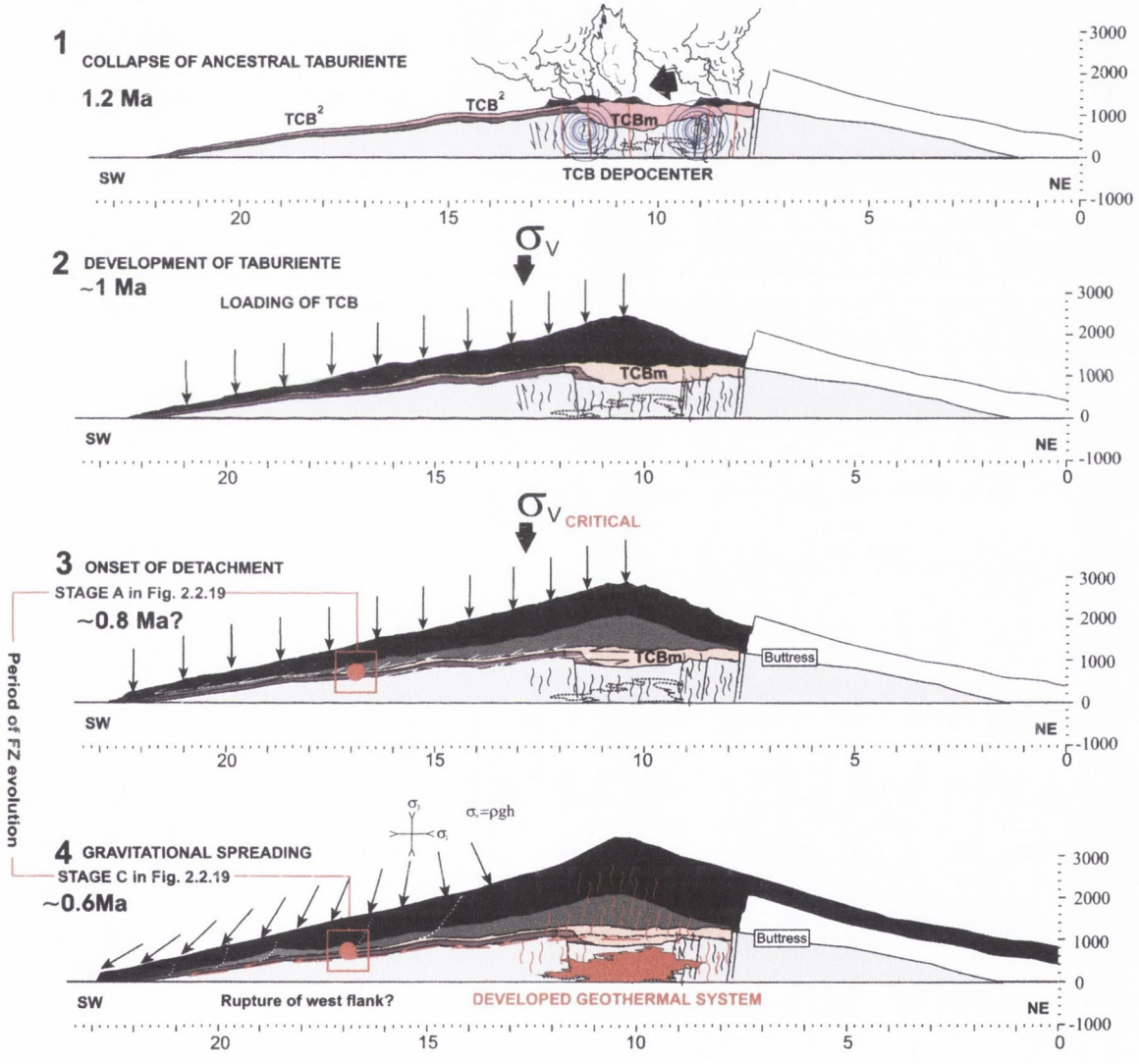


**Fig. 2.2.18.** Re-development of the Taburiente edifice and the onset of substratum deformation and fault zone evolution. $\sigma_V$ is the vertical stress induced by loading of the TCB.

It is possible however that the basement rocks were abnormally weak and sensetive to regimes of abnormal fluid pressure and shifting and increasing loads; hence the differential stress required for the onset of fracturing may have been lower than that required to cause fracturing in more compentant/intact rocks. It is implied that the increasing and shifting loads of the mobilizing had induced a basal traction in the footwall of the TCB causing detachment, basement rock dissgregation, comminution and particle size reduction, the essential mechanical processes involved in decollement zone maturation.

### 2.2.2.3 Kinematic evolution of the detachment

Throughout the evolutionary history of the Cumbre Nueva detachment, displacement along the fault zone was partitioned through (1) slip on the fault plane (2), through distributed granular flow in the assemblages of granular/clay and banded gouge and (3) localized slip along shear structures. Most of the shear is interpreted to have been concentrated in the finest-grained material, i.e., the 10 to 30 cm contiguous zone of UFG-gouge in contact with the hanging wall, and some of the ancillary Y-slip surfaces. This structural element of 'confined comminution' is in common with the Punchbowl [*Chester*, 1999] and Turtleback Detachments [*Cladouhous*, 1999a], where slip has been concentrated in extremely narrow zones, termed "Euclidean layers" by *Ben-Zion and Sammis*, [2003].

The exhumed Cumbre Nueva detachment presents a snapshot of the ultimate stages in the fault zones' evolution or growth sequence, prior to its exhumation by the Cumbre Nueva collapse (see *Hull* [1988] and *Shipton and Cowie* [2001]. Information on the development of the fault zone is contained in the orientations, persistence and zonations of internal structures and in the distributions of fault rock fabrics. These have an important bearing on the spatial and temporal development of cross-fault strain. The zoned internal structure records the operation of different deformation processes at different locations in the fault zone. The damage zone for instance can be defined as the region where accumulated strain or localized slip was perhaps some orders of magnitude less than the fault core, but brittle deformation was greater than that of the surrounding protolith. The fault core is therefore that interval of the Cumbre Nueva detachment that has accommodated net slip. The transformation of disaggregated host rocks into assemblages of breccia and then gouge, records a progressive increase in the total shear strain imposed by cumulative slip. Widening of the fault core through cumulative slip can be represented conceptually in three main evolutionary stages that evolve towards geometric simplicity [see *Ben-Zion and Sammis*, 2003]. Fig. 2.2.19 illustrates the conceptual evolution of the footwall.

Although the deformation induced by basal traction appears to have been responsible for much of the grain size reduction and fabric development within the fault zone, field and laboratory criteria for elevated fluid pressures and seismo-genesis (e.g. veins, hydro-fractures, psuedotachylite) are absent. However, this does not necessarily negate the involvement of fluids in the evolution of the Cumbre Nueva detachment. It is posible that the fault rocks have undergone varying degrees of post-kinematic leaching and alteration.. Moreover, the fact that the fault zone penetrates the exposed geothermal and intrusive core of the volcano makes it likely that fluids of different concentrations, temperatures and chemistries were involved in its dynamic evolution. Therefore, what appears to distinguish the Cumbre Nueva detachment from continental thrust faults is its intimate spatial relationship with sheeted intrusions, which according to recent studies on volcano instability, may influence the kinematic capacity for flank failure under highly specific circumstances (often invoking high fluid pressures as a critical process) [e.g., *Iverson*, 1995; *Elsworth and Voight*, 1995, 1996; *Day*, 1996]. This topic is addressed further in Ch. 3.2).

From a purely fault dynamics perspective, the emplacement of sheeted intrusions into the fault zone has another interesting effect on its theoretical evolution - particle size distributions in particular.

Each intrusion feeding the subaerial shield would transect the detachment, typically sub-vertically. That part of the intrusion traversing the fault core/damage zone had to be assimilated into it by progressive disaggregation of new intact rock among pulverized fault rocks. The newly emplaced intrusión(s) thereby locally reset the particle size distributions over narrow distances. This may explain why areas of the fault core appear under-developed (being dominated by coarse crush breccias), perhaps reflecting dissagregation of sheeted intrusion swarms.

Displacement along the detachment appears to have been localized by cooperative slip on ephemeral R-shears and long-lived Y-slip surfaces during grain-scale fracturing and granular flow in the surrounding medium. The amalgamating shear fractures reflect complex slip patterns that locally concentrated towards the removal of asperities due to the convoluted relief of the footwall. Other zones of comminuted hangingwall material, that do not display limiting shear fractures, may have developed in a similar way, but the eroding P shear plane was subsequently abandoned perhaps due to vertical/lateral changes in the shear stress conditions (by intrusions for example).

Fig. 2.2.11c attempts to capture the relationship between what have been interpreted as P and Y shears where they have congregated at an asperity and begun the process of hangingwall erosion. The scenario in Fig. 2.2.11a is more difficult to interpret. Here an array of R-shears form a mesh-like fabric bounding packages of foliated granular banded gouge, while a well-developed lens-shaped mass of non-foliated cataclastite has formed in the shadow of a non-deformed asperity. Perhaps this arrangement of shear structures and associated particles size distributions capture the initial stages of asperity removal. Distributed crush breccias can develop during the removal of local asperities [*Sibson,* 1986]. In Fig. 2.2.11b, millimetre-thick synthetic R-shears of variable inclination are seen to localize onto a major through-going Y-shear where the sense of shallow dip invariably changes along strike.

### 2.2.4.3. Displacement and fault scaling relationships

The displacement and, more specifically, the timing of displacement along the Cumbre Nueva detachment could not be measured directly. The period of fault zone evolution illustrated in Fig. 2.2.18 should be thus treated as speculative, based on a highly tentative analogy with Mt. Etna, where, over a 0.3 Ma period, the net displacement on the east flank amounts to approximately 1.2 km [*Borgia et al.*, 1992]. The question arises whether fault scaling relations can be applied to the Cumbre Nueva detachment where the sense of slip is, in essence - normal, albeit a shallow-dipping normal fault by any standards. As an absolute maximum the active cycle of the detachment is temporally constrained between two cataclysmic flank collapse events (~1.2 Ma and ~0.55 Ma), the latter, the Cumbre Nueva collapse, represents the point in time when the detachment was exhumed. Total displacement occurred at some stage in the 0.65 Ma period of volcano re-growth since the partial collapse of Ancestral Taburiente.

In order to be realistic, an assessment of the temporal evolution of the fault zone must be calibrated with the loading and uplift history of Taburiente and the finite size of the island. This is based on the assumption that gradual instability during loading, uplift and slope steepening lead to the onset of detachment, possibly in the later stages of volcano re-growth. However, the unknown parameters required to mathematically model the onset of detachment (e.g., differential loading rates, *in situ* rock mass strength/viscosity, effects of uplift eccentricity etc), outweigh the practicality and usefulness of such an endeavour in the present study. Radiometric dating of fault rocks and crosscutting intrusions was beyond the capacity of the project. The extent of hydrous metamorphism/fault rock weathering may even preclude the suitability of such a procedure and the validity of its estimates.

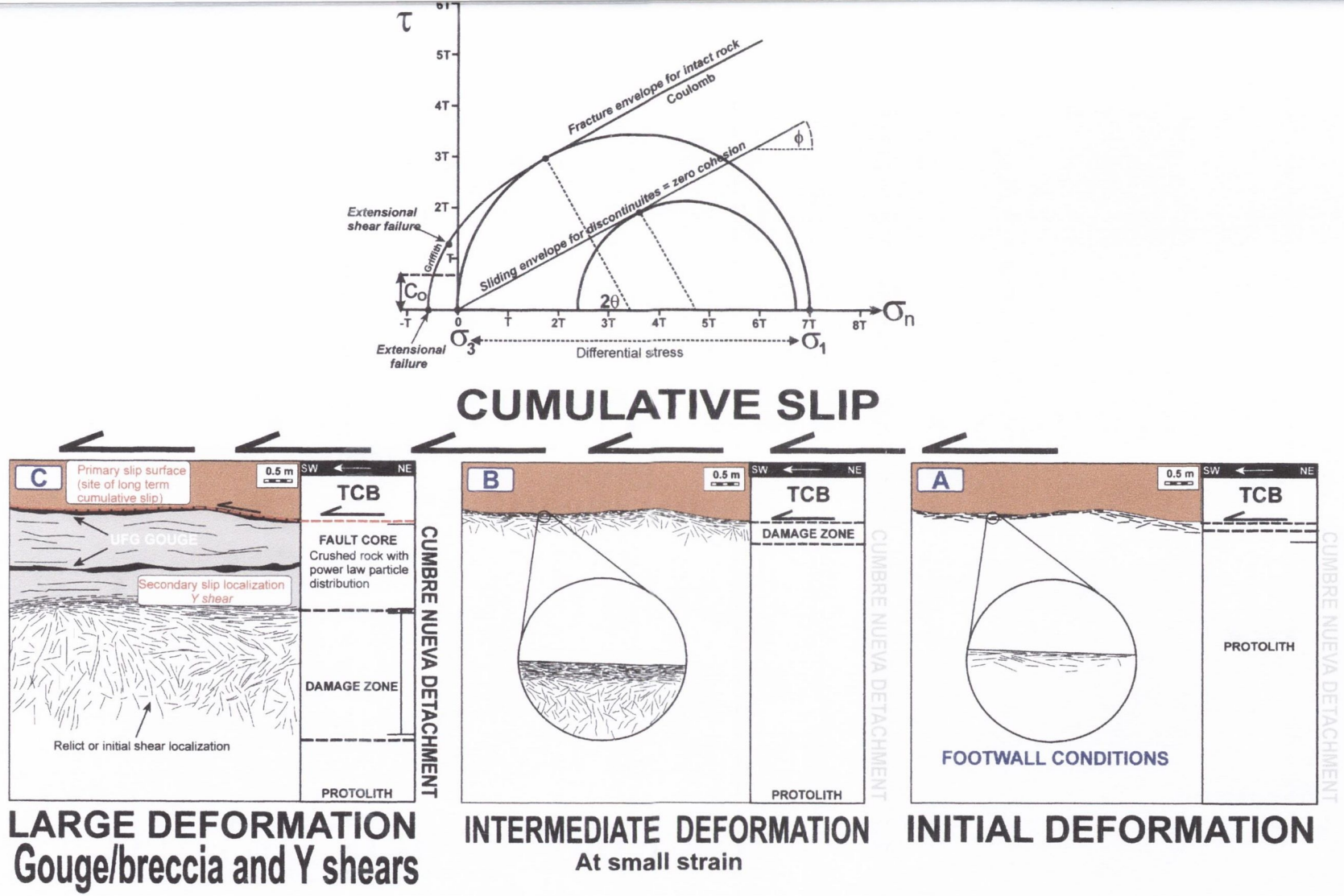


**Fig. 2.2.19.** Conceptual evolution of the footwall with cumulative slip, adapted from *Ben-Zion and Sammis* [2003] with finite strain axes in two dimensions for a steady state simple shear deformation. A, Initial deformation associated with strain hardening. B. Localizaion to tabular primary slip surfaces accompanied by a transition to strain weakening. C. Large deformation dominated by strain weakening and evolution toward geometric simplicity.

Moreover, alkali basaltic dikes are normally unsuitable for radiometric test-work since they trap excess argon. One option is to attempt to scale the fault zone thickness with published data.

It is well established that the production and thickening of fault gouge during frictional sliding tends to increase with increasing displacement up until a certain limit, as is consistent with a steady-state frictional wear mechanism [*Scholz*, 1987, 1990]. Since displacements over fault surfaces vary systematically, a corresponding variation in fault zone thickness is to be expected [*Walsh et al.*, 1998]. Scaling laws based on the empirical relationships between fault zone thicknesses (*T*) and finite displacements (*D*) have been developed for normal faults and mylonites, which demonstrate a log-linear relationship [e.g., *Scholz*, 1987; *Hull*, 1988; *Walsh et al*, 1998]. Fault zones containing assemblages of gouge and breccia generally have a *D/T* ratio >10:1 [*Walsh et al.*, 1998], although the ratio can reach 1000:1 [*Little,* 1995] (Fig. 2.1.20 a, b). *D/T* ratios of 1:53 and 1:1030 have been calculated for interlaced gouge assemblages adjacent to the Awatare Fault Zone (New Zealand) suggesting competing processes in gouge formation [*Little*, 1995].

When plotted against published data for normal faults and other brittle deformation zones (including detachments) there is considerable variation in the possible values of *D* for the Cumbre Nueva detachment. Assuming a process zone thickness of approximately 3 m and a *D/T* of 100, the corresponding value of displacement is around 300 m. However, fault rock thickness data for different fault types show a considerable variation and, given the available data, it is possible that D/T values approaching 1:1000 may apply, suggesting that kilometer-scale displacements may have occurred on the Cumbre Nueva Detachment. A more discriminating approach, given the low angle nature of the Cumbre Nueva Detachment, would be to compare associated fault rock thicknesses with those of other detachments (Fig. 2.2.20c; Table 2.2.2). This comparison suggests that rather high displacements (>300 m to kilometer-scale) are more likely.

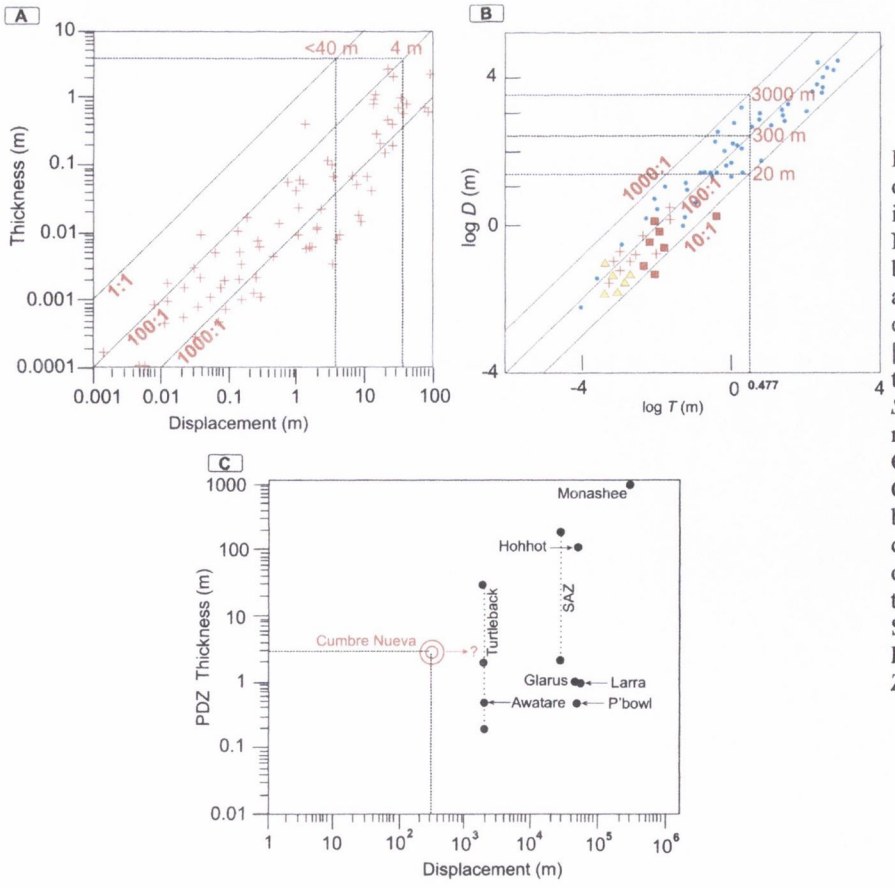


**Fig. 2.2.20.** D/T data from outcropping faults with interpolation of Cumbre Nueva fault thickness between *D/T* ratios of 10:1 and 100:1. (a) Published data (+) from *Walsh et al.* [1998] and references therein. (b) Data from *Scholz* [1987] and references therein. (c) Comparison between Cumbre Nueva (upper bound) with the principle displacement zones of other detachments listed in table 2.2.2. Abbreviations SAZ – Sub Andean Zone. P'bowl – Punchbowl Fault Zone.

| Fault system | DZT (cm) | Structure | D (km) | References |
|---|---|---|---|---|
| Punchbowl | 50 | Ultra-cataclastite | 40 | *Chester*, 1999 |
| Turtleback | 10-30 | Cataclastite | 2 | *Cladouhous*, 1999a |
| Monashee | 100,000 | Ductile shear zone | 300 | *Crowley et al.*, 2001 |
| SAZ | 20,000 | Cataclastite/slip bands | 20 | *Labaume and Moretti*, 2001 |
| Larra | 100 | Calcite veins | 5 | *Teixell et al.*, 2000 |
| Awatare | 30 | Ultra-cataclastite | 2 | *Little*, 1995 |
| Glarus | 25-200 | Myloinitc | ~40 | *den Brock and Jagoutz*, 2000 |
| Hohot | 10,000 | Mylonitic | >40 | *Davis et al.*, 2002 |

**Table. 2.2.2.** Summary data for large and small displacement thrusts spanning brittle and ductile deformation. Abbreviations DZT – displacement zone thickness, D: displacement distance.

### 2.2.2.5 Conclusions

The Cumbre Nueva detachment is located at the interface between the Pliocene basement and base of the subaerial shield of Taburiente Volcano. The fault rocks forming the detachment consist of systematically zoned assemblages of predominantly chloritic granular gouge, clay gouge, breccia (cataclastite) and ultra-fine grained gouge (or ultra-cataclastite). These rocks form a near contiguous fault core which is subjacent to the Tenerra Collapse Breccia. Parts of the TCB are assimilated into the fault core where asperities in the hangingwall have been mechanically removed during the maturation of the fault zone. Downward from the fault core, the damage zone consists of partially disaggregated and heavily fractured seamount/intrusive core rock, transitional with TCB-like materials within the confines of the Caldera. The overthrust fault plane displays dip-slip slickenside lineations preserved mostly along the SW-striking Cumbre Nueva sector. Most of the slip accrued along the detachment was accommodated within ultra-cataclastite adjacent to the fault plane. The period of fault zone evolution can be characterised by complimentary processes involving constrained comminution, distributed granular flow together with the development of Reidel shears particularly around asperities. The fault zone conveyed the SW flank of Taburiente, and perhaps Cumbre Nueva, towards the ocean (gravitational spreading), and ultimately towards its destruction at around 0.55 Ma. The period of fault activity and the net slip along the fault are undetermined although preliminary estimates based on fault scaling relationships indicate near kilometre scale displacements possibly over a period in excess of 0.2 Ma. Whether or not fluids were involved in the fault cycle is also undetermined, leaving scope for future studies that may answer this through isotope and/or mineralogical studies.

# 3.1. Debris Avalanche Deposits and Source Regions

The development of the island of La Palma has involved four major Quaternary deconstructive events. Each collapse structure appears to be related in geometry to a predecessor escarpment and/or its associated debris avalanche deposit, a factor in common with many other volcanoes.

**Fig. 3.1.2.** A view from the northern part of Cumbre Vieja Volcano towards the dismantled summits of Taburiente and Bejenado, with cloud cascading over the arcuate segment of the Cumbre Nueva embayment on the right. Photograph by Juan Socorro.

### 3.1.1 Introduction

The submarine slopes around La Palma are mantled with debris avalanche and turbidite deposits, generated by cataclysmic mass wasting events and sediment mass flows [*Urgeles et al.*, 1999; *Wynn et al.*, 2000]. In this section, the existing bathymetric database is revised and several new constraints are formulated regarding the topography of the onshore embayments and the spatial limits of the associated debris avalanches. The giant landslide deposits can be correlated with the dismantled subaerial slopes and older escarpments buried within the Taburiente edifice [*Ancochea et al.*, 1994; *Carracedo et al.*, 2001; *Masson et al.*, 2002]. The nested relationship between old collapse scars and developing instability sectors can be reconciled with the west flank of Cumbre Vieja Volcano where the distribution of cinder cones on the rift axis mimics the shape of the escarpment beneath. Rupture and normal displacement of the west flank, during the 1949 eruption, occurred in front of the Cumbre Nueva escarpment which is buried only a few hundred meters beneath the modern rift axis [*Day et al.*, 1999]. The alignments of vents along the active rift zone can thus be correlated with the enveloped southern segment of the Cumbre Nueva embayment. Furthermore, a debris avalanche boundary, delineated by side-scan surveys [*Urgeles et al.*, 1999; *Masson et al.*, 2002], exhibits a geographic correlation with the expected southern limit or 'outlet' of the embayment – based on these vent alignments. Older debris avalanche units on the western slopes may be related to landslides/slumps that were initiated on the submarine flanks. Finally, a debris avalanche unit emanating from the eastern part of La Palma may form the distal part of the TCB. In retrospect, the sizes of subaerial landslides on La Palma have generally decreased throughout the 1.7 Ma period of evolution. This may have implications for the development of the west flank of Cumbre Vieja.

### 3.1.2 Debris avalanche deposits

#### 3.1.2.1. Nomenclature of landslides in marine environments

Giant landslide deposits are ubiquitous in marine environments, from around oceanic island volcanoes [*Moore et al.*, 1989], spreading centres [*Tucholke*, 1992] and continental slopes [*Driscoll et al.*, 2000]. The three end-member types of mass movement:- (1) slumps, (2) debris avalanches and (3) turbidites, show systematic variation in the extent of slope/flank disintegration and run-out length (i.e., the distance between the source scarp or re-entrant and the leading edge of the debris avalanche deposit). These end members are depicted from a ternary perspective in Fig. 3.1.3, in terms of coherence, fragmentation and dispersal patterns. The archetypal Hawaiian slump structure, characteristic of Kilauea and Mauna Loa, takes the form of an actively creeping and disjointed flank, displaced away from a bounding rift zone, undergoing thrust-related uplift and sediment accretion in the process [*Morgan et al.*, 2000; *Lipman et al.*, 2002; 2003].

Debris avalanches are characterised by large-scale flank disintegration and resultant dispersal of kilometre-sized allochtonous masses of the former edifice/slope. These blocks/slabs are frequently rafted and undergo partial subsidence upon the voluminous syn-depositional volcaniclastic matrix; thickening down-slope into a bulging depo-centre [*Labuzy*, 1996; *Urgeles et al.*, 1999; *Watts and Masson*, 2001]. The run-out lengths and spatial dimensions of debris avalanches are controlled by the topography encountered during emplacement (e.g., scarps, benches and submarine cones), the proximity of neighbouring island pedestals, and the surface characteristics of the volcaniclastic apron (ponded volcanic and pelagic sediment, landslide blocks) [e.g., *Watts and Masson*, 2001; *Legros,* 2002]. Debris avalanches are the most frequently interpreted type of mass movement from around the Canary Archipelago (Fig. 3.1.4), slumps are less distinct [*Urgeles et al.*, 1998, *Masson et al.*, 2002; *Mitchell et al.*, 2002].

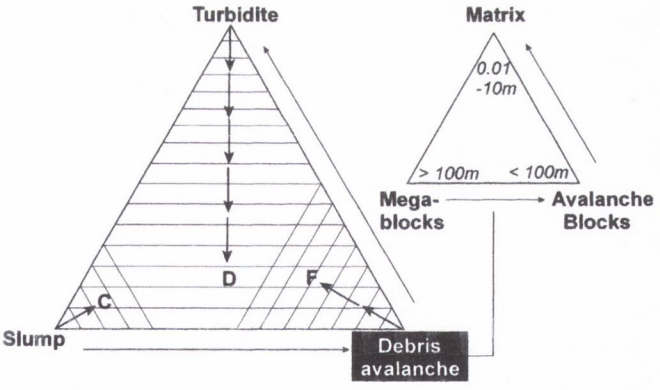


**Fig. 3.1.3.** End-member classification scheme depicting the fundamental aspects of mass wasting events from oceanic volcanoes. The ternary system is described in terms of coherence (C), fragmentation (F) and dispersal (D) or run out. The graduations are merely depictive of run out magnitude, which for many turbidites would be impossible to represent on a graduated scale whilst attempting to include the other end members. The exterior arrows represent the chain of mass movement transformations that may occur during slope failure. The smaller ternary plot specifies the size range of components from a debris avalanche deposit.

The third type of mass movement associated with growth and destruction of oceanic volcanoes is the far travelling abyssal turbidite. Turbidites can develop by the 'agitation' of pre-existing volcanic and pelagic sediments due to the impetus of a giant landslide or by a critically destabilizing seismic event. Turbidite deposits are, by comparison to slumps and debris avalanches, extremely thin (10-50 m) although they exceed both of these end-member types in terms of run-out length. Far-reaching debris avalanche-generated turbidites have been identified from both the Hawaiian and Canarian archipelagic regions [*Garcia*, 1996]. The Canary debris flow; a 600 km long, 40,000 km$^2$ turbidite was generated in the wake of the El Golfo collapse on the NW flank of El Hierro [*Masson et al.*, 2002]. The sediment wave fields identified around the submarine slopes of La Palma were generated by unconfined turbidity currents that originated on the flanks of the island [*Wynn et al.*, 2000].

The pool of data obtained from ocean drilling, seismic stratigraphy and bathymetric surveying indicate that debris avalanche deposits, slump structures, turbidites and pelagic/volcaniclastic sediments are a major volumetric component of the stratigraphic architecture of oceanic volcanoes [*Garcia*, 1996; *Schmincke and Sumita* , 1998; *Ye et al.*, 1999]. To this end the evolutionary stages between a seamount and a subaerial volcano are punctuated by innumerable flank collapses and structural re-developments that occur within and around the collapsed part of a flank [e.g., *Vogt and Smoot*, 1984, *Mitchell*, 2001]. Further on in the evolutionary time-scale, during the rapid subaerial shield-building stage, a substantial amount of mass is transferred into the ocean by submarine and littoral venting, continuous tube-feed of subaerially degassed lavas at lava delta fronts and subsequent bench collapses, ash fall-out from eruption columns and by erosion in areas of lesser volcanic activity. The 'clastic flank facies' of oceanic volcanoes may therefore represent between 20 and 30% of the volume of the volcanic system [*Schmincke and Sumita*, 1998] possibly more.

The debris avalanche deposits sourced from La Palma and its submarine pedestal are among a series of slide deposits flanking the volcaniclastic aprons around the insular volcanoes (Fig. 3.1.4). The bathymetric data of *Urgeles et al.* [1999] and other workers since have clearly demonstrated the scale and significance of mass wasting events from La Palma, in line with observations of similar scale on Tenerife, El Hierro [*Watts and Masson* 1995, *Urgeles et al.*, 1998] and other Canarian volcanoes. However, the origin and extent of the debris avalanche deposits around La Palma have generally lacked detailed correlations with the onshore geology and appear to have been misinterpreted from a dimensional/volumetric perspective. The discussions that follow demonstrate how with special reference to the Cumbre Nueva collapse.

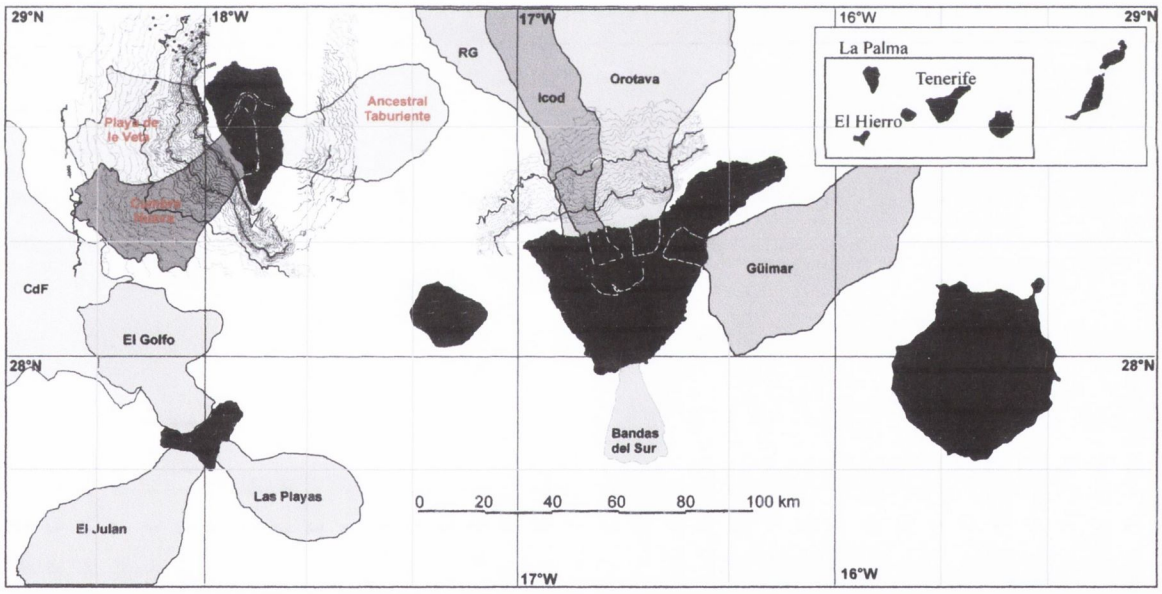


**Fig. 3.1.4**. Debris avalanches in context with others in the Canary Archipelago. Abbreviation CdF – Canary Debris Flow. Debris avalanche deposit geometries and source regions from *Urgeles et al.* [1999], *Krastel et al.* [2001], *Gee et al.* [2001] and Roa [2003].

### 3.1.2.2. Contemporary interpretations of landslide deposits around La Palma

This section outlines the criteria that have been used to delineate the debris avalanche deposits around the subamarine slopes off La Palma, their subaerial source regions (re-entrants) and the extrapolated volumes and areas (see *Urgeles et al.* [1999]; *Krastel et al.* [2001]; *Masson et al.* [2002]; *Mitchell et al,* [2002]). The first integrated bathymetric studies around La Palma were focused on surveying the sea-floor opposite the Cumbre Nueva embayment/Caldera de Taburiente [*Urgeles et al.*, 1999; *Krastel et al.*, 2001]. A Towed Oceanographic Bathymetric Imaging system (TOBI) was used to investigate the surface structure of the seafloor, while seismic reflection surveys provided some sub-structural definition. The acoustic back-scatter intensity, derived from an EM12 multibeam system, was used as an indication of the amount of sediment drape, and hence the relative age of the debris avalanche deposits, summarized in table 3.1.1.

| Debris avalanche unit | Area | Volume | Runout | Age | H/L | Source | References |
|---|---|---|---|---|---|---|---|
| | $km^2$ | $km^3$ | *km* | *Ma* | | | |
| 1. Cumbre Nueva | 780 | 95 | 80 | 0.42-0.5 | 0.075 | West flank | *Urgeles et al.* [1999] |
| 2. Playa de la Veta | 2000 | ~650 | 80 | 0.8-1 | 0.075 | West flank | *Urgeles et al.* [1999] |
| 3. Santa Cruz | 1000 | ? | 50 | >1 | 0.070 | East flank | *Masson et al.* [2002] |

Table 3.1.1. Debris avalanche deposits, source, geometry and age data for La Palma.

The Cumbre Nueva deposit forms a prominent topographic bulge on the submarine slopes, between submarine contours -2500 and -4000 m (Fig. 3.1.6a) [*Masson et al.*, 2002]. This hummocky depo-centre is characterized by an ensemble of sub-kilometre-scale debris avalanche blocks and associated matrix, up to 500 m thick [*Urgeles et al.*, 1999]. The depocentre which is up to 35 km across, is connected or projected up-slope via a narrow topographic chute towards the arcuate Cumbre Nueva headwall (Fig. 3.1.6c). The northern limit of the 8 km wide chute intercepts the right-lateral fault forming the Hacienda sector, although the southern limit has no clear shoreward topographic expression. The postulated closure of the embayment occurs north of Puerto Naos, 9 km down-slope from where the arcuate segment of the escarpment has been overlapped by Cumbre Vieja (Fig. 3.1.6c). However, numerous authors have stated that the Cumbre Nueva escarpment continues for some distance underneath Cumbre Vieja Volcano [e.g., *Carracedo et al.*, 1999a,b; *Day et al.*, 1999], and this is key to understanding both the total geometry of the embayment and the potential limits of future instability on the west flank of Cumbre Vieja. The chute region represents the transport pathway of the debris avalanche mass as it made its descent below sea level [*Masson et al.*, 2002]. The debris avalanche margins have been overlapped by well-developed submarine drainage systems consisting of flat-floored channels with numerous distributaries [*Urgeles et al.*, 1999]. The margins of adjacent debris avalanche deposits have been delineated based on the positioning of these channels [*Urgeles et al.*, 1999; *Masson et al.*, 2002]. Discontinuous ridge-like linear features (Fig. 3.1.6b) are also well developed within the margins of debris avalanche units, paralleling each other down to the –3000 m contour, after which they are no longer distinguishable.

The Cumbre Nueva deposit overlies an older amalgamation of debris avalanche units that have been collectively designated as the Playa de la Veta Debris Avalanche Complex (Fig. 3.1.6a) [*Urgeles et al.* 1999; *Krastel et al.*, 2001; *Masson et al.* 2002]. The namesake locality (*Playa de la Veta* - Fig. 3.1.5a) is located below the vertical sea cliffs, near the village of Tijarafe, in an area of localized stratigraphic discordance. The discordance surfaces are composed of distinct rust red scoriaceous materials that bound lens-shaped outcrops of distal a'a lavas and stacked pahoehoe sub-units, possibly unconformably[T].

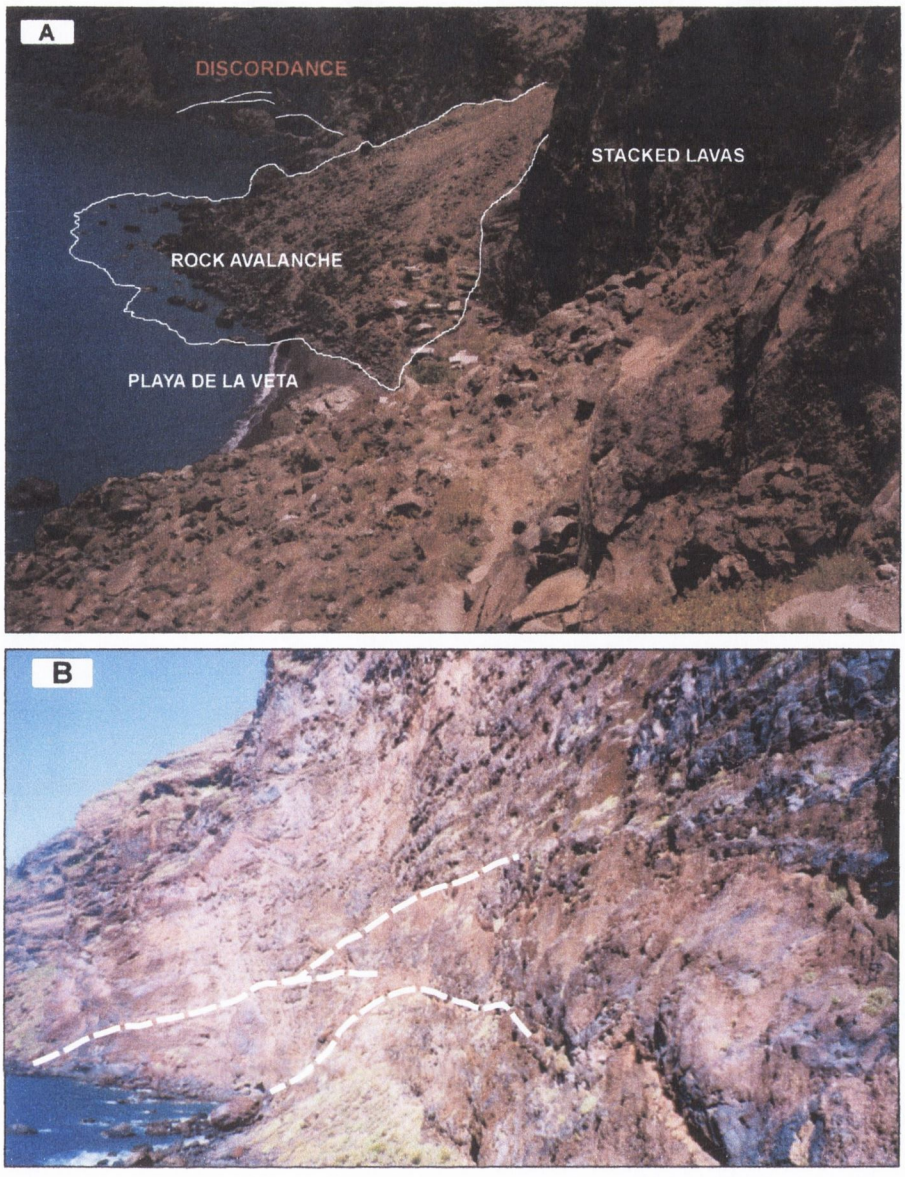


**Fig. 3.1.5.** A: Outcrop pattern of the discordance surfaces at the locality of Playa de la Veta. Photograph by J.C. Carracedo. B: Close up of the discordance system.

There is no evidence for offset or comminution on the discordant segment examined in Fig. 3.1.5b and no age data exist to determine the time intervals between the adjacent lava flow sequences.

An escarpment has been interpolated by *Urgeles et al.* [1999] and *Masson et al.* [2002] to extend from Playa de la Veta inland, bounding most of the Cumbre Nueva embayment, opening to the south near El Remo (Fig. 3.1.6c). The interpolated escarpment is bound by the Ancestral Taburiente inliers north of the present Caldera rim, and it encompasses the Jieque inlier on the western flank. The bathymetric data indicate that the Playa de la Veta Debris Avalanche Complex comprises three topographic bulges with rough surface topography.

A reconnaissance bathymetric survey, carried out to the east of La Palma, identified a lobate debris avalanche deposit emanating from the eastern flank in the vicinity of Santa Cruz de La Palma and south of the east rift zone at Puntallana [*Masson et al.*, 2002] (Fig. 3.1.6a). This, the Santa Cruz Debris Avalanche, lacks topographic evidence for a source escarpment on the upper submarine slopes; its source may lie buried on land [*Masson et al.*, 2002].

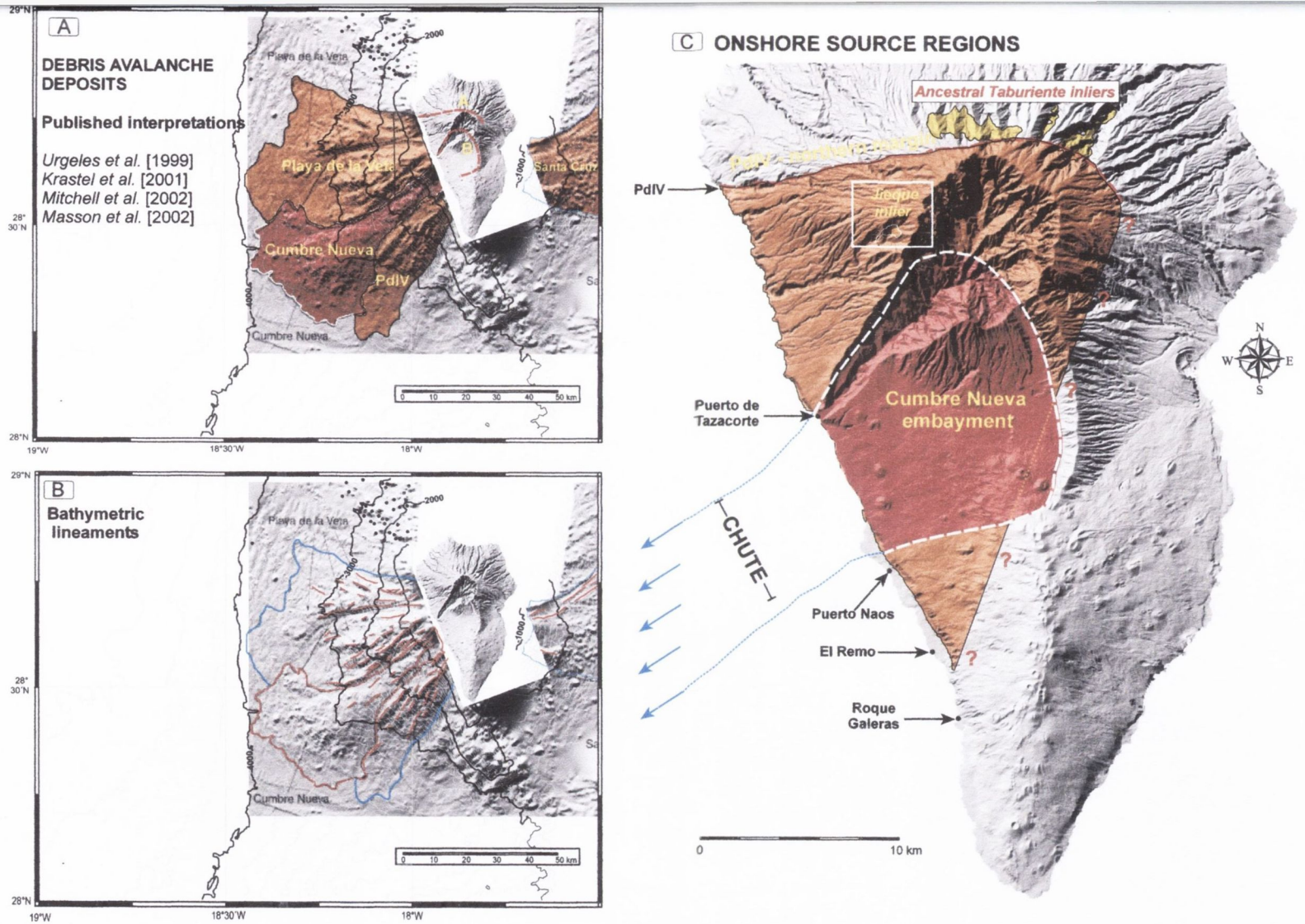


**Fig. 3.1.6**. A. Debris avalanche boundaries and onshore source regions as defined by *Urgeles et al.* [1999], *Krastel et al,* [2001], *Mitchell et al.* [2002] and *Masson et al.* [2002]. Abbreviations relating to red stipple. A: northern limit of the Playa de la Veta collapse scarp. B: Extent of the Cumbre Nueva embayment. B. Linear ridge-like features accentuated along the debris avalanche chute regions. C: Source regions as interpreted by *Urgeles et al.* [1999] and *Masson et al.* [2002]. The abbreviation PdlV is the locality of Playa de la Veta.

### 3.1.3 Re-appraisals of geometry; source regions and debris avalanche deposits

#### 3.1.3.1 The Cumbre Nueva embayment and avalanche deposit

There are a number of distinct structural components of the Cumbre Nueva embayment. The remarkably linear north wall (the Hacienda sector), forms the right-lateral strike slip fault-like structure [*Carracedo et al.*, 1997;1999a] that partitioned the west flank into a creeping sector, overlying the Cumbre Nueva detachment, and a stable or buttressing northern sector. Slide-bounding faults such as this are increasingly recognised on developing landslides in mountain environments (e.g., the Slumgullion earth-flow, Colorado [*Gomberg et al.*, between the Caldera/Cumbre Nueva embayment and the former mobile sectors.

A topographic feature named Bejenado embankment (BE in Fig. 3.1.7), stands at a distance of up to 700 m from the base of the arcuate headwall. Lavas on the east flank of Bejenado Volcano were dammed against the higher part of the Cumbre Nueva escarpment during the Quaternary and subsequently preserved its geometry along the embankment. As the relic spreading sectors re-adjusted to the new stress regime, brought about by the Cumbre Nueva lateral collapse, the unconfined TCB began to extrude from beneath the headwalls [*Roa,* 2003]. Retrogression of the scarp, both vertically and horizontally, formed a topographic breach between the scarp walls and Bejenado. The distance between these features should therefore reflect the processes of residual gravitational spreading of the east flank as well as differential erosion [*Roa,* 2003].

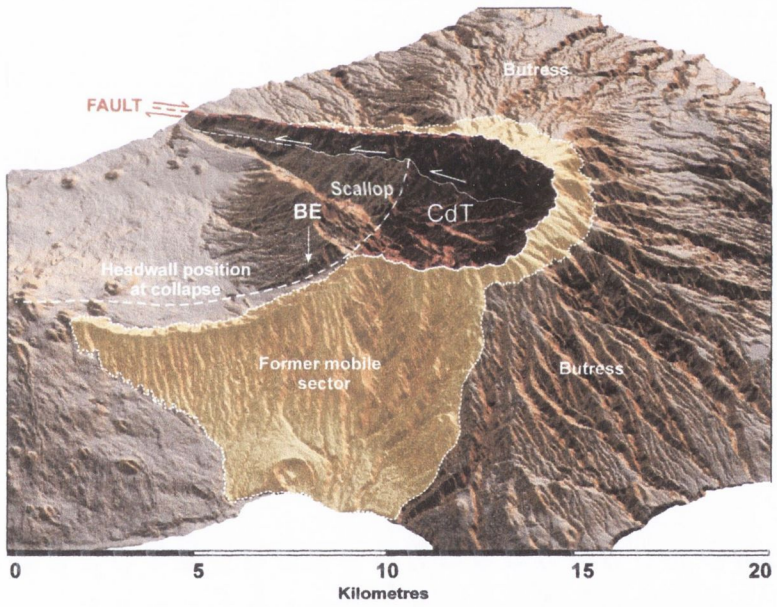


**Fig. 3.1.7.** Shaded relief image of northern La Palma looking west showing the major structural elements of the Cumbre Nueva embayment. The abbreviation BE is Bejenado embankment. The former mobile sectors overlie the TCB.

In its primitive position the Cumbre Nueva headwall was located over a kilometre west of the present eroded escarpment [*Carracedo et al.*, 1999a,b], intersecting the faulted northern margin between Tenerra and Risco Liso (Fig. 3.1.7). The significance of Bejenado embankment therefore, is that it preserves the former geometry of the escarpment prior to retrogression to its present position. The northernmost segment of the escarpment may have been subsequently scalloped as the un-supported summit region collapsed into the embayment, thereby forming the Caldera de Taburiente [*Roa*, 2003].

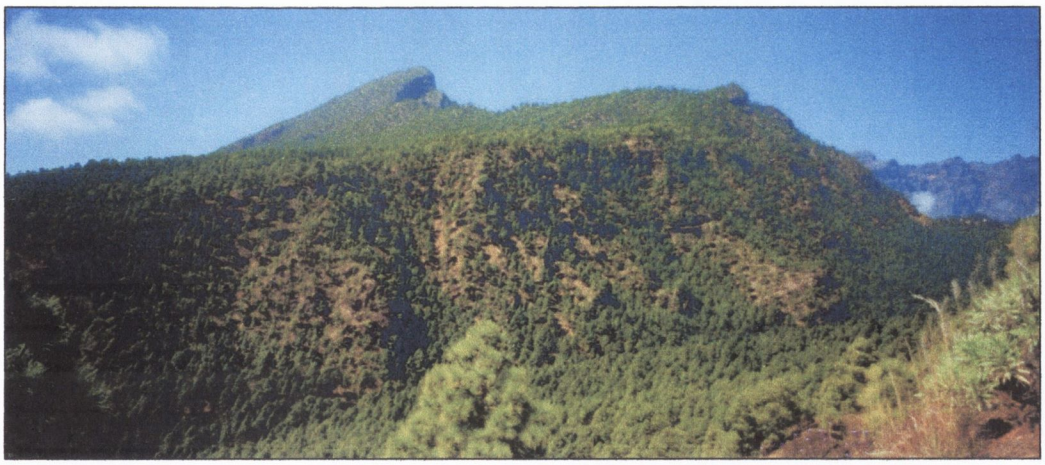

**Fig. 3.1.8**. Bejenado embankment with the incomplete stratocone of Bejenado in the background.

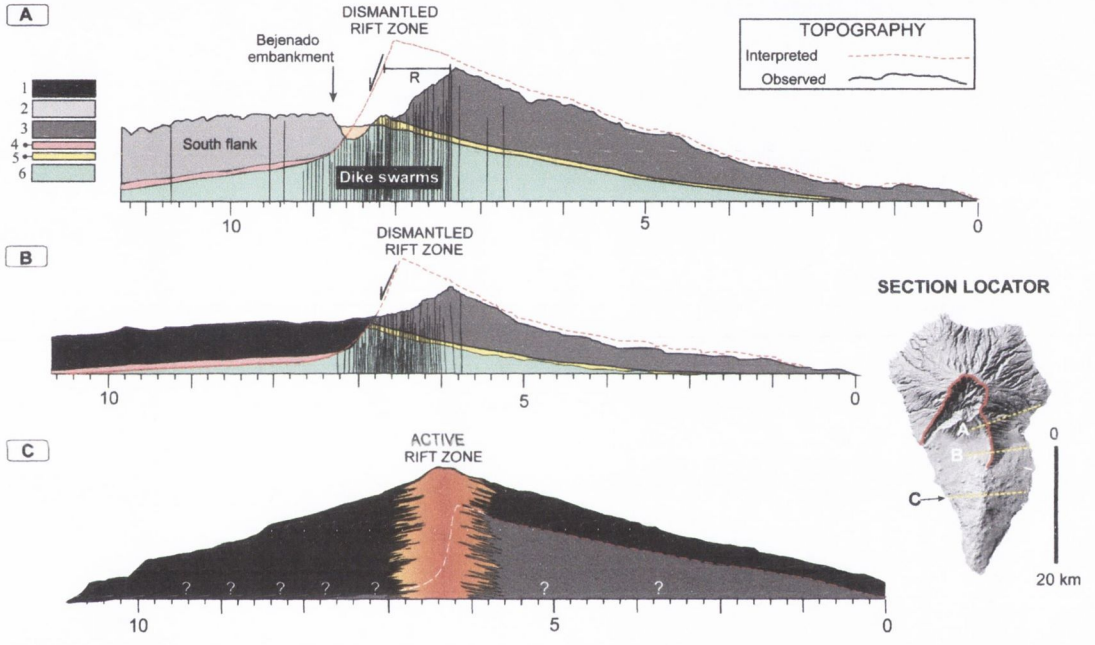


**Fig. 3.1.9.** Scaled E-W sections illustrating the extent of embayment-filling volcanism and associated landslide unconformities. Volcanic successions as follows: 1: Cumbre Vieja, 2: Bejenado, 3: Cumbre Nueva. Collapse-filling volcaniclastics: 4: Cumbre Nueva. 5: TCB. 6: Uplifted basement. Section A is based partially on borehole data [*Carracedo et al.*, 1997; 1999a,b]. In section B the elevation of the basement is extrapolated. In section C the basement elevation is unknown. In A the abbrevation R represents the distance of headwall regression.

The largely submerged floor of the embayment was covered with volcaniclastic materials associated with the lateral collapse, and subsequently infilled by two stages of intra-collapse volcanism [*Carracedo et al.,* 1999a,b; *Day et al.*, 1999] (Fig. 3.1.9). Vents along the higher part of the Cumbre Vieja rift zone developed along the contours of the escarpment, thus reflecting/preserving its geometry (Fig. 3.1.9c). The development of the Cumbre Vieja rift zone would thus appear to have been partially controlled by gravitational stresses along the escarpment Furthermore, the southern margin of the Playa de la Veta Debris Avalanche Complex continues upslope to where the expected southern limit or outlet of the Cumbre Nueva embayment should daylight in the vicinity of Roque Galeras (Fig. 3.1.10b). Therefore, the coincidence between the debris avalanche boundary and the eastward inflection of the Cumbre Vieja vent population could indicate that the Cumbre Nueva embayment and associated debris avalanche deposit is larger than has been previously assumed.

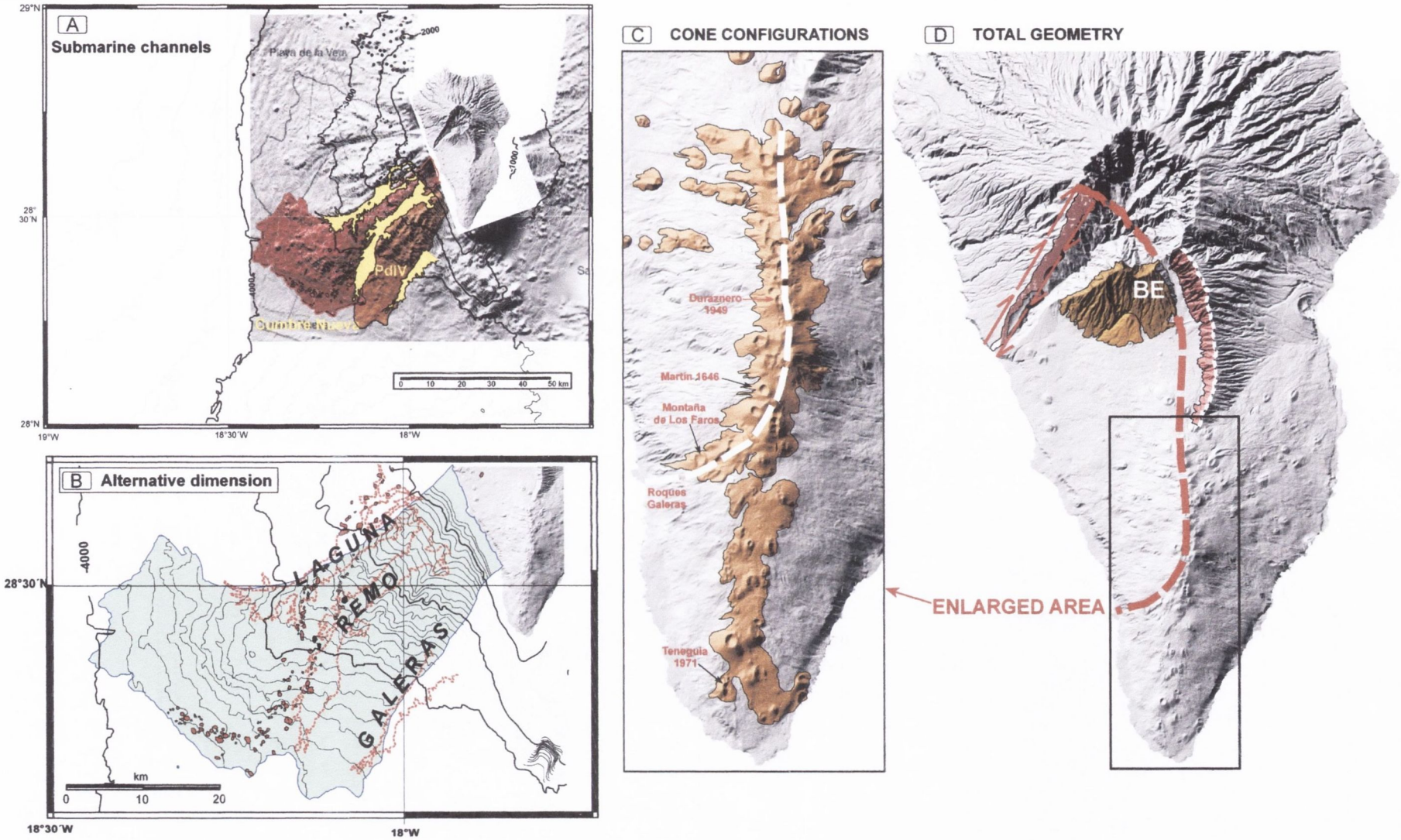


**Fig. 3.1.10.** A: Submarine channels (in yellow) used to delineate the boundaries of the Cumbre Nueva and southern Playa de la Veta (PdlV) debris avalanche deposits. B: An alternative interpretation of the Cumbre Nueva debris avalanche deposit that incorporates the southern PdlV component. C: Distribution of Holocene/historic cones along the N-S ridge of Cumbre Vieja, with the distinct inflection towards Roque Galeras. D: Proposed total geometry of the Cumbre Nueva embayment.

The southern limit of the Playa de la Veta Debris Avalanche Complex is therefore re-evaluated as an integral component of the Cumbre Nueva deposit and is annexed to it as such in Fig. 3.1.10b. The planimetric area of the modified debris field is 1160 km². The total inferred geometry of the embayment is indicated in Fig. 3.1.10d. In its adjusted form the outlet is nearly 16 km wide, twice that of previous estimations, and the adjacent broader chute region expands below the –3000 m bathymetric contour into two lobes, each one having smaller frontal protrusions with an overall self similar shape (Fig. 3.1.11a). The west lobe reaches the -4000 m contour, 63 km west of the escarpment. The area bounded by the reconstructed embayment is 146 km² although the precise volume of material removed is difficult to calculate since the pre-slide height variation is unknown. *Carracedo et al.* [1997, 1999a] estimate a figure in excess of 200 $km^3$, roughly 33% of the present subaerial volume of La Palma.

The scatter-plot in Fig. 3.1.11b illustrates the planimetric areas of 104 distinct landslide blocks sourced from the Cumbre Nueva re-entrant. The distributions of these slide blocks has been normalised along line-of-site with respect to the reconstructed headwall scarp. The scattergram does not simulate the trajectories of each block throughout progressive disintegration time, nor can it account for post-emplacement settling motion. However, it is evident that the distribution of blocks is relatively homogenous even though some of the largest blocks appear to have travelled the furthest distance from source. This is not an unusual characteristic of Canarian landslide deposits. For example, the Icod debris field (Fig. 3.1.4), emanating from northern slopes of Tenerife, is characterized by innumerable sub-kilometre sized blocks surrounded at is margin by blocks up to 1.5 km across [*Watts and Masson*, 2001; *Masson et al.*, 2002].

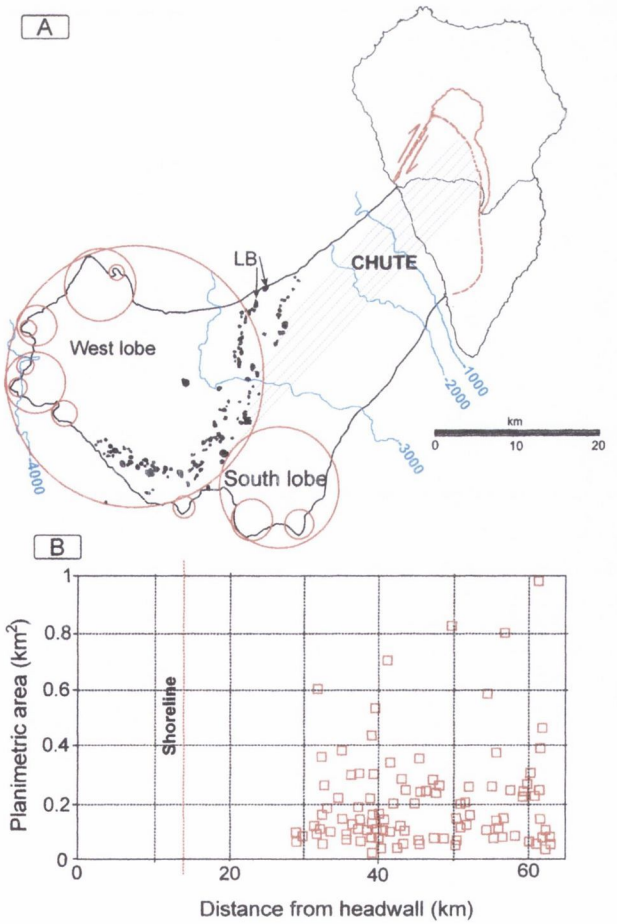


**Fig. 3.1.11.** A: Map of the Cumbre Nueva debris avalanche deposit showing a swath of 104 submarine landslide blocks interpreted from Fig. 11 of *Urgeles et al.* [1999]. Circles show frontal protrusions displaying self-similarity to the overall debris avalanche shape. B. Scatter-plot illustrating the planimetric areas of the landslide blocks as a function of normalized distance from the reconstructed headwall. Areas estimated using Arcview. Circles denote geometric self similarity of the debris avalanche lobes.

The mobility of the Cumbre Nueva debris avalanche deposit is plotted in relation to a range of continental and oceanic volcano debris avalanche deposits in Fig. 3.1.12 (see also Appendix 2). The dimensional parameters are the ratio of the maximum fall height relative to the maximum run-out distance ($H_{max}/L_{max}$), versus the area and volume respectively. The maximum elevation of the Cumbre Nueva scarp is estimated to have been between 2.2 and 2.6 km above sea level. The vertical fall height ($H_{max}$) is calculated with respect to the base elevation of the most distant frontal lobe of the deposit (-4000 m), thus summed as 4+2.2=6.2. The most distant lobe is 63 km ($L_{max}$), when measured horizontally from the escarpment in its inferred primitive position. These dimensional relationships are illustrated schematically in Fig 3.1.12. The equivalent apparent coefficient of friction ($\mu = H_{max}/L_{max}$), is 0.1 The previous evaluations of $\mu$ = 0.153 for Cumbre Nueva [*Urgeles et al.*,1999] lead these authors to suggest a low mobility on the basis of comparisons with other landslides around the Hawaiian Archipelago and Tenerife. Although some authors stress the ambiguity of the value of $\mu$ [*Legros*, 2002], one may stipulate that, from the continuum of $\mu$ values plotted in Fig. 3.1.12 that the Cumbre Nueva landslide represents a relatively efficient mass movement (or sequence of mass movements, emplaced rapidly.

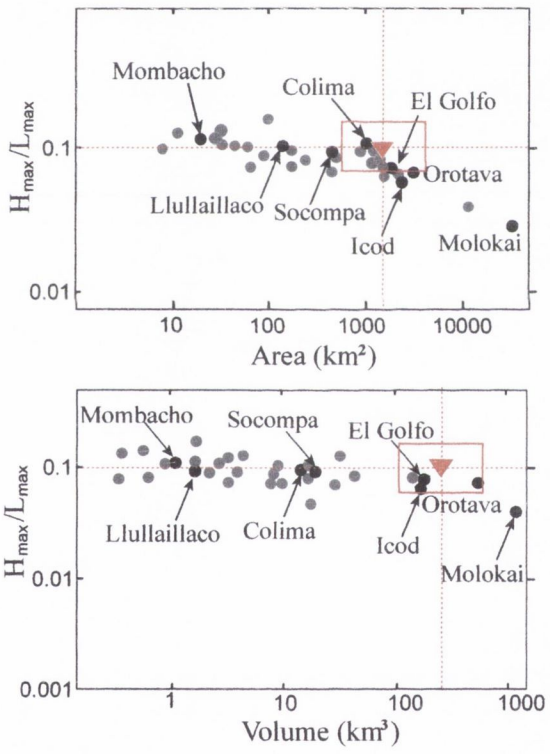


**Fig. 3.1.12.** Relationships between the total fall height ($H_{max}$) and run-out distance ($L_{max}$) versus volume and area for debris avalanche deposits from oceanic and continental volcanoes. Data extracted form *Richards and Villaneuve* [2001] and references therein *Legros* [2002], *Masson et al.* [2002].

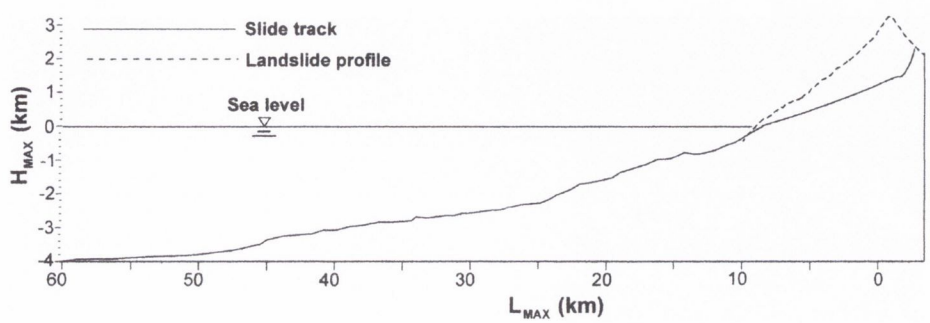


**Fig. 3.1.13.** Slide track and landslide profile of the Cumbre Nueva debris avalanche. VE = 2.5

A lingering question regarding the failure kinematics of the Cumbre Nueva collapse is whether or not it occurred as a single mass or if it was staged in multiple events. For the El Golfo collapse on El Hierro (Fig. 1.3.15), *Wynn and Masson* [2003a] note that the width of the chute region is less than width of the re-entrant. They question whether it is possible for the landslide material to pass through the chute region as a coherent mass. Furthermore, piston cores obtained from the Canary and Agadir basins show stacked volcaniclastic turbidites originating from two of the most recent landslides in the Canary archipelago (El Golfo and Icod). The stacked sub-units within single turbidite beds have been interpreted to indicate multiple stages of landslide failure from each re-entrant [*Wynn and Masson,* 2003b]. The Cumbre Nueva re-entrant is also slightly wider than the chute region, while further down slope the debris avalanche deposit terminates at two distinct lobes (Fig. 3.1.11a). However, in the absence of correlative core data from the abyssal plains west of La Palma, and based on re-evaluations of the existing bathymetric data and their onshore correlations, the preferred interpretion for the Cumbre Nueva collapse is that wholesale flank disintegration occurred on-land thus carving out the 16 km wide chute region.

### 3.1.3.2 Playa de la Veta Debris Avalanche Complex; a submarine origin?

As emphasized in Ch. 1.3, the island of La Palma is the emergent part of larger submarine construct, and may only represent 5% of the complete edifice by volume [*Urgeles et al.*, 1998; *Schmincke and Sumita*, 1998]. Therefore, the volcano-shaping processes of growth and destruction have, from a statistical perspective, occurred mostly in the submarine section. The conventional view is that the foregoing debris avalanche deposits (table 3.1) have been sourced from the subaerial edifice [*Urgeles et al.*, 1999; *Krastel et al.*, 2001; *Masson et al.*, 2002]. However, there are reasons to believe that the Playa de la Veta Debris Avalanche Complex (herein PdlV), has been sourced from the submarine slopes. The occurrence of Ancestral Taburiente lavas in the galerías around Puntagorda/Tijarafe [*Coello,* 1989], together with outcropping ancestral volcanic successions at the Jieque inlier [*Navarro and Coello*, 1993; *Carracedo et al.*, 2001] (Fig. 3.1.6), indicates that something is amiss with the interpretation of an exclusively subaerial source. The broadly unified constraints on the growth and destructive stages of northern La Palma [e.g., *Navarro and Coello*, 1993; *Ancochea et al.*, 1994; *Carracedo et al.*, 1999a,b; 2001], make it difficult to verify the existence of a subaerial collapse structure, that either predates the collapse of Ancestral Taburiente, or occurs between the ancestral and Cumbre Nueva collapses. In essence, if the PdlV collapse was initiated on land, how might Ancestral Taburiente volcanics remain in place on the west flank (Tijarafe)? In other words, what stage of subaerial deconstruction does the PdlV collapse actually represent outside of those firmly identified? Although the structural and stratigraphic significance of the discordance at PdlV is poorly understood, it is probably not as important, on a flank-tectonic scale, as assumed by previous interpretations. It is more likely therefore that the PdlV collapse was initiated almost entirely on the upper submarine slopes west of the NW rift zone. If so the steep topographic gradient on the upper submarine slopes (Fig. 3.1.15c) could represent a relict escarpment or region of depletion. The collapse scarp may have localized onshore around Playa de la Veta, but it can not have penetrated much further inland (i.e., towards the Jieque inlier). The avalanche deposit is spread over an area in excess of 1000 km², although the volume of the deposit is unknown. As noted by *Masson et al.* [2002], the PdlV deposit consists of structurally distinct components of as yet undetermined age relationships.

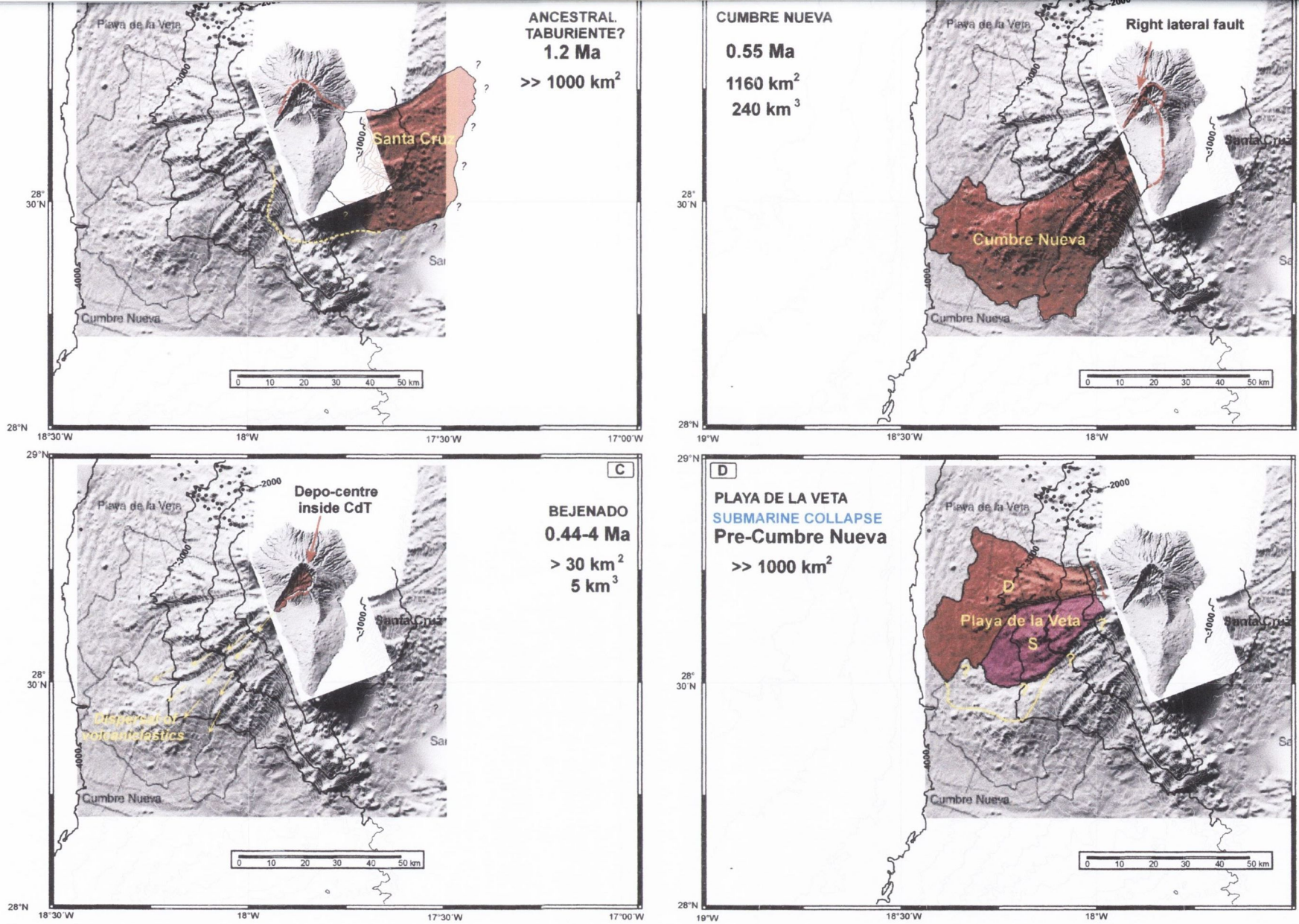


**Fig. 3.1.14.** Synopsis of the extent, relative timing and source regions of the debris avalanche deposits around La Palma. Note: In D, the abbreviations D and S denote debris avalanche and slump-like components of the PdlV Complex.

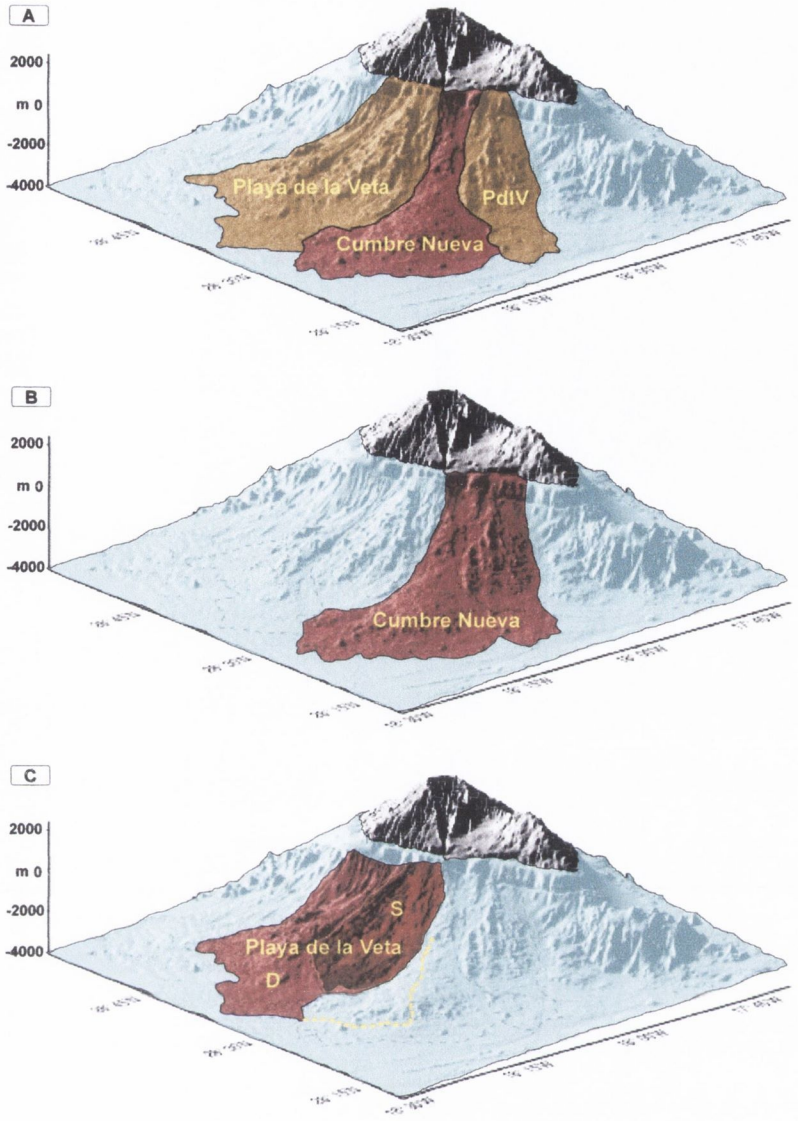


**Fig. 3.1.15.** A: Shaded relief images depicting A: the published interpretations of the debris avalanche units around La Palma. B and C are modifications of these interpretations. Modified from *Urgeles et al.* [1999] and *Masson et al.* [2002]. Note, in C, the abbreviations S and D refer to the slump-like and debris avalanche components of the Playa de la Veta debris avalanche complex respectively.

A relatively coherent bulging mass abutting the Cumbre Nueva debris field is slump-like in morphology (marked S in Fig. 3.1.15c), while an adjacent unit with distal protrusions forms a more disperse debris avalanche deposit (D in Fig. 3.1.15c).

### 3.1.3.3. Santa Cruz, the distal part of the TCB?

Although the total extent of the Santa Cruz debris avalanche deposit is undetermined [see *Masson et al.*, 2002], the northern limit exhibits a spatial correlation with the inferred eastern opening of the buried Ancestral Taburiente collapse escarpment (Fig. 3.1.14a). The southward direction of failure of the ancestral edifice is confirmed on-land by the outcrop and correlative sub-crop extent of the TCB, with the linear wall forming the eastern part of the headward escarpment. It is possible that a significant volume of the TCB, possibly forming the distal part of the Ancestral Taburiente debris avalanche deposit, has been overlapped by the Cumbre Nueva and Cumbre Vieja stages of rift development. Additional bathymetric imaging is required to fully delineate the extent of this debris avalanche deposit.

### 3.1.3 Summary – landslide locations and size characteristics

The 1.7 Ma evolutionary cycle of volcanism on La Palma was affected by four major flank deconstruction events, each with a common source region or an underlying causative weak layer generated by a predecessor collapse, or inherited from the uplifted basement. Table 3.1.2 gives a concise re-evaluation of the collapse events and their source regions, identified and inferred (see also Appendix 2).

| Debris avalanche unit | Area | Volume | Runout | Age | H/L | Source | References |
|---|---|---|---|---|---|---|---|
| | $km^2$ | $km^3$ | *km* | *Ma* | | | |
| *Subaerial* | | | | | | | |
| 1. Bejenado | 30 | ~5 | 6 | 0.4? | 0.24 | Bejenado | *Roa* [2003] |
| 2. Cumbre Nueva | 1160 | *>200* | 80 | *0.55* | 0.1 | West flank | *Carracedo et al.* [1999a] |
| 2a. Caldera de Taburiente | ? | ~30 | ? | 0.55 | ? | Summit | *Roa* [2003] |
| 3. Ancestral Taburiente | 1000 | >200? | 50 | *1.2* | 0.070 | South flank | *Ancochea et al.* [1994] |
| *Submarine* | | | | | | | |
| 4. Playa de la Veta | *>1000* | *~650* | 80 | ? | *0.075* | Western slopes* | *Urgeles et al.* [1999] |
| 5. Cumbrecita | ? | ? | ? | >1.7 | ? | Summit region* | *Ancochea et al.* [1994] |

Table 3.1.2. Modifications to table 3.1.1. *Italicised* text refers to quoted authors. Note: in the case of the Bejenado north flank collapse event, the debris avalanche has been remobilised, forming the El Time fan delta. * Inferred source.

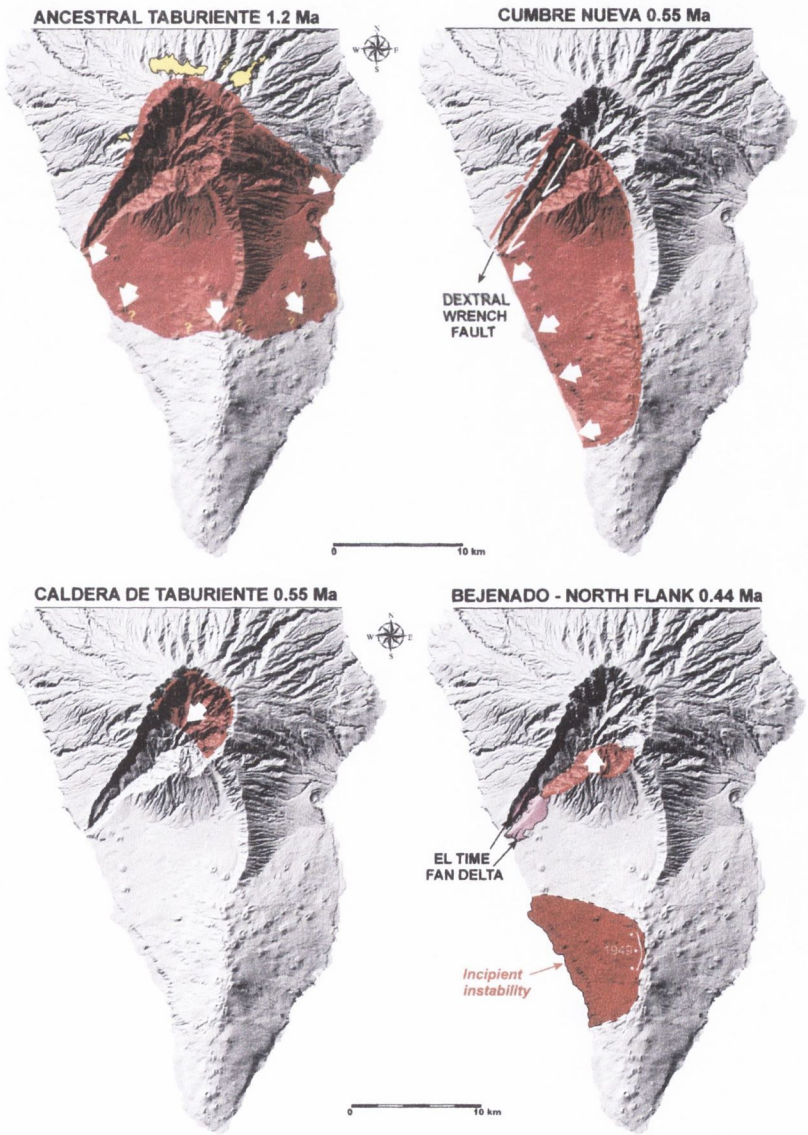


**Fig. 3.1.16.** Spatial and temporal evaluation of the subaerial collapse sectors/embayments.

The largest subaerial landslide event may have been the southward-directed collapses of Ancestral Taburiente, spawning a landslide which had important implications for the development of slumping on the SW flank of Taburiente. The reason for this inference stems from the subsequent development of a spreading sector within the confines of the ancestral embayment, bisected at a later stage by the Cumbre Nueva rift zone. The direction of ancestral flank failure may have been influenced by structural anisotropies in the uplifted basement where there is evidence of mass wasting during the submarine stage (the Cumbrecita group volcaniclastics – Ch. 1.2). The volume removed during the ancestral collapse is difficult to constrain as is the volume of the pre-collapse ancestral edifice itself. *Ancochea et al.* [1994] infer a constructional volume of around 145 $km^3$, which is <25% of the current volume of La Palma (594$km^3$) in its dismantled state. It is perhaps more likely, as suggested by *Carracedo et al.* [2001b] that Ancestral Taburiente had reached an elevation (~3000 m) or a volume similar to that of the successor Taburiente edifice. A constructional volume in the region of 500 or 600 $km^3$ is possible, nearly half of which may have been mass wasted during the explosive disintegration of the south flank.

The development of the Cumbre Nueva detachment, nested within the topographic confines of the ancestral embayment, is perhaps key to understanding how future instabilities may accentuate along the west flank of Cumbre Vieja. The incipient instability sector delineated initially by *Carracedo et al.* [1997] (outlined in Fig. 3.1.16) is nested within the southern part of the Cumbre Nueva embayment. Preliminary ground deformation analyses indicate that the west flank is stable during inter-seismic periods [*Moss et al.*, 1999] although eruptions on the ridge crest may trigger further slip events characteristic of the 1949 rupture [*Carracedo*, 1996]. *Ward and Day* [2001] have modelled a scenario involving the wholesale disintegration of the flank, and the submarine foundations, generating far reaching tsunami in the process, although the source dimensions and physics of the tsunami they propose have been contested [*Madder* 2001, *Pararas-Carayannis*, 2002]. If it can be said that the rupture surfaces that appeared during the 1949 eruption represent the incipient development of a landslide [e.g., *Carracedo,* 1994], there is reason to believe that future flank displacements as such may be controlled by volcano-seismicity along the axis of Cumbre Vieja [e.g., *Carracedo*, 1994,1996; *Moss et al.*, 1999]. However, in comparison to other large basaltic shield/strato shield volcanoes that display elaborate geological histories of flank displacement (with associated fault networks, benches, slumps etc), the events of 1949 should be interpreted with caution in the light of the high tsunami risk portrayed by the media before and since the Asian Tsunami of 2005. Moreover, the nested relationship of collapse structures and common source regions on La Palma (as outlined in Ch. 1.2.6.4), gives a more realistic framework for understanding the volume of potentially unstable flank material. This volume is considerably less than that of the re-entrant into which the bulk of the west flank of Cumbre Vieja has been constructed (i.e., within Cumbre Nueva). Combined with the evidence from other Canary Island volcanoes that slope failure is staged in multiple events [*Wynn and Masson*, 2003b] there is a high probability that the severity of the scenario depicted by *Ward and Day* [2001] is over-stated.

# 3.2. The Cumbre Nueva Lateral Collapse

The Cumbre Nueva collapse may have been triggered by failure of weak hydrothermally altered basement rocks significantly below the Cumbre Nueva Detachment, by either magmatic or climatically-induced high fluid pressures.

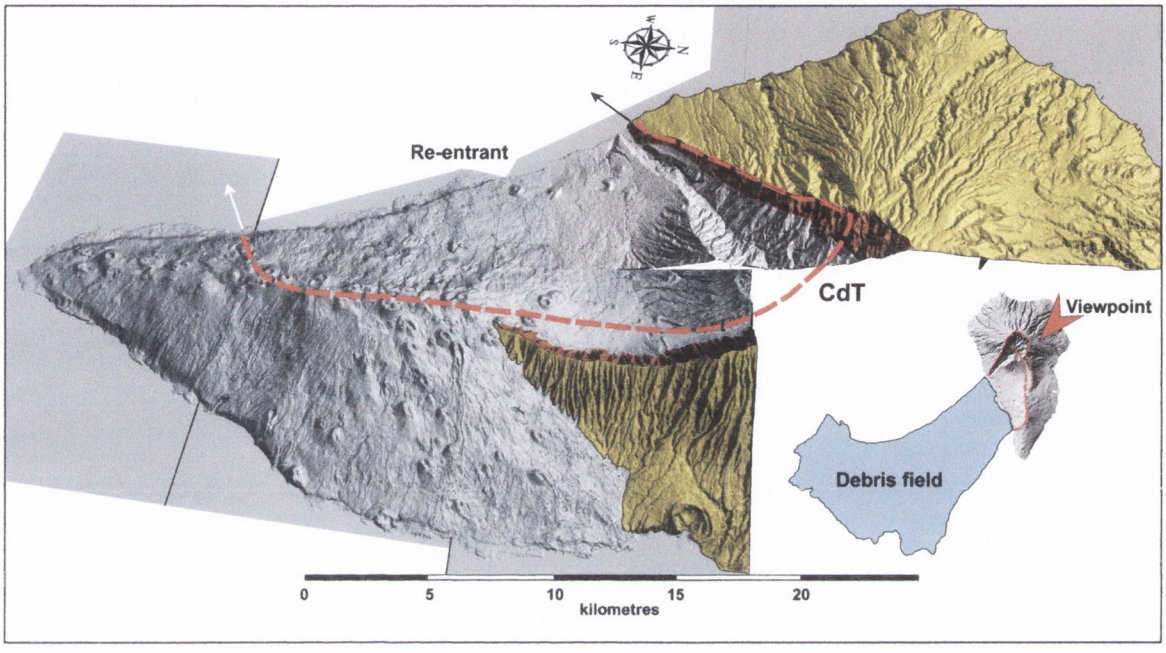


**Fig. 3.2.1.** High oblique shaded relief image looking west upon La Palma showing the total extent of the Cumbre Nueva embayment. The image was generated by the fusion of 5 DEM's (southern and central La Palma) spliced with the two DEM's of northern La Palma. The high RAM requirements for the 3D image-generating process prohibit fusion of all 9 DEM's. Abbreviation CdT – Caldera de Taburiente.

### 3.1.1 Introduction

In this section, rotational slope failure of the composite Taburiente/Cumbre Nueva edifice west flank (Fig. 3.2.1) is modeled using elements of limit equilibrium theory in an attempt to reconcile development parameters (uplift, tilting, superficial detachment, differential loading), with conceptual triggering mechanisms (intrusions, seismicity and climatic effects). The boundary conditions of the Cumbre Nueva embayment, particularly the base of the re-entrant and the total extent of the pre-slide Cumbre Nueva detachment, are difficult to delineate. However, an assumption of circular failure with simplified ground-water conditions and homogenous slope is in agreement with other modelling procedures of giant oceanic island landslides, such La Orotava on Tenerife [*Hurlimann*, 1999], and observations of rock slope failures in general [*Sjöberg*, 1999]. Exhumation of the detachment, the preservance of relict coherent slumps still attached to the onshore escarpments (the amphitheatre bench zone), together with the anomalous sub-detachment relief, compliment the model approach wherein failure was initiated below the footwall, undercutting the detachment by up to 400 m. The increasing depth of undercut towards the headwalls of the Caldera may further indicate that the collapse was initiated beneath the Caldera and Cumbre Nueva rift system such that both of the major re-entrants formed at the exact same moment. Alternatively, the collapse amphitheatre-forming event may represent a retrogressive failure immediatley or shortly after the larger Cumbre Nueva collapse. Hydrothermal alteration in the intrusive core and rift system, with resultant weakening of rock mass, may have pre-conditioned the loss of flank strength as has been inferred for Piton de la Fournaise [*Merle and Lénat*, 2003] and observed from volcanoes in continental environments [e.g., *van Wyk de Vries et al.*, 2000; *Reid et al.*, 2001].

### 3.2.2. Landslide triggering mechanisms

In the engineering science of landslide mechanics a triggering mechanism is, by definition, a stimulus that causes a near-immediate response in the form of a landslide, by rapidly increasing the stresses or by reducing the strength of slope materials [*Wieczorek*, 1996 p 76]. The flank of a volcano becomes susceptible to large scale failure under the right conjunction of geological processes, namely (1) the stress conditions in the pre-slide flank, including the effects of seismic acceleration and groundwater pressure, (2) the geological structure; in particular the presence of large-scale features (fracture belts, normal faults and throughgoing basal detachments), (3) the flank geometry and morphology, and (4) the rock mass strength. The distribution of past landslides, the steepness of rapidly developed slopes, the migration of rift zones and the heterogeneous geo-technical architecture of a volcano are factors that influence the development of unstable flanks and the staging of subsequent failure events [e.g. *Voight and Ellsworth*, 1997; *Masson et al.* 2002]. At a point of critical instability a total loss of equilibrium can occur by a small perturbation relative to the stress levels present in the unstable flank [*Laouafa and Darve*, 2002]. The most commonly recognized landslide triggering mechanisms are described in this section, and examples are provided for which cause and effect relationships have been observed or inferred.

#### 3.2.2.1. Rainfall

The rapid infiltration of rainfall and the subsequent saturation of soil and rock, causes a temporary rise in pore-water pressure and is generally believed to be the mechanism by which many shallow-seated landslides and some open pit failures are generated during rain storms [*Wieczorek*, 1996 p 76; *Sjöberg*, 1999, *Iverson*, 2000]. The loading induced by heavy rainfall perturbs the stress distributions throughout a volcano, causing a pore pressure increase and a reciprocal decrease in the effective normal stress on faults [*Cervelli et al.*, 2002] (Fig. 3.2.2). Basaltic lavas, typical of oceanic island volcanoes, are closely and randomly fractured and thus sustain optimal hydraulic conductivity at rock mass and flank scales. As discussed in Ch. 1.2, the Canary Islands are particularly prone to severe seasonal sub-tropical cyclones and recent preliminary studies indicate a 99% correlation between periods of intense rainfall and micro-seismicity on Tenerife [*Jimenéz and García Fernández*, 2000]. La Palma experiences the most precipitation in the Canary Archipelago, with mean annual precipitation values approaching 100 cm in the upland regions; the wettest months are between October and April [*Graham*, 2003]. Some authors regard periods of intense rainfall as a causal or contributing mechanism for the gigantic landslides of Oahu and Moloka'i, Hawaii [*Yokose*, 2002; *Clague and Moore*, 2002] and Orotava on the north flank of Tenerife [*Hurlimann*, 1999].

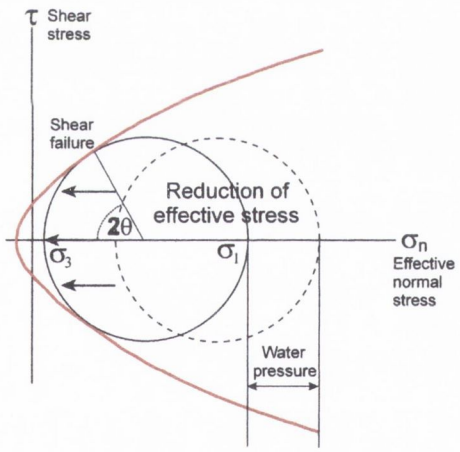


**Fig. 3.2.2.** Mohr diagram illustrating the stress perturbation influenced by fluid pressure increase in permeable rocks.

The timing of a major storm immediately prior to the November 2000 aseismic slip event on the south flank of Kilauea volcano suggests a possible causal relationship between rainfall and aseismic slip on the fault network [*Cervelli et al.*, 2002]. Other examples in which periods of intense rainfall have induced slope failure include the 1997 landslide of Mt. Adams Volcano in Washington State, and the landslide at Casita Volcano (Nicaragua) in 2000, neither of which showed signs of precusory volcano-seismicity [*van Wyk de Vries et al.*, 2000].

### 3.2.2.2 Seismicity and intrusions

Evidence of giant land-sliding is prolific in high relief mountain belts and extensional zones in continental interiors that are subject to seismicity of high magnitude. Examples were cause and effect relationships have been established between earthquakes and landslides in fault-bound mountain belts include the gigantic palaeo-landslide event associated with slip along the recently active (1957) Bogd Fault in the Gobi-Altai region of western Mongolia [*Philip and Ritz*, 1999]. The kilometer-scale escarpments surrounding the Summer Lake Basin (Basin and Range province of south-central Oregon) were produced by giant landslides triggered by ground acceleration associated with the Winter Ridge-Slide Mountain fault which is capable of producing M $\geq$7 seismic events [*Badger and Waters*, 2004].

In contrast to continental deformation zones, volcanoes commonly develop over markedly less protracted time frames, and, depending on their tectonic environment, are subjected to internal and external forces that influence edifice growth, eruption dynamics and flank instability. However, external forces (for example far-field stresses) are probably of lesser influence in flank stability in intra-plate oceanic island environments where insular rift zones often form the key structural control in the construction and destabilization of the flanks. The often simultaneous interaction between tectonics, magmatism and volcanism in rift systems [e.g., *Dauteil et al.*, 2000] is fundamental to understanding the long and short-term behaviour of destabilizing volcano flanks. For instance, ground acceleration during volcano-seismic events can induce slope failure by interrupting or changing the kinetic energy in slope friction planes, thereby increasing the stress on a fault. Examples include the M7.2 Kalapana earthquake in 1975 which occurred on the high relief section of the south flank of Kilauea Volcano [see *Owen et al.*, 2000]. It has been suggested that the seismic events of 1975 may have caused or been amplified by rapid flank displacement (totaling 3.5 m) along a 40 km segment of Kilauea's south coast [*Smith et al.*, 1999]. In similarity, the over-steepening west flank of Cumbre Vieja Volcano is considered to be at the incipient stage of flank instability ever since the flank displacement event that occurred during the 1949 rift eruption [*Carracedo*, 1996; *Day et al.*, 1999]. Another example is the events that took place during the formation of extensional fractures/faults and grabens that accompanied intrusion and subsequent volcanic activity at Mt. Etna during the July-August 2001 eruption [*Billi et al.*, 2003].

Since sheeted intrusions form fundamental building blocks in the construction of oceanic island volcanoes [*Stillman*, 1987; *Walker*, 1992], the possibility that intrusive events and their counterpart seismicity could induce critical flank destabilization must only occur under extraordinary circumstances [e.g., *Iverson*, 1995; *Voight and Elsworth*, 1997]. Empirical assessments of the forces acting within an oceanic island volcano allow theoretical limitations to be placed on the criteria that may facilitate flank failure of such large magnitude. A primary triggering agent that is envisioned by many workers is a seismogenic intrusion itself. The cause and effect relationship involves concurrent development of mechanical/thermal fluid pressures along a basal decollement (existing or hypothetical), and magma-static pressures at the dike interface [*Ellsworth and Voight*, 1995; 1996; *Voight and Elsworth*, 1997; *Elsworth and Day*, 1999]. Understandably, the de-volitilization of high pressure/temperature magmas as they ascends through a rift zone can lead to perturbations in the shear strength of the confining wall rocks especially if pressurized pore water is in abundance (Fig. 3.2.3). The most obvious outcome of such an interaction is phreato-magmatic volcanism if a dike reaches the surface, but this is only a point-source effect. The stress changes bought about by an intrusion decay as a function of distance from the dike [*Elsworth and Voight*, 1997] hence, in order to plausibly create enough stress to trigger flank-scale failure, the minimum requisite dike horizontal length is around one kilometer and the evolving geometry of the failing block is largely controlled by the geometry of the intrusion(s) [*Elsworth and Day*, 1999].

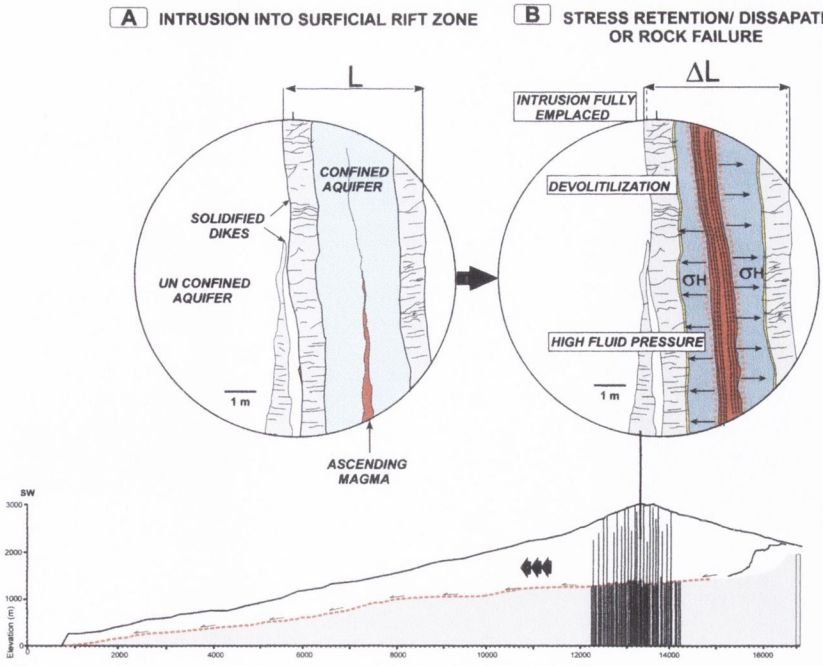


**Fig. 3.2.3.** The intrusion of magma into a dike-bound aquifer in the surficial rift zone and the possible end effects. $\sigma_H$ is the horizontal stress induced by dike injection. $\Delta L$ denotes the amount of reciprocal strain accommodated by the rock mass.

Intrusions within the Taburiente/Cumbre Nueva edifice have a converging geometry on the embayment, in parallel with the arcuate segment and approximately orthogonal to the right lateral fault (Fig. 1.3.12) with their nexus at the dismantled summit region; this marking the volcanoes geometric and structural center.

### 3.2.3. Rock mass strength

Volcano flanks are constructed of poorly consolidated and/or disjointed rocks, often upon older sediments, debris avalanche and pyroclastic deposits that are compressed by the weight of the edifice. Gravitational instability of the flanks is controlled in terms of location, geometry and magnitude by the interplay between the three-dimensional stress field and the spatial distribution of rock mass shear strength [*Reid et al.*, 2001; *Zimbelman et al.*, 2004]. Rock mass can be defined as an aggregate material consisting of both intact rock and associated fractures, bedding planes and major discontinuities, which, over a range of normal and shear stress, behave as Mohr Coulomb materials [*Schultz*, 1996]. The range of shear strength condtions that may be encountered at rock mass scale are illustrated in Fig 3.2.4b. The strength of a disjointed rock mass depends on the properties of the intact rock components and their freedom to slide and rotate under different stress conditions [*Hoek*, 2000]. This freedom is controlled by the geometry of the components as well as the condition of the surfaces separating them. For instance, angular rock pieces with clean, rough discontinuity surfaces will result in a much stronger rock mass than those with weathered and altered materials. Therefore, rock mass composed predominantly of cubically/columnar disjointed basaltic lavas will have a relatively higher shear strength than fissile pyroclastic/epiclastic deposits or hydrothermaly altered rock mass. Rock mass alteration caused by cooling and neutralization of hot acidic fluids that interact with host rocks and ground-waters, is often cited as an important process in the weakening of volcanic constructs both in oceanic and continental environments [e.g., *Voight and Elsworth*, 1997, *Reid et al.*, 2001, *Zimbelman et al.*, 2004]. Stressed and/or altered rock mass, perturbed for example by a seismic shock or an intrusion, can undergo extensional failures such that the Mohr circle approaches the failure envelope in the extensional fracturing field (Fig. 3.2.4a).

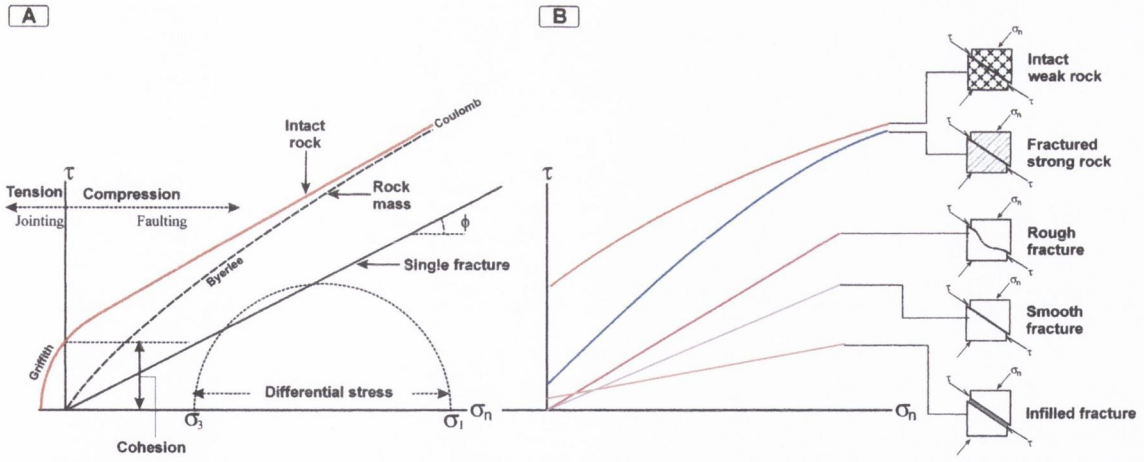


**Fig 3.2.4.** A. Relationship between normal and shear stress showing the curved shear envelope for rock mass strength Modified from *Schultz* [1996]. B. Same relationship on rupture surfaces under different geological conditions. From *Wyllie and Norish* [1996].

From the preceding discussion can it be implied that the geotechnical architecture of a volcano can control the flank disintegration characteristics during slope failure and the subsequent dispersal of failed mass? This is perhaps evident to an extent by the sizes and dispersal patterns of landslide blocks distributed across the volcaniclastic aprons of different archipelagos. Slide blocks sourced from some of the Hawaiian re-entrants (Nuuanu and Wailau) are exceptional for their size and longitudinal alignments* and can be partially pieced together to their pre-slide positions [*Moore and Clague,* 2002; *Yokose*, 2002]. Other slide blocks in the Hawaiian Archipalego, Canary Islands, Tahiti and Reunion are heavily fragmented and preclude re-assembly into a coherent mass [e.g., *Clouard et al.*, 2001; *Masson et al.*, 2002]. Some authors speculate that fragmentation/disruption patterns may reflect the types of rock masses that have failed [*Carracedo et al.*, 1998; *Masson et al.*, 2002]. For example, a higher degree of fragmentation may reflect a signifcant content or structural control by poorly consolidated tephra and epiclastics. However, flow transfomation and fluidization are important processes operative during flank disintegration and mass flow [e.g., *Iverson and Vallance*, 2001; *Legros,* 2002], especially when debris avalanches are projected down narrow chute regions, forcing interactions between slide-blocks [*Michell et al.*, 2002].

On rift-centred volcanoes such as La Palma and El Hierro there is a distinct demarcation in the structure of rock mass - between the flanks that are predominantly built of successions of basanitic lavas, and the rift zones that are constructed by vertically amalgamated pyroclasic deposits and interlaced dikes [e.g., *Hurlimann*, 1999; *White and Schmincke*, 1999]. Rift zones act as a loading apex, building successive, nested scoria cones and adding lavas that spread downslope at a rate that is dependant on their viscosity and the eruption duration. The mass of a volcano can be further conveyed downslope by gravitational spreading of the flanes provided there is a weak layer in the basement [e.g., *Borgia*, 1994]. Rift zones, penetrating the subaerial and submarine section of the Canary Island volcanoes, have clearly acted as the break-away zones for the development of rift-lateral or intra-rift collapses [*Carracedo*, 1994; 1996], for example Orotava [*Hürlimann*, 1999] and El Hierro [*Gee et al.*, 2001]. For La Palma, the demarcation of rock mass structure between rift zones, the adjacent flanks and the Pliocene basement is illustrated in Fig. 3.2.5 with outcrop-scale observations at each of these levels. This is further complimented by a concise rock mass characterization with relative strength ranking in table 3.2.1.

*Tuscoloosa seamount, a fragment of the Koolau submarine pedestal, is 30 km across.

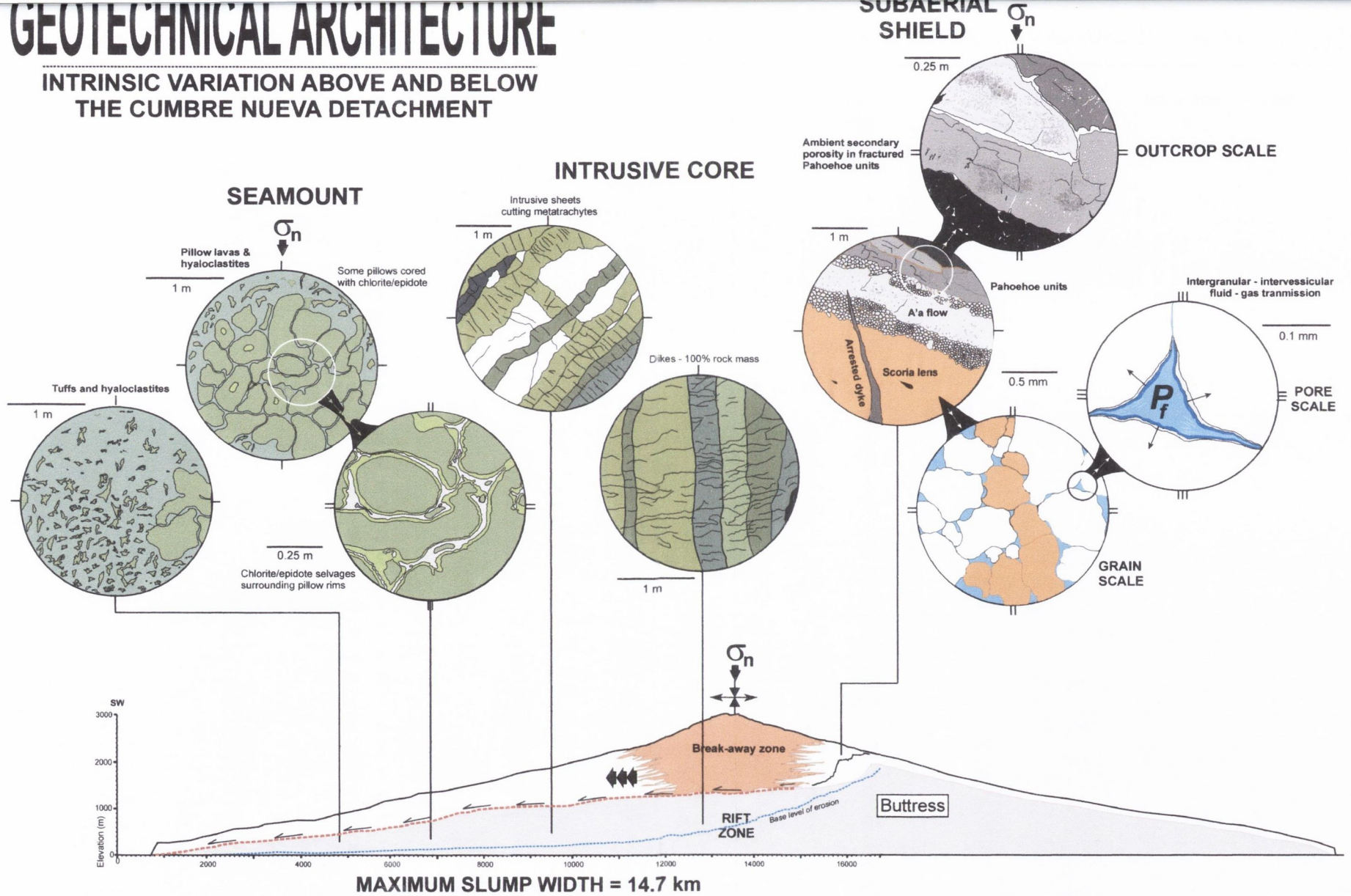


**Fig. 3.2.5.** Elements of the geotechnical architecture of northern La Palma, combining field sketched of the various rock units and their relative positions. The buttress is formed by the dismantled edifice of Ancestral Taburiente and the underlying basement.

# APPROXIMATE GEOTECHNICAL CLASSIFICATION OF COHESIVE VOLCANICLASTICS, LAVAS AND PLUTONICS AMSL

| Strength rank | RM Character | RM Fabric | $\sigma_c$ (MPa) | U W $KN/m^3$ | Cohesion $c = kPa$ | Int: friction $\phi$ | % RM |
|---|---|---|---|---|---|---|---|
| Incompetent | Unconsolidated scoria / ash or *hyaloclastic tuff.* | Multi-dimensional, mod-well sorted grain-grain contact with ambient intergranular porosity (30-40%) | 0.04 – 2 | | | | 15 |
| Incompetent | Clastic successions related to debris avalanche | Open framework, matrix supported multi-dimensional clasts of diverse origins and RM specifications Massive – compacted - unconsolidated | 0.04 – 0.5 | | | | 5 |
| Marginal | Partially consolidated or welded scoria and ash | Graded – laminated with spatter clots and sporadic bombs. | 0.08 – 25 | | | | 10 |
| Marginal | Case hardened scoria / ash | Exposed surface is extremely durable, otherwise concealing a F-M-CG alternately laminated interior | 0.15 – 15 | | | 30 | 5 |
| Resistant | Lithified – silified epiclastics | Open-tight framework of multidimensional clasts suspended in disaggregated matrix. Crystalline RM if silicified. | 10 – 200 | | | | 1 |
| Incompetent | Fault rocks | Progressive deformation to fault gouge – rock flour **(cohesive/incohesive)** Banded – disaggregated fabric subjected to transient pore fluid pressure highs. | 0.01 – 1 | | 190- | 10-15 | 0.5 |
| Incompetent | RM subjected to persistent geothermal activity, fluid flow and argillic alteration | **Variable**:- potential for complete RM disintegration RM may exhibit numerous oxidation fronts, selvages and halos. Potential for resistant core-stones. | 0.1 – 10 | 21 | 300 | 28 | 5(%) |
| Incompetent | A'a auto-breccia | Unsupported carapace agglomerate. | 0.5 – 10 | | | | 5 |
| Marginal/Res. | Entrail – spongy pahoehoe Phonolitic neck / dome | RM may be up to 50% micro-vesicular – gas blisters Concentric vesiculation, intense prismatic or sporadic jointing with master / peripheral lava tubes Phonolitic RM frequently exhibits persistent. transverse fracture sets with significant aperture widths. | 50 – 100 | 23-29 | 100 –300 | 35 | 10 |
| Resistant | Dense basalt (A´a interior, *dike*) | Variably aphyric-megracrystic-holcrystaline with transverse cooling cracks (colonades – entablature) and well developed curvaceous jointing. *Possibility of medial re-injection (dikes).* | 100 – 250 | 24-29 | | 42 | 40 |
| Resistant | Massive basalt (blue rock) Gabbro – syenite. | Macro-vesicular disjointed RM Holcrystalline – cumulate layering. Infrequent jointing | >200 | 27-31 | | 42 | 7.5 |

The abbreviation **U W** denotes unit weight. Abbreviation – Res: resistant

Data compiled and modified from *Hoek and Brey* [1981], *Lockner,* [1995], *Sjöberg* [1999], *Schultz* [1996], *Hurlimann* [1999], *Bos et al.* [2000] and *Reid et al.* [2001].

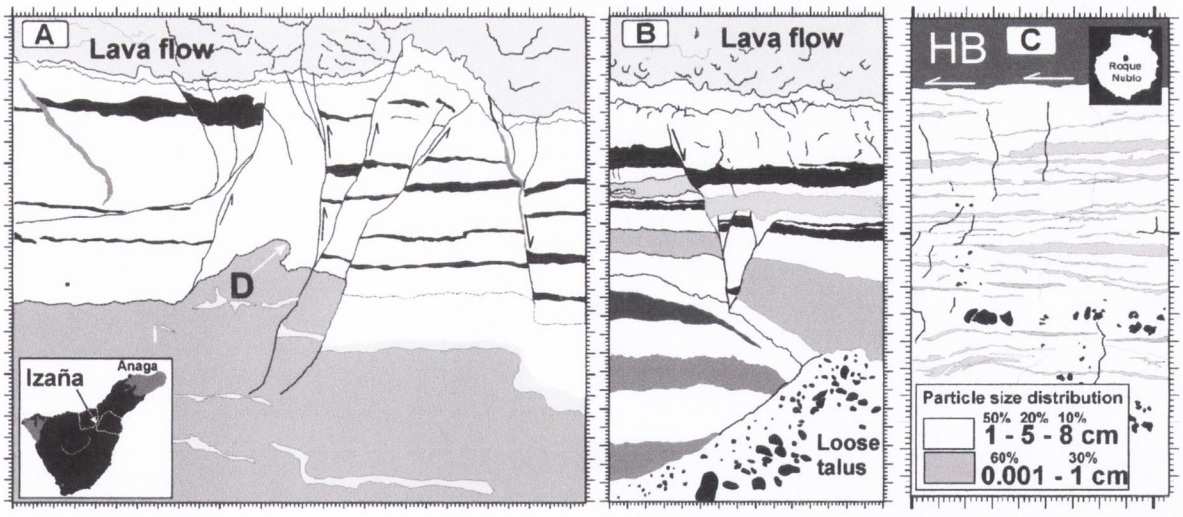


**Fig. 3.2.6.** A and B: Deformation structures visible along a road-cut near Izaña, Tenerife. Diapir (D) producing a small flower structure in fine-bedded purple scoria. B: Oblique normal fault array cutting bedded scoria. C: Shallow-seated fault rocks exposed near Ayacata, Gran Canaria. The abbreviation HB dentotes hangingwall breccias. Scale graduated in centimetres.

In the subaerial section, the rock mass fabrics of the Canarian volcanoes show evidence of deformation and shear at different scales. For example, soft-pyroclast deformation structures are visible along the NE rift zone of Tenerife, skirting the headwall apex of the Orotava/Guimar embayments (Figs 3.2.6a,b). The composite fabric of minor faults and diapiric structures indicates the susceptability of the highly heterogenous rock mass to gravitational deformation even at relatively low confining pressures. At higher confining pressures, for example at the base of the Miocene Anaga edifice (locality of Antaquerra), the volcanic successions are locally traversed by close-spaced, steeply dipping conjugate faults, formed perhaps by settling of the superior units upon the heavily loaded basal successions, although this may also tie in with the picture of edifice spreading being developed for the Miocene of Tenerife [see *Walter et al.* 2001].

At larger scales of observation, more consequential in terms edifice stability (i.e., at flank scale) the Canarian volcanoes are notable particularly for through-going collapse-related fault structures, both incipient and relatively mature. Fig. 3.2.6c shows a layer of fault gouge along the Ayacata Fault Zone on Gran Canaria, a shallow-seated structure exhumed by the Pliocene Roque Nublo deconstructive stage [*Pérez-Torrado*, 1992]. The Roque Nublo fault rocks are between 1.2 and 2.5 m thick and are composed of a clay-rich pale grey-brown to brick red banded gouge and breccia containing dispersed millimeter-scale clasts (microbreccia) and large centimeter-scale angular survivor clasts of dense basalt and phonolite. As indicated by *Day* [1996], the gouge appears to have been quite mobile during deformation; made evident by the localized injection and fluidisation of fine-grained crushed materials into overlying foliated assemblages. The well-developed and laterally continuous foliation is disrupted by variably deformed veinlets and Reidel fractures, which in similarity to the Cumbre Nueva detachment, appear to have developed around areas of asperity removal. In contrast to the Cumbre Nueva fault rocks the particle size distributions have evolved more toward self-similarity (e.g., homogenization of particle size) although how this textural evolution is related to protolith geology, maturation characteristics (i.e., diagenesis) and fault roughness is undetermined. Pseudotachylite-bearing fault rocks have also been identified on the south east flank of El Hierro, backing the aborted/incipient San Andres landslide structure [*Day et al.*, 1997].

### 3.2.3. Pre-slide components of the Cumbre Nueva collapse

The abrupt, high relief landforms generated by flank collapses are the most conspicuous topographic features of oceanic island volcanoes and their submarine flanks. Wide-ranging variations in morphology exist between the landslide escarpments/re-entrants in different archipelagos and between individual volcanic edifices. For instance, in the western Canary Archipelago there are numerous examples of straight-walled or rectilinear collapse escarpments with shallow-seated, seaward-dipping slip planes and headwalls located between 11 and 14 km inland (e.g., Orotava [*Hurlimann*, 1999;] Cumbre Nueva (*Carracedo et al.*, 1999a]). In contrast, the larger flank collapses sourced from the Hawaiian volcanoes, such as Wailau (Moloka'i) and Nuuanu (O'ahu), are deep-seated and the resultant headwall scarps are located offshore [*Clague and Moore*, 2002; *Moore and Clague*, 2002]. These authors suggest that the imposing sea-cliffs remaining onshore are relict listric faults located upslope of the dismantled slide blocks. Present-day active slumps around Hawaii and Maui are assumed to be translated along landward-dipping decollements that interface with sediment layers atop of the oceanic crust [*Borgia and Treves,* 1992*; Lipman et al.*, 2003; *Eakins et al.,* 2003].

The four structural/morphological components of the Cumbre Nueva embayment are illustrated in Fig. 3.2.7. These are (1) the seaward-dipping (to the SW) Cumbre Nueva Detachment that is exposed entirely above sea level along the Hacienda sector, the southern extent and the dip along strike are undetermined, (2) the SW striking right-lateral fault forming the northern limit of the embayment [*Carracedo et al.,* 1999a,b], (3) the arcuate headwall escarpment, the total geometry of which is concealed by Cumbre Vieja while the northern segment has been scalloped by the collapse amphitheatre. (4) The south rim of the embayment, which, as discussed in Ch. 3.1.3.1 is defined by the westward deviation in vent alignments along the Cumbre Vieja rift axis.

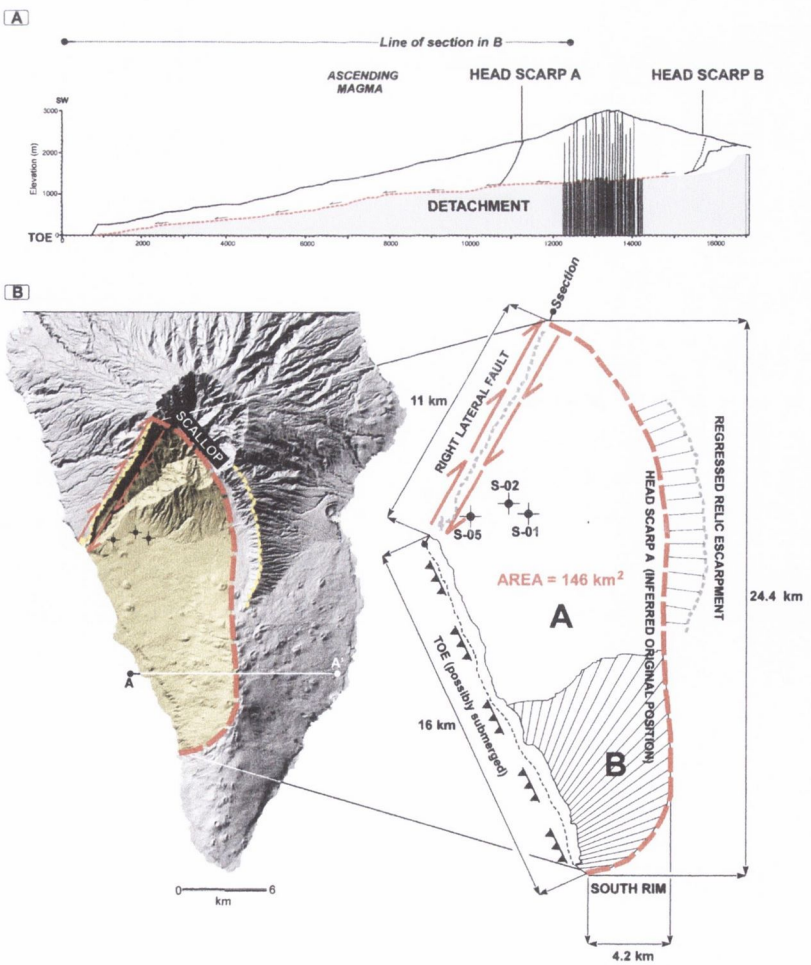


**Fig. 3.2.7.** Structural and morphological components of the Cumbre Nueva embayment. Boreholes are marked S-01, S-02 and S-03. Section A-A' mid flank of Cumbre Vieja is from *Day et al.* [1999]. Region A is the inferred extent of the TCB, the substratum conditions of region B are speculated upon in Fig. 3.2.9.

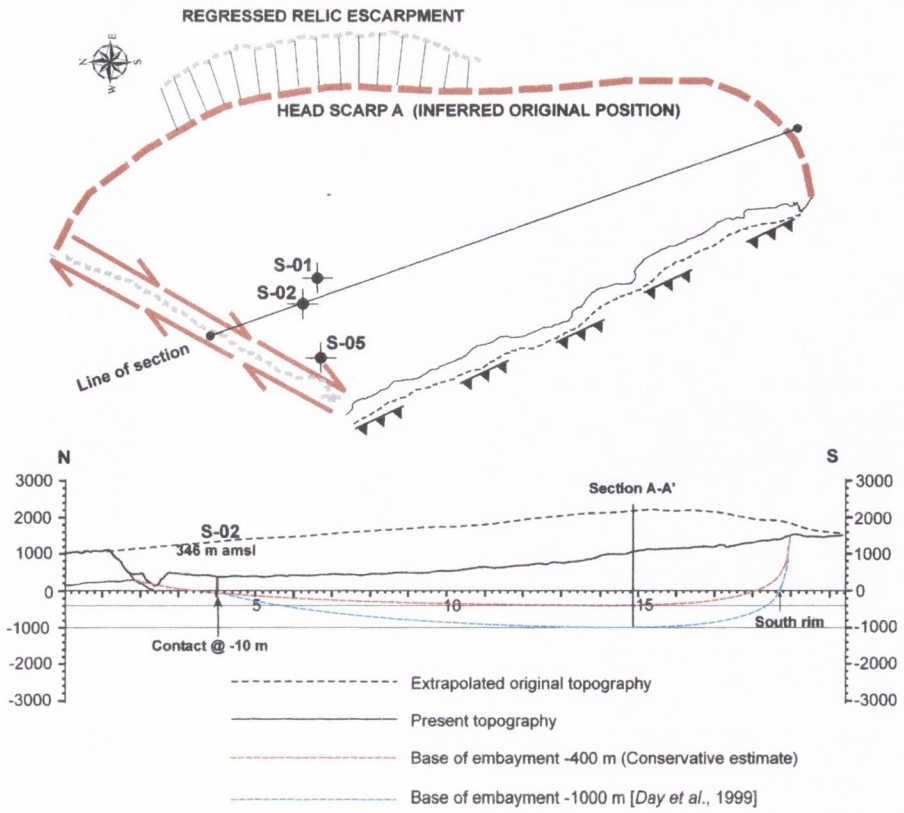


**Fig. 3.2.8.** Plan and interpretative north-south cross-section of the embayment based on borehole data. The contact at –10 m is between embayment filling breccias and subjacent seamount series pillow lavas. Section A-A' is from *Day et al.* [1999].

The paucity of sub-structural data precludes an accurate evaluation of the location and southward continuation of the failure surface. Tunnelling operations beneath the escarpment for the TF-47 highway are largely excavated through subaerial lavas, dikes and TCB-like materials while boreholes, drilled in the vicinity of Los Llanos, allow sub-structural interpretation of the northern part of the embayment only (Fig. 3.2.8). Intact seamount rocks are encountered in borehole S-02 (collar elevation 340 m amsl) at a depth of 10 m (bmsl) [*Carracedo et al.*, 1999a]. Towards the bottom of this and other boreholes nearby are structureless volcaniclastics up to 100 m thick that have been interpreted as embayment-filling breccias derived from the Cumbre Nueva collapse [*Carracedo et al.*, 1999a,b]. *Day et al.* [1999] postulate that the embayment bottoms at around 1 km below sea level (based on their Fig. 13), although there is no bathymetric evidence for an offshore continuation of the embayment [*Urgeles et al.*, 1999]. It is worth mentioning however, that there is no bathymetric data coverage for the littoral zone extending between 1 and 2 km from the coastline (Fig. 3.2.4b). This is an important point to consider since the toe of the developing landslide may have day-lighted within this zone. It is for this reason that the base of the embayment is estimated more conservatively (400 m below sea level) in the present study, allowing the toe region of the re-entrant to be contained geographically within the littoral zone.

Fig 3.2.2 illustrates two distinct instability domains separated in terms of observed and inferred substratum geology. The largest of these (region A in Fig. 3.2.7) was founded upon the TCB, visible from the walls of the enclosing embayment, although the southern limits of TCB subcrop are very difficult to define. A second domain is also inferred (region B), formed by the onlap of Cumbre Nueva onto southern flank of Taburiente at a later stage (post 0.8 Ma as proposed by *Guillou et al.* [2001]). A proviso for the mergence is that the west flank underwent accelerated loading and differential gravitational spreading in the north and central parts, while loading and critical over-steepening occurred in the southern part.

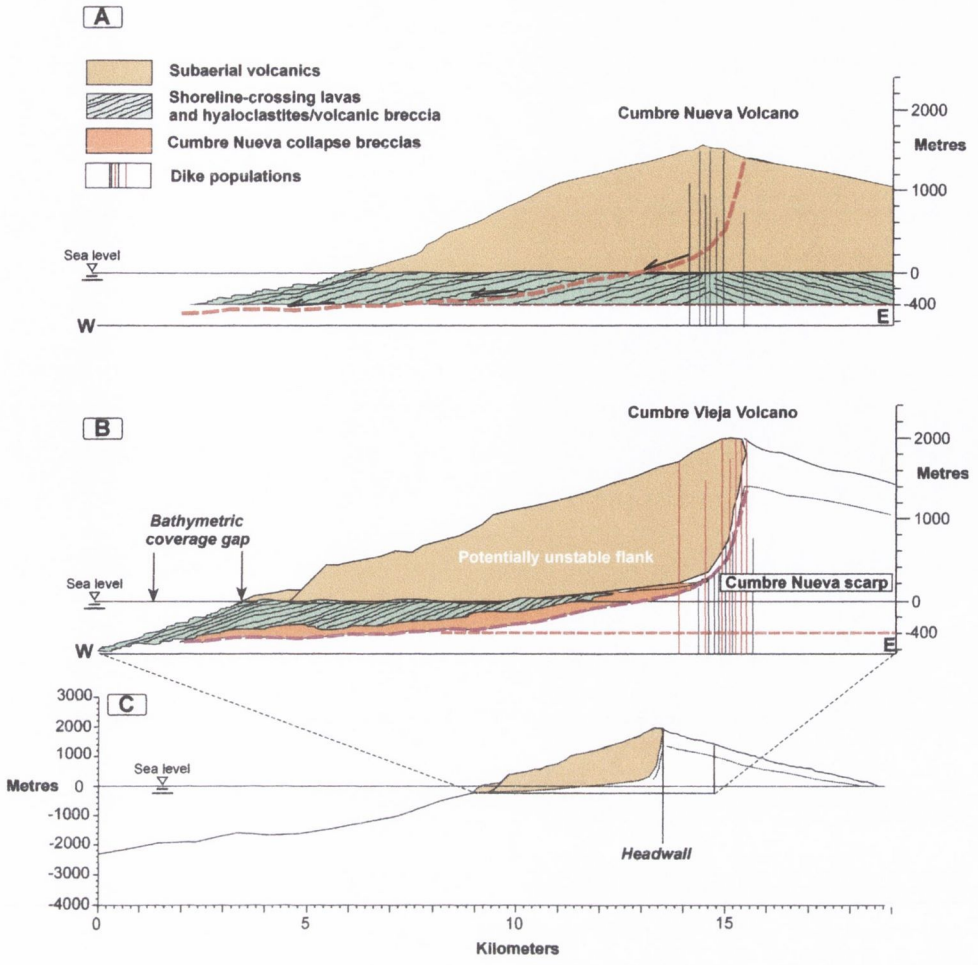


**Fig. 3.2.9.** Cross-section of the western flank of Cumbre Vieja Volcano illustrating A: the inferred topography of Cumbre Nueva Volcano and B, the inferred depth extent of the Cumbre Nueva embayment and superior volcaniclastic successions. Section B is modified from *Day et al.* [1999]. C shows the submarine slopes west of Cumbre Vieja. Submarine slope extracted from Mitchell et al. [2002]

In terms of rock composition and geological structure the littoral zone adjacent to the subaerial shield-building Hawaiian volcanoes consists of poorly consolidated masses of subaerially degassed, shoreline-crossing lavas, pillow lavas and derivative hyaloclastites [e.g., *Lipman et al.*, 2002, *Clague et al.*, 2002]. Voluminous amounts of volcanic sand and breccia accumulate out of the passive and explosive interactions that occur between lavas and the ocean, and from marinel erosion thereafter. The littoral zone forming the western part of Cumbre Vieja consists at its upper bounds (i.e., the subaerial interface) of partially collapsed lava deltas and derivative rock debris and sands which, based on analogies with Kilauea Volcano, are assumed to merge downward and laterally along prograding forsets composed of volcanic breccia, hyaloclastites and subaerial/submarine-derived epiclastics (Fig. 3.2.9). The base of these successions is defined by the Cumbre Nueva landslide unconformity that separates the embayment-filling debris and hyaloclastites (Fig. 3.2.4b see *Day et al.* [1999]) from the older submarine and subaerial-derived volcaniclastic successions, lavas and intrusions forming ancestral Fuencaliente Ridge. Although distant to the littoral zone, core samples recovered during ODP Leg 157 from around volcaniclastic apron of Gran Canaria and Tenerife contained basaltic tuffs, lapillistones, breccias, and turbidites, overlain by trachytes and rhyolites [*Delius et al.*, 1998].

### 3.2.5 Limit equilibrium analysis

The gigantic scale and Quaternary age of the Cumbre Nueva collapse, the lack of detachment-wide correlation, complete envelopment and erosive under-cutting of the embayment floor (i.e., along the course of the Bco. De Las Angustias) together with the lack of geotechnical data on both intact rock and fault rock make it imposible at this stage to back analyse the landslide with the aim of deducing causative factors. Therefore, the discusion that follows reflects only on the choice of stability analysis adopted and the model parameters assumed given the lack of tangible mechanical constraints.

Most existing models of flank-scale instability employ limit equilibrium theory, a technique that is suitable for the analysis of how failure may initiate [e.g. *Ellsworth and Voight*, 1995, 1997; *Iverson*, 1995; *Voight and Ellsworth*, 1997, *Hürlimann*, 1999]. Although it is only an empirical alternative to rigorous geo-mechanical testing, the main benefit of limit equilibrium analysis is its relative simplicity. The limit equilibrium procedure enables a quantitative assessment of the kinematic capacity for flank failure and its use is often justified in civil and mining engineering practices by the positive results they generate and the financial benefits they bring [*Fredlund*, 2003]. When applied to the scale of an oceanic island volcano, limit equilibrium analyses are typically used to gauge the mechanical and thermal effects of dike intrusions upon the hydro-mechanical properties of an inclined decollement [e.g. *Iverson*, 1995; *Ellsworth and Voight*, 1995]. The critical block width (i.e., the width of the instable flank) is controlled by the dike horizontal length, indicating the potentially significant influence of magmastatic pressure on the evolving flank failure [*Ellsworth and Day*, 1999]. Fig. 3.2.10 shows the generic geometric relationships between the force components acting in a hypothetical instability scenario modified for Cumbre Nueva.

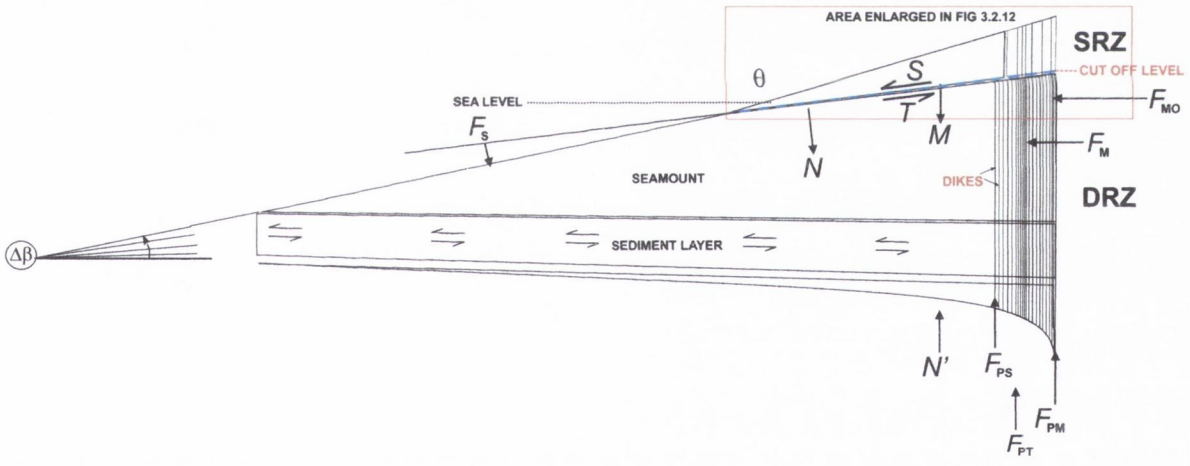


**Fig. 3.2.10.** A limit equilibrium model for the entire volcanic construct of La Palma, modified from *Voight and Ellsworth* [1997]. The forces are as follows:- block weight M, magma force $F_M$, over-pressured magma force $F_{MO}$, static groundwater force $F_{PS}$, seawater pressure $F_S$, and induced pore pressure forces that result from mechanical ($F_{PM}$) and thermal strains ($F_{PT}$). N and its counterforce N′ are effective forces acting normal to the failure surface. The total force driving wedge moment is S and the mobilized resisting force is T. Abbreviations SRZ (20-30% dilation), Surficial rift zone, DRZ – Deep rift zone (100% dilation), Δβ - slope angle change. Basal differential shear (illustrated in the supporting sediment layer) is postulated in order to accomodate dilation of the DRZ and associated thermal/fluid dynamic effects.

The limit of equilibrium is reached when intrinsic and extrinsic forces act in unison to create a critical stress situation that tips the kinematic balance of instability towards collapsing the flank. A parameter that is used to describe this scenario is the non-dimensional scalar termed the 'Factor of Safety' (FOS), defined as the factor by which the shear strength of the slope materials have to be reduced in order to bring the slope to a state of failure [*Laouafa and Darve*, 2002]. The FOS can be summated as

FOS = Σ Resisting forces / Σ driving forces or FOS = Σ (Shear Strength) / Σ (Actuating Shear Stress)

A FOS ≤1 indicates a propensity for failure. The condition of limit equilibrium strictly means that the only admissible factor of safety is 1, at which point the resisting and driving forces (or moments) reach unity [*Sjöberg*, 1999]. The factor of safety is not necessarily a reliable indicator of the probability that a slope will fail or remain stable. This is because the factor of safety analysis utilizes average values of parameters and thus can mask the wider variation (uncertainty) in the values of the different parameters affecting stability [*Laouafa and Darve*, 2002]. A slope can have a factor of safety higher than that of another but still have higher risk of failure, for example an FOS = 1.1 means that the slope strength is only 10% greater than the driving forces.

A failure criterion (usually the Mohr-Coulomb criterion) is used to describe the stress relationships under consideration. A Mohr-Coulomb material is one in which the shear strength of the sliding surface is expressed in terms of the cohesion (c) and the friction angle ($\phi$). When an effective normal stress ($\sigma'$) acts on the failure surface, the shear strenght ($\tau$) that develops is described by the equation

$$\tau = c + \sigma' \tan \phi$$

The Mohr-Coulomb failure criterion may be idealized as a linear envelope touching all Mohr circles that represent critical combinations of principal effective stresses [*Schultz*, 1996; *Hurlimann*, 1999] (Fig. 3.2.4). By converting gravitational forces into stresses acting normal and parallel to the slope, it is possible to define the normal and shear stresses

$$\text{normal stress} \qquad \sigma = \rho\, g\, h \cos \beta$$

$$\text{shear stress} \qquad \tau = \rho\, g\, h \sin \beta$$

By summing the vertical forces and rotational moments acting on each rock column above the potential failure surface, a factor of safety for that surface can be computed [*Reid et al.*, 2000].

The processes causing slope failure involve a continuous series of events and contributing circumstances (e.g., deteriorating structural conditions) [e.g., *Voight and Elsworth*, 1997] that can be represented as a conceptual flow chart in Fig. 3.2.11. The flow chart incorporates elements of the case specific nature of Taburiente Volcano (e.g., uplift, detachment) but most of the parameters are applicable at all scales to volcanic and non-volcanic landslides alike. Sensitivity analysis performed as part of a two and three-dimensional stability study employing limit equilibrium and finite element analysis, implied that the pre-slide integrity of the gigantic Orotava failure on Tenerife was related to slope angles, material properties and hydrological conditions, but these factors alone were insufficient to iniate slope failure. [*Hurlimann*, 1999]. Intrinsic mechanisms related to volcanic activity or volcano-tectonic processes were deemed necessary to create the adverse stress conditions.

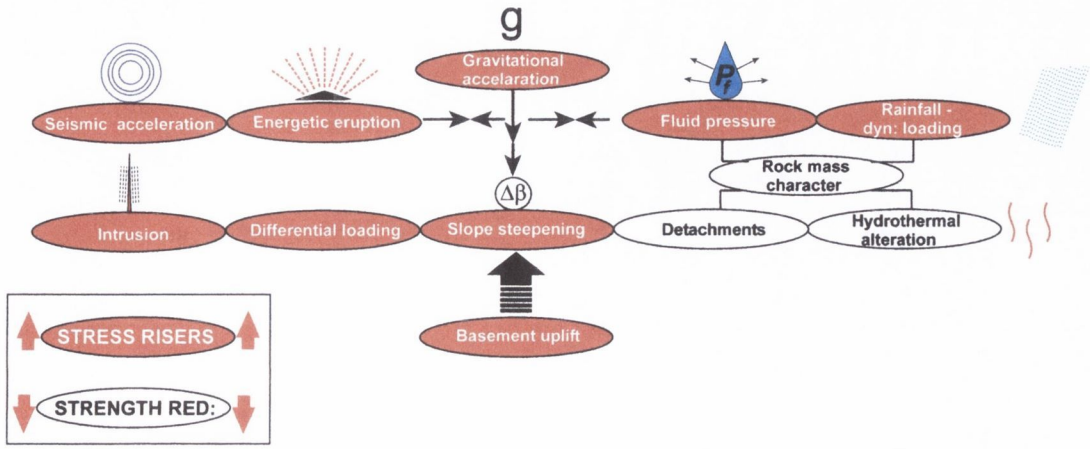


**Fig.3.2.11.** The relationships of force components contributing to flank instability. Abbreviations, dyn: - dynamic, RED:- reducers.

### 3.2.4.1 Location of the critical failure surface

The most important aspect in the design of a limit equilibrium model is determining the location of the failure surface, which has the theoretical lowest factor of safety and the highest probability of failure. The position of the failure surface is often found on a trial and error basis but in some cases it is predicted [*J.J. Walsh*, writ com]. Criteria for the embayment-wide geometry of the Cumbre Nueva-CdT failure surface are lacking, although the relief along the Barranco de Las Angustias, and the source drainage system in the Caldera (Fig. 1.2.5), may facilitate reconstruction of the failure surface at its northern-most and widest extent. The Angustias catchment area has heavily incised the Pliocene basement, producing a heavily serrated topography of canyons separated by steep interfluves, with up to 400 m of relief between the Cumbre Nueva detachment and the interfluve apices (Fig. 3.2.13). The super-position of post-Cumbre Nueva landslide blocks (toreva remnants) upon the interfluve apices is suggestive that the relief is anomalous with respect the regime of fluvial erosion that has been implied for centuries to have shaped the Caldera [e.g., *Lyell*, 1855; *Carracedo et al.*, 2001].

Under the assumption that post-Cumbre Nueva volcanism continued without a significant hiatus (i.e., for the construction of Bejenado stratocone) one may stipulate that volcanism and large scale mass-wasting predominated over gradual fluvial erosion as landform-shaping processes. Age data for the dismantled remains of Bejenado Volcano suggest a rapid constructive stage based on samples obtained from the highest remaining point (Pico Bejenado) and the base of the El Time sedimentary sequence below the southwest flank of the edifice. *Guillou et al.* [2001] estimate an age range, based on cross correlated K-Ar and $^{40}Ar/^{39}Ar$ dating, of between 0.537±0.08 Ma and 0.490±0.06. K-Ar data for geographically similar lava sequences *Hildenbrand et al.* [2003], constrain the constructional period to between 0.501±0.11 Ma and 498+0.08 Ma. However, the toreva remnants, derived from the dismantled north flank of Bejenado [*Roa*, 2003], may hold the key for to the upper age limit of Bejenado, although as yet, no age data exist.

The positions of the toreva remnants perched upon the interfluve apices, seems to indicate emplacement upon a relict topography that was inherited from the Cumbre Nueva deconstructive stage. The toreva remnants display evidence in the form of comminuted basement rocks and striated slip surfaces (the striae are mostly aligned in parallel with the interfluve apices), of motion from areas higher within the collapse amphitheatre [*Roa*, 2003]. These kinematic data further support the hypothesis in Ch.1.2 that the Caldera already existed in order to have accommodated the growth and subsequent partial collapse of Bejenado. These observations suggest that the positions of the toreva remnants, at the canyon apices, are the closest approximation of the base level from which the current amphitheatre drainage system was initiated. It is proposed therefore that the Bejenado failure surface had localized at approximately the same level as the Caldera-forming failure surface. For the latter, the failure surface is listric in geometry and step-shaped inside the Caldera, descending seaward at an angle of around 6° (Fig. 3.2.12). The depth to which it undercuts the detachment increases toward the Caldera but decreases 2 km ahead of the amphitheatre headwalls where it roughly coincides with the detachment. The depth of undercut decreases seaward so that the failure plain again coincides with the toe of the detachment where it daylights offshore. The sudden drop of interfluve topography (point D in Fig. 3.2.12) may be explained by the confluence of the entire amphitheater drainage system at Dos Aguas where a higher flow regime canyon begins (the Bco. de Las Angustias)*. Fig. 3.2.13 illustrates a simple 2D model characterised by a wedge-shaped flank with a constant slope angle with only a minor offshore component for the northern and speculated southern limits of the embayment.

*The flow regime of the Angustias catchment area has been heavily depleted since the construction of galerías in the 18th century

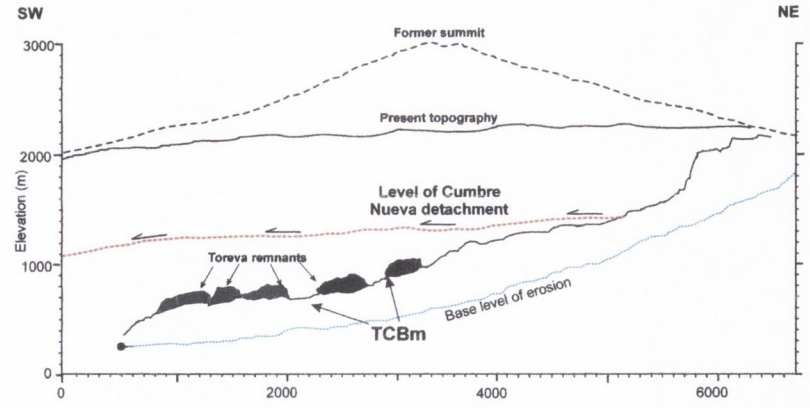


**Fig. 3.2.12.** Scaled topographic sections through the Caldera showing A: the positions of the toreva remnants relative to the detachment surface and B: the extent of anomalous relief and extrapolated level at which failure may have been initiated.

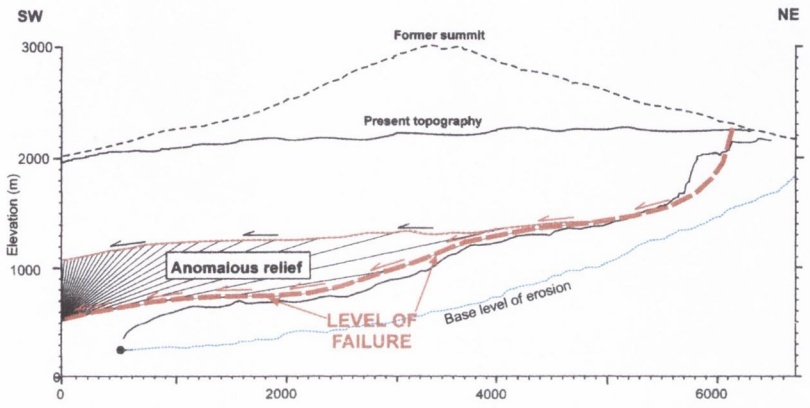


The longitudinal section along the Hacienda sector (below) illustrates the total inferred geometry of the critical failure surface for the northern part of the embayment. Note the sharp drop in relief at point D (Dos Aguas) where the Bco. de Las Angustias begins.

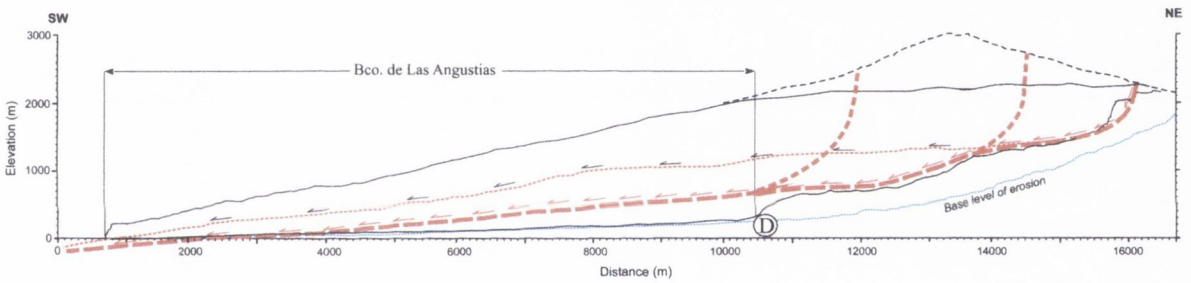


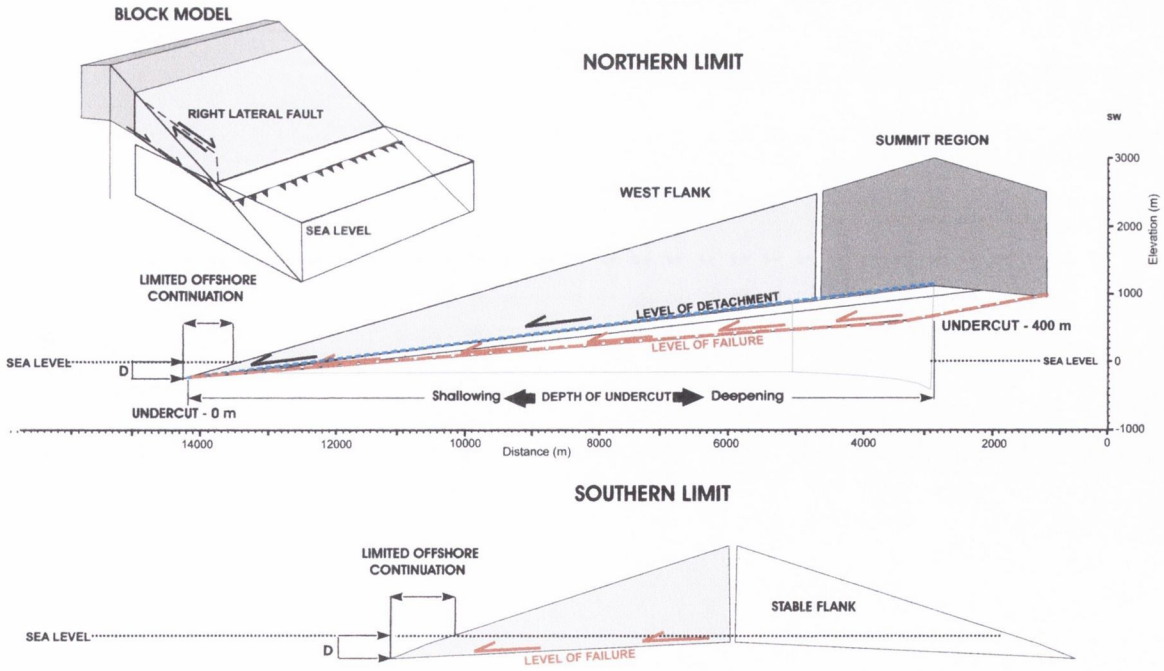


**Fig. 3.2.13**. Limit equilibrium model incorporating undercut for the northern and postulated southern limits of the Cumbre Nueva embayment. The toe of the failure plane daylights offshore, extending a distance D below sea level. The insert block model is a simplified isometric view of the west flank, highlighting the right lateral fault and thrust offshore front.

### 3.2.4.2 A circular failure mechanism for the Cumbre Nueva collapse?

Circular failures are one of the most commonly assumed failure mechanisms for large-scale rock slopes. A circular failure surface approximates the arc of a circle and is not necessarily controlled by pre-existing through-going structural discontinuities [*Sjöberg*, 1999]. Slope movements at the crest of the slope tend to be very steep, whereas movements at the toe tend to be sub-horizontal [*Norish and Wyllie*, 1996]. Rock types that are particularly susceptible to circular failures include those which are partially to completely altered and those which are closely and randomly fractured [*Norish and Wyllie*, 1996]. Currently there is limited knowledge of the failure mechanism involved in the formation of a circular failure surface and what factors effect the 2D shape of the surface [*Sjöberg*, 1999]. In general the shape of a failure surface appears to be primarily controlled by the relationship between material strength parameters and the slope geometry [*Sjöberg*, 1999 and references therein]. Analysis of the Orotava lateral collapse on Tenerife utilized a circular failure mechanism with several low angle failure surfaces interacting at the same instant [*Hurlimann*, 1999]. At Mt. St. Helens a slip surface formed just behind the summit crater and propagated downward with other discrete successive failures, conforming in geometry to a major circular failure [*Glicken*, 1996].

For the Cumbre Nueva/Caldera de Taburiente collapses, two alternate models are possible for the structural and temporal development of slope failures. The first (Fig. 3.2.15a) involves failure initiated along the west flank (1) instantaneously triggering retrogressive collapse of the summit (2). If the summit withstood the SW-directed collapse of the flank, this would have caused the instantaneous redistribution of horizontal stresses around the summit region. The buttressing effect of the bounding ancestral collapse headwalls may have further conditioned the volume of material and direction of failure of the destabilizing summit region, un-butressed to the southwest.

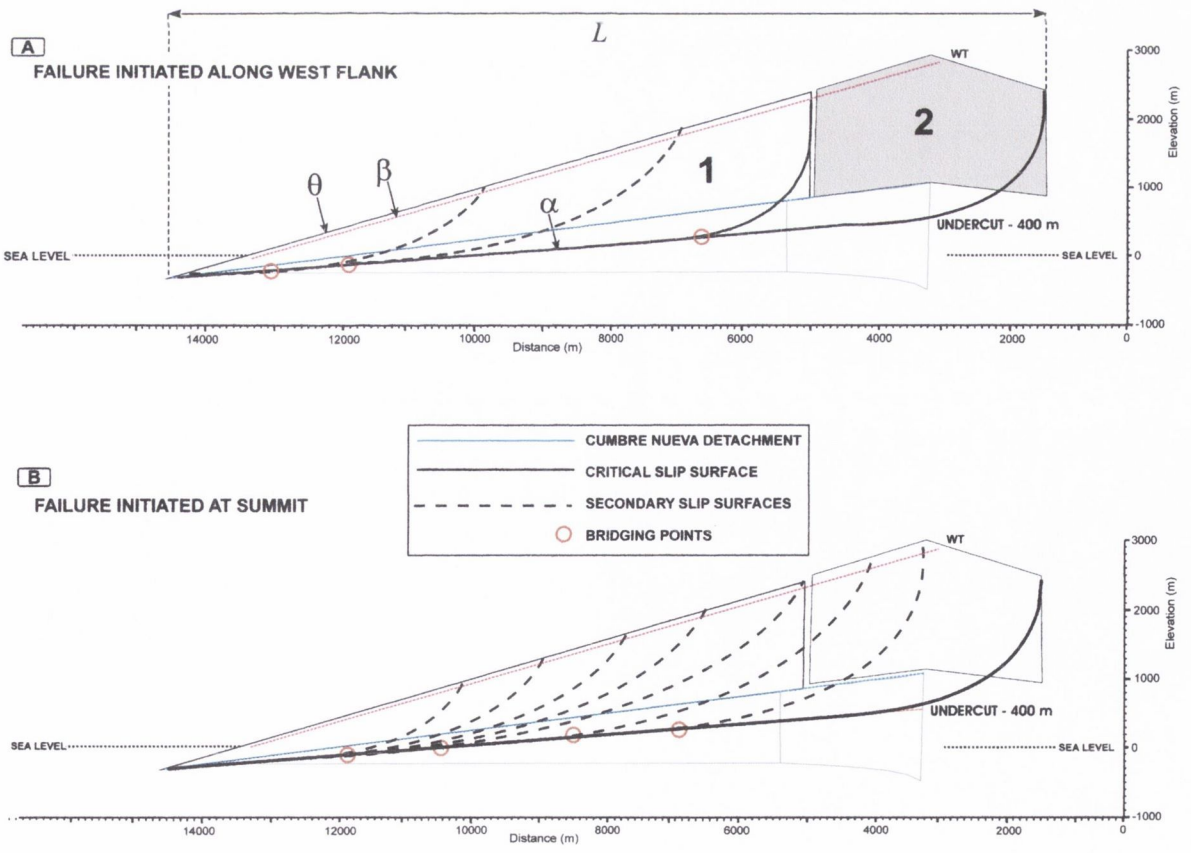


**Fig. 3.2.15**. A: circular failures (with arbitrary circular failure surfaces) initiated along the west flank (1) with a retrogressive collapse (2) of the summit region (formation of the Caldera de Taburiente) B: circular failure initiated beneath the summit region. Abbreviation WT – water table. See table 3.2.2 for abbreviations.

The alternative model (Fig. 3.2 15b) implicates contemporaneous rotational failure of the summit region and west flank based on the increasing depth of undercut towards the headwalls of the Caldera. For both models the shape of the water table, which depends on the slope geometry, is relatively close to the ground surface. The critical circular failure surface terminates within the 2 km wide littoral zone and starts close to the top of the volcanic edifice. The envisioned failure mechanism is relatively complex, involving rotational failure through intact rock displaying strength anistropies (e.g., sills), and structurally weak materials, especially the poorly consolidated La Cumbrecita group volcaniclastics derived from the seamount stages of edifice instability.

Each failure consists of a number of discrete circular failure surfaces intersecting each other at bridging points. The basic model parameters are listed in table 3.2.1. The slide block can be divided into a number of vertical fictitous slices, a measure that is neccessary since the problem is statistically indeterminate [*Sjöberg*, 1999]. Theoreitically, if a condition of equilibrium is satisfied for each and every slice it is also satisfied for the entire mass. The forces acting on a slice are shown in Fig. 3.2.16.

Table 3.2.2. Geometric paramters for circular failure

| Geometric parameter | symbol | magnitude |
|---|---|---|
| slope angle | $\theta$ | 11° |
| angle of water table | $\beta$ | 10° |
| angle of slip surface | $\alpha$ | 3-50° |
| total model length | L | 14000 m |

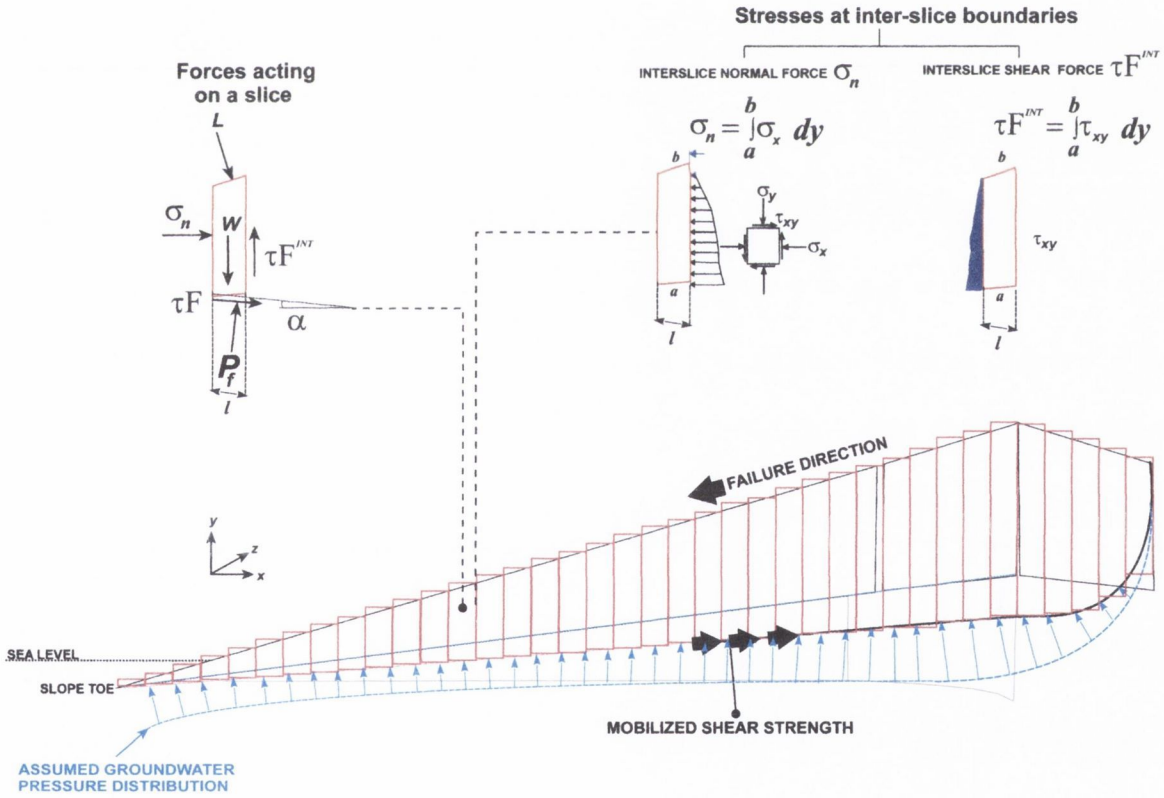


**Fig. 3.2.16.** Method of slices illustating the resolutuon of forces acting on a slice and its boundaries.

Table 3.2.3. Parameters effecting stability of each slice

| | |
|---|---|
| L = external load | $\alpha$ = base of slice inclination |
| W = weight of slice | $\tau F_a$ = shear force along failure surface |
| $\sigma_n$ = effective normal force between slices | $\tau F^{INT}$ = shear force between slices |
| Pf = pore fluid pressure | |

### 3.2.5. The collapse initiator

It is important to understand how giant landslides are foreshadowed and initiated in oceanic island/island arc environments due to the extreme tsunami hazards such events can pose. Geodetic surveys, structural investigations and remote sensed data are increasingly employed to monitor flank displacement patterns and fault slip rates on active volcanoes where gravity-driven lateral displacements are relatively rapid [e.g., *Cervelli et al.*, 2002; *Billi et al.*, 2003]. Where slope failures have occurred (partially or completely), site investigations have been used to assess pre-slide kinematics and force components of the collapse systems [e.g., *Day et al.*, 1997; *Hurlimann*, 1999]. It is understood that all of the islands in the Canary Archipelago have undergone multiple flank collapses throughout their evolutionary period [e.g., *Guillou et al.*, 1998; *Krastel et al.*, 2001; *Walter and Schmincke*, 2002]; those of La Palma and neighbouring El Hierro are the most recent [*Carracedo et al.,* 1999a]. Existing models on how the Cumbre Nueva collapse may have developed are summarized as follows.

1: Intense volcanic activity and overgrowth of the Cumbre Nueva rift zone [*Carracedo et al.,* 1999a]

2: Gravitational spreading of the SW flank and resultant rift zone activity [*Walter and Troll*, 2003]

3: Uplift, steepening and faulting of the basement [*Hildenbrand et al.*, 2003]

Although there is no direct field evidence for the exact cause of the collapse, the discovery of the Cumbre Nueva detachment is a direct indication that the southwest and eastern flanks were mobile for an as yet undetermined but perhaps geologically significant period of time up until the moment of slope failure. An important factor in the location and geometry of the collapse may have been the shifting distributions of flank mass during gravitational spreading, since the location, magnitude and direction of loads acting on a volcano slope play a significant role in stabilizing or destabilizing it [e.g., *Hurlimann*, 1999; *Tibaldi*, 2001]. For Taburiente, significant loading occurred within the confines of the ancestral collapse caldera, detaching the nascent Taburiente edifice perhaps before its lavas over-spilled the ancestral caldera walls. The southwest and eastern flanks are assumed to have detached from the basement as the edifice was still undergoing significant volumetric increase, augmented by the onlap/amalgamation of Cumbre Nueva which added more mass to the spreading flanks. As down-slope detachment and uplift ensued, the evolving fault zone steepened, thus increasing the gravitational potential for failure, with the detachment itself a suitable (kinematic) candidate for failure.

However, the exhumation of the Cumbre Nueva detachment and the extent of sub-detachment relief, seem to implicate failure at a deeper level. If this assumption is correct, then, in order to have survived the cataclysmic collapse, the relic sliver of pre-slide flank still attached to the headwall highs (the Hacienda sector), must have been partitioned from the southwest spreading slump sector by the right lateral fault at an early stage in the development of the slump. The Hacienda sector fronts the buttressing headwalls of the ancestral collapse structure and must therefore be coupled to it. Consequently, it is implied that attempts to model the collapse should take into consideration mechanisms that invoke failure of intact or structurally anisotropic rocks, for instance by high fluid pressure and/or temperature conditions in the DRZ/intrusive core. High fluid pressures can be generated by dehydration reactions in metamorphic rocks [*Scholz*, 1990] particularly adjacent to degassing intrusive complexes [*Sibson*, 1996]. The notion that high fluid pressures, perhaps related to the geothermal system of Taburiente, were involved in the kinematics of the detachment and the lateral collapse itself - is intuitively appealing although difficult to demonstrate at this stage.

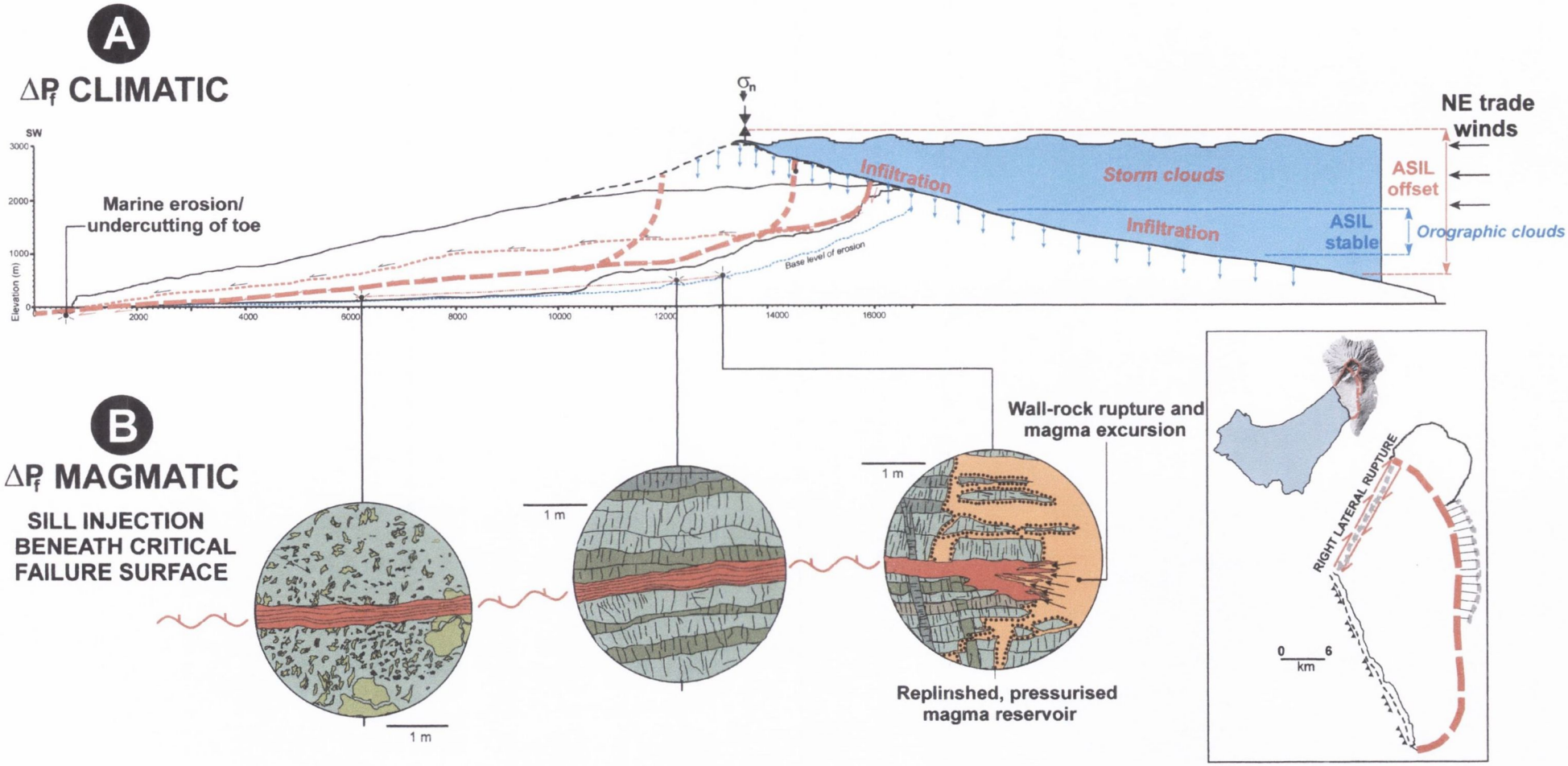


**Fig. 3.2.17.** Hypothetical scenarios for the Cumbre Nueva lateral collapse related to fluid pressure changes ($\Delta P_f$) in the basement. The abbreviation ASIL denotes the atmospheric subsidence inversion layer that is influenced by the Azores High Pressure System.

Fluid pressure excess is, in general, a major actualistic and theoretical component of fault/flank stability in volcanic and non-volcanic environments [e.g., *Hsü*, 1969, *Sibson*, 1996, 2000; *Iverson*, 1995; *Day*, 1996; *Elsworth and Voight*, 1995, 1996, *Voight and Elsworth*, 1997] (Fig. 3.2.2.), particularly on stratovolcanoes where acid-sulfate hydrothermal systems and associated rock mass alteration zones are well developed [e.g., *van Wyk de Vries et al.*, 2000; *Reid et al.*, 2001; *Reid*, 2004; *Zimbelman et al.*, 2004]. On La Palma, hydrothermal alteration assemblages (e.g., *Schiffman and Staudigel* [1994]) and dike-bound deposits of poorly consolidated La Cumbrecita Group volcaniclastics are ubiquitous throughout the intrusive core. Pipe-like zones of hydrothermal mineralization, mainly zeolite-cemented breccia along the margins of dikes in the seamount, are interpreted by *Ellsworth and Day* [1999] to have formed by explosive brecciation driven by the thermal fluid pressurization mechanism they advocate. Centimetre-scale veinlets and stockworks exposed sporadically within the intrusive core (Ch. 1.2) may also attest to high P/T water-rock interactions. Altered, fractured rocks, particularly planar intrusions*, occur sporadically throughout the intrusive core, with pervasive to selective replacement by advanced argillic ranks. In essence, there is field evidence at least that the rockmass within the basement was prone to large scale failure under the right conjunction of circumstances and events. The critical failure surface may have exploited structural anisotropies such as horizontal/sub-horizontal sill injection planes, again bearing in mind that sills occur as stacks up to 600 m thick, particularly around the periphery of the intrusive core and as isolated sheets within the cumulate plutonics and dike plexus.

Fig. 3.2.17 illustrates two hypothetical triggering mechanisms, climatic and magmatic, each one involving the development of high fluid pressures in the geothermal basement. Scenario A invokes intense rainfall brought about by a seasonal disturbance in the atmospheric subsidence inversion layer, giving rise to a major meteroic water infiltration event such that the rate of water influx exceeded the rate of water escape. A pore water pressure excess ($\Delta P_f$ CLIMATIC) is generated within the subaerial carapace and in the high-level geothermal system, resulting in cooperative failure of the basement rocks and overlying shield volcanics. In scenario B, a replenished and overpressured high-level magma reservoir undergoes wall-rock rupture, injecting a sill sub-level to the critical failure surface, thereby inducing a transient fluid pressure high ($\Delta P_f$ MAGMATIC) in excess of the compressive strength of the enclosing wall rocks along the length of the intrusion. Emplacements of sills, judging by the significant stratigraphic extent of sheeted sill stacks, are interpreted to have been an integral process in the uplift of La Palma and thus relatively high frequency events. When failure was initiated the shifting loads instantaneously overstressed the overlying flank, removing the kinematic restraints by basal and right lateral detachments. The key question remains whether the flank was gravitationally stable (e.g., FOS >2) or marginally stable (FOS >1) without the impetus of dynamic loading (rainfall ± intrusion ± seismic shock)? Future studies using more advanced modeling concepts and techniques may further our understanding of the dynamics of the Cumbre Nueva collapse and its relevance to other oceanic island volcanoes.

*Holocrystaline dikes (dunite, oceanite) are particularly altered.

# Conclusions and Contributions

This study reveals new data pertaining to the structural evolution of La Palma, specifically the mechanisms and/or features associated with the chain of subaerial landslides which dramatically changed the shape of the volcanoes during the Quaternary. The thesis presents a detailed evaluation of the two volcano-tectonic units located at the break in slope between the subaerial shield (Taburiente Volcano) and the uplifted Pliocene basement, neither of which have been the subject of previous academic study. It is proposed that two new unit names should be added to the stratigraphic nomenclature of the island. These are:-

***1. The Cumbre Nueva detachment***

***2. The Tenerra Collapse Breccia (TCB)***

Accordingly, a revised stratigraphic nomenclature is presented (Fig. 4.3) in order to take account of these important tectonic units. Fig 4.3 illustrates schematic stratigraphic sections of the island/seamount from three localities, north to south.

- ***The Cumbre Nueva detachment*** is a fault zone exposed discontinuously over a strike length of nearly 10 km along a 5° to 17°, northeast to southwest-striking slope. It is tabular in geometry and is composed of asymmetrically zoned and predominantly incohesive assemblages of fault gouge and breccia, typically 3 m in total thickness. The striated fault surface displays a convoluted topography of asperities; emulated by the overthrust hangingwalls.
    - The fault zone is qualitatively differentiated into two zones; first, a region of clay-rich granular banded gouge, 'the fault core', where the protolith is obliterated. Below this is a 'damage zone' composed of heavily brecciated and oxidized rock that merges with altered but otherwise undeformed host rocks composed of seamount series extrusives, sheeted intrusions and ancestral TCB-type volcaniclastics. Large subrounded, embayed and slightly fractured clasts of protolith are held in suspension within the fine and coarse granular assemblages. These are referred to as survivor clasts, having resisted dissaggregation during distributed granular flow.
    - The fault rock mass is typically pale chloritic green although it is often heavily infiltrated by dark brown, dark blue, green and pale purple colour-banded-alteration-zones. The colour bands have sharp inter-band margins and are often enriched with cohesive, scaly clay minerals. The present study has not determined the relevance of these minerals with respect to the diagenetic or post-kinematic evolution of the fault zone or if fluids were unequivocally involved in the fault zones' evolution although this is considered likely considering the close spatial relationship between the fault zone and the geothermal intrusive core.
    - At its upper bounds the fault zone consists of a narrow (10 to 30 cm thick) Euclidean layer of ultra-fine grained (UFG) fault rock (or ultra-cataclasite), below which are other discrete anatomizing seams of UFG gouge that roughly parallel the bulk northeast to southwest sense of shear. Most of the shear is interpreted to have been concentrated in these fine-grained materials
    - The fault zone is transected by arrays of Riedel fractures and P shears (the latter occasionally form the hangingwall boundary) and subordinate yet strike-persistent Y-slip surfaces. P shears that occasionally step into the hangingwall would appear to do so in order to mechanically erode asperities.

- A unique characteristic that appears to distinguish the Cumbre Nueva Detachment from thrust faults in continental settings, is the increasing abundance (towards the northeast) of dikes in varying states of deformation.
- No distinctive relationship has been determined between fault zone thickness (*T*) and net displacement (*D*) along it. Provisional estimates based on scaling laws suggest a possible lower limit of displacement in the order of 300 m assuming a *D/T* ratio of 1:100. The extent of comminuted fault rock (up to 3 m thick) comprising the fault core, further supports a significant displacement history.

- ***The Tenerra Collapse Breccia (or TCB)*** is a 50 to 350 m thick hangingwall sequence of well-consolidated to locally silicified volcaniclastic deposits that overly the Cumbre Nueva detachment. One of the most conspicuous features of this unit is the abundance of juvenile pyroclastic matrix – often comprising around 30%vol of the rock mass. The TCB accumulated during the explosive lateral collapse and collapse embayment-forming events of Ancestral Taburiente at around 1.2 Ma. The TCB is differentiated on the basis of the distribution of its constituent blocks, clasts and matrix into a layered and a chaotic facies, the significance of this difference is unresolved.
  - Laterally persistent scoria horizons (at least three have been identified), form an integral part of the TCB. These 'ash members', are composed of altered-yellow scoria rich phreato-magmatic deposits, up to 20 m in thickness, strata-bound between identical successions of TCB volcaniclastics.
  - Fold structures (chevron and polyclinal), flame-like diapirs and shear bands within the ash members are interpreted to have formed by ignimbrite-like rheomorphism during the aggradation and down-slope hot-state mass transfer of the TCB during what is referred to as the La Farola eruption.
  - Structurally and lithologically identical volcaniclastic units (referred to as TCBm) are exposed from the steep canyon walls inside the Caldera de Taburiente, often separated from the TCB by the Cumbre Nueva detachment. These are interpreted as an integral component of the ancestral collapse breccia, the distinction being the appearance of metasomatic mineralization due to burial within the re-developing intrusive core/geothermal system of Taburiente Volcano. The TCBm is interpreted to represent part of the ancestral collapse breccia that filled a depo-centre created by rapid downsag of the central portion of the basement along an array of fault zones.
  - Over-thrusting of the TCB, is related to the process of post-collapse substratum expulsion generated in response to horizontal stress re-distributions subsequent to the Cumbre Nueva/Caldera de Taburiente collapses. Lithostatic unloading of the volcanic edifice by the collapse(s) caused the TCB to extrude out towards the low pressure areas beneath the escarpments that survived the cataclysm. The overthrust surfaces define the day-lighting toes of major intra-Caldera and intra-embayment slumps, causing the ongoing deterioration of the escarpments. Substratum expulsion is characterized by overthrusting, the development of tension fractures parallel to overthrust surfaces, and eventual collapse and spall of the TCB. The spall blocks are gravity-fed down-slope forming the voluminous boulder train deposits below the escarpments.

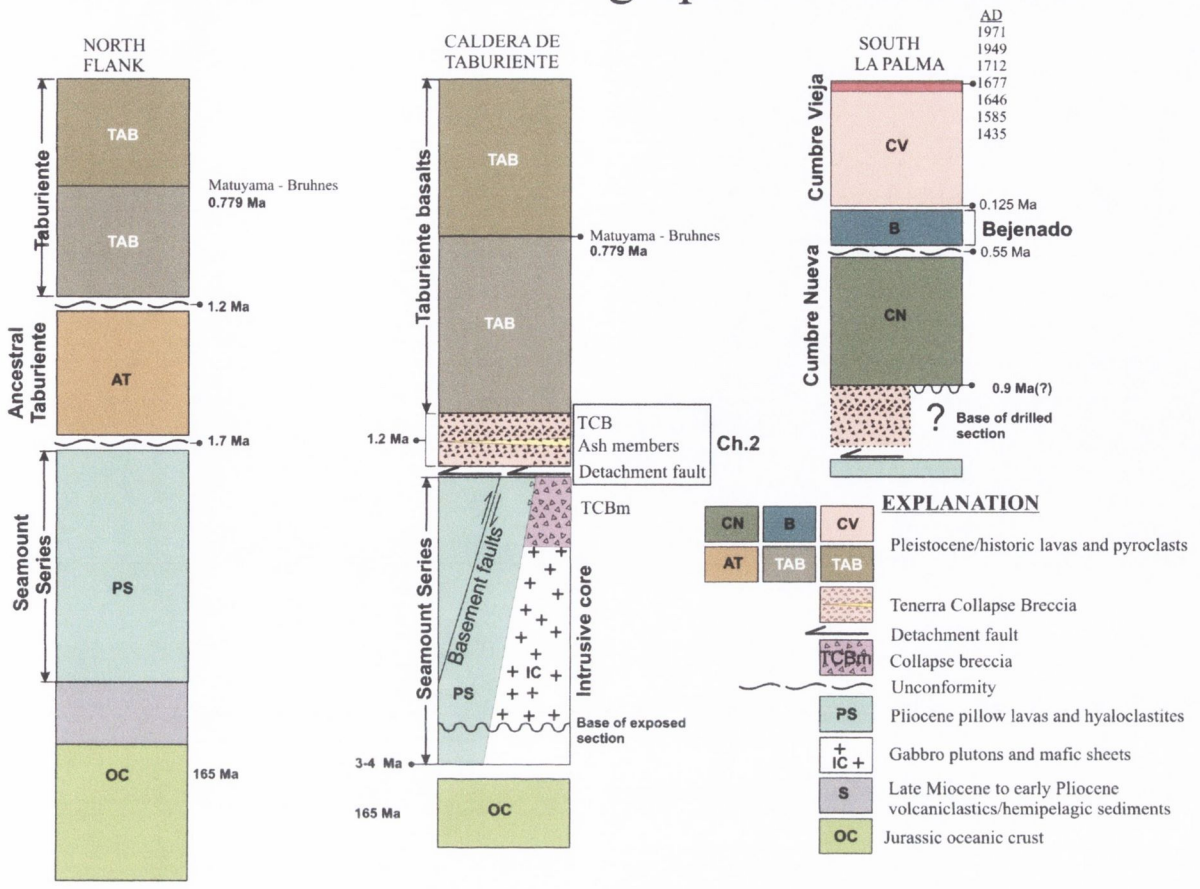


Fig. 4.1. Revised stratigraphic nomenclature of La Palma, taking account of the TCB (and its constituent ash members) and the Cumbre Nueva detachment.
Abbreviations in explanation as follows: CN – Cumbre Nueva, B – Bejenado, CV Cumbre Vieja, AT – Ancestral Taburiente, TAB – Taburiente (note magnetic polarity change) [see *Guillou et al.*, 2001], TCBm – Tenerra Collapse Breccia (mid Caldera), IC – intrusive core, S – submarine sediment, OC – oceanic crust.

- ***Rift zone volcanism, an inherited trait?***

  In terms of the structural controls that governed the directional growth of intrusions, Taburiente Volcano was constructed along an array of diffuse (or divergent) multiaxial rift zones. These rift zones, forming the northern part of the edifice, extended to the east, the northeast and a more diffuse rift striking northwest. A coherent rift zone, topographically similar to present-day Cumbre Vieja, developed in the south, overlapping and increasing the volume of Taburiente. No succinct explanation is tenable for the disparate modes of rift zone evolution or their exact temporal evolution. It is possible that lithostatic unloading and gravitational stresses imposed by the southward flank collapse (s) of Ancestral Taburiente, together with flexural stress perturbations in the upper mantle had some bearing on the evolution of the rift systems, but vital constraints (e.g., from bathymetric, structural, seismic constraints) are necessary to understand the spatial and temporal evolution of the rift system.

  However, in contrast to contemporary interpretations (that the rift zones formed late in the evolutionary history of La Palma) it is argued that they should be a facet of the submarine stage of the volcanoes evolution, inherited from and uplifted with the Pliocene seamount. This is in agreement with the recent concepts and observational data on how oceanic volcanoes develop from nascent seamounts to large subaerial shields. The Cumbre Nueva rift zone, which overlapped the south flank of Taburiente, was destroyed during the lateral collapse at around 0.55 Ma. Although existing radiometric and palaeomagmetic data provide important structural/stratigraphic constraints e.g., [*Guillou et al.*, 2001], it is difficult to determine if a rift zone(s) existed during the development of the Ancestral Taburiente.

- ***Flank failure geometries, past and future***

  During the cataclysmic flank collapses of La Palma, the geometries, directions or failure and volumes of edifice removed have been partially or completely controlled by structures in the basement (e.g., fault zones, weak substrates) and/or by the topography of underlying (ancestral) collapse embayments. Fig. 4.1 illustrates the spatial overlap of sector instabilities, and how each landslide event is associated with its predecessor embayment. It also shows the potential limits of future ruptures on the western flank of Cumbre Vieja

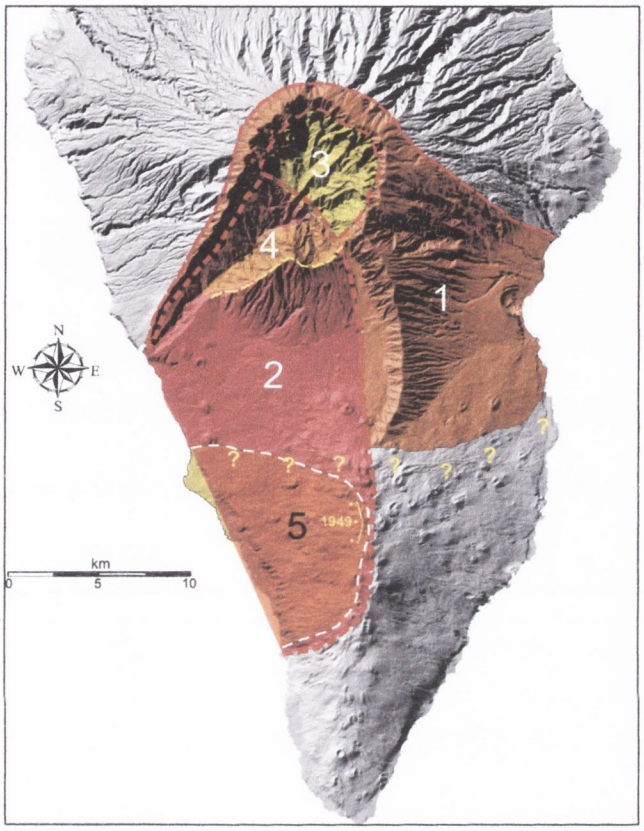


**Fig. 4.2.** Composite map of La Palma illustrating the relative overlay of landslide dimensions and their source regions through time. Questions marks denote the uncertainty of the limits of the collapse(s) of Ancestral Taburiente. The location of the 1949 flank rupture event is shown.

1. Ancestral Taburiente,
2. Cumbre Nueva.
3. Caldera de Taburiente,
4. Benejado.
5. Incipient instability sector developing on Cumbre Vieja.

  - Gravitational spreading of the southwest flank of Taburiente (2:- the slump sector) and the amalgamated Cumbre Nueva edifice, was initially spatially restricted within the confines of the Ancestral Taburiente collapse structure.
  - Accelerated loading of the slump sector during the growth of the Cumbre Nueva rift zone lead to the southward propagation of sector instability. Cataclysmic collapse of the slump is correlated with a lobate debris avalanche deposit, spread over an area of 1160 km² around the submarine slopes off western La Palma.

Since the failure of the slump sector, the morphology of the resultant Cumbre Nueva escarpment has been substantially modified by post-collapse volcanism, fluvial erosion, residual gravitational spreading and associated piecemeal collapses, partially dismantling or overprinting its primitive form. However, the form of the southern segment of the scarp, which has been enveloped by Cumbre Vieja Volcano, is still reconcilable from the distribution of vents along the axis of the active rift zone. As illustrated in Fig 4.2., the size and shape of the potentially unstable sector developing on the west flank [e.g., *Carracedo*, 1994, *Day et al.*, 1999], should reflect certain morphometeric elements of the antecedent landslide structures. Furthermore, the size of the potentially unstable sector should follow a reduced volume pattern, since the bulk of Cumbre Vieja Volcano is contained within the spatial confines of the larger Cumbre Nueva embayment.

***Bejenado Volcano – collapse and toreva emplacement***

The rapid construction of a post-shield intra-collapse stratocone (Bejenado Volcano) climaxed with the collapse of its northern flank inside the Caldera de Taburiente and the northern part of the adjoining Cumbre Nueva escarpment. Toreva remnants (intact blocks of the former flank) from the collapse event are preserved along the canyon interfluves inside the Caldera [*Roa*, 2003]. Although no radiometric data exist (at the time of writing in late 2004) to unequivocally correlate the toreva remnants to the heavily dismantled north flank of Bejenado, there are several substantiating criteria with which to make direct and indirect correlations. These are.

(1) the proximity of the toreva remnants to the relic Bejenado escarpments,
(2) The pyroclastic dominated stratigraphy of the toreva remnants, together with the fossil fumarole deposits is suggestive of a central vent region or summit source.
(3) the available radiometric data constrain the age of the Cumbre Nueva collapse (0.55 Ma [*Guillou et al.*, 2001]), and hence the synchronous formation of the Caldera (as put forth by this study). Therefore, the positions of the toreva remnants - shunted within the earlier-formed Caldera - are an indication of their later relative age, thus excluding an origin from the cataclysmic Caldera-forming event itself.
(4) The existence and position of the El Time sediments, together with the fact that they have been deeply dissected by the Barranco de las Angustias, lends support to the hypothesis that a relatively rapid cycle of erosion and deposition had occurred subsequent to a spatially confined flank collapse event.

***Development; from seamount to shield***

The temporal development of both the subaerial and submarine stages of La Palma is represented in the context of a geological/magnetic polarity time scale in Fig. 4.3. The bulk (>95%) of the present volume of La Palma is formed by its submarine foundations, the Pliocene seamount, from where palaeontological criteria and radiometric data (from sheeted intrusions) indicate a maximum possible age of between 3 and 4 Ma [*Staudigel and Schmincke*, 1984; *Staudigel et al.*, 1986]. Since the earliest dated subaerial volcanics are >1.7 Ma [*Guillou et al.*, 2001], it would appear that the bulk of the volume of erupted submarine material and intrusions had accumulated over a time period more or less equivalent to the subaerial growth stage. Taking account of the subaerial volumes of material that were removed by recurrent giant landslides (perhaps <10%), then the underlying volume of 90% accumulated at a near order of magnitude rate relative to the subaerial stage.

Upon shoaling, the Ancestral Taburiente edifice built itself up over the uplifting submarine foundations which had succumbed to at least one identifiable sector collapse represented by La Cumbrecita group volcaniclastics. This (late Pliocene!) submarine sector collapse may have delayed the event of incipient shoaling for a significant period of time despite uplift. Moreover, it is probable that the submarine volume of La Palma accumulated at a relatively steady state, with growth towards shoaling compromised by recurrent gigantic submarine sector collapses of equivalent or greater scale to those which later affected the subaerial volcanoes.

The gap in radiometric age data between the termination of volcanism on northern La Palma (Taburiente/Bejenado) and the onset of the Cumbre Vieja stage, reflects the limits of sampling the earliest Cumbre Vieja lavas. The gap makes the apparent hiatus in volcanic activity incongruous in the scheme of relatively continuous volcanism presented in Fig 4.3. The apparent hiatus is perhaps an artefact of the present limitations in radiometric dating key stratigraphic units and unified structural geologic control. It is possible however that volcanism in this period of the geological evolution of the Canary Islands had been focused on the construction of El Hierro [*Carracedo et al.*, 1999b]. For certain there is much scope for further studies to constrain the structural and volcanological evolution of La Palma, particularly the timing of the Cumbre Nueva detachment and its role in the development of the namesake cataclysmic landslide.

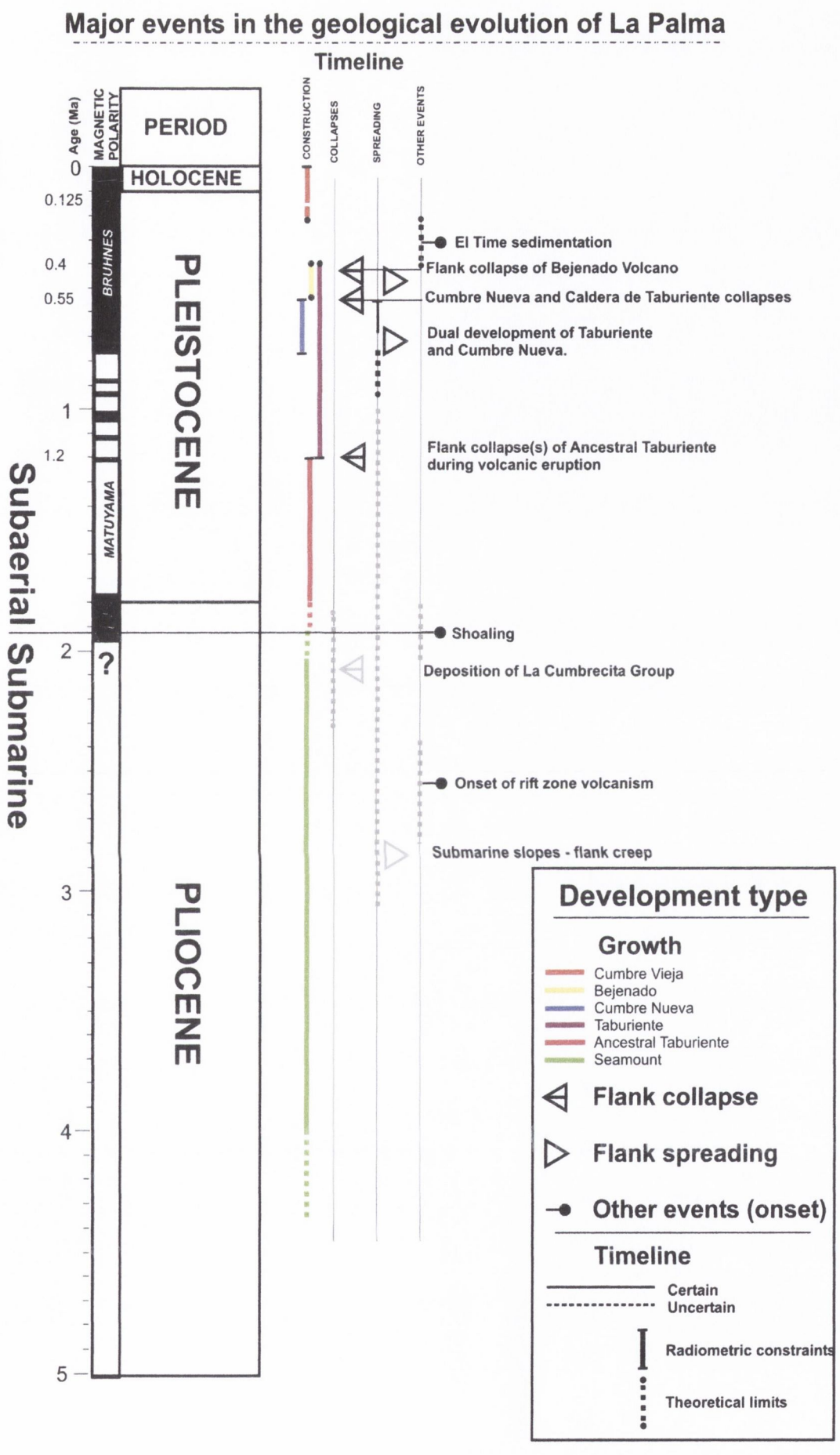


Fig. 4.3. Event chronology spanning the construction of the Pliocene seamount to the present stage of Cumbre Vieja rift zone volcanism. Grey stippled timeline and events reflect the high temporal uncertainty particularly in relation to the most voluminous Pliocene seamount stage. Magnetic polarities for the Pleistocene are from *Guillou et al.* [2001].

Available online at www.sciencedirect.com
SCIENCE DIRECT
Journal of volcanology and geothermal research
ELSEVIER
Journal of Volcanology and Geothermal Research 125 (2003) 191–214
www.elsevier.com/locate/jvolgeores

# Nature and origin of toreva remnants and volcaniclastics from La Palma, Canary Islands

Karl Roa *

*Department of Geology, Trinity College, Dublin 2, Ireland*

Received 4 April 2002; accepted 4 February 2003

**Abstract**

New data pertaining to the origin of volcaniclastic fan delta deposits (the El Time group) and previously unreported toreva remnants (intact landslide blocks) are presented in terms of their relationships with the Quaternary flank destruction of Bejenado volcano on La Palma, Canary Islands. Bejenado volcano is the heavily dismantled relic of a stratocone which developed at the confluence of the Cumbre Nueva embayment and the Caldera de Taburiente collapse amphitheatre. Both of these giant landslide structures formed at around 0.55 Ma after ~0.2 Ma of gravitational spreading on the western and eastern flanks of the Taburiente–Cumbre Nueva shield volcanic complex. Evidence is presented on the basis of stratigraphic, photogeologic and Geographic Information System studies that both the toreva remnants and the El Time group can be related to the sequential collapses of the north flank and summit region of Bejenado inside the Caldera de Taburiente and the northernmost part of the adjoining Cumbre Nueva embayment. The collapses probably occurred between 0.44 and 0.4 Ma and they involved a volume of around 5 $km^3$. The toreva remnants display a deformed volcanic architecture, traversed by discontinuities which developed during impact and post-collapse dislocation during slip. They are composed of layer-differentiated scoria with ancillary ankaramite and basanite–tephrite lavas and occasional dikes. They rest upon a thin veneer of sheared volcaniclastic deposits in relative proximity to the disfigured north flank of Bejenado. The collapse event(s) is distinguished by its extremely low mobility due to the deceleration of the debris avalanche mass within the confines of the Caldera de Taburiente. The high friction coefficient ($H/L = 0.22$) reflects this topographic factor. Reworking of the avalanche matrix gave rise to the accumulation and offshore progradation of the fan delta deposits at the SW base of Bejenado. Contemporaneous fluvial sediments, sourced by the retrogressive erosion of the pre-Bejenado collapse scarps, were fed into the subaerial confines of the Cumbre Nueva embayment. Piecemeal scarp failure and the extrusion of substratum from beneath the scarps also contributed to the sediment budget. The fluvial sedimentation rates subsequently increased with the onset of Cumbre Vieja volcanism prior to 0.125 Ma. These processes have contributed to the development of the flat-floored submarine channels which extend onto the volcaniclastic apron west of La Palma. These new data give a fresh insight into the role of epiclastic processes, landsliding and volcanism in the morphology and sediment mass balance of an oceanic island volcano system.
© 2003 Elsevier Science B.V. All rights reserved.

*Keywords:* Toreva remnants; giant landslides; volcaniclastics; Bejenado volcano; Caldera de Taburiente; La Palma

* Fax: +353-1-671-1199.
*E-mail address:* karlroa@hotmail.com (K. Roa).

0377-0273/03/$ – see front matter © 2003 Elsevier Science B.V. All rights reserved.
doi:10.1016/S0377-0273(03)00069-6

## 1. Introduction

### 1.1. Objectives and methods

This paper describes the structure and significance of the large landslide blocks (toreva remnants) which occupy the central part of the Caldera de Taburiente – the giant amphitheatre-shaped depression which forms the morphological centre of northern La Palma. It also examines the role of epiclastic processes in the reworking of a coeval debris avalanche deposit which is now shunted along the lower course of the ravine which drains the Caldera de Taburiente into the Atlantic – the Barranco de Las Angustias. The objective of this study is to elucidate the origin of the toreva remnants and the 370-m-thick El Time volcaniclastic fan (pronounced El Teemay) by assessing the structural and temporal relationships between the formation of the Caldera de Taburiente with the growth and collapse(s) of Bejenado stratovolcano. The palaeogeographic reconstruction is based on the inferred relationship between the toreva remnants and the El Time volcaniclastics, and how these deposits relate to the sequential collapses of the north flank and summit of Bejenado inside the Caldera de Taburiente and the northern part of the adjoining Cumbre Nueva embayment. This interpretation is based on: (1) the heavily disfigured structure of the remaining part of the stratocone; (2) the extrapolated amount of missing mass ($\sim 5$ km$^3$); (3) the disposition and structure of the toreva remnants; and (4) the predominance of a 'debris flow' facies architecture amongst the El Time deposits. These new data highlight the importance of epiclastic processes which concentrate towards the degradation of collapsed volcanic terrain. This work also introduces a new chapter to the geology of La Palma following the discovery of subaerial decollement zones on Taburiente volcano (Roa, 2003). The contribution of substratum deformation, as interpreted from Taburiente, is here considered as an important process which influenced the instability of Bejenado. It is proposed therefore that the sequential collapses of Bejenado developed by the loading of volcaniclastic materials forming the edifice substratum.

The field studies underpinning this paper encompassed detailed stratigraphic profiling, supplemented by the mapping of panoramic and aerial photographs. Geographic Information System (GIS) data that were sourced from the *Spanish Geological Map* were used for the analysis of dimensional data and in the calculation of volumes (see Appendix for methods used).

### 1.2. Geological setting

La Palma is the northwesternmost of the seven hot spot-related volcanic islands of the Canary archipelago (Dañobeitia and Canales, 2000). Shield-building subaerial volcanism on La Palma began prior to 1.6 Ma with the construction of Ancestral Taburiente (Staudigel et al., 1986) and was punctuated by gigantic subaerial flank collapses at around 1.2 Ma and 0.55 Ma (Ancochea et al., 1994; Guillou et al., 2001) (Fig. 1). These were the Ancestral Taburiente and Cumbre Nueva/Caldera de Taburiente collapses, respectively. The Cumbre Nueva/Caldera de Taburiente instability sectors developed upon the debris and pyroclasts which had accumulated within the spatial confines of the Ancestral Taburiente collapse structures (Roa, 2003).

The final stage of volcanic activity on northern La Palma, between 0.55 and 0.4 Ma, was centred on the construction of Bejenado volcano while residual rift zone volcanism continued on the flanks of the Taburiente volcano (Guillou et al., 2001). Neo-volcanism on La Palma is focused along the N–S elongate, rift-centred edifice of Cumbre Vieja which forms the southern part of the island. The most recent eruption from Cumbre Vieja was in 1971 whilst the oldest dated rocks are 0.125 Ma (Carracedo et al., 1999a), yet this only reflects the limit of sampling. It is possible that Cumbre Vieja lavas are older than 0.2 Ma.

Bejenado volcano is a relic alkali basalt stratocone that was constructed upon the unroofed foundations of the earlier Taburiente shield. It is located in the northern part of the giant Cumbre Nueva embayment which is open to the west and restricted by its bounding headwalls to the east (Figs. 1 and 2). The embayment formed by the

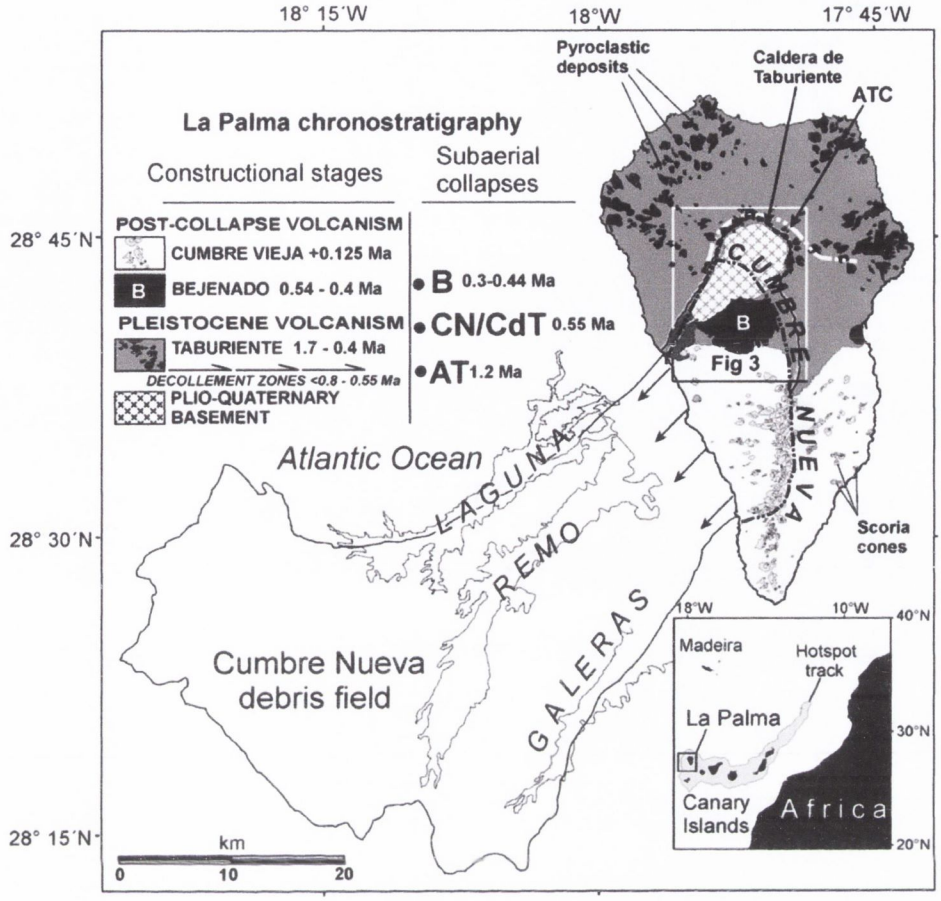


Fig. 1. Geological map of La Palma showing the relationship between the submarine Cumbre Nueva debris avalanche deposit and its onshore embayment. Abbreviations: B, Bejenado; CN, Cumbre Nueva; CdT, Caldera de Taburiente; AT, Ancestral Taburiente. ATC is the subcrop pattern of the Ancestral Taburiente collapse structure. Modified from Ancochea et al. (1994) and Carracedo et al. (2001). Laguna, Remo and Galeras are the flat-floored submarine channels defined and labelled 'C, D and E' by Urgeles et al. (1999).

lateral collapse of a 240-km$^3$ subaerial slump sector which developed by the gravitational spreading of the west flank of the Taburiente–Cumbre Nueva volcanic complex (Roa, 2003). Cataclysmic slope failure of the west flank was succeeded by the collapse of the summit of Taburiente, leading to the formation of the Caldera de Taburiente which scalloped the northern end of the embayment. Throughout this work reference is made to the Caldera de Taburiente as it is known locally on La Palma as 'the Caldera' or from a genetic perspective as the 'collapse amphitheatre'. The 6.5-km-diameter Caldera has sub-vertical headwalls (700–950 m high) that enclose an area of some 24 km$^2$ and opens into the larger Cumbre Nueva embayment to the SW (Fig. 2a,b).

### 1.3. Terminology

The emplacement of 'toreva blocks', former segments of a volcanic edifice, is a frequent if not ubiquitous phase of giant landsliding (i.e. mass movements $>1$ km$^3$) on volcanoes. Torevas in varying states of dislocation, shattering and erosion are well described (e.g. slump block, block facies, megablock) from Mount Shasta, California (Crandell, 1989), Roque Nublo, Gran Canaria (Mehl and Schmincke, 1999), Socompa, Chile (Wadge et al., 1995), Mount St. Helens, Washing-

ton (Glicken, 1996), Shiveluch, Kamchatka (Belousov et al., 1999), Parinacota, Chile (Clavero et al., 2002), and from a range of volcanoes in the Trans-Mexican volcanic belt (Capra et al., 2002). The degrees of back rotation, emplacement distances, and dispersal patterns concurrent with peak landslide momentum, indicate considerable variation in the mobility and disruption of torevas during the formation of developing collapse structures and associated debris avalanche deposits. Landslides initiated on oceanic volcanoes show the widest dispersal patterns and block coherence, with kilometre-sized blocks dispersed over great distances along the submarine pedestals and onto the mergent abyssal plains (e.g. Urgeles et al., 1999; Watts and Masson, 2001).

In subaerial environments there is no size discrimination of torevas provided that significant volcanic architecture is identifiable. For example, Glicken (1996) adapted a range of block facies sizes from centimetres to a few hundred meters wide for the debris avalanche deposit of Mount St. Helens.

Mehl and Schmincke (1999) define megablocks (>100 m) and debris avalanche blocks (0.25–100 m) amongst many other components and facies of the Pliocene Roque Nublo debris avalanche deposit. These authors emphasize that the smallest and largest components are members of a continuous series characterised by the progressive fracturing, disaggregation, and mixing that occurs during flow transformations that are inherent in large-scale debris avalanching. The Bejenado toreva remnants are not differentiated as such, since erosive processes have degraded their primary form, hence the initial dimensions and volumes are difficult to extrapolate.

The term 'volcaniclastics' encompasses all volcanic particles regardless of their mode of origin (Fisher and Schmincke, 1984). Epiclastics can be specifically related to the deposits produced by the erosion of volcanic rock (see Cas and Wright, 1987) although juvenile fragments can be important (accidental) components. Nonetheless, the emphasis of epiclastic processes, as implied here, lies in the remobilisation of mass wasted or eroded volcanic materials. Agglomerate generally encompasses lithologically homogenous, primary volcanic particles (bombs, lapilli, spatter) that may or may not be fused together during deposition. The term can also be applied to the carapace fragments produced during the bodily disintegration of active lavas and it is synonymous with autobreccia.

## 2. Previous studies

### 2.1. The Caldera de Taburiente

The long-standing view that the eponymous Caldera de Taburiente had formed as a result of erosive processes (e.g. Lyell, 1855; Middlemost, 1970) was first refuted by Ancochea et al. (1994). These authors realised that the erosional form of the Caldera is second only to landslide activity. In spite of this, the hypothesis of a fluvially enlarged 'erosion caldera', initiated by the Cumbre Nueva collapse is still argued by Carracedo (1994) and Carracedo et al. (1999a,b, 2001). According to this hypothesis, the Caldera developed by the erosional retreat of the Cumbre Nueva escarpment along a lineament reflected now by the Barranco de Las Angustias. However, there are four major inconsistencies in this hypothesis which are irreconcilable from a structural, climatological and temporal perspective. Firstly, the Caldera has developed within the structural confines of the pre-existing collapse structure of ancestral Taburiente which is exposed only in water capture tunnels that penetrate the interior stratigraphy of northern La Palma (Coello, 1987; Ancochea et al., 1994). As the latter authors suggest the structure of this ancestral caldera (AT in Fig. 1) has controlled the collapse amphitheatre-shaped morphology and location of the Caldera de Taburiente.

Secondly, at the base of the Caldera and the Cumbre Nueva escarpments are major decollement zones exposed in pristine section. The hanging wall consists of a 100–300-m-thick ductile deformed volcaniclastic unit, here named the Tenerra Collapse Breccia (TCB), which contains an important component of interbedded juvenile pyroclasts that contributed to the TCB's in situ solidification (Roa, 2003).

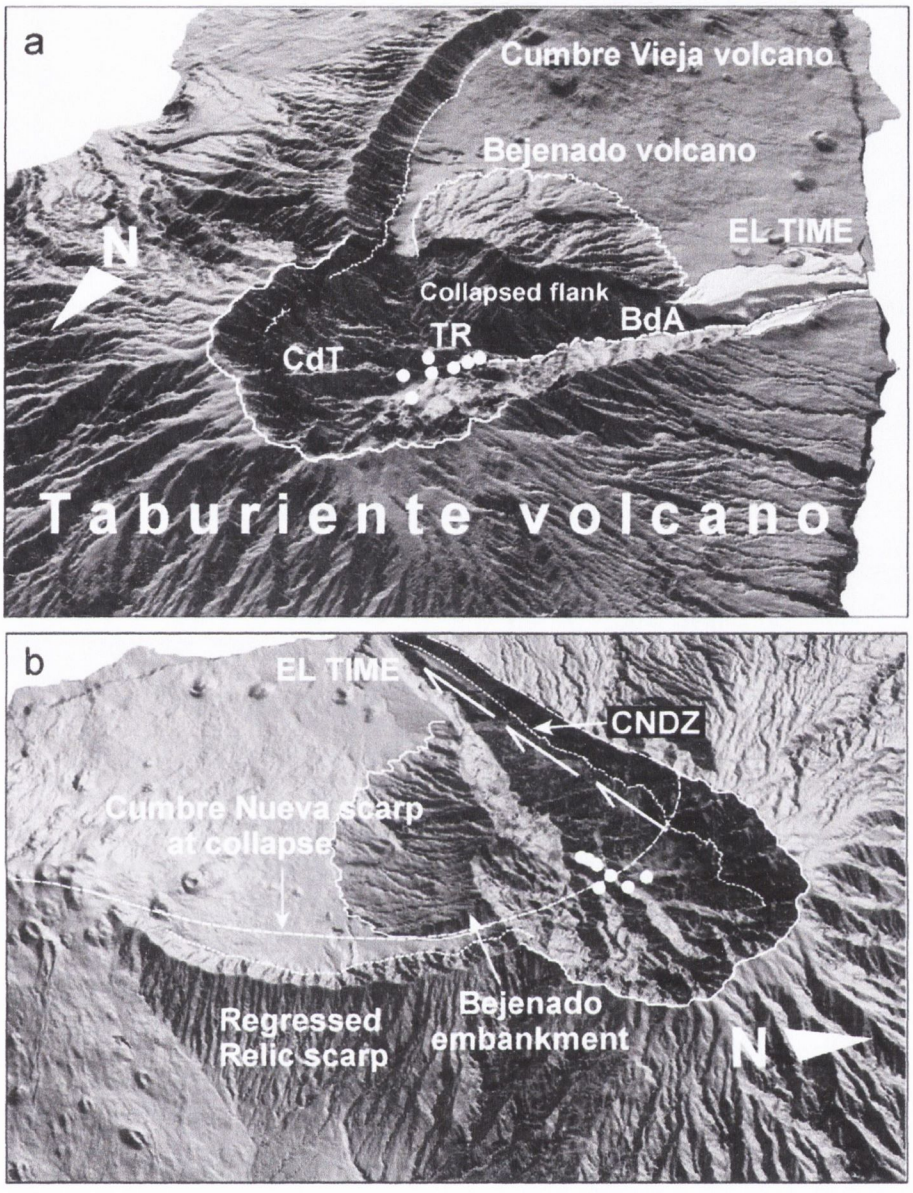


Fig. 2. High oblique shaded relief images of north-central La Palma. (a) The perspective is 19.25 km across. Decollement zones (see text) are outlined below the lateral collapse escarpments. (b) The reconstructed geometry of the Cumbre Nueva headwall scarp is outlined along with the Cumbre Nueva Decollement Zone (CNDZ). The N–S distance is 18.75 km. Abbreviations: BdA, Barranco de Las Angustias; CdT, Caldera de Taburiente; TR, toreva remnants.

This substratum overlies a 3–8-m-thick fault gouge and breccia zone in the footwall composed of angular to subangular foliated assemblages of severely damaged basement rock. Both of these tectonic units comprise the Cumbre Nueva decollement zone (CNDZ in Fig. 2) are separated by a master detachment fault which geometrically emulates the domal topography of the uplifted basement. With this new structural perspective it is possible to demonstrate conclusively that substratum deformation, fault zone diagenesis, and the build up of a SW-directed deviatoric stress had forced the collapse of the entire summit region of Taburiente during or shortly after the

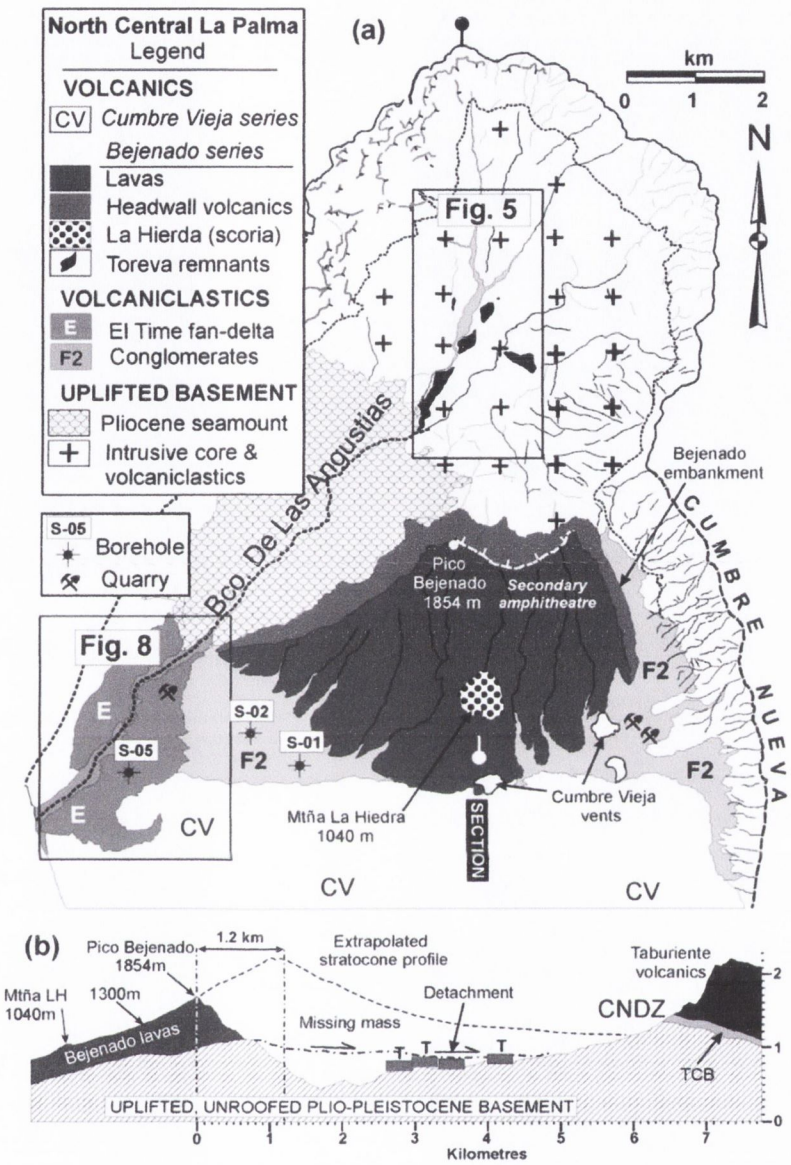


Fig. 3. Simplified geologic map and scaled reconstructed section of north-central La Palma. The tick marks on the NE face of the CdT represent major scarps. Abbreviations: CNDZ, Cumbre Nueva decollement zone; TCB, Tenerra Collapse Breccia (see text).

Cumbre Nueva collapse (Roa, 2003). The third point which needs to be considered is that the differential erosion of La Palma has been clearly dominated by northeasterly trade winds and the impact this has had on the depth and distribution of extra-Caldera canyons is quite distinctive. For instance, canyons up to 0.54 km deep predominate on the northern to eastern flanks whereas the leeward western slopes are better preserved. If the purported 'erosion caldera' model was valid, then northern La Palma should be in an advanced state of erosional degradation, moreso than the aspect-controlled erosional regime implies. Finally, the disposition of the toreva remnants within the Caldera and up to 450 m below the decollement zones is a clear indication that a substantial

void space (the Caldera) already existed for the development and subsequent collapse of the north flank of Bejenado.

### 2.2. The toreva remnants and the El Time fan delta

Previous studies from inside the Caldera have referred to the *Roques centrales* or *Serie de los Roques* (e.g. Gastesi et al., 1966; De la Nuez, 1983), which have Spanish or Guanche (pre-Conquest) names that correspond geographically to the positions of the toreva remnants. When translated from Spanish, the word *roque* denotes a detached hill or a butte of resistant strata (erosional remnant), in the sense of its conspicuous geomorphology or in the colloquial sense without any geological connotations. The only published interpretation is 'an accumulation of sediments and flows, filling a palaeovalley' (Ancochea et al., 1994).

Studies of the El Time fan delta by Vegas Salamanca et al. (1999) have defined the bulk stratigraphy and lithofacies variation and they also provide preliminary although highly imprecise K–Ar data. Furthermore, the palaeogeographic reconstruction by these authors does not specifically single out the north flank collapse of Bejenado as a major event in the Quaternary sedimentology of La Palma. In terms of facies architecture and provenance, the El Time sediments are similar to the Chiancone volcaniclastic fan deposits of Mount Etna which are sourced from the Valle del Bove collapse amphitheatre (Calvari and Groppelli, 1996). The El Time group can be subdivided accordingly on the basis of comparable facies variations. These include debris flow units, fluvial conglomerates with frequent erosional boundaries, mudstones and cross-stratified sandstones, and locally interbedded pyroclasts and lavas (Vegas Salamanca et al., 1999). These successions have been remobilised along the flat-floored channels which extend up to 60 km across the submarine pedestal of La Palma (Urgeles et al., 1999). These channels are here named Laguna, Remo and Galeras in Fig. 1, corresponding with channels C, D and E of Urgeles et al. (1999).

### 2.3. Volcaniclastic stratigraphy below the Cumbre Nueva decollement zones

The floor of the Caldera comprises the uplifted and unroofed intrusive complex of northern La Palma and the mergent seamount series volcanics (Staudigel and Schmincke, 1984). It is heavily dissected by a harsh terrain of narrow canyons, between 220 to 340 m deep, which drain out over a length of 14 km towards the SW through the Barranco de Las Angustias (Fig. 3) and onto the submarine slopes. The Quaternary collapse structures and the subsequent Angustias catchment area expose a diverse range of volcaniclastic successions in terms of depositional environments (e.g. fluvial–deep marine) which, from a temporal perspective, encompasses over 2 Ma of deposition (Table 1).

Groups F2 and F1 are unconsolidated fluvial

Table 1
Grouping of volcaniclastics on northern La Palma

| Group | Name/classification | Characteristics | Thickness (m) | Age range (Ma) |
|---|---|---|---|---|
| F2 | Basinal epiclasticss | Unaltered, some pyroclasts | 40–200(?) | 0.55–Holocene |
| F1 | Intra-caldera epiclastics | Unaltered epiclastics | 30–170 | Holocene |
| E | El Time fan delta | Unaltered, intercalated lavas | 370 | 0.41–0.44(?) |
| B | Bejenado (relic debris) | Unaltered, base of torevas | 1–2 | 0.44(?) |
| C | Cumbre Nueva (breccia) | Unaltered, 1–2% dikes | 100 | 0.55 |
| TCB | Ancestral Taburiente | Unaltered, 5–20% dikes (Tectonised) | 100–350 | 1.2 |
| TCBm | Ancestral Taburiente | Partially metasomatised, 20–30% dikes | 100–200 | 1.2 |
| H2 | Submarine – debris | Hydrous metamorphosed, many dikes | 400(?) | Pliocene |
| H1 | Submarine – clastics | Hydrous metamorphosed, many dikes | 3000(?) | Pliocene |

Preliminary age data are discussed and referenced in text

conglomerates and rock avalanche deposits derived from the ongoing retrogressive erosion of the Caldera and the Cumbre Nueva escarpments. Groups H2 and H1 are the hydrous metamorphosed clastic sequences which formed during the Pliocene-stage submarine evolution of La Palma (see Staudigel and Schmincke, 1984; Ancochea et al., 1994). Groups TCB and TCBm (the largest subaerial volcaniclastic sequence) relate to the partial destruction of Ancestral Taburiente during a paroxysmal caldera-forming eruption associated with a lateral flank collapse (Roa, 2003). Group TCBm is locally incorporated into the footwall of the CNDZ and is partially metasomatised, increasingly so with stratigraphic depth. Group B represents the veneer of volcaniclastic materials which are exposed at the base of the toreva remnants. Group C includes sediments and collapse-filling breccias which accumulated early within the Quaternary collapse structures (Carracedo et al., 1999a,b, 2001); they partially form the substratum of Bejenado.

## 3. Morphology and geology of Bejenado volcano

Bejenado volcano developed opposite the intersection between the Caldera and the Cumbre Nueva escarpment (Ancochea et al., 1994). This would place the summit palaeoposition approximately 1.2 km north of Pico Bejenado (1854 m) in very close proximity to the opening of the Caldera (Fig. 3a). The growth of Bejenado along a S–SW dipping basal topographic gradient, against the topography incurred by lateral collapses, resulted in the projection of most of its lavas toward the south and southwest. During the Quaternary, the north flank developed inside the Caldera whilst the south flank extended unbuttressed for up to 10 km. Lavas on the east flank were dammed against the higher part of the Cumbre Nueva escarpment and subsequently preserved its geometry along an embankment which faces the headwall over a length of 3 km. This feature, Bejenado embankment (Fig. 4A), presents slopes averaging 42° with a maximum height of 350 m. The embankment now stands at a distance of up to 700 m from the base of the headwall, yet this distancing was not produced by erosion alone. Following the Cumbre Nueva/Caldera de Taburiente collapses, the horizontal stresses that were generated by edifice unloading re-equilibrated to the gigantic void spaces around the collapse escarpments. As the relic spreading sectors re-adjusted to the new stress regime, the unconfined substratum beneath Taburiente began to extrude from beneath the headwalls (Roa, 2003). Therefore the distance between Bejenado embankment and the Cumbre Nueva escarpment reflects the process of residual gravitational spreading (headwall recline and slumping) as well as retrogressive escarpment erosion.

The present form of Bejenado is compared with its hypothetical original shape in Fig. 3b. It is difficult to precisely constrain the pre-collapse morphology and, more specifically, the volume of the original cone given the irregularity and planimetric asymmetry of its base. The volume concealed by Cumbre Vieja and the severity of edifice destruction and subsequent erosion further frustrates this attempt. Hence, one can only speculate upon the volume of material that was involved in the collapse and this will be discussed in a later section. What remains of the stratocone measures 9 km (NE–SW) × 5 km (N–S), and it encompasses an exposed surface area of 25 $km^2$, and an exposed volume of 14 $km^3$. The south flank slopes at 12° for over 3 km from its current base. The slope increases around the 1300-m contour to 28°, rising to Pico Bejenado (1854 m), and then drops dramatically over a horizontal distance of 1.3 km into the intrusive domain exposed by the Caldera. The headwalls facing into the Caldera present an imposing, abrupt morphology of substantial relief (Figs. 2 and 4B), which is heavily modified by gullying and piecemeal slope failure. A distinct relic scarp, 2.1 km in perimeter and 600–700 m deep, is visible to the east of Pico Bejenado, confirming that a secondary collapse occurred after a more voluminous slope failure event (Ancochea et al., 1994). The stratocone morphology is reconstructed (Fig. 3b) using the 1300-m slope inflection as the topographic control on the overall slope asymmetry and the summit elevation of around 2100 m. The original stratocone may have resembled the present form of the

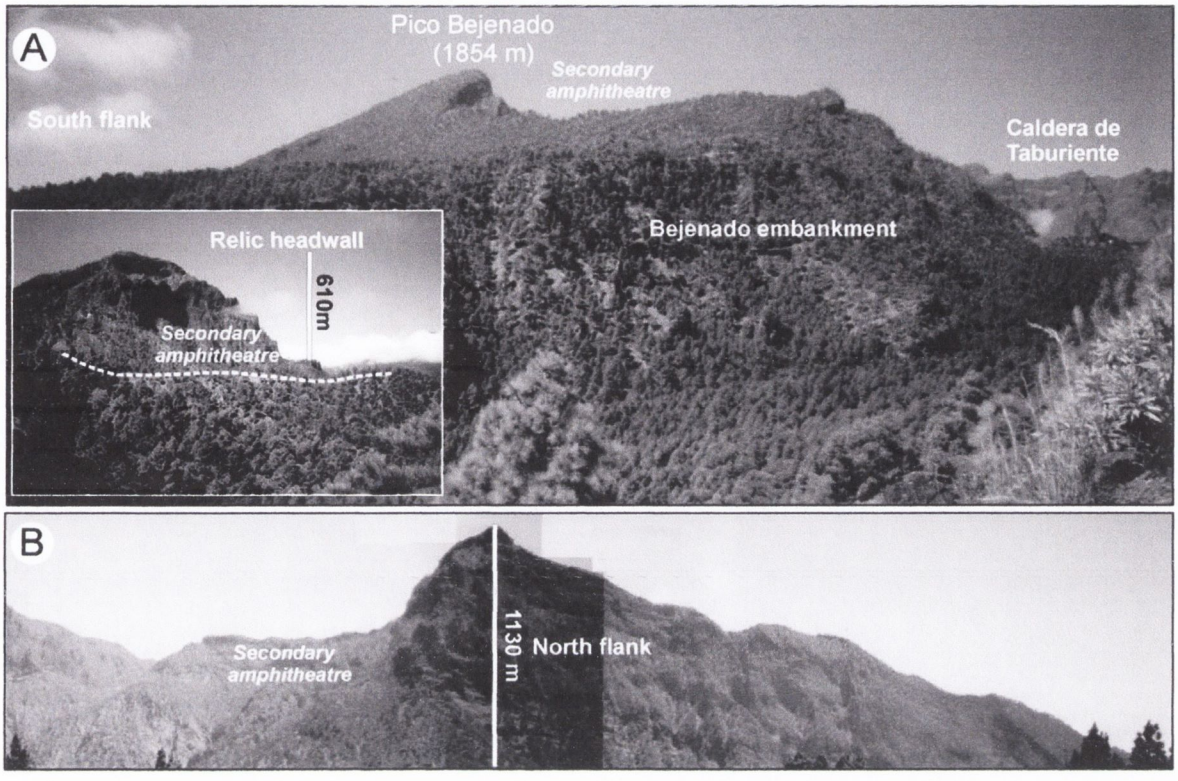


Fig. 4. (A) Panoramic photograph of Bejenado taken at decollement zone level from below the arcuate segment of the Cumbre Nueva scarp. The inset image shows the north flank headwall viewed across the rim of the secondary amphitheatre (dashed line). (B) Photomosaic of the disfigured north flank of Bejenado viewed from the limit of the Caldera de Taburiente. The image is 8 km across.

steep-sided cones of Pico (Azores) or Fogo (Cabo Verde).

The south flank of Bejenado is still partially surfaced with well-preserved pahoehoe lavas and spatter ramparts at its upper reaches, whilst the lower reaches display stacked, tube-fed pahoehoe flow units amongst numerous 'a'a flows which have the most distal subaerial coverage. The south flank has succumbed locally to advanced gullying, up to 100 m deep, although a younger drainage system, set up since the eruption of the only visible parasitic vent, Montaña La Hiedra (Fig. 3a), overlaps the older gullies. Several other scoria cones are located at the south base of the volcano; all of which belong by stratigraphic ordering to the Cumbre Vieja phase of volcanism (Navarro and Coello, 1993). The Holocene/subhistoric lava flows from the northern part of Cumbre Vieja onlap and are diverted west by Bejenado. The base of Bejenado has been identified by Carracedo et al. (1999a, 2001) in a number of boreholes on the southwest flank (Fig. 3a) that have bottomed in successions of collapse-filling group C volcaniclastic deposits up to 100 m thick. Borehole S-01 (collar elevation 395 m) intersected over 300 m of ankaramite and basanite lavas and scoria before terminating in group C (Carracedo et al., 2001). The observable base of the edifice, outcropping from inside the Caldera, also comprises volcaniclastic successions that correlate with the borehole data. One of the most interesting aspects of the S-01 borehole is a K–Ar age of $0.710 \pm 0.11$ Ma (H. Guillou, unpublished data) obtained from an 80-m interval of intact volcanics towards the bottom of the hole.

This incongruous age is suspected of representing an earlier toreva sourced from the Cumbre Nueva collapse headwall during the embayment-forming event (J.C. Carracedo, pers. commun.). Other boreholes drilled in proximity to S-01

have bottomed in Pliocene submarine volcanic successions. However, a detachment surface from the Cumbre Nueva collapse is not apparent (Carracedo et al., 2001).

Bejenado volcanics are composed predominantly of ankaramite and basanite with lesser amounts of phonolitic lava limited in subaerial coverage to the upper reaches of the south flank (Coello, 1987; Ancochea et al., 1994). The available age data (from cross correlated K–Ar and $^{40}Ar/^{39}Ar$ determinations on lava flow sequences) range between $0.537 \pm 0.08$ Ma and $0.490 \pm 0.06$ Ma (Guillou et al., 2001). However, the same authors estimated an age of $0.590 \pm 0.04$ Ma for Montaña La Hiedra which exceeds the probabilistic age they designate for the Cumbre Nueva collapse (0.55 Ma) and further conflicts with the relative youth of Montaña La Hiedra. Earlier K–Ar age determinations from singular lava flows, which range between $0.71 \pm 0.05$ and $0.65 \pm 0.04$ Ma (Ancochea et al., 1994), are inconsistent with the probabilistic Cumbre Nueva collapse threshold date. Guillou et al. (2001) discuss the difficulties in obtaining reliable K–Ar-based age data due to the presence of excess argon in Canarian lavas.

## 4. Structure and disposition of the toreva remnants

Several toreva remnants have been identified between 2 and 4 km from Pico Bejenado (Fig. 4; Table 2). Examples of the preserved structure and volcano-stratigraphic sequencing are illustrated by profiles A–D in Fig. 5. The tilted and locally jointed sequencing is predominantly composed of layer-differentiated scoria whilst ancillary 'a'a autobreccia, pahoehoe flow units, dikes and areas of fumarolic alteration are also present. The sequencing is identical to the myriad scoria layers and lavas that constitute the stratigraphy of the surrounding walls of the Caldera and the headwalls of Bejenado itself. The toreva remnants can be distinguished at a distance by their anomalous oxidised colours and their conspicuous basal slip surfaces. The oxidation colours are revealed by continuous fragmentation (or spall); an ongoing process which has produced the dense accumulations of spall blocks below the toreva remnants. Individual blocks are up to 5 m across. Where fragmentation is not apparent, the oxidation colours are less distinct and subsequent case hardening and dull colored palagonitisation predominates.

The toreva remnants are mostly distributed along a major interfluve, sloping 12–15° to the SW, whilst the remainder lie either side on steep ridges. They are separated by distances no greater than 440 m and most of them overlie a structureless veneer of poorly indurated yet compacted volcaniclastic materials up to 2 m thick (group B volcaniclastics).

Group B is composed of lithologically heterogeneous, centimetre-scale, subangular clasts that are held in a pulverised and locally sheared matrix of lithic fragments, lapilli and relic crystals. They have been interpreted as a debris avalanche unit which formed during the first stages of the genesis of the Caldera (Ancochea et al., 1994). However, the superimposition of the toreva remnants

Table 2
Dimensions of the toreva remnants and their associated basement characteristics

| Name | Dimensions (m) | Altitude (m) | Azimuths | D (km) | BD (m) | C (m) |
|---|---|---|---|---|---|---|
| Roque del Huso | 211×67×80 | 950 | – | 4.1 | 1.2–1.4 | – |
| Roque Salvaje | 300×150×160 | 1071 | 219° | 3.8 | 0.1 | 0.3 |
| El Negrito | 380×160×60 | 1027 | 304° | 3.4 | 1.8 | 0.2 |
| Brevera Macha | 420×210×164 | 971 | 223° | 3.3 | 1.1 | 0.4–1.2 |
| Picos de Teruel | 740×300×150 | 865 | 217° | 2.9 | 1.6–1.8 | – |
| Lajas del Viento | 490×160×120 | 712 | ? | 2 | ? | ? |

Total volume 0.1 $km^3$. Abbreviations: Azimuths, azimuths of basal striations; D, horizontal distance from Pico Bejenado; BD, thickness of basal debris; C, maximum thickness of basement rock comminution.

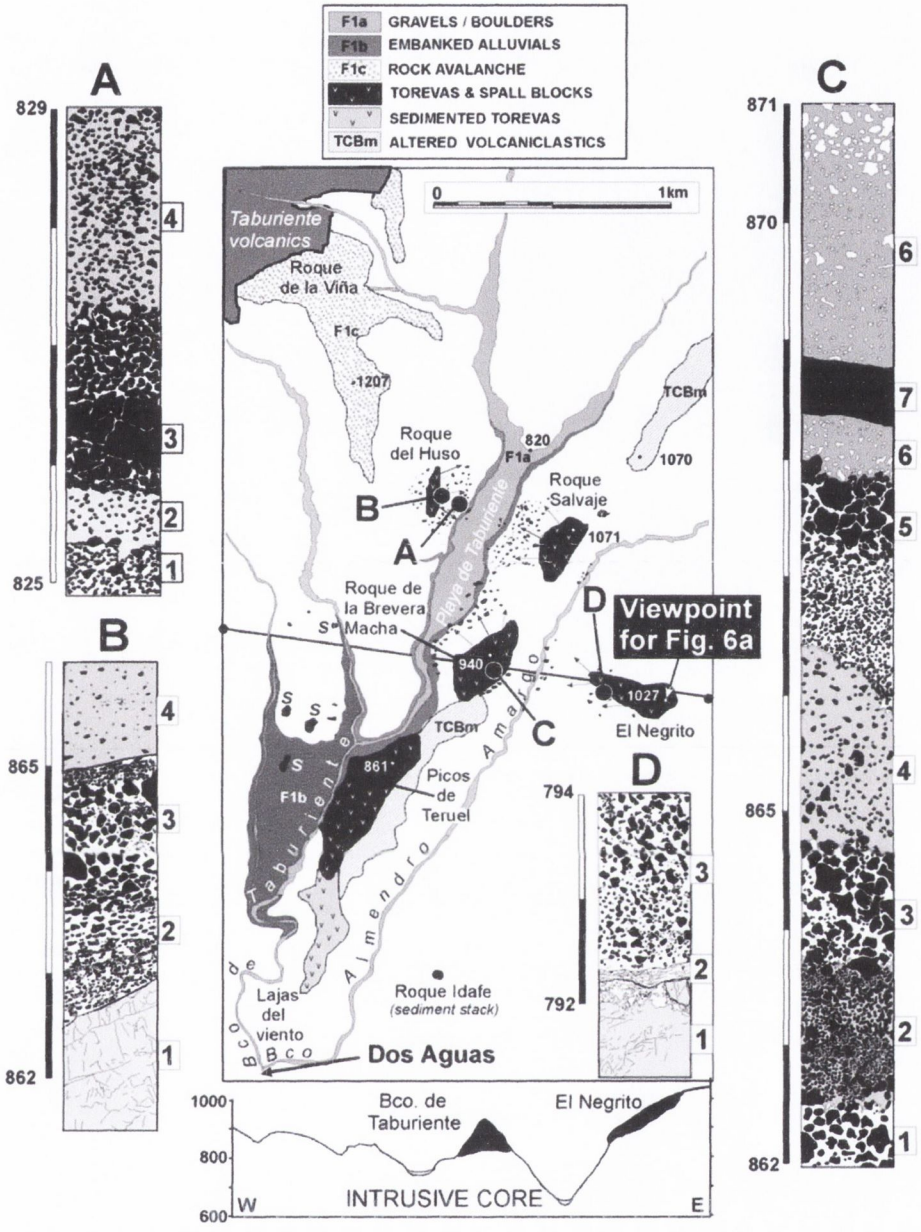


Fig. 5. Geologic map of the central Caldera de Taburiente drawn from a 1:5000 aerial ortho-photograph. Graphic profiles of the toreva remnants are scaled in meters. Profile A. Spall block from Roque del Huso: (1) dark purple oxidised scoria with fragments of dense aphyric lava; (2) altered dark yellow lapilli layer; (3) dense lava core with mergent vesicular autobreccia (20% clinopyroxene crystals) forming part of an 'a'a flow carapace; (4) pale yellowish brown lapilli with abundant plagioclase-phyric scoria. Profile B: (1) stacked aphyric sills below base of Roque del Huso; (2) smoothened planar overhanging surface of avalanche debris (no apparent striations); (3) oxidised and case hardened debris with occasional shear bands; (4) base of toreva remnant, dark-red altered scoria. Profile C: (1) disaggregated 'a'a flow (5–10% cpx-ol); (2) deep red agglutinated spatter and scoria; (3) disaggregated 'a'a flow (15–20% clinopyroxene); (4) dark brown altered lapilli and agglomerate; (5) disaggregated 'a'a flow (5–10% clinopyroxene–olivine crystals); (6) altered scoria horizon with clasts of dense ankaramite; (7) aphyric intrusion. Profile D: (1) hydrous metamorphosed aphyric dikes; (2) heavily comminuted basement rock; (3) poorly indurated debris adhering to base of toreva remnant.

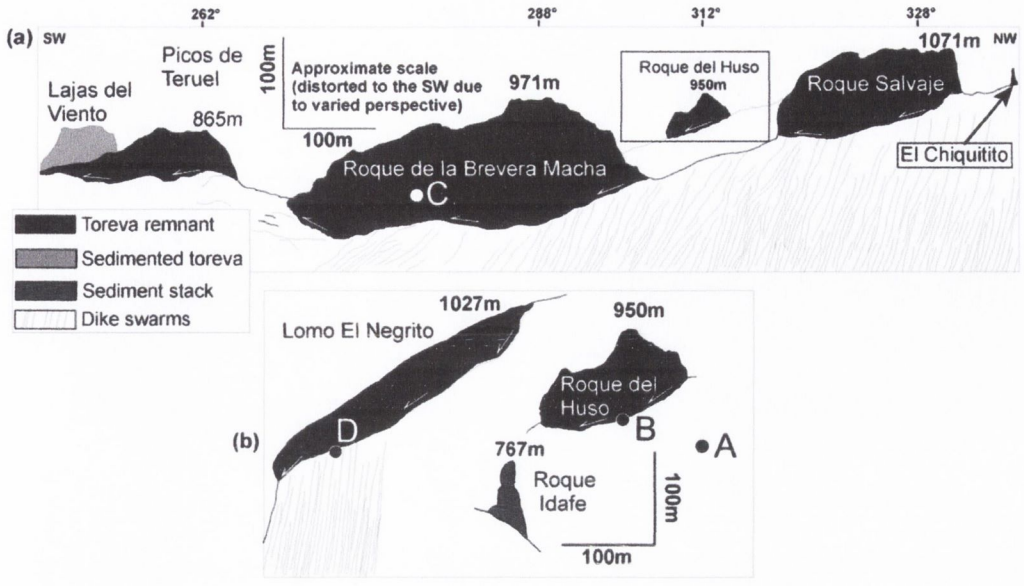


Fig. 6. Sketches drawn from panoramic photographs showing the relative dimensions of the toreva remnants. The main panoramic image is taken from the summit of El Negrito (1027 m) across Barranco Almendro Amargo (see Fig. 5 for the location of the viewpoint).

strongly suggests that they are an integral component of the later Bejenado slope failure event. They have also been interpreted as agglomerates (Gastesi et al., 1966; Hernández Pacheco and Afonso, 1974; De la Nuez, 1983) which is inconsistent with the terminology cited in Section 1.3.

The undersides of the toreva remnants frequently display survivor grooves or finer striations etched in paralleling surfaces of basal debris or decapitated basement dikes. Some of the toreva remnants have evidently slipped off their basal debris (e.g. Roque Salvaje), in which case post-collapse toreva motion has resulted in severe comminution of the hydrothermally altered basement rocks. Fine lustrous striations on internal discontinuities provide evidence of internal dislocation subsequent to emplacement. Each toreva remnant acts as a perched aquifer and their discoloured bases show evidence of prolonged seepage and leaching of iron and sulphate bearing fluids. It is certain that many of them formed unified toreva blocks of greater dimensions prior to the incision of the amphitheatre catchment area. Weathering and erosion have resulted in substantial modification of their morphology, with smoothened longitudinal profiles mostly elongated along the canyon axes, the exception being El Negrito where the slip axis is aligned against the general SW trend. The toreva elongation axes are frequently twice their widths, and aspect ratios average around 0.4. The most distant remnant, Roque del Huso, is 4.1 km from Pico Bejenado. Other pinnacles such as Roque Idafe appear to be sediment stacks, surviving from the initial reworking of the Bejenado debris avalanche deposit.

### 4.1. The interfluve toreva remnants

Toreva remnants lying on the steep and narrow interfluve that separates Barranco Almendro Amargo from Barranco de Taburiente are visible discontinuously over a distance of 2.5 km, each one separated by a small saddle (Figs. 5 and 6). Sediment accretion is accentuated toward the SW, eventually giving way to perched epiclastic successions below Dos Aguas. No toreva remnants have been identified below this point. Roque Salvaje is the highest standing toreva remnant, displaying the most conspicuous basal slip surface. Basal striations are directed toward the SW and the immediate basement rocks are strongly comminuted. The NW face is locally desurfaced and nu-

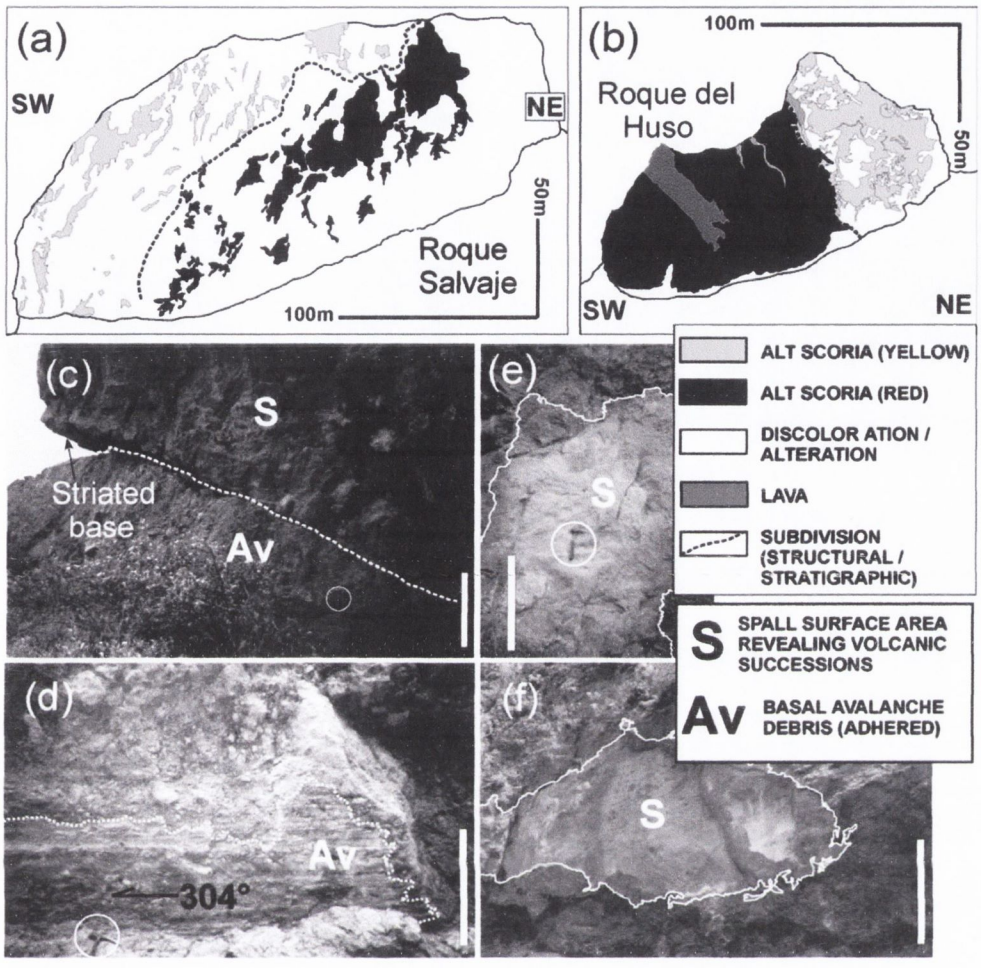


Fig. 7. Geologic sections drawn from photographs of (a) Roque Salvaje, and (b) Roque del Huso. Close detail of the toreva remnants showing: (c) basal section of the NE end of Picos de Terruel; (d) striated debris avalanche material (group B) that has adhered to the overhanging base of El Negrito; (e) spall point on the lower NW face of Roque de la Brevera Macha; (f) spall point on the NW face of Roque Salvaje. Note that the vertical scale bar in each photo is 1 m.

merous spall blocks have accumulated at its base, above Playa de Taburiente. The SE face is heavily desurfaced and shows a striking scoria-based colour contrast which indicates the disposition of at least two distinct volcano-stratigraphic units (Fig. 7a). A small unnamed and precariously balanced pinnacle to the NE of Roque Salvaje is also composed of scoria. The name El Chiquitito (Spanish; 'the little one') has been assigned to it in Fig. 6.

Roque de la Brevera Macha, located 230 m SW of Roque Salvaje, is the only toreva remnant that is partly accessible for more detailed field observation. Profile C (Fig. 5) shows a typical section comprising sequences of texturally differentiated scoria that are locally traversed by sheeted intrusives. Several internal dislocation faults are evident on the SE face, each showing variable orientation and persistence. The volcanic architecture is partially or completely shattered, made evident by diffuse contacts or offset stratification. Glicken (1996) describes similar features in the block facies of the Mount St. Helens debris avalanche deposit. A sequence of adjoined toreva remnants begins 240 m SW of Roque de la Brevera Macha (Figs. 5 and 6), the first of which, Picos de Teruel, has evidently slipped into Barranco de Taburiente during the course of its incision. The NE end of the toreva remnant is composed of

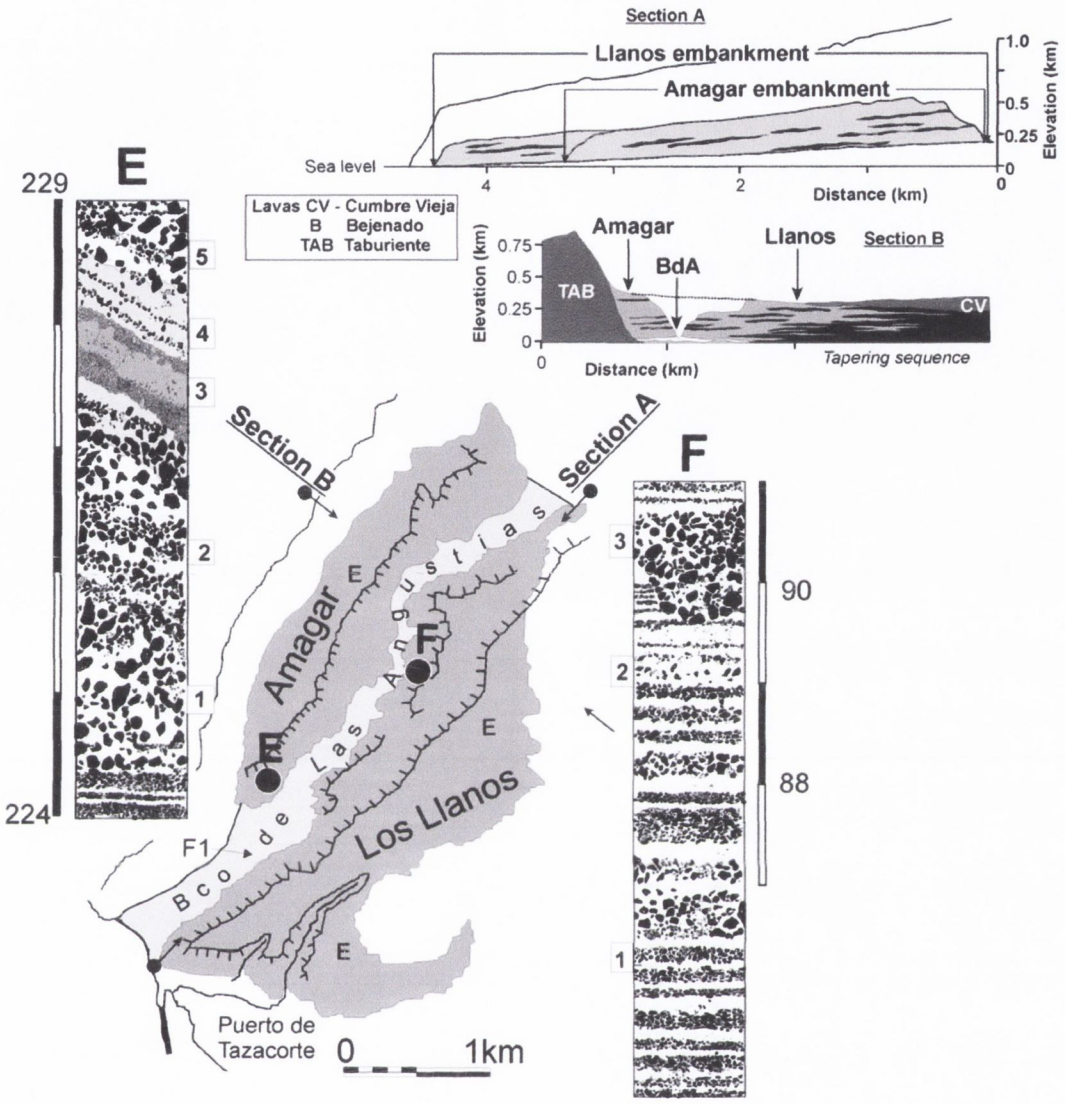


Fig. 8. Scaled sections and plan of the El Time fan delta, with graphic profiles (E) and (F). Profile (E): (1) large debris flow unit overlying fine–coarse fluvial beds; (2) debris flow unit with fine fluvial beds; (3) 'a'a flow unit; (4) lapilli and scoria; (5) debris flow unit in erosive contact with altered lapilli and scoria clots. Profile (F): (1) sequence dominated by coarse fluvial units and minor debris flows; (2) multiple minor debris flow units interbedded with coarse and fine fluvial beds; (3) debris flow filling small palaeochannel.

dark purple–red scoria that has produced pervasive iron oxide dissolution throughout the group B volcaniclastics upon which it rests (Fig. 7c). Observable striations on its overhanging base are directed towards the SW. However, striated surfaces which indicate a NW slip vector are visible from the undercut base above Barranco de Taburiente. Further SW, the difficult terrain prohibits outcrop-scale access to the amalgamated toreva remnants that terminate at Lajas del Viento. They have accreted substantial amounts of epiclastic material, increasingly so toward the SW.

### 4.2. *Isolated toreva remnants*

Two toreva remnants lie either side of the in-

Fig. 9. Photograph of the Amagar embankment.

terfluve group on opposing ridges. To the west, Roque del Huso (Figs. 5 and 7b) rests upon a narrow ridge formed by a stack of sheeted sills inclined 12° toward the NW. It overlies a 1.3-m thick veneer of compacted group B volcaniclastics, the base of which is exposed as a smooth non-striated hanging wall. Prominent volcanostratigraphic subdivisions are visible on the east face (Fig. 6b) below which is an extensive field of spall blocks that have been used for stratigraphic profiling. Profile A (Fig. 5) shows the dense interior of an 'a'a flow with a carapace of oxidised clinker, interbedded between related successions of vent-building pyroclasts. To the east of the interfluve group is El Negrito (Figs. 5 and 6), an elongate and steeply dipping (17–28°) toreva remnant. Fresh faces are revealed by fragmentation, but most of the associated spall blocks have shattered during impact upon descent into Barranco Almendro Amargo. Sheared group B volcaniclastics have adhered to its overhanging base and appear striated along the toreva elongation axis (Fig. 7d). Decapitated hydrous metamorphosed dikes are also striated along parallel bearings. Profile D (Fig. 5) illustrates a section of comminuted basement rock.

## 5. Structural and sedimentary characteristics of the El Time and F2 conglomerate groups

### *5.1. Group E – the El Time fan delta*

The El Time group has been identified from previous studies to consist of fan delta deposits, largely comprising reworked volcaniclastics with locally interbedded lavas and pyroclastic horizons (Vegas Salamanca et al., 1999). They are exposed in section over a length of 4.5 km at the lower course of the Barranco de Las Angustias where they have been eroded down to the base of the sedimentary sequence. Spatially, the deposition of the fan delta was accommodated along the lower segment of the linear wall of the Cumbre Nueva embayment, and along the lowermost shallow slopes on the remaining part of the west flank of Bejenado (Figs. 2 and 8). These topographic features controlled the geometry, thickness and the facies architecture of the fan delta. The prograded delta front has been truncated by littoral mass wasting, whilst the current Barranco de Las Angustias has deeply incised the delta plain into two embankments (Fig. 8).

Further exposure by ephemeral ravines and gul-

lies provides good 2-D and 3-D sections of the sediment body geometries. The Amagar embankment (Fig. 9) comprises a surface area of 1.7 $km^2$ and a volume of approximately 0.45 $km^3$. It slopes 3–5° to the SW and decreases from 370 to 200 m in thickness downslope. The embanked deposits which extend within the localities of Los Llanos and Tazacorte are 3.5 $km^2$, with an estimated volume of 0.76 $km^3$. In these environs the sedimentary sequence is visible in small gullies and building foundations, and must extend further south beneath the NW rift zone of Cumbre Vieja volcano, hence the quoted volume is a minimum. The total subaerial volume, prior to the incision of the current Barranco de Las Angustias and the encroachment by Cumbre Vieja lavas, is estimated to have been $\geq 2$ $km^3$.

The near-shore base of the fan delta is composed of pale indurated sandstones and stratified, lens-shaped conglomerate horizons. The clastic composition and depositional characteristics of the overlying deposits, which make up the main body of the fan delta, are broadly similar to a much larger sequence of volcaniclastics described by Calvari and Groppelli (1996) which outcrop on the eastern flank of Mount Etna. These authors consider the Chiancone volcaniclastic fan deposits to be sourced from the Valle del Bove, the amphitheatre-shaped depression east of the summit cones of Mount Etna. Both El Time and Chiancone comprise repetitive sequences of gravels, boulder breccias/conglomerates, silts and cross-stratified sands in horizontal–subhorizontal beds. Both groups show occasional intercalation with contemporaneous basaltic lavas and pyroclastic deposits (see sections A and B and profile E in Fig. 8), which, in the case of El Time, were derived from the waning stages of Bejenado volcanism subsequent to its collapses.

At least six distinct lithofacies are distinguishable within the El Time deposits, the simplified breakdown of which is presented in Table 3 in a scheme which is in general accordance with the one adopted by Vegas Salamanca et al. (1999).

Many subunits exist within each lithofacies, the thickness, grading, geometry and lateral continuity of which reflect the environmental controls on each depositional event. Based on the depositional characteristics, these events are interpreted to represent a spectrum of flow types and regimes that encompassed the emplacement of cold debris flows, lahars, scoriaceous-debris flows and fluvial sequences. Debris flow units of varying thicknesses are the most recurring lithofacies. They

Table 3
Lithofacies variation within the El Time fan delta

| Facies | Thickness variation (m) | Interpretation |
|---|---|---|
| Debris flows | 1–6 | Chaotic angular blocks of lava and dike (0.5–3 m), block- or clast-supported, or supported in moderately indurated 0.5–2-cm matrix. Matrix is generally dull brown or yellow and of sand to gravel grade. Representative of single and multiple event debris flow deposits |
| Debris flows (mixed) | 1–6 | Chaotic angular blocks and multi-lithic clasts with distinct juvenile pyroclastic horizons |
| Lahar | 0.4–1.1 | Coarse subangular to subrounded blocks (0.2–0.5 m), matrix supported with tree moulds representing mudslides (lahars). |
| Fluvial conglomerate-rich | 0.6–2 | Coarsely stratified well sorted and normally graded bodies of gravel, cobbles, sand and silt, representing deposits of single waning floods. |
| Fluvial sand-rich | 0.01–0.6 | Normally graded lenses of fine sand, silt and clay with occasional larger subrounded clasts. Large lenticular and sheet-like channels with irregular interconnected gravels, representing the deposits of gravely, braided alluvial systems. |
| Volcanic | 1–7 | Thin pahoehoe flow units, massive 'a'a, agglomerate, diffusely intercalated lapilli or ash horizons |

are moderately to well indurated and ungraded to normally graded and poorly sorted, exhibiting a lateral variation between clast-supported and matrix-supported constituents. The clasts are mainly angular to subangular blocks of dense fractured lava, tabular dike segments, vesicular lava and lesser scoria fragments. The clasts are lithologically heterogeneous, comprising olivine basalts, ankaramites, trachybasalts and lesser phonolites, sometimes with large oxidation selvages and halos extending into the matrix. This brown, brownish red matrix is composed of sand and clay-sized particles with locally abundant relic crystals of olivine and augite. Hydrous metamorphosed clasts (typically 10–30 cm) of basalt and gabbros/pyroxenites, either subrounded or subangular, occur frequently at the base of the sequence but not exclusively so. Stratification boundaries show frequent erosive contacts with irregular, troughed or lens-shaped palaeochannel fills, commonly as debris flows (profile F; Fig. 8). Subhorizontal tree moulds are visible in debris and mud flow (lahar) units whilst palaeosols with bioturbation features (burrow forms) and soft-sediment deformation structures (folds) are locally well exposed. Gradational contacts between some debris flow units are suggestive of a chronology of successive flow emplacement events at times when net erosion was less significant (e.g. during droughts or lava dams). Other debris flow units show no apparent grading.

The limited and conflicting radiometric data that exist for lava flows interbedded within the fan delta are difficult to reconcile with a coherent sedimentation chronology and it has not been possible to elucidate this discrepancy with new radiometric analyses. Ancochea et al. (1994) sampled a lava flow from the Barranco de Las Angustias which yielded a K–Ar age of $0.78 \pm 0.1$ Ma. However, the El Time stratigraphic sequence accumulated within the Cumbre Nueva embayment, therefore the age interval of accumulation can only postdate the 0.55-Ma age assignment for the Cumbre Nueva collapse (Carracedo et al., 1999a; Guillou et al., 2001). It must also predate the earliest available age for the onset of Cumbre Vieja volcanism, i.e. 0.125 Ma (Carracedo et al., 1999a) since the Cumbre Vieja lavas onlap the El Time sequence. When allowance is made for the probabilistic $< 0.1$-Ma growth period of Bejenado (Carracedo et al., 2001) the temporal window for the onset of deltaic sedimentation is further constrained. Vegas Salamanca et al. (1999) report a K–Ar age of $0.2 \pm 0.1$ Ma for this time of onset but as its statistical error is simply too large this date is devoid of any value.

Since the drainage system inside the Caldera postdates the emplacement of the torevas (it downcuts the toreva remnants and the surrounding basement rocks), it is logical to surmise that the toreva remnants occupy positions along the canyon apices which are the closest approximation to the Bejenado failure surface (Fig. 3b). Allowance must be made for post-emplacement toreva slip into their current positions. By using the fluvial erosion rates of Gee et al. (1993), estimated between 1 and 2 mm/yr, it is possible to deduce a lower limit for the Bejenado north flank/summit collapse. The canyon depths within the Caldera (between 220 and 340 m) imply an erosion interval of roughly 0.37 Ma subsequent to emplacement and this age is used as a provisional estimate for the onset of deltaic sedimentation.

### 5.2. *Group F2 – the basinal conglomerate groups*

Unconsolidated to poorly indurated sedimentary successions have accumulated around the south flank of Bejenado, locally choking the lower reaches of gullies and onlapping the peripheral vents of Cumbre Vieja. They fan out over a surface area of 9.3 $km^2$ and are measurable in sections up to 47 m thick in the gravel quarries below Bejenado embankment (Fig. 3a) although the base is nowhere exposed. Most of the sedimentary sequence has been overlapped by Cumbre Vieja lavas, making a realistic estimate of the volumetric extent impossible to determine. From the sections exposed in the gravel quarries and from the small drainages that downcut them, they are seen to be composed of subhorizontally bedded, normally graded cobbles, pebbles, sands and silts which are often very well rounded and sorted. The planar to slightly undulatory beds are 0.4–1.1 m thick. Palaeosols are locally identifiable from these beds although juvenile volcanic frag-

ments occur to a lesser degree except in the vicinity of peripheral Cumbre Vieja vents. Vegas Salamanca et al. (1999) have carbon-dated charcoal samples from the gravel quarries and have defined a stratigraphic age range from 938 to 33 206 equivalent $^{14}C$ years. If these dates are reliable, then they imply a time-averaged sediment accumulation rate of 0.15 cm/yr, given the quarry depth at this locality (47 m).

## 6. Discussion

### 6.1. Toreva emplacement

In a retrospective analysis of the Bejenado north flank/summit failure events there are a number of key structural elements which place important constraints on the cause of flank instability and the emplacement of the debris avalanche deposit: (1) the topographic confinement (24 $km^2$) of the enclosing collapse amphitheatre/embayment headwalls; (2) the counter-slope surface of the collapse amphitheatre floor (i.e. 7–8° against the gradient of the debris avalanche deposit); (3) the pre-collapse summit elevation of Bejenado (between 2100 and 2200 m) which is based on the shape of the reconstructed cone illustrated in Fig. 3b; (4) the substratum geology of Bejenado – group C volcaniclastics; and (5) the basal striations, associated basement rock comminution and the dislocation faulting within the toreva remnants. The latter indicate that post-emplacement settling motion occurred as the torevas slipped towards their current positions from their primary emplacement areas.

Furthermore, toreva slip during the course of the erosion of the Caldera resulted in the thinning and expulsion of the group B volcaniclastics under the load of the torevas. Based on the extent of basement rock comminution and slip-surface polishing, a minimum range of 0.1–0.5 km of settling motion is inferred to have taken place up until the erosion of the Caldera to its present form.

Attention needs to be drawn at this stage to the substratum conditions of Bejenado since it is at this level that the structural integrity of many volcanic edifices is most influenced (e.g. van Wyk de Vries and Borgia, 1996; van Wyk de Vries et al., 2001; Clavero et al., 2002). Moreover, Taburiente volcano exemplifies this understanding of the structural control on volcano instability at basement level since laterally extensive, pristine decollement zones are exposed in section (Roa, 2003). The partial construction of Taburiente upon the TCB, to which the developing edifice was cohesively bound, led to the loading and deformation of the TCB and the decoupling of the edifice stresses from the basement. The edifice spread under a high gravitational potential upon its uplifted and seaward-tilted basement within the subaerial confines of the Ancestral Taburiente collapse embayment (Roa, 2003). The west flank and summit subsequently developed into a slump-like structure whilst a separate rift-centred volcano, the Cumbre Nueva edifice (Ancochea et al., 1994) merged onto the south flank. The 240-$km^3$ slump eventually collapsed into the Atlantic, incorporating most of the Cumbre Nueva rift axis. It produced a debris avalanche deposit that spread over 1160 $km^2$ across the submarine pedestal (Roa, 2003). Once the Caldera had formed, the water table around the destroyed summit region of Taburiente experienced instantaneous draw-down to a new level (the amphitheatre floor) that was largely over-run by the intra-collapse edifice of Bejenado.

Given that Bejenado volcano had developed upon foundations of similar mechanical incompetence (debris and toreva blocks associated with the earlier collapse amphitheatre/embayment-forming events), one may surmise that the instability of its north flank developed under similar conditions to the gravitational spreading-related collapses of Taburiente. It is proposed therefore that the north flank and summit of Bejenado destabilised by the loading of water-saturated group C volcaniclastics which deformed under the weight of the edifice. When the edifice failed it did so sequentially in order to have produced the discrete secondary amphitheatre. What triggered the collapse(s) is unknown at this stage. It is of course possible to envision a combination of factors such as the load bearing capacity and fluid pressurisation tolerance of group C, the distribu-

tion of edifice stress and the influence of seismic shock on these factors. Upon collapse, the disintegrating edifice (nascent torevas and volcaniclastic matrix) travelled no more than five radial kilometres against the slopes of the amphitheatre/embayment floor. Due to the proximity of the enclosing amphitheatre/embayment walls it is further suggested that the debris avalanche impacted against these escarpments before coming to rest. This deduction is substantiated by the very high value of the apparent coefficient of friction ($H/L$). The summit elevation range of Bejenado implies a fall of 1000–1200 m which, for the associated run out length, gives an apparent coefficient of friction between 0.2 and 0.24. These values are not an indication of flow efficiency; they merely reflect the deprivation of run out due to the confined environmental conditions.

The diffuse contacts and the intrusion of layering from adjacent strata within the toreva remnants are interpreted to indicate a transient breakdown of the cohesive strength of the constituent scoria deposits during peak landslide momentum and impact. The predominance of stratified scoria in the toreva remnants may also indicate that they are characteristic of the summit region of Bejenado where the stratocone-building emission centres were clustered.

### 6.2. *The sediment mass balance of Bejenado volcano*

There are a number of parameters which control the balance between erosion and sedimentation in collapsed volcanic terrains, specifically the collapse scarp morphology and the slope aspect, whilst the regional hydrology, eruptive activity and the debris avalanche dispersal characteristics are important modulating influences. Under suitable climatic and tectonic conditions, a large, unconsolidated debris avalanche deposit can undergo relatively rapid mobilisation from its source depocentre to peripheral borderlands, and thereafter further afield into larger basins (Cas and Wright, 1987; Fisher and Schmincke, 1994). For example, the Chiancone volcaniclastics are considered to reflect the reworking of detritus sourced from the Valle del Bove, substantial amounts of which must have accumulated initially by landsliding (Calvari and Groppelli, 1996). They are dispersed over a much wider area (40 $km^2$ at least) than El Time and are up to 30 m thick at outcrop (Calvari and Groppelli, 1996). However, these authors consider 300 m to be the mean thickness of Chiancone, which implies a volume in the order of 12 $km^3$. This is comparable to the missing mass of the source region – the Valle del Bove. Calvari and Groppelli (1996) further suggest that the Chiancone sediments were deposited during or later than the life span of ancestral Etna (Ellittico volcano) between 40 000 and 15 000 yr BP. Another example is the 25-$km^2$ Juan Grande alluvial fan on Gran Canaria which is sourced from the Barranco de Tirajana, a broad basin-shaped valley which developed by fluvial erosion and by multiple landslides that were individually smaller ($< 1$ $km^3$) than the events which dismantled Bejenado (Lomoschitz et al., 2002).

With these parameters and examples in mind, a speculative although detailed sediment mass balance model is put forth based on the positioning, sedimentary characteristics and the post-depositional downcutting of the El Time fan delta. These factors are interpreted to be indicative of: (1) an exclusive source region – the disfigured north flank of Bejenado volcano; (2) a primary depocentre the Caldera de Taburiente and the northernmost part of the Cumbre Nueva embayment; and (3) a limited time span for epiclastic mass transfer to have occurred. The palaeogeographic reconstruction in Fig. 10a illustrates this hypothesis in that the debris avalanche deposit was mobilised, almost in its entirety, from the Caldera toward the SW, between the collapsed north flank of Bejenado and the linear scarp forming the northern end of the Cumbre Nueva embayment. The debris avalanche deposit may have been bounded within the confines of the primary depocentre for some time before the steep topography was breached by the forerunner to the Barranco de Las Angustias. This proto-canyon was perhaps characterised by a narrow outwash channel, or sediment chute, that served the development and littoral progradation of the fan delta.

The fan delta thickened due to its constricted outlet and eventually it spread out over the gentle

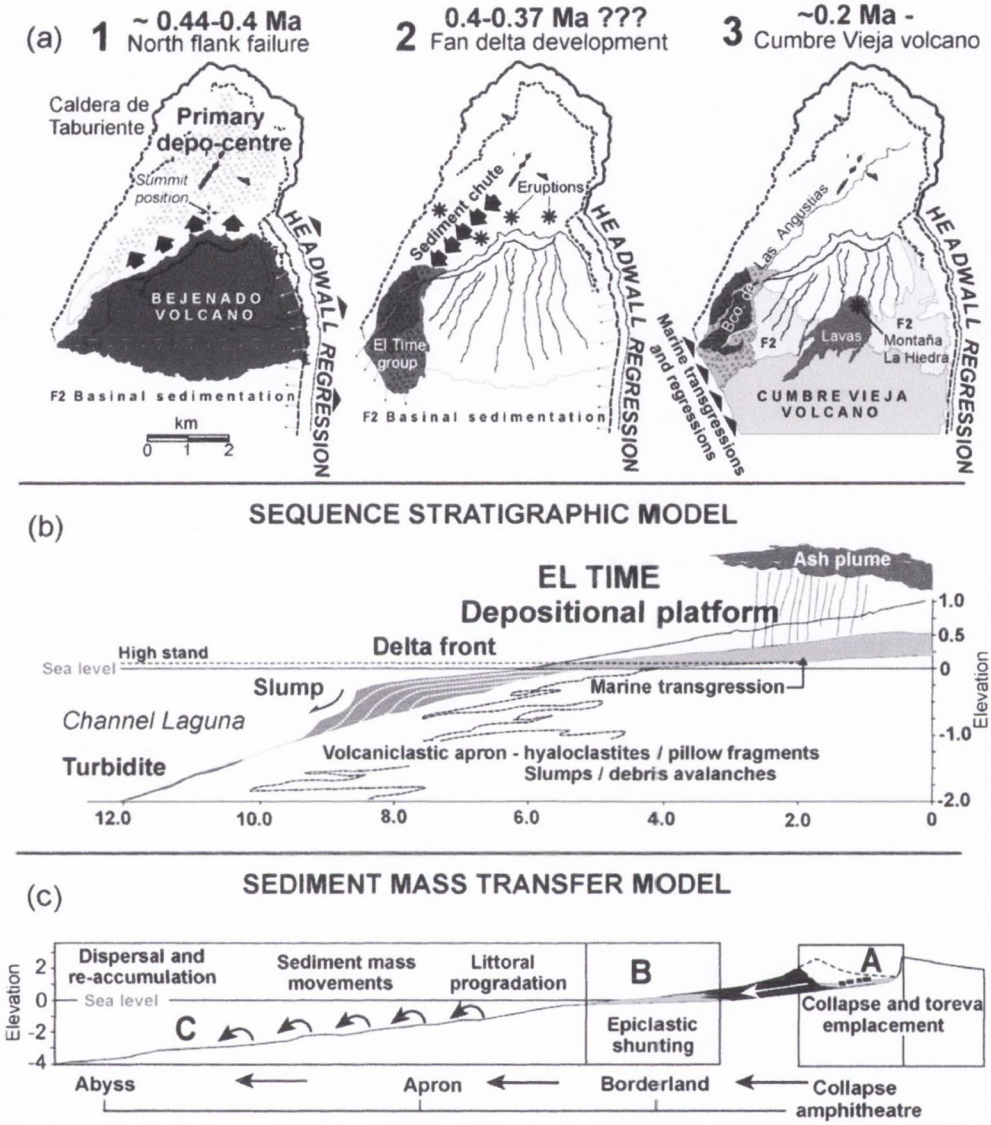


Fig. 10. (a) Palaeogeographic reconstructions 1–3 of Bejenado based on sedimentological data and extrapolation of available radiometric data: (1) collapse of the north flank of Bejenado within the confines of the Caldera/Cumbre Nueva embayment; (2) reworking of the north flank debris and accumulation of the El Time group; (3) continued erosion of the Caldera and growth of Cumbre Vieja volcano. (b) Sequence stratigraphic model of the entire depositional platform (all distances in meters). (c) Sediment mass transfer model tracing the progression of the Bejenado debris avalanche deposit from its primary depocentre to the abyssal plains at around −4000 m.

slopes of Tazacorte once it exceeded 100 m in thickness. The transfer of volcaniclastic materials between the primary and secondary depocentres probably occurred with most frequency during seasonal flash floods, yet simple dry gravity slides could have been just as frequent given the head of the proto-canyon. Bulk mass transfer of the reworked debris avalanche material may have been completed within a few tens of thousand of years based on a tentative comparison with the Chiancone volcaniclastics. Given that the El Time fan delta is a fraction of the size of Chiancone, and there are no major sequence stratigraphic unconformities, it is reasonable to assume

an accumulation interval of either comparable of lesser duration. Pronounced channel development, palaeosol horizons, erosional boundaries and the aggradation of debris flow units over significant thicknesses, are interpreted to indicate that the inter-eruptive periods of Bejenado were long throughout the period of deltaic sedimentation. The rate of sediment accumulation cannot have been constant in time since sea-level fluctuations, droughts, lava dams and landslides had modulated the erratic sedimentation rates during the progradation and retreat of the delta front.

The sequence stratigraphic model in Fig. 10b is based on a progradational delta front with a limited surface above sea level, which extends outward from the shoreline (the transgressive surface) to encompass a delta plain up to 10 $km^2$ in surface area above sea level. Progradation onto the volcanic apron contributed significantly to the development of the submarine channels as did turbulent mass flows generated by submarine sediment slides (Urgeles et al., 1999). Marine transgressions and regressions subsequently modified the subaqueous distribution of deltaic foresets by altering the depositional sequencing under the influence of tidal forces. The first non-eustatic marine transgression may have occurred soon after the Cumbre Nueva collapse, leading to the deposition of the sandstone–conglomerate unit outcropping at the base of El Time.

The floor of the Cumbre Nueva embayment was filled with fluvial sediments (F2) sourced from the bounding escarpments and from the south flank of Bejenado. The sediment outwashed into the Atlantic through a subaerial drainage system that is now enveloped, almost in its entirety, by Cumbre Vieja lavas. The flat-floored submarine channels to the west of the embayment may thus have developed as the submarine counterparts of a 'basinal' embayment drainage system characterised by high surface run-off. Based on their comparable backscatter (acoustic reflectance) the submarine channels could reflect a coeval input from the subaerial sediment outlets. The rate of sediment discharge entering these channels may have increased dramatically during the incipient subaerial stage of Cumbre Vieja volcanism prior to 0.125 Ma, as soft pyroclastic deposits were fed into the developing drainage system. The $^{14}C$ age determinations of the conglomerate groups (Vegas Salamanca et al., 1999) are thus an absolute minimum since the onset of F2 sedimentation must correlate with the interval of retrogressive erosion of the arcuate segment of Cumbre Nueva headwall (after 0.55 Ma). The F2 conglomerates accumulated over shallower slopes and at low rates of sedimentation relative to that of the El Time group.

Downcutting of the El Time group since the development of the current Caldera drainage system has resulted in the discharge of $\gg 2$ $km^3$ of post-El Time sediment (i.e. Taburiente basement rock) onto the volcaniclastic apron. It is in this environment that the bulk of the missing mass of Bejenado volcano has been distributed. This concept of cyclic sedimentation is illustrated in the total sediment discharge model (Fig. 10c) whereby the Bejenado debris avalanche deposit has undergone multiple stages of mobilisation from the Caldera to the lower submarine flanks leading onto the Madeira Abyssal plain. What remains to be discussed is the question of the total volume of collapsed Bejenado materials which have been mobilised from area A to C (Fig. 10c).

The current subaerial volume of the El Time group (1.21 $km^3$) and the insignificant volume of the toreva remnants (0.1 $km^3$) represent a fraction of the initial volume of the debris avalanche deposit at the time of its emplacement. Under the assumption that a large transgressive surface spread out below sea level away from the structural confines of the Cumbre Nueva escarpment, incorporating a volume greater than or equal to the onshore volume of El Time, then the total volume of remobilised volcaniclastic matrix should exceed 4 $km^3$. By including a conservative estimate of the initial volume of the toreva remnants (0.5 $km^3$), then the total volume of the debris avalanche may be constrained between 4.5 and 5 $km^3$.

Whilst the initial growth of Cumbre Vieja contributed to sedimentation processes within the subaerial confines of the Cumbre Nueva embayment, the encroachment of the Cumbre Vieja lavas upon the F2 fluvial conglomerates and the source headwalls in the last 0.1 Ma has totally

countered this effect. Moreover, most of the outcropping conglomerates will be mantled completely by further lavas vented from the northern part of Cumbre Vieja over the next 10–50 000 years. The most recent eruption on the northern segment of the Cumbre Vieja rift was from Montaña Quemada around the 15th century AD (Ancochea et al., 1994).

## 7. Conclusions

Bejenado stratovolcano developed upon the unroofed foundations of the earlier Taburiente shield volcano within the confines of the Caldera de Taburiente collapse amphitheatre and the northern part of coalescing Cumbre Nueva embayment. The stratocone reached an elevation of up to 2100 m above mean sea level and it was founded largely upon volcaniclastic materials that were emplaced within the Taburiente landslide structures. After $<0.1$ Ma of volcano growth the entire north flank and summit of Bejenado collapsed northwards and northwestwards into the Caldera/embayment subsequent to the deformation and failure of its mechanically incompetent substratum. Associated with the collapse were the large blocks of former volcanic edifice (torevas) that were transported intact within the sequential landslides. The toreva remnants are composed predominantly of layer-differentiated scoria with ancillary lavas and intrusives. Although the strata are relatively coherent, they are invariably disrupted and tilted due to the effects of the initial impact during emplacement and post-emplacement settling motion. The latter has resulted in basement rock comminution and internal faulting. The bulk of the debris avalanche deposit was mobilised from its primary depocentre (the Caldera) towards the SW at the northern opening of the Cumbre Nueva embayment. The secondary depocentre is characterised by the remains of a $>2$-km$^3$ fan delta deposit at El Time.

The fan delta stratigraphy records the shunting and reworking of the mass wasted volume of Bejenado whilst residual volcanism continued. Additional work is required to constrain the period of deltaic sedimentation by dating the lava flows interbedded within the sedimentary sequence with the use of rigorously tested radiometric cross correlations. Offshore progradation of the fan delta contributed to the development of flat-floored submarine channels via turbidity currents and other mass flow mechanisms (Urgeles et al., 1999). The escarpments generated by the Cumbre Nueva collapse regressed by residual gravitational spreading and erosion, feeding a subaerial basinal area with abundant sediment. The sediment load increased with the onset of Cumbre Vieja volcanism but decreased subsequently as volcanic activity overwhelmed the sedimentation rate.

## Acknowledgements

I am indebted to Chris Stillman, Pauline Agnew, J.C. Carracedo, Valentin Troll, John Murray, and Kate Walsh for their help with this project. Constructive reviews by Roger Urgeles and Sharon Allen significantly improved the original manuscript and are greatly appreciated. This work was partly supported by research grants and awards from Trinity College Dublin, a scholarship from the Spanish Ministry of Foreign Affairs, the Spanish National Map Project, and personal funding from Chris Stillman and Carl Laverty. Permission and assistance from the staff of the Parque Nacional de La Caldera de Taburiente and the CSIC in Tenerife are gratefully acknowledged.

## Appendix. Volume calculations in GIS

GIS matrices and CAD drawings are geo-referenced (or calibrated) to a coordinate system (e.g. UTM) which can be used for the spatial analysis of dimensional data. This enables volumetric calculations and the creation of the 3-D images as in Fig. 2. The volumes of most geological units (e.g. El Time, the toreva remnants, and the remaining exposed part of Bejenado) have been calculated by the use of a GIS extension called 3-D Analyst in Arcview version 3.2. The volume calculating procedure is as follows. The exact dimensions of

the geological unit are outlined to form a polygonal shape which forms the dimensional basis of a shape file. The 3-D attributes of this polygon are sourced from a digital elevation model which is constructed from a matrix or a CAD-based composite. The 3-D shape file is then converted into a geographic theme known as a TIN file. The surface area and volume attributes of this theme are calculated with reference to a datum or a plane (e.g. sea level or the lower limit of outcrop). The volume which is calculated represents the space that is above this datum and below the surface of the geographic theme.

## References


Ancochea, E., Hernán, F., Cendrero, A., Cantagrel, J.M., Fuster, J.M., Ibarrola, E., Coello, J., 1994. Constructive and destructive episodes in the building of a young Oceanic Island, La Palma, Canary Islands, and the genesis of the Caldera de Taburiente. J. Volcanol. Geotherm. Res. 60, 243–262.

Belousov, A., Belousova, M., Voight, B., 1999. Multiple edifice failures, debris avalanches and associated eruptions in the Holocene history of Shiveluch volcano, Kamchatka, Russia. Bull. Volcanol. 61, 324–342.

Calvari, S., Groppelli, G., 1996. Relevance of the Chiancone volcaniclastic deposit in the recent history of Etna Volcano (Italy). J. Volcanol. Geotherm. Res. 72, 239–258.

Capra, L., Macías, J.L., Scott, K.M., Abrams, M., Garduñoy-Monroy, V.H., 2002. Debris avalanches and debris flows transformed from collapses in the Trans-Mexican volcanic belt, Mexico – behavior and implications for hazard assessments. J. Volcanol. Geotherm. Res. 2362, 1–30.

Carracedo, J.C., 1994. The Canary Islands: an example of structural control on the growth of large oceanic-island volcanoes. J. Volcanol. Geotherm. Res. 60, 225–241.

Carracedo, J.C., Day, S., Guillou, H., Torrado, J.P., 1999a. Giant Quaternary landslides in the evolution of La Palma and El Hierro, Canary Islands. J. Volcanol. Geotherm. Res. 94, 169–190.

Carracedo, J.C., Day, S., Guillou, H., Gravestock, P., 1999b. The later stages of the volcanic and structural evolution of La Palma, Canary Islands: The Cumbre Nueva giant collapse and the Cumbre Vieja Volcano. Geol. Soc. Am. Bull. 111, 755–768.

Carracedo, J.C., Guillou, H., Rodríguez Badiola, E., 2001. Mapa Geológico De España (*MAGNA*). Norte y sur de La Palma. Hojas 1083–1087.

Cas, R.A.F., Wright, J.V., 1987. Volcanic Successions: Modern and Ancient. Chapman and Hall, London, pp. 1–528.

Clavero, J.E., Sparks, R.J.S., Huppert, H.E., Dade, W.B., 2002. Geological constraints on the emplacement mechanism of the Parinacota debris avalanche, northern Chile. Bull. Volcanol. 64, 40–54.

Coello, J., 1987. Las Aguas subterráneas en las formaciones volcánicas del norte de La Palma (islas Canarias). Com. Simp. Int. Rec. Hidraul. Canarias Agua 2000, 19 pp.

Crandell, D.R., 1989. Gigantic debris avalanche of Pleistocene age from ancestral Mt. Shasta Volcano, California, and debris avalanche hazard zonation. U.S.G.S. Bull. 1861, 1–32.

Dañobeitia, J.J., Canales, J.P., 2000. Magmatic underplating in the Canary Archipelago. J. Volcanol. Geotherm. Res. 103, 27–41.

De la Nuez, J., 1983. El complejo intrusivo subvolcánico de la Caldera de Taburiente, La Palma. Col. Tesis Doctórale, Ed. Complutense, 401 pp.

Fisher, R.V., Schmincke, H.-U., 1984. Pyroclastic Rocks. Springer, Berlin, 472 pp.

Fisher, R.V., Schmincke, H-U., 1994. Volcaniclastic sediment transport and deposition. In: Pye, K. (Ed.), Sediment Transport and Deposition Processes. Blackwell, Oxford, pp. 351–388.

Gastesi, P., Hernández-Pacheco, A., Muñoz, M., 1966. Los rocas holocristalinas de la Caldera de Taburiente, Isla de la Palma (Canarias). Estud. Geol. 23, 113–134.

Gee, J., Staudigel, H., Tauxe, L., Pick, T., Gallet, Y., 1993. Magnetization of the La Palma Seamount Series: Implications for seamount palaeopoles. J. Geophys. Res. 98, 11743–17767.

Glicken, H., 1996. Rockslide debris avalanche of May 18, 1980, Mount St. Helens Volcano, Washington. U.S.G.S. Open-file Report 96–677, 90 pp..

Guillou, H., Carracedo, J.C., Duncan, R.A., 2001. Unspiked K–Ar, $^{40}Ar$–$^{39}Ar$ dating and magnetostratigraphy of Brunhes and Matuyama lava sequences from La Palma Island. J. Volcanol. Geotherm. Res. 106, 175–194.

Hernández-Pacheco, A., Afonso, A., 1974. Mapa geológica de la Caldera de Taburiente, Isla de San Miguel de La Palma. *M.O.P., D.G.O.H., S.G.O.P.*, Madrid.

Lomoschitz, A., Meco, J., Corominas, J., 2002. The Barranco de Tirajana basin Gran Canaria (Spain). A major erosive landform caused by large landslides. Geomorphology 42, 117–130.

Lyell, C., 1855. A Manual of Elementary Geology, II. London, 498 pp.

Mehl, K.W., Schmincke, H.-U., 1999. Structure and emplacement of the Roque Nublo debris avalanche deposit, Gran Canaria, Spain. J. Volcanol. Geotherm. Res. 94, 105–134.

Middlemost, E.A.K., 1970. San Miguel de la Palma. A volcanic island in section. Bull. Volcanol. 34, 216–239.

Navarro, J.M., Coello, J., 1993. Geological map of the Caldera de Taburiente. Ministerio de Medio Ambiente, Organismo Autónom, Madrid.

Roa, K., 2003. The Influence of Volcanic Spreading in the Structural Evolution and Landslide Kynematics of Taburiente Volcano, La Palma, Canary Islands. Ph.D. Thesis, University of Dublin, Dublin, 208 pp.

Staudigel, H., Schmincke, H-U., 1984. The Pliocene seamount series of La Palma, Canary Islands. J. Geophys. Res. 89, 1195–1215.

Staudigel, H., Féraud, G., Giannérini, G., 1986. The history of intrusive activity on the island of La Palma (Canary Islands). J. Volcanol. Geotherm. Res. 27, 299–322.

Urgeles, R., Masson, D.G., Canals, M., Watts, A.B., Le Bas, T., 1999. Recurrent large scale landsliding on the west flank of La Palma, Canary Islands. J. Geophys. Res. 11, 20331–20348.

van Wyk de Vries, B., Borgia, A. 1996. The role of basement in volcano deformation. In: McGuire, Jones, Neuberg (Eds.), Volcano Instability on the Earth and other Planets. Geol. Soc. Spec. Pub. 110, pp. 95–100.

van Wyk de Vries, B., Self, S., Francis, P.W., Keszthelyi, L., 2001. A gravitational spreading origin for the Socompa debris avalanche. J. Volcanol. Geotherm. Res. 105, 225–247.

Vegas Salamanca, J., Hernández Pacheco, A., Marfil Pérez, R., 1999. Los depósitos volcanoclásticos de la isla de La Palma (Canarias): su relación con la evolución de las calderas de Taburiente y Cumbre Nueva. Bol. Geol. Min. 110, 135–158.

Wadge, G., Francis, P.W., Ramirez, C.F., 1995. The Socompa collapse and avalanche event. J. Volcanol. Geotherm. Res. 66, 309–336.

Watts, A.B., Masson, D.G., 2001. New sonar evidence for recent catastrophic collapses of the north flank of Tenerife, Canary Islands. Bull. Volcanol. 63, 8–19.

# CHAPTER 3

# THE QUATERNARY COLLAPSES OF LA PALMA

**Fig. 3.1.1.** View to the northeast of the dismantled Plio-Pleistocene volcanoes forming northern La Palma. Solid white lines mark escarpments. Cumbre Vieja lavas and scoria cones (foreground) have infilled most of the Cumbre Nueva embayment floor. White stipple is the postulated summit cone of Taburiente. Yellow stipple is the Cumbre Nueva detachment fault. Photograph by Juan Socorro.

# EVOLUTION OF THE STRATIGRAPHIC NOMENCLATURE OF LA PALMA

## PLEISTOCENE

| STAGES OF VOLCANIC EVOLUTION | | | | | | | SUBAERIAL COLLAPSES | |
|---|---|---|---|---|---|---|---|---|
| | RIFT ZONES | | RIFT ZONES | | CENTRAL VENT | RIFT ZONES | | |
| **DIACHRONOUS MAGMATISM** IC | **SUBMARINE VOLCANISM** PS | **ANCESTRAL SHIELD** AT | **SUBSEQUENT SHIELD** TAB | **MATURE SHIELD** TAB-CN | **INTRA-COLLAPSE VOLCANISM** B | **RIFT VOLCANISM** CV | ?, 1.2, 0.55, >0.3 | *REFERENCES* |
| **Intrusive core** | Seamount Series | Ancestral Taburiente | Taburiente **TCB / La Farola ash - CND** **DECOLLEMENT ZONE** | Taburiente – CN | Bejenado stratocone | Cumbre Vieja Volcano | SUB, AT, CN-CdT, B | **THIS WORK** |
| **Intrusive complex** | Seamount Series | Garafia Volcano (1.722-1.208) | Lwr Taburiente (1.12 – 0.78) | Uppr Taburiente (0.78 – 0.41) | Bejenado Volcano (0.55-0.44) | Cumbre Vieja rift > 0.125 | GC, CN | *Guillou et al.* [2001] *Carracedo et al.* [2001] |
| **Basal Complex** | Basal Complex | Lower Old Series (2.03-1.3) | Upper Old Series (1.05 – 0.51) | Cumbre Nueva (0.88 – 0.72) | Bejenado Massif (0.77 – 0.6) | Cumbre Vieja Series <0.54 | AT, CN, CdT | *Ancochea et al.* [1994] |
| **Basal Complex** | Basal Complex | Taburiente I | Taburiente II | Cumbre Nueva | Bejenado stratocone | South rift | AT, CN | *Navarro and Coello* [1993] |
| **Old Series 1** | Old Series 1 | Old Series 2 | Old Series 3 | Old Series 4 | Old Series 4 | - | - | *Coello* [1987] |
| **Basal Complex** | Old Series | ← Series de la Pared → | | | | - | - | *De La Nuez* [1983] |
| **Basal Complex** | Old Series | Coberta Series (1.61 – 1.05) | Coberta Series 0.83 – 0.78 | | | Cumbre Vieja Series 0.62 | - | *Abdel Monem et al.* [1972] |
| | EROSIONAL UNCONFORMITY → | | | | | | | **ALL PREVIOUS WORKS** |
| **Basal Complex** | Pre-tilt G1 – 4.0 – 2.9 Syn tilt G2 (sills) >1.6 | | Post tilt <1.6 | | | | | *Staudigel et al.* [1986] |
| **Plutonic Complex** | Seamount Series | | | | | | | *Staudigel & Schmincke* [1984] |

Notes: CND – Cumbre Nueva Decollement. TCB – Tenerra Collapse Breccia.
All ages in Ma (millions of years). HOL – Holocene era
Abbrevitions as follows:- AT – Ancestral Taburiente, CN – Cumbre Nueva, CdT – Caldera de Taburiente, GC - Garafia Collapse.
SUB – Submarine slope failure.
Radiometric data of *Abdel-Monem et al.* [1972], *Staudigel et al.* [1986] and *Ancochea et al.* 1994 are K/Ar determinations
Radiometric data of *Guillou et al.* [2001] are K/Ar with cross correlated Ar/Ar determinations and paleomagnetism

## APPENDIX 2

# GIANT LANDSLIDES SOURCED FROM THE CANARY ISLAND VOLCANOES

| Location | Source | Name | Age (Ma) | Volume ($km^3$) | Area ($km^2$) | Runout | Type / cause | References |
|---|---|---|---|---|---|---|---|---|
| **El Hierro** | NW flank | El Golfo | 0.015-0.017 | 150-180 | 1500 | 65 | Debris avalanche | *Holcomb and Searle*, 1991; *Gee et al.*, 2001 |
| | SW flank | El Julán | >0.2 | 130 | 60-120 | 60 | Slump / debris avalanche | *Urgeles et al.*, 1998; *Gee et al.*, 2001 |
| | SE flank | San Andres | 0.17-0.54 | - | - | - | Possible aborted slump | *Gee et al.*, 2001; *Masson et al.*, 2002 |
| | SE flank | Las Playas II | 0.145-0.176 | <30 | 950 | 52 | Debris avalanche | *Gee et al.*, 2001; *Masson et al.*, 2002 |
| **La Palma** | N. flank | Bejenado | 0.44-0.3 | >5 | - | <5 | Possible slump collapse | [*Roa, 2003*] |
| | Summit | CdT | 0.55 | >30 | | - | Slump collapse | This work; *(chapters 2.6 and 4) Guillou et al.*, 2001* |
| | W flank | Cumbre Nueva | 0.55 | ~240 | 1160 | 63 | Slump collapse | This work; (*chapters 3.3 and 4*) *Guillou et al.*, 2001* |
| | S. flank | Ancestral Tab:‡ | 1.2 | >100 (?) | - | ~60 | Explosive caldera collapse | This work; *Ancochea et al.*, 1994* |
| | W. flank | Playa de la Veta | - | - | >1000 | 70 | Submarine flank failure | This work (*chapter 3.3*) *Urgeles et al.*, 1999; |
| | E.. flank | Santa Cruz ‡ | - | - | >1000 (?) | | (*see notes*) | *Masson et al.*, 2002 |
| | Summit (?) | La Cumbrecita | >1.7 | - | - | - | Submarine summit failure | This work (*chapter 2.6*) |
| **Tenerife** | S flank | Bandas de Sur | <2 | 25 | 500 | ~40 | - | *Krastel et al.*, 2001 |
| | SE flank | Güimar | 0.78-0.84 | >120 | 1600 | >50 | Debris avalanche | *Teide Group*, 1997; *Masson et al.*, 2002 |
| | N. flank | Orotava | 0.5-0.8 | 500 | 2100 | 90 | Slump collapse | *Teide Group*, 1997; *Hürlimann*, 1999; This work (ch.*6*) |
| | N. flank | Icod | 0.13-0.18 | >150 | 5500 (?) | 105 | Debris avalanche | *Ancochea et al.*, 1999 |
| | Summit | Roques de Garcia | 0.6-1.3 | 1000 | 5500 | 130 | Debris avalanche | *Cantagrel et al.*, 1999 |
| | - | Tigaiga | >2.3 | - | - | - | Debris avalanche | *Cantagrel et al.*, 1999 |
| | NE flank | Anaga | >>1 | - | >400 | - | - | *Ancochea et al.*, 1999 |
| | NW flank | Teno | >2 | - | - | - | - | *Ancochea et al.*, 1999 |
| **Gran Canaria** | Summit | Roque Nublo | 3.5 | 14 ↑ / 20 ↓ | 180 ↑ / 150 ↓ | >30 | Multiple slump collapses | *Mehl and Schmincke*, 1999, this work |
| | - | Fataga | 9-11.5 | - | - | - | Debris avalanche | *Schmincke and Sumita*, 1998 |
| | NW flank | Agaete | 14-15 | >50 | >500 | <30 | Debris avalanche | *Funck and Schmincke*, 1998 |
| | W flank | Horgazales basin | 14-15 | >80 | >1000 | >40 | Debris avalanche | *Funck and Schmincke*, 1998 |
| | North flank | N.C. Re-entrant | 12-15 | >60 | >700 | - | Possible debris avalanche | *Schmincke and Sumita*, 1998 |
| **Lanzarote** | NW flank | Famara | ? | - | - | - | - | |
| **Fuerteventura** | SW flank | Jandia | >17 | - | - | - | - | *Stillman*, 1999 |
| | SW flank | Jandia | <2 | 25 | 250 | - | Debris avalanche | *Krastel et al.*, 2001 |
| | W flank | CVC | >17 | - | - | - | Slump collapse | *Fernández et al.*, 1997; *Stillman* 1999; This work (ch.6) |

NOTE:
* Authors referenced for age data
↑ Onshore / ↓ offshore
‡ Possibly one of the same event

Appendix 3

## Poster Presentation – Abstract

Presented at the

## 45th Annual Irish Geological Research Meeting 2002

Friday 22nd – Sunday 24th February 2002
University College Dublin

# Volcanic spreading and lateral collapses at Taburiente volcano, La Palma, Canary Islands

Karl Roa
Department of Geology, Trinity College, Dublin 2

Taburiente is a Pleistocene oceanic island volcano in the western Canary islands. The most important events in its evolution are the giant lateral collapses that occurred at around 1.2 Ma and 0.55 Ma. Ancestral volcano growth was disrupted by a cataclysmic flank failure that was triggered by an eruption. Taburiente volcano developed inside the resultant collapse embayment upon successions of debris avalanche material and juvenile pyroclast deposits. After <0.4 Ma of post-collapse volcano growth, the volcaniclastic substratum began to deform under the weight of the Taburiente edifice. The volcanic superstructure decoupled from its uplifted basement along this substratum, leading to the inception of a giant slump sector along the west flank. Decollement zone maturation led to cataclasis and granular flow within basement rocks with particle size distributions strongly controlled by Reidel fractures, authigenesis and attendant fluid pressures. The slump sector was bounded by a major south striking rift zone that developed coherently as a consequence of flank spreading. Highly diffuse rift zones developed to the north of the edifice in areas of dense fracture connectivity activated by the spreading flanks. Flank instability culminated in the 0.55 Ma giant landslide (200 km3) that spread over an area of 1160 km² of the volcanic apron.

Available online @ www.geomond.ucd/htdocs/mpgrg/html/igrm-2002-abstracts.pdf

# REFERENCES


Acocella V., T. Korme, F. Salvini, R. Funiciello, Elliptic calderas in the Ethiopian Rift: control of pre-existing structures. *J. Volcanol. Geotherm.* Res. 2512,,1-15, 2002.

Abdel-Monem, A., N.D. Watkins and P.W. Gast. Potassium-Argon ages, volcanic stratigraphy and geomagnetic polarity of the Canary Islands: Tenerife, La Palma and Hierro. *Am. J. Sci.*, ***272,*** 805-825, 1971.

Ablay, G.J. and J. Martí. Stratigraphy, structure, and volcanic evolution of the Pico Teide-Pico Viejo formation, Tenerife, Canary Islands. *J. Volcanol. Geotherm. Res. 103*, 175-208, 2000.

Abratis, M, Schmincke, H.U. and Hansteen T.H., Composition and evolution of submarine volcanic rocks from the central and western Canary Islands. *Int J Earth Sci (Geol Rundsch),* 91:562–582, 2002.

Ancochea, E., F. Hernán, A. Cendrero, J.M. Cantagrel, J.M. Fuster, E. Ibarrola, and J. Coello, Constructive and destructive episodes in the building of a young Oceanic Island, La Palma, Canary Islands, and the genesis of the Caldera de Taburiente, *J. Volcanol Geotherm Res., **60,*** 243-262, 1994.

Anderson, E.M., Cone sheets and ring dykes; the dynamical explanation. *Bull. Volcanol.* **1**, 35-40, 1937.

Anguita, F. and F. Hernán, A propagating fracture model versus a hot-spot origin for the Canary Islands. *Earth. Plan. Sci. Lett., **27***, 11-19, 1975.

Anguita, F. and F. Hernán, The Canary Islands origin, a unifying model, *J. Volcanol Geotherm Res., **103,*** 1-26, 2000.

Araña. V and R. Ortiz, The Canary Islands: Tectonics/magmatism and geodynamic framework. In Kampunzu. A.B., Lubala, R.T. (eds) magmatism in extensional structural settings: the Phanerozoic African Plate. Springer-Verlag, Berlin, pp 189-198, 1991.

Ask, M.V.S., Mechanical tests on claystone from Ocean Drilling Program Hole 1070A (Leg 173) - implications for elevated pore-fluid pressure in sediments within the ocean–continent transition zone, West Iberia. *Mar. Geol., **177***, 395-410, 2001.

Azzaro, R., M. Mattia and G. Puglisi, Fault creep and kinematics of the eastern segment of the Pernicana fault (Mt. Etna, Italy) derived from geodetic observations and their tectonic significance. *Tectonophys. 333,* 401-415, 2001.

Badger, T.C. and R.J. Watters, Gigantic seismogenic landslides of Summer Lake basin, south-central Oregon. *Geol. Soc. Am. Bull., **116***, 687–697, 2004.

Barton, N., R. Lien and J. Lunde, Engineering classification of rock masses for the design of tunnel support. *Rock Mechanics*, ***6***, 189-236, 1974.

Barry, T.L., M.J. Branney and G. Andrews, Rapid welding and rheomorphism in unconfined (sheet-like) ignimbrites in Idaho, England and Pantelleria. *Geophys. Res. Abs. **5**, 01719*, 2003.

Belousov, A., M. Belousova and B. Voight, Multiple edifice failures, debris avalanches and associated eruptions in the Holocene history of Shiveluch volcano, Kamchatka, Russia. *Bull. Volcanol., **61***, 324-342, 1999.

Ben-Zion, Y. and C G. Sammis, Characterization of Fault Zones, *Pure Appl. Geophys. **160***, 677–715, 2003.

Bertrand, H., The Mesozoic tholeiitic province of Northwest Africa: a volcano-tectonic record of the early opening of the Central Atlantic. In Kampunzu. A.B., Lubala, R.T. (eds) magmatism in extensional structural settings: the Phanerozoic African Plate. Springer-Verlag, Berlin, pp. 147-188, 1991.

Billi, A., V. Acocella, R. Funiciello, G. Giordano, G. Lanzafame and M. Neri, Mechanisms for ground-surface fracturing and incipient slope failure associated with the 2001 eruption of Mt. Etna, Italy: analysis of ephemeral field data *J. Volcanol Geotherm Res., **122,*** 281-294, 2003.

Borgia, A. and B. Treves, Volcanic plates override the ocean crust: Structure and dynamics of Hawaiian volcanoes. *Geol. Soc. Spec. Pub., London, **60***, 277-299, 1992.

Borgia, A., L. Ferrari and G. Pasquare, Importance of gravitational spreading in the tectonic and volcanic evolution of Mount Etna. *Nature, **357***, 231-235, 1992.

Borgia, A. Dynamic basis of volcanic spreading. *J. Geophys. Res., **99***, 17,791–17,804, 1994.

Borgia, A., P.T. Delaney and R.P. Denlinger. SPREADING VOLCANOES. *Ann. Rev. Earth Planet. Sci. **28***, 539–70, 2000.

Borgia, A and B. van Wyk de Vries, The volcano tectonic evolution of Concepción, Nicaragua. *Bull. Volcanol. **65***, 248-266, 2003

Bos, B., C.J. Peach and C.J. Spiers. Frictional-viscous flow of simulated fault gouge caused by the combined effects of phyllosilicates and pressure solution. *Tectonophys.* ***327,*** 173-194, 2000.

Bosworth, W., K. Burke and M. Strecker, Effect of stress fields on magma chamber stability and the formation of collapse calderas, *Tectonics, 22*, 1-21, 2003.

Bravo Expósito, T. and J. Coello Armenta, Contribución a la hidrogeología de la Caldera de Taburiente, La Palma, Islas Canarias. 189-206, 1979.

Brodie, K.H., D. Fettes, B. Harte and R. Schmidt. Towards a unified nomenclature for metamorphic rocks. 5. Structural terms including fault rock terms. A proposal on behalf of the *IUGS Subcomission on the systematics of metamorphic rocks.* Web version 31.10.2002. 8 pp 2002

Cambridge Polymer Group, Inc. Cambridge Polymer Group Silly Putty™ "Egg". Consultation, Testing, and Instrumentation for Polymeric Materials. 3 pp. 2002. http://www.campoly.com/notes/sillyputty.pdf

Canales, J.P. and J.J. Dañobeitia. The Canary Islands swell: a coherence analysis of bathymetry and gravity. *Geophys. J. Int., 132*, 479-488. 1998.

Cannat, M., A. Briais, C. Deplus J. Escartín, J. Georgen , J .Lin, S. Mercouriev, C. Meyzen, M. Muller, G. Pouliquen, A. Rabain, P. da Silva, Mid-Atlantic Ridge–Azores hotspot interactions: along-axis migration of a hotspot-derived event of enhanced magmatism 10 to 4 Ma ago. *Earth Plan.. Sci. Letts., 173*, 257–269, 1999.

Cannat, M., M. Maia C. Deplus C. Durand, P. Agrinier, A. Belarouchi, G. Dubuisson E. Humler, J. Reynolds, Thin crust, ultramafic exposures, and rugged faulting patterns at the Mid-Atlantic Ridge (22°–24°N). *Geology*; 23, 49–52, 1995,

Carracedo, J.C., S. Day, H. Guillou, H. The Cumbre Nueva collapse and Cumbre Vieja volcano. La Palma geological excursion guidebook. 1-27, 1997.

Carracedo, J.C., S. Day, H. Guillou, H. Rodríguez, E. Canas and F.J. Pérez Torrado, Hotspot volcanism close to a passive continental margin. *Geol. Mag.* ***135***, 591-604, 1998

Carracedo, J.C., S. Day, H. Guillou and P. Gravestock, Later stages of volcanic evolution of La Palma, Canary Islands: Rift evolution, giant landslides and the origin of the Caldera de Taburiente. *Geol. Soc. Am. Bull.,* ***111***, 755-768, 1999a.

Carracedo, J.C., S. Day, H. Guillou and F.J. Pérez Torrado, Giant Quaternary landslides in the evolution of La Palma and El Hierro, Canary Islands. *J. Volcanol. Geotherm. Res.,* ***94,*** 169-190, 1999b.

Carracedo, J.C., H. Guillou, and E.R. Badiola, Mapa Geológico de España *(MAGNA).* Norte y sur de La Palma. Hojas 1083 a 1087, 2001a.

Carracedo, J.C., E.R. Badiola, J. de la Nuez and F.J. Perez Torrado, Geology and volcanology of La Palma and El Hierro, Western Canaries. *Estud. Geol. 57*, 175-273, 2001b.

Cervelli, P., P. Segall, K. Johnson, M. Lisowski and A. Miklius, Sudden aseismic fault slip on the south flank of Kilauea Volcano. *Nature,* ***415***, 1014-1018, 2002.

Chester, F.M. and J.M. Logan, Implications for mechanical properties of brittle faults from observations of the Punchbowl fault zone, California, *Pure, App. Geophys.,* ***124***, 79-106, 1986.

Chester, F. M. and J.S. Chester, J. S. Ultracataclasite Structure and Friction Processes of the Punchbowl Fault, San Andreas System, California, *Tectonophys 295*, 199–221. 1998.

Chester, F.M. Field Guide to the Punchbowl Fault Zone at Devil's Punchbowl, Los Angeles County Park, California. *Texas A&M University*, v. 2.1. 15 pp. 1999.

Childs, C., J. Watterson and J.J. Walsh, A model for the structure and development of fault zones, *J Geol. Soc. Lon.,* ***153***, 337-340, 1996.

Christiansen, R.L. and D.W. Peterson, Chronology of the 1980 eruptive activity, in Lipman. P.W., and Mullineaux D.R., (eds). The 1980 eruption of Mount Saint Helens, Washington. *USGS Prof. Pap.* ***1250,*** 743-756, 1981.

Christiansen, L.B. and G. Garven, Transient hydrogeologic models for submarine flow in volcanic seamounts: 2. Comparison of the Hawaiian, Canary, and Marquesas Islands, *J. Geophys Res.,* ***109***, 1-18, 2004.

Cladouhos, T. T., Shape preferred orientations of survivor grains in fault gouge. *J. Struct. Geol.,* ***21***, 419-436, 1999a.

Cladouhos, T. T., A kinematic model for deformation within brittle deformation zones. *J. Struct. Geol.,* ***21***, 437-488, 1999b.

Clague, D.A., and R.P. Delinger, Role of olivine cumulates in destabilizing the flanks of Hawaiian volcanoes. *Bull. Volcanol.*, ***56***, 425-434, 1994.

Clague, D.A., K.A. Hon, J.L. Anderson, W.W. Chadwick, and C.G. Fox, Bathymetry of Puna Ridge, Kilauea Volcano, Hawaii, in *U.S. Geological Survey Miscellaneous Investigations Series Map MF-2237*, 1994.

Clague, D.A. and J.G. Moore, The proximal part of the giant submarine Wailau landslide, Molokai, Hawaii. *J. Volcanol. Geotherm. Res* **113**, 259-287, 2002.

Clague, D.A., J.G. Moore and A.S. Davis, Volcanic Breccia and Hyaloclastite in Blocks from the Nuuanu and Wailau Landslides, Hawaii. In: Hawaiian Volcanoes; deep underwater perspectives (Takahashi, Lipman, García, Naka, Aramaki – Eds). Geophysical Monograph 128. American Geophysical Union, Washington, 279-296, 2002

Clement, J-P., Legendre, C., Caroff, M., Guillou, H., Cotton, J., Bollinger and G.,Guille. Epiclastic deposits and 'horseshoe-shaped' calderas in Tahiti (Society Islands) and Ua Huka (Marquesas Archipelago), French Polynesia. *J. Volcanol Geotherm Res., 120*, 87-101, 2002.

Clouard, V., A. Bonneville and P-Y. Gillot, A giant landslide on the southern flank of Tahiti Island, French Polynesia. *Geophys. Res. Letts,* 28, 2253-2256, 2001.

Coello, J., Las Aguas subterráneas en las formaciones volcánicas del norte de La Palma (islas Canarias). *Com. Simp.* Int. Rec. Hidraul. Canarias Agua 2000, 19pp, 1987.

Cronin, S.J., M. Bebbington and C.D Lai, A probabilistic assessment of eruption recurrence on Taveuni volcano, Fiji, *Bull, Volcanol.* ***63***, 274-288, 2001.

Crough, S.T., Seamounts as recorders of hotspot epeirogeny. *Geol. Soc. Am. Bull., 95*, 3-8, 1984.

Crowley, J.L., R.L. Brown and R.R. Parish. Diachronous deformation and a strain gradient beneath the Silkirk allochton, northern Monashee Complex, southeastern Canadian Cordillera. *J. Struct. Geol., 23*, 1102-1121, 2001.

Dañobeitia, J.J. and J.P. Canales, Magmatic underplating in the Canary Archipelago. *J. Volcanol Geotherm Res.,* ***103***, 27-41, 2000.

Dauteuil, O., J. Angelier, F. Bergerat, S. Verrier and T. Villemin, Deformation partitioning inside a fissure swarm inside the northern Icelandic rift. *J. Struct. Geol.,* ***23***, 1359-1372, 2000.

Davis, G.A., B.J. Darby, Z. Yadong and T.L. Spell, Geometric and temporal evolution of an extensional detachment fault, Hohhot metamorphic core complex, Inner Mongolia, China. *Geology,* ***30***, 1003–1006, 2002.

Day, S., Hydrothermal pore fluid pressure and the stability of porous, permeable volcanoes. In: Volcano Instability on the Earth and other Planets. (Eds. McGuire, Jones and Neuberg).*Geol Soc Publication* **110**, 77-93, 1996.

Day, S., J.C. Carracedo, H. Guillou, Age and geometry of an aborted rift flank collapse: the San Andres fault system, El Hierro, Canary Islands, *Geol. Mag.* ***134***, 1-14, 1997.

Day, S., J.C. Carracedo, H. Guillou and P. Gravestock, Recent structural evolution of the Cumbre Vieja volcano, La Palma, Canary Islands: volcanic rift zone configuration as a precursor to volcano flank instability? *J.Volcanol. Geotherm. Res.,* ***94***, 135-167, 1999.

Delaney, P.T., R.P. Delinger, M. Lisowski, A. Miklius, P. Okubu, A.T. Okamura, and M. Sako, Volcanic Spreading at Kilauea, 1976-1996. *J. Geophys. Res.,* ***103***, 18,003-18,023, 1998.

Delinger, R.P., and P. Okubo, Structure of the mobile south flank of Kilauea volcano, Hawaii, *J. Geophys. Res.*, ***102***, 18,091–18,100, 1997.

Delius, H., C. Bücker and J. Wohlenberg, DETERMINATION AND CHARACTERIZATION OF VOLCANICLASTIC SEDIMENTS BY WIRELINE LOGS: SITES 953, 955, AND 956, CANARY ISLANDS. In Weaver, P.P.E., Schmincke, H.-U., Firth, J.V., and Duffield, W. (Eds.), *Proceedings of the Ocean Drilling Program, Scientific Results,* ***157***, 29-37, 1998

De La Nuez Pestana, J., 1983. El complejo intrusivo subvolcanico de la Caldera de Taburiente, La Palma. Tesis Doctórales, Ed. Complutense, 401 pp.

De Voogd, B., S. Pou Palome, A. Hirn, P. Charvis J. Gallart, Vertical movements and material transport during hotspot activity: seismic reflection profiling offshore La Reunion. *J. Geophys. Res.* ***104***, 2855–74, 1999.

Deplus, C, A. Le Friant, G. Boudon, J-C. Komorowski, B. Villemant, C. Harford, Jes Ségoufin, J-L. Cheminée, Submarine evidence for large-scale debris avalanches in the Lesser Antilles Arc. *Earth Plan. Sci. Letts,* ***192***, 145-157, 2001

den Brok, B. and O. Jagoutz, The Glarus thrust an erosional unconformity? An old idea of Otto Ampferer revisited. Abstract for *17th Swiss Tectonics Studies Group Meeting* Mar. 31 - April 1 2000.

Devey, C.W., K.S. Lackschewitz, D.F. Mertz, B. Bourdon, J.-L. Cheminée, J. Dubois, C. Guivel, R. Hekinian, P. Stoffers, Giving birth to hotspot volcanoes: Distribution and composition of young seamounts from the seafloor near Tahiti and Pitcairn islands. *Geology, **31***, 395–398, 2003.

Deniel, C., G. Kieffer and J. Lecointre, New $^{230}Th$–$^{238}U$ and $^{14}C$ age determinations from Piton des Neiges volcano, Reunion - A revised chronology for the differentiated series. *J. Volcanol. Geotherm. Res. **51***, 253–267. 1992.

Driscoll, N.W., J.K. Weissel and J. A. Goff, Potential for large-scale submarine slope failure and tsunami generation along the U.S. mid-Atlantic coast. *Geology,* 28, 407–410, 2000.

Eakins, B.W., J.E. Robinson, T. Kanamatsu, J.Naka, J.R. Smith, E. Takahashi and D. Clague, Hawaii's Volcanoes Revealed. *USGS Geological Investigation Series I-2809*, 2003

Ellsworth, D. and B. Voight, Dike intrusion as a trigger of large earthquakes and the failure of volcano flanks. *J. Geophys. Res. **100***, 6005-6024, 1995

Ellsworth, D. and B. Voight, Evaluation of volcano flank instability triggered by dyke injection. In Volcano Instability on the Earth and other Planets. *(eds McGuire, Jones and Neuberg). Geol Soc Publication **110***, 45-53, 1996.

Ellsworth, D. and S.J. Day, Flank collapse triggered by intrusion: the Canarian and Cape Verde Archipelagoes *J. Volcanol. Geotherm. Res.*, ***94***, 323–340, 1999.

Fernández, C., Casillas, R. Ahijado, A. Perelló, V., and A. Hernández-Pacheco. Shear zones as a result of intraplate tectonics in oceanic crust: the example of the Basal Complex of Fuerteventura (Canary Islands), *J. Struct. Geol. **19***, 41-57, 1997.

Fernández, C., J de la Nuez, R. Casillas and E. García Navarro, Stress fields associated with the growth of a large shield volcano (La Palma, Canary Islands), *J. Geophys Res., 21.,* 1-18, 2002.

Féraud, G., G. Giannérini, R. Campredon and C.J. Stillman, Geochronology of some Canarian dike swarms: Contribution to the volcano-tectonic evolution of the archipelago. *J. Volcanol. Geotherm. Res.*, **25**, 29-52, 1985.

Fiske, R.S., and E.D. Jackson, Orientation and growth of Hawaiian volcanic rifts: the effect of regional structure and gravitational stresses. *Proc. R. Soc London. **329***, 299-326, 1972.

Francis, P.W., M. Gardeweg, C.F. Ramirez and D.A. Rothery, Catastrophic debris avalanche deposit of Socompa volcano, northern Chile. *Geology **13***, 600-603, 1985.

Fredlund, D.G., What is the Future for Slope Stability Analysis? (Are We Approaching the Limits of Limit Equilibrium Analices?). Second Symposium and Short Course on Unsaturated Soils and Environmental Geotechnics. Powerpoint presentation, Budapest, Hungary November 4-5, 2003.
Available online at: www.gtt.bme.hu/2nd SCUSEG/FREDLUNDSlopeStabilityFuture4.ppt

Gallego, D., Garcia, R., Hernandez, E, Gimeno, L. and Ribero P. NAO influence on precipitation in the Canary Islands. Universidad Complutense Madrid/University of Vigo. Poster presentation. 2000.

Garcia, M.O., Turbidites from slope failure on the Hawaiian Volcanoes. In Volcano Instability on the Earth and other planets, Eds McGuire, Jones and Neuberg. *Geol. Soc. Public.*, ***110***, 281-294, 1996.

Gastesi, P., Hernández-Pacheco, A. and Muñoz, M., Los rocas holocristalinas de la Caldera de Taburiente, Isla de la Palma (Canarias). *Estud. Geol.*, ***23***, 113-134, 1966.

Gee, J., H. Staudigel, L. Tauxe, T. Pick and Y. Gallet. Magnetization of the La Palma seamount series: Implications for seamount palaeopoles. *J. Geophys Res., **98***, 11,743-11,767, 1993.

Gee, M.J.R., D.G. Masson, A.B. Watts and P.A. Allen, The Saharan debris flow: an insight in the mechanics of long run-out submarine debris flows, *Sedimentology, **46***, 317-335, 1999.

Gee, M.J.R., D.G. Masson, A.B. Watts and N.C. Mitchell, Offshore continuation of volcanic rift zones, El Hierro, Canary Islands. , *J. Volcanol Geotherm Res., 105,* 107-119, 2001a.

Gee, M.J.R, A.B. Watts, D.G. Masson, and N.C. Mitchell, Landslides and the evolution of El Hierro in the Canary Islands, *Mar. Geol., **177***, 271-293, 2001b.

Geist, D., W. M. White, F. Albarede, K. Harpp, R. Reynolds, J. Blichert-Toft and M. D. Kurz, Volcanic evolution in the Galapagos: The dissected shield of Volcán Ecuador. *Geochem, Geophys, Geophys, 3*, 1-32, 2002.

Geist, D., T. Naumann, J. Standish, K. Harpp, M. Kurz, and D. Fornari, Diffuse Rift Zones: Subaerial and submarine satellite vents at Wolf Volcano, Galapagos. Abstract. *AGU Fall Meeting*, 2003.

Gomberg, J., P. Bodin, W. Savage and M. E. Jackson, Landslide faults and tectonic faults, analogs?: The Slumgullion earth-flow, Colorado. *Geology*, **23**, 41–44, 1995

Gomez, F., W. Beauchamp and M.Barazangi, Role of the Atlas Mountains (northwest Africa) within the African-Eurasian plate-boundary zone. *Geology*, ***28***, 775-778, 2000.

Graham, E., Temperature and Precipitation Changes at La Palma, Canary Islands (1971-2000). 2003 http://www.eso.org/gen-fac/pubs/astclim/espas/espas_reports/LaPalma.Climate.pdf

Guillou, H., J.C. Carracedo and S.J. Day, Dating the Upper Pleistocene-Holocene volcanic activity of La Palma using the unspiked K-Ar technique, *J. Volcanol Geotherm Res.*, ***84***, 137-149, 1998.

Guillou, H., J.C. Carracedo and R.A. Duncan, K-Ar, $^{40}$ Ar-$^{39}$Ar ages and magnetostratigraphy of Brunhes and Matuyama lava sequences from La Palma Island. *J. Volcanol Geotherm Res.*, ***106***, 175-194, 2001.

Gudmundsson, A., L.B. Marinoni and J. Martí. Injection and arrest of dykes: implications for volcanic hazards. *J. Volcanol. Geotherm. Res.*, ***88***, 1999 1–13.

Guest, J.E., J.L. Gaspar, P.D., Cole, G. Queiroz, A.M. Duncan, N., Wallenstein, T. Ferreira, and J-M. Pacheco. Volcanic geology of Furnas Volcano, Sao Miguel, Azores, *J. Volcanol. Geotherm. Res.*, ***92*** 1–29, 1999.

Hansteen, T.H., A. Klügel and H-U. Schmincke, Multi-stage magma ascent beneath the Canary Islands: evidence from fluid inclusions, *Contrib. Minerol. Petrol.*, ***132***, 48-64, 1998.

Hernández-Hernández, P., Natura y cultura de las Islas Canarias, Tafor, 704 pp 2003

Hernández-Pacheco, A. and E. Ibarrola. Geochemical variation trends between the different Canary Islands in relation to their geological position. *Lithos*, ***6***: 389-402, 1973.

Hekinian, R., J.L. Cheminee, J. Dubois, P. Stoffers, S. Scott, C. Guivel, D. Garbe-Schönberg, C. Devey, B. Bourdon, K. Lackschewitz, G. McMurtry, E. Le Drezen, The Pitcairn hotspot in the South Pacific: distribution and composition of submarine volcanic sequences. *J. Volcanol Geotherm Res.*, ***2546***, *1-27, 2002.*

Hildenbrand, A., P-Y. Gillot, V. Soler and P. Lahitte, Evidence for a persistent uplifting of La Palma (Canary Islands), inferred from morphological and radiometric data. *Earth Plan. Sci. Letts.*, ***210***, 277-289, 2003.

Hoek, E. and W.J. Bray, Rock Slope Engineering. Institute of Mining and Metallurgy, London. 358 pp., 1981.

Hoernle, K. and H-U. Schmincke, The role of partial melting in the 15-Ma geochemical evolution of Gran Canaria: a blob model for the Canary hotspot. *J. Petrol.34*, 599–626, 1993.

Hsü, K.J., Role of Cohesive Strength in the Mechanics of Overthrust Faulting and of Landsliding, *Geol. Soc. Am. Bull.*. ***80***, 927-952, 1969.

Hull, J., Thickness-displacement relationships for deformation zones, *J. Struct. Geol.* ***10***, 431-435, 1988.

Hürlimann, M., Geotechnical analysis of large volcanic landslides: The La Orotava events on Tenerife, Canary Islands. Ph.D dissertation. Technical University of Catalonia. 205 pp., 1999.

Hürlimann, M., J.O. Garcia-Piera and A. Ledesma, Causes and mobility of large volcanic landslides: application to Tenerife, Canary Islands. *J. Volcanol Geotherm Res.*, ***103***, 121-134, 2000.

Iverson, R.M., Can magma-injection and groundwater forces cause massive landslides on Hawaiian volcanoes? *J. Volcanol. Geotherm. Res.*, ***66***. 295-308, 1995.

Iverson, R.M., Landslide triggering by rain infiltration, Water Resources Research, 36, 1897-1910, 2000.

Iverson, R.M. and J.W. Vallance, New views of granular mass flows. *Geology*, ***29***, 115–118, 2001.

Janssen, C., A. Hoffman-Rothe, S. Tauber and H. Wilke, Internal structure of the Precordilleran fault system (Chile) – insights from structural and geophysical observations. *J. Struct. Geol.*, ***24***, 123-143, 2002.

Jimenéz, M-J., and M. García Fernández, Aftershock sequence of the 9 May 1989 Canary Islands earthquake. *Tectonophysics, 255*, 157-162, 1996.

Jimenéz, M-J., and M. García Fernández, Occurrence of shallow earthquakes following periods of intense rainfall in Tenerife, Canary islands. *J. Volcanol Geotherm Res., 103*, 463-468, 2000.

Kaátson, D. and J-C. Thouret. Reply to the comment on the article "Erosion calderas: origins, processes, structural and climatic control. *Bull. Volcanol. 63*, 291-292, 2001.

Kampunzu, A.B. and M. Popoff, Distribution of the main Phanerozoic African rifts and associated magmatism: introductory notes. In. Kampunzu, A.B. Lubala. R.T. (eds) *Magmatism in extensional structural settings: the Phanerozoic African Plate.* Springer-Verlag, Berlin, pp. 2-10, 1991.

Kehl, R.O., Analysis of gravity sliding and Orogenic Translation. *Geol. Soc. America Bull.,* ***91***, 1641-1644, 1970.

Krastel, S., H-U. Schmincke, C.L. Jacobs, R. Rihm, T.P. Le Bas and B. Ailbés, Submarine landslides around the Canary Islands. *J. Geophys. Res., 106,* 3977–3997, 2001.

Krastel, S. and H-U. Schmincke, Crustal structure of northern Gran Canaria, Canary Islands, Spain deduced from active seismic tomography. *J. Volcanol Geotherm Res. 115,* 153-177, 2002.

Labaume, P. and I Moretti, Diagenesis dependence of cataclastic thrust fault zone sealing in sandstone: examples from the Bolivian Sub-Andean Zone, *J. Struct Geol., 23* 1659-1675, 2001.

Labuzuy, P., Recurrent landslide events on the submarine flank of Piton de la Fournaise Volcano (Reunion Island). In. McGuire, Jones, Neuberg (eds) Volcano instability on the Earth and other planets. *Geol. Soc. Spec. Pub. 110.* 295-306, 1996.

Laouafa, F., and F. Darve, Modelling of slope failure by a material instability mechanism. *Computers and Geotechnics,* ***29***, 301-235, 2002.

Lancelot, J.R., Allegre, C.J., Origin of carbonatite magma in the light of the Pb-U-Th isotope system. *Earth Planet. Sci. Lett., 22*, 233-238, 1974.

Le Friant, A G. Boudon, C. Deplusand and B. Villemant, Large-scale flank collapse events during the activity of Montagne Pele´e, Martinique, Lesser Antilles, *J. Geophys. Res., 108*, 2003. (Pages not specified by AGU)

Legros, F., The mobility of long runout landslides. *Eng. Geol., 63*, 301-331, 2002.

Lipman, P.W., T.W. Sisson, T. Ui., J. Naka and R. Smith, Ancestral submarine growth of Kĩlauea volcano and the instability of its south flank. In: Hawaiian Volcanoes; deep underwater perspectives (Takahashi, Lipman, Garcia, Naka, Aramaki – Eds). Geophysical Monograph 128. American Geophysical Union, Washington, 161-191, 2002.

Lipman, P.W., B.W. Eakins and H. Yokose, Ups and downs on spreading flanks of oceanic island volcanoes: Evidence from Mauna Loa and Kĩlauea. *Geology, 31*, 841-844, 2003.

Little, T.A., Brittle deformation adjacent to the Awatere strike-slip fault in New Zealand: Faulting patterns, scaling relationships, and displacement partitioning. *GSA Bulletin*, 107, 11, 1255–1271, 1995.

Lockner, D.A., Rock failure. In: Rock physics and phase relations. A handbook of physical constants, edited by T.J. Ahrens. *AGU Reference Shelf, 3*, 127-146, 1995.

Lyell, C., *A Manual of Elementary Geology*. London, 498 pp., 1855.

Mader, C.L., MODELING THE LA PALMA LANDSLIDE TSUNAMI *Science of Tsunami Hazards*, 19, 150-170, 2001.

MacLeod, C.J., J. Escartín, D. Banerji, M. Gleeson, D.H.B. Irving, R.M. Lilly, A.M. McCaig, Y. Niu, S. Allerton and D.K. Smith. Direct geological evidence for oceanic detachment faulting: The Mid-Atlantic Ridge, 15°45'N. *Geology,* 30, 879–882, 2002.

Magloughlin F., F. Chester and J. Spray, Penrose Conference Report: Fine Grained Fault Rocks. *Extended version from GSA Today* (6, 4, 1996). 12pp. 1996.

Malengreau, B., J.F. Lenat and J.F. Froger, Structure of Reunion Island, Indian Ocean inferred from the interpretation of gravity anomalies. *J. Volcanol and Geotherm. Res.*, 88, 131–146, 1999.

Martí. J. and A. Gudmundsson, The Las Cañadas caldera (Tenerife, Canary Islands): an overlapping collapse caldera generated by magma chamber migration. *J Volcanol Geotherm Res.* ***103,*** 161-173, 2001.

Marinoni, L.B. and G. Pasquare, Tectonic evolution of the emergent part of a volcanic ocean island: Lanzarote, Canary Islands. *Tectonophys 239*, 111-135, 1994.

Marinoni, L.B. and Gudmundsson, A., Dykes, faults and palaeostresses in the Teno and Anaga massifs of Tenerife (Canary Islands). *J. Volcanol. Geotherm. Res.,* 103, 83-103, 2000.

Marinoni, L.B., Crustal extension from exposed sheet intrusions: review and method proposal. *J. Volcanol. Geotherm. R.es.,* ***107,*** 27-46, 2001.

Masson, D.G., A.B. Watts, M.J.R. Gee, R. Urgeles, N.C. Mitchell, T.P. Le Bas and M. Canals, Slope failures on the flanks of the western Canary Islands, *Earth Sci. Rev.,* ***57***, 1-35, 2002.

Mazzarini, F., and P. Armienti, Flank cones at Mount Etna volcano: Do they have a power-law distribution?

*Bull. Volc.*, ***62***, 420-430, 2001.

McDougall, I., The geochronology and evolution of the young volcanic island of Reunion Indian Ocean. *Geochim. Cosmochim. Acta 35 3* , 261–288. 1971.

McKinnon, S.D., I. Garrido de la Barra, Fracture initiation, growth and effect of stress field: a numerical investigation. *J. Struct. Geol.* ***20***, 1673-1689, 1998.

Mehl, K.W. and H-U. Schmincke, Structure and emplacement of the Pliocene Roque Nublo debris avalanche deposit, Gran Canaria, Spain. *J. Volcanol. Geotherm. Res.*, ***94***, 105–134, 1999.

Merle, O. and J-F. Lenat, Hybrid collapse mechanism at Piton de la Fournaise volcano, Reunion Island, Indian Ocean, *J. Geophys Res.*, ***108***, 1-11, 2003

METOC https://metoc.npmoc.navy.mil. 2003

Middlemost, E.A.K., San Miguel de La Palma – a volcanic island in section, *Bull. Volcanol.* ***34***, 216-239, 1970.

Mitchell, N.C., Transition from circular to stellate forms of submarine volcanoes. *J. Geophys. Res.*, ***106***, 1987-203, 2001.

Mitchell, N.C., D. G. Masson, A.B. Watts, M. J. R. Gee and R. Urgeles, The morphology of the submarine flanks of volcanic ocean islands. A comparative study of the Canary and Hawaiian hot spot islands. *J. Volcanol. Geotherm. Res.*,***115***, 1-26, 2002.

Mitchell, N.C., W.B. Dade and D.G. Masson. Erosion of the submarine flanks of the Canary Islands. *J. Geophys. Res.*, ***108***, 2003. Pages not listed on AGU website

Mitchell, N.C., Susceptibility of mid-ocean ridge volcanic islands and seamounts to large-scale land-sliding *J. Geophys Res* 108, 2003. Pages not listed on AGU website

Monzier, M., C. Robin, P. Samaniego, M.L. Hall, J. Cotton, P. Mothes, P. and N. Arnaud, Sangay Volcano, Ecuador: structural development, present activity and petrology. *J. Volcanol. Geotherm. Res.*,***90***, 49-79, 1999.

Moore, J.G., D.A. Clague, R.T. Holcomb, P.W. Lipman, W.R. Normark, and M.E. Torresan, Prodigious submarine landslides on the Hawaiian Ridge, *J. Geophys. Res.*, ***94***, 17465-17484, 1989.

Moore, J.G. and D.A. Clague, Mapping the Nuuanu and Wailau Landslides in Hawaii. In: Hawaiian Volcanoes; deep underwater perspectives (Takahashi, Lipman, Garcia, Naka, Aramaki – Eds). Geophysical Monograph 128. American Geophysical Union, Washington. 223-244, 2002

Moss, J.L., W.J. McGuire and D. Page Ground deformation monitoring of a potential landslide at La Palma, Canary Islands, *J. Volcanol. Geotherm. Res.*, 94, 251–265, 1999.

Morgan, W.J., Hotspot tracks and the early rifting of the Atlantic. *Tectonophysics, 94*, 123-139, 1983.

Morgan, J.K and M.S. Boettcher, Numerical simulations of granular shear zones using distinct element method 1. Shear zone kinematics and the micromechanics of localization. *J. Geophys. Res.*, ***104***, 2703–2719, 1999.

Morgan, J.K., F. Gregory, D.J. Moore, S. Leslie, Overthrusting and sediment accretion along Kilauea's mobile south flank, Hawaii. Evidence for volcanic spreading from marine seismic reflection data. *Geology, **28**,* 667-670, 2000.

Morgan, J.K. and D.A. Clague, Volcanic spreading on Mauna Loa Volcano, Hawaii: Evidence for accretion, alteration and exhumation of volcaniclastic sediments. *Geology, 31*, 411-414, 2003.

Müller, C., F. Theilen and B. Milkereit, Large gas-prospective areas indicated by bright spots. *World Oil*, Jan., 60-67, 2000.

Munro, D.C. and S.K. Rowland, Caldera morphology on the western Galápagos and implications for volcano eruptive behaviour and mechanisms of caldera formation. *J. Volcanol. Geotherm. Res.*, ***72***, 85-100, 1996.

Naumann, T. and Geist, D., Physical volcanology and structural development of Cerro Azul Volcano, Isabela Island, Galápagos: implications for the development of Galápagos-type shield volcanoes. *Bull. Volcanol.*, ***61***, 497-514, 2000.

Navarro Latorre, J.M., Farrujía, I. Bases para el planeamiento hidrologico insular: aspectos geológicos e hidrogeológicos. Plan Hidrológico Insular de Tenerife. Cabildo Insular de Tenerife, *Sección de Planifación Hidráulica*, 135 pp., 1989

Navarro Latorre, J.M. and J.J. Coello Bravo, Geological map of the Caldera de Taburiente. *Ministerio de Medio Ambiente*, Madrid, 1993.

Neumann, E.R., V.B. Sørensenb, S.L. Simonsen and K. Johnsen, Gabbroic xenoliths from La Palma, Tenerife and Lanzarote, Canary Islands: evidence for reactions between mafic alkaline Canary Islands melts and old oceanic crust *J. Volcanol. Geotherm.Res., 103*, 313-342, 2000.

Nikogosian, I. K., T. Elliott and J.L.R. Touret, Melt evolution beneath thick lithosphere; a magmatic inclusion study of La Palma, Canary Islands. *Chem. Geol.*, ***183***, 169-193, 2002.

Norrish, N. I. and D.C. White, Rock slope stability analysis. *In:* Landslides; Investigation and mitigation A.K. Turner and R.L.Schuster Eds. Special Report 247. Transport and Research Board. *National Academy Press, Washington* 675 pp.

Oehler, J.F., P. Labazuy and J.F. Lénat, DEBRIS AVALANCHE DEPOSITS ON THE SUBMARINE FLANKS OF REUNION ISLAND. IMPLICATIONS ON ITS EVOLUTION MODEL. *Geophysical Research Abstracts*, Vol. 5, 06258, European Geophysical Society 2003

Owen, S., P. Segall, M. Lisowski, A. Miklius, R. Delinger and M. Soko, Rapid deformation of Kilauea Volcano: Global Positioning System measurements between 1990 and 1996, *J. Geophys. Res.*, ***105***, 18,983-18,998, 2000.

Pararas-Carayannis, G., EVALUATION OF THE THREAT OF MEGA TSUNAMI GENERATION FROM POSTULATED MASSIVE SLOPE FAILURES OF ISLAND STRATOVOLCANOES ON LA PALMA, CANARY ISLANDS, AND ON THE ISLAND OF HAWAII. *Science of Tsunami Hazards*, 20, 251 – 277, 2002.

Paris, R. and J.C. Carracedo, Formation d'une caldera d'érosion et instabité récurrente d'une île de point chaud; Caldera de Taburiente, La Palma, Iles Canaries. Géomorphologie, 2, 93-105, 2001.

Pérez-Torrado, F.J., Volcanoestratigrafía del Grupo Roque Nublo (Gran Canaria). Ph.D Thesis. Univ. De Las Palmas, Gran Canaria. 510 pp. 1992.

Pérez-Torrado, F.J., J..Martí, I. Queralt and J. Mangas. Alteration process of the Roque Nublo ignimbrites (Gran Canaria, Canary Islands). *J. Volcanol. Geotherm. Res.*, ***65***, 191-204, 1995

Peterson, S., P.M. Herzig, M.D. Hannington, I.R. Jonasson and A. Arrabis JR., Submarine Gold Mineralization Near Lihir Island Fore Arc, Papau New Guinea. *Econ. Geol., 97*, 1795-1813, 2002.

Philip, H. and J-F. Ritz, Gigantic paleolandslide associated with active faulting along the Bogd fault (Gobi-Altai, Mongolia). *Geology; **27***, 211–214, 1999.

Ranero, C.R. and T. J. Reston, Detachment faulting at ocean core complexes, *Geology, 27*, 983–986, 1999.

Reston T.J., O. Ruoff, J. H. McBride C. R. Ranero and R.S. White, Detachment and steep normal faulting in Atlantic oceanic crust west of Africa. *Geology*; 24; 811–814, 1996.

Reid, M.E., T.W. Sisson and D.L. Brien, Volcano collapse promoted by hydrothermal alteration and edifice shape, Mount Rainier, Washington. *Geology;* 29, 779–782, 2001.

Reid, M.E., Massive collapse of volcano edifices triggered by hydrothermal pressurization. *Geology, **32***, 373–376, 2004.

Richards, J.P. and M. Villeneuve, The Llullaillaco volcano, northwest Argentina: construction by Pleistocene volcanism and destruction by sector collapse, *J. Volcanol. Geotherm. Res. 105*, 77-105, 2001.

Roa, K., Volcanic spreading and lateral collapses at Taburiente volcano, La Palma, Canary Islands. Poster and abstract presented at the *45th Annual Irish Geological Research Meeting 2002* University College Dublin. 48 pp. 2002. Abstract available online at: www.geomond.ucd/htdocs/mpgrg/html/igrm-2002-abstracts.pdf.

Roa, K., Nature and origin of toreva remnants and volcaniclastics from La Palma, Canary Islands, *J. Volcanol. Geotherm. Res.*, ***125***, 191-214, 2003.

Rodríguez-Losada, J.A., J. Martinez-Frias, M.A. Bustillo, A. Delgado, A. Hernandez-Pacheco and J.V. de la Fuente Krauss, The hydrothermally altered ankaramite basalts of Punta Poyata (Tenerife, Canary Islands) *J. Volcanol. Geotherm. Res.*, 103 367-376, 2000.

Roberts, J.A. and A. Cramp, Sediment stability on the western flanks of the Canary Islands. *Mar. Geol.*, ***134***, 13-30, 1996.

Robertson, A.H.F., and C. J. Stillman, Late Mesozoic sedimentary rocks of Fuerteventura, Canary Islands: implications for west African continental margin evolution, *J. Geol. Soc. Lon.*, ***136***, 47-60, 1979.

Robin, C., J.P. Eissen and M. Monzier, Giant tuff cone and 12 km-wide associated caldera at Ambryn Volcano (Vanuatu, New Hebrides Arc). *J. Volcanol. Geotherm. Res.*, ***55***, 225-238, 1993.

Roest, W.R., J.J. Dañobeita, J. Verhoef and B.J. Collette. Magnetic anomalies in the Canary Basin and the Mesozoic evolution of the central north Atlantic. *Mar. Geophys. Res.*, ***14***, 1-24, 1992.

Romero Ruiz, C. L. Garcia Cacho, V. Araña, A.Yanes Luquea and A. Felpeto, Submarine volcanism surrounding Tenerife, Canary Islands: implications for tectonic controls, and oceanic shield forming processes. *J. Volcanol. Geotherm. Res.*, ***103***, 105-119, 2000.

Sandwell, D.T., H.F. Walter, S.G. Smith, J. Steven K Soofi and B. Coakley, Bathymetry from Space: White paper in support of a high-resolution, ocean altimeter mission. Version 1.5 June 28, 54 pp. 2001

Schiffman, P., and H. Staudigel, Hydrothermal alteration of a seamount complex on La Palma, Canary Islands: Implications for metamorphism on accreted terranes. *Geology, **22**,* 151-154, 1994.

Shipton, Z.K. and P.A. Cowie, Damage zone and slip surface evolution over μm to km scales in high-porosity Navajo Sandstone, Utah. *J. Struct. Geol., **23**,* 1825-1844, 2001.

Schmidt, R. and H.U. Schmincke. From seamount to oceanic island, Porto Santo, central East-Atlantic. *Int J Earth Sci **91***: 594-614, 2002.

Schmincke, H-U., and M. Sumita, Volcanic evolution of Gran Canaria reconstructed from apron sediments: Synthesis of VICAP project drilling. *Proc. ODP, Sci. Results, **157**,* 443-465, 1998.

Schmincke, H-U., A. Klügel, T. Hansteen, K. Hoernle and P. van den Bogaard. Samples from the Jurassic oceanic crust beneath Gran Canaria, La Palma and Lanzarote (Canary Islands). *Earth Plan. Sci. Lett., **163***, 343-360, 1998.

Scholz, C.H., The mechanics of earthquakes and faulting. Cambridge University Press, New York. 439 pp. 1990.

Scholz, C.H., Wear gouge formation in brittle faulting. *Geology, **15***, 493-495, 1987.

Schultz, R.A., Relative scale and the strength and deformability of rock masses. *J. Struct. Geol., **18***, 1139-1149, 1996.

Schultz-Ela, D.D., Excursus on gravity gliding and gravity spreading, *J. Struct. Geol. **23***, 725-731, 2001

Seber, D., M.Baranzangi, A.Ibenbrahim and A.Demnati, Geophysical evidence for lithospheric delamination beneath the Alboran Sea and Rif-Betic Mountains. *Nature, **379**,* 785-790, 1996.

Seber, D., M.Baranzangi, B.A.Tadili, M.Ramdami, A.Ibenbrahim and D. Ben Sari, Three-dimensional upper mantle structure beneath the intra-plate Atlas and inter-plate Rif Mountains of Morocco. *J. Geophys. Res. **101***, 3125-3138, 1996.

Seront, B., T. Fong Wong, J.S. Caine, C.B. Forester, R.L. Bruhn and J.T. Fredrich. Laboratory characterization of hydro-mechanical properties of a seismogenic normal fault system, *J. Struct. Geol., **20***, 865-881, 2001.

Sibson, R.H., Fault rocks and fault mechanics. *J. Geol. Soc. London **133***, 191-213, 1977.

Sibson, R.H., Structural permeability of fluid-driven fault-fracture meshes, *J. Struct. Geol., **18***, 1031-1042, 1996.

Sibson, R.H., Fluid involvement in normal faulting, *J. Geodyn., **29***, 469-499, 2000.

Simkin, T., J. D. Unger, R. I. Tilling, P. R. Vogt and H. Spall. World Map of Volcanoes, Earthquakes, Impact Craters, and Plate Tectonics. *The Dynamic Planet presentation.* 9 pp. 1994.

Sjöberg, J., Analysis of large-scale rock slopes. Doctoral thesis, Luleå University of Technology, 788 pp., 1999.

Smith, J.R., A. Malahoff and A. N. Shor Submarine geology of the Hilina slump and morpho-structural evolution of Kilauea volcano, Hawaii. *J. Volcanol. Geotherm. Res., **94***, 59–88, 1999.

Staudigel, H., and H.U. Schmincke, The Pliocene seamount series of La Palma, Canary Islands, *J. Geophys Res. **89**,* 1195-1215, 1984.

Staudigel, H., G. Feraud and G. Ginanerini, The history of intrusive activity on the island of La Palma (Canary Islands). *J. Volcanol Geotherm Res., **27**,* 299-322, 1986.

Stillman, C.J., A Canary Islands dyke swarm: implications for the formation of oceanic islands by extensional fissural volcanism. In: Mafic dyke swarms. (eds. Halls & Fahrig) *Geol. Soc. Canada Special Paper, 33*, 243-255, 1987.

Stix, J., B. Kennedy, M. Hannington, H. Gibson, R. Fiske, W. Mueller and J. Franklin, Caldera-forming processes and the origin of submarine volcanogenic massive sulfide deposits. *Geology,* 31, 75–378, 2003.

Sumner. M. and J. Michael J. Branney, The emplacement history of a remarkable heterogeneous, chemically zoned, rheomorphic and locally lava-like ignimbrite: 'TL' on Gran Canaria. *J. Volcanol. Geotherm. Res., 115*, 109-138, 2002.

Swanson, D.A., W.R. Duffield and R.S. Fiske, Displacement of the south flank of Kilauea volcano: the result of forceful intrusion of magma into the rift zones. U.S. Geol. Surv., Prof. Pap. 963, 39 pp, 1976.

Szakács. A. and M. Ort. Comments on the article ""Erosion calderas: origins, processes, structural and climatic control" by Karátson D., Thouret J-C., Moriya I., Lomoshitz A. *Bull. Volcanol. 61:174-193.*

*Bull. Volcanol, **63**,* 289-290, 2001.

Teixell, A., D. W. Durney and M-L. Arboleya, Stress and fluid control on decollement within competent limestone *J. Struct. Geol.,**22***, 349-371, 2000.

Tibaldi, A., Multiple sector collapses at Stromboli volcano, Italy: how they work. *Bull Volcanol., 63*, 112–125. 2001.

Toutin, T., A. Redmond; E. Hoeppner, D. Hoja and C. King. Radarsat and DEM data fusion for 3D visualization over the Reunion Island for geoscientific applications. 11 pp. 1998

Tucholke, B.E., Massive submarine rockslide in the rift valley wall of the Mid Atlantic Ridge, *Geology, 20*, 129-132, 1992.

Troll, V.R., Walter, T.R., Schmincke, H.U., Cyclic caldera collapse: Piston or piecemeal subsidence? Field and experimental evidence. *Geology, 30*, 135-38, 2002

Urgeles, R., M. Canals, Jesus Baraza and Belen Alonso. Seismostratigraphy of the western flanks of El Hierro and La Palma (Canary Islands): a record of Canary Islands volcanism. *Marine Geology 146*, 225–241,1998.

Urgeles, R., D.G. Masson, M. Canals, A.B. Watts and T. Le Bas, Recurrent large scale landsliding on the west flank of La Palma, Canary Islands. *J. Geophys. Res., **104**, 25,331-20,348, 1999.*

Urgeles, R., M. Canals, J. Roberts and the SNV "Las Palmas" Shipboard Party. Fluid flow from pore pressure measurements off La Palma, Canary Islands. *J. Volcanol. Geotherm Res., 101*, 253–271, 2000

van Bemmelen, R.W., The geology of Indonesia. *1A*, 732 pp. The Hague, 1949.

van Wyk de Vries, B. and P.W. Francis, Catastrophic collapse at stratovolcanoes induced by gradual volcano spreading. *Nature **387**,* 387-390, 1997.

van Wyk de Vries, B. N. Kerle and D. Petley.2000, Sector collapse forming at Casita volcano, Nicaragua: *Geology, **28**,* 167–170

van Wyk de Vries, B., S. Self, P.W. Francis, and L. Keszthelyi, A gravitational spreading origin for the Socompa debris avalanche. *J. Volcanol. Geotherm. Res., **105**,* 225-247, 2001.

Vine, F.J and P. Kearey, Global Tectonics 2nd edition: Blackwell Science, 344 pp, 1996

Voight, E., and D. Ellsworth, Failure of volcano slopes. *Geotechnique, **47***, 1-31, 1997.

Vogt., P. and N. Christian Smoot, The Geisha Guyots: Multibeam Bathymetry and Morphometric Interpretation. *J. Geophys. Res., **89**.* 11085-11107, 1984.

Von Buch, L., Physikalische Berschrebung der Canarischen Inslen, 201 pp. Koenigl. Akad. Wiss., Berlin. 1825.

Walker, G.P.L., Downsag calderas, ring faults, caldera sizes and incremental caldera growth. *J. Geophys. Res. **89***, 8407-8416, 1984.

Walker, G.P.L., Gravitational (density) controls on volcanism, magma chambers and intrusion. *Aus. J. Earth. Sci., **36**,* 149-165, 1989.

Walker, G.P.L., "Coherent intrusion complexes" in large basaltic volcanoes – a new structural model, *J. Volcanol Geotherm Res. **50**,* 41-54, 1992.

Walsh, J.J., J. Watterson, A.E. Heath and C. Childs, Representation and scaling of faults in fluid flow models. *Pet. Geosci.* 4, 241-251, 1998.

Walter, T.R., V.R. Troll and H-U. Schmincke, Rift architecture in volcanoes: from single rift to triaxial rifts. *Forth international dike conference (IDC4), South Africa,* 8 pp, 2001.

Walter, T.R. and Schmincke, H-U. Rifting, recurrent landsliding and Miocene structural reorganization on NW-Tenerife (Canary Islands). *Int J. Earth Sci. (Geol Rundsch) **91***, 615–628, 2002.

Walter, T.R., Butressing and fractional spreading of Tenerife, an experimental approach on the formation of rift zones. *Geophys. Res. Lets, **30***, 1-4, 2003.

Walter, T.R. and V.R. Troll, Experiments on rift zone evolution in unstable volcanic edifces. *J. Volcanol. Geotherm. Res. **127**,* 107-120, 2003

Watts, A.B., and D.G. Masson. A giant landslide on the north flank of Tenerife, Canary Islands, *J. Geophys. Res., **100,*** 24,487-24,498, 1995.

Watts, A.B., C. Pierce, J. Collier, R. Dalwood, J.P, Canales, T.J. Henstock, A seismic study of lithospheric flexure in the vicinity of Tenerife, Canary Islands. *Earth Planet. Sci.Lett. **146***, 431-447. 1997.

Watts, A.B., and D.G. Masson. New sonar evidence for recent catastrophic collapses of the north flank of Tenerife, Canary Islands. *Bull. Volcanol.* ***63***, 8-19, 2001.

Watts, A.B., Isostacy and Flexure of the Lithosphere. *Cambridge University Press*. 458 pp. 2001.

White, J. D. L., and H-U. Schmincke, phreatomagmatic eruption and depositional processes during the 1949 eruption of La Palma (Canary Islands). *J. Volcanol Geotherm Res.* ***94***, 428-304, 1999.

Wieczorek, G.F., Landslide triggering mechanisms. *In:* Landslides; Investigation and mitigation A.K. Turner and R.L.Schuster Eds. Special Report 247. Transport and Research Board. *National Academy Press, Washington* 675 pp.

Wolfe, E.W. and J. Morris, Geologic map of the island of Hawaii. *USGS MAP* ***I-2524-A***, 1996.

Wooller L., B. van Wyk de Vries, J.B. Murray, H. Rymer and S. Meyer, Volcano spreading controlled by dipping substrata. *Geology,* 32, 573–576; 2004

Wylie, D.C. and N.I. Norish. Rock strength properties and their measurement. *In:* Landslides; Investigation and mitigation A.K. Turner and R.L.Schuster Eds. Special Report ***247***. Transport and Research Board. *National Academy Press, Washington* 675 pp.

Wynn, R.B., D.G. Masson, D.A.V. Stow and P.P.E. Weaver, Turbidity current sediment waves on the submarine slopes of the western Canary Islands. *Mar. Geol.*, ***163***, 185-198, 2000,

Wynn, R.B. and D.G. Masson, Canary Islands landslides and tsunami generation: myth or legend? PDF presentation. 20 pp 2003. http://www.soc.soton.ac.uk/CHD/staff_stu/Russel-Wynn/canaries_gy306.pdf

Wynn, R.B. and D.G. Masson, Can we use turbidite deposits to interpret landslide processes? Canary Islands landslides and tsunami generation. In: Proc. 1st Int. Symposium on Submarine Mass movements and their Consequences (Ed. by J. Mienert and J. Locat), EGS-AGU-EUG Joint Assembly, Nice, April, 8 pp, (in press) 2003

Ye, S., J.P. Canales, R. Rihm, J.J. Dañobeitia and J. Gallart, A crustal transect through the northern and northeastern part of the volcanic edifice of Gran Canaria Canary Islands *Geodynamics* ***28***, 3-26, 1999.

Yokose, H., Landslides on the Windward Flanks of Oahu and Molokai, Hawaii: SHINKAI 6500 Submersible investigations. In: Hawaiian Volcanoes; deep underwater perspectives (Takahashi, Lipman, Garcia, Naka, Aramaki – Eds). Geophysical Monograph 128. American Geophysical Union, Washington. 245-261, 2002

Zimbelman, D. R., R. J. Watters, I. R. Firth, G.N. Breit and G. Carrasco-Nunez, Stratovolcano stability assessment methods and results from Citlaltépetl, Mexico. *Bull Volcanol,* ***66***, 66–79, 2004